

SASCOM

Introductory course on composite materials 2021

Albertino Arteiro & Pedro P. Camanho

INEGI, University of Porto, Porto, Portugal

SASCOM

Introductory course on composite materials 2021

Constituent materials and semi-products

References

Marques AT. Composite Systems: Design and Manufacture for Durability, University of Porto, September 2019.
Miravete A. Materials, Composites Design Workshop XXI, Stanford University, July 2021.

Constituent materials

Composite materials are a combination of two materials that result in better properties than the constituents alone.

The two main constituents of **advanced composite materials** are:

- A **continuous fibre**, which carries most of the external load and gives the composite material its major strength and stiffness. It dominates other properties such as the coefficient of thermal expansion and conductivity.
- A **(polymer) matrix**, which binds the fibres together, transfers external loads to the fibres, protects the fibres from the surrounding environment and gives the composite material its surface appearance.

Fibres

Boron fibres

Boron fibres are produced by deposition of boron in vapour phase on a tungsten wire or carbon, which acts as substrate.

The diameter of the fibres that act as a substrate is about 12 μm and the result, after deposition of boron, is a fibre that can reach 200 μm .

- Due to their high cost, composites with boron fibres are essentially used in the aerospace industry.

Fibres

Carbon fibres

- **Carbon fibres** - with carbon content between 80% and 95%.
- **Graphite fibres** - carbon content above 95%. Most widely used in aerospace applications.

The production of carbon fibres is based on thermal decomposition of several organic precursors:

Cellulose (“rayon fibres”)

Pitch (“pitch fibres”)

Polyacrylonitrile (PAN)

Fibres

Carbon fibres

- **Carbon fibres** - with carbon content between 80% and 95%.
- **Graphite fibres** - carbon content above 95%. Most widely used in aerospace applications.

The production of carbon fibres is based on thermal decomposition of several organic precursors:

Cellulose (“rayon fibres”)

Pitch (“pitch fibres”)

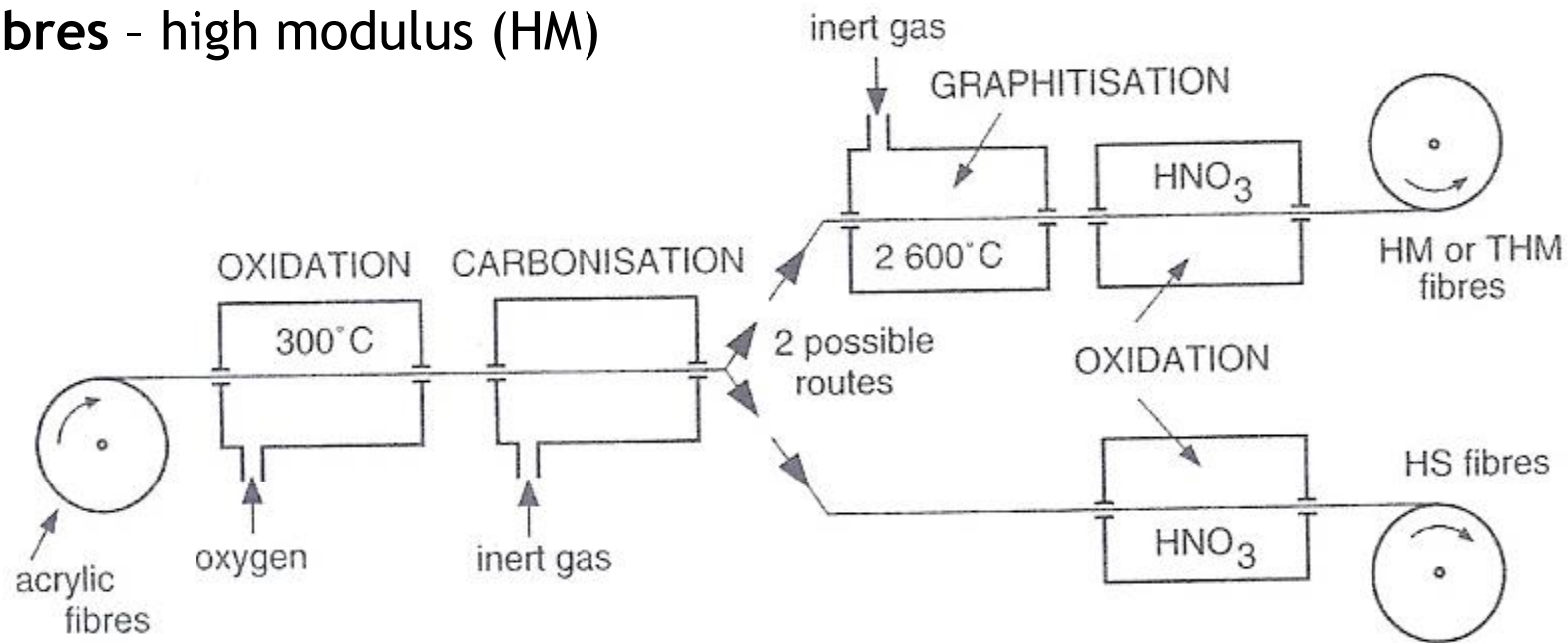
Polyacrylonitrile (PAN)

- Currently the most widely used precursor.

Fibres

Carbon fibres

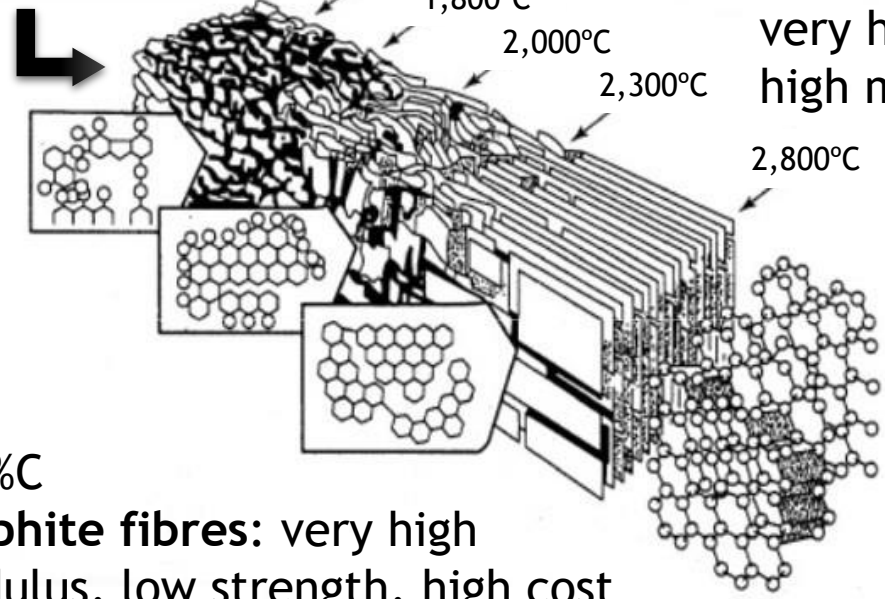
- Carbon fibres - high strength (HS)
- Graphite fibres - high modulus (HM)



Fibres

Carbon fibres

PAN fibres



92% C - 95% C
Carbon fibres:
very high strength,
high modulus

≈99% C
Graphite fibres: very high
modulus, low strength, high cost

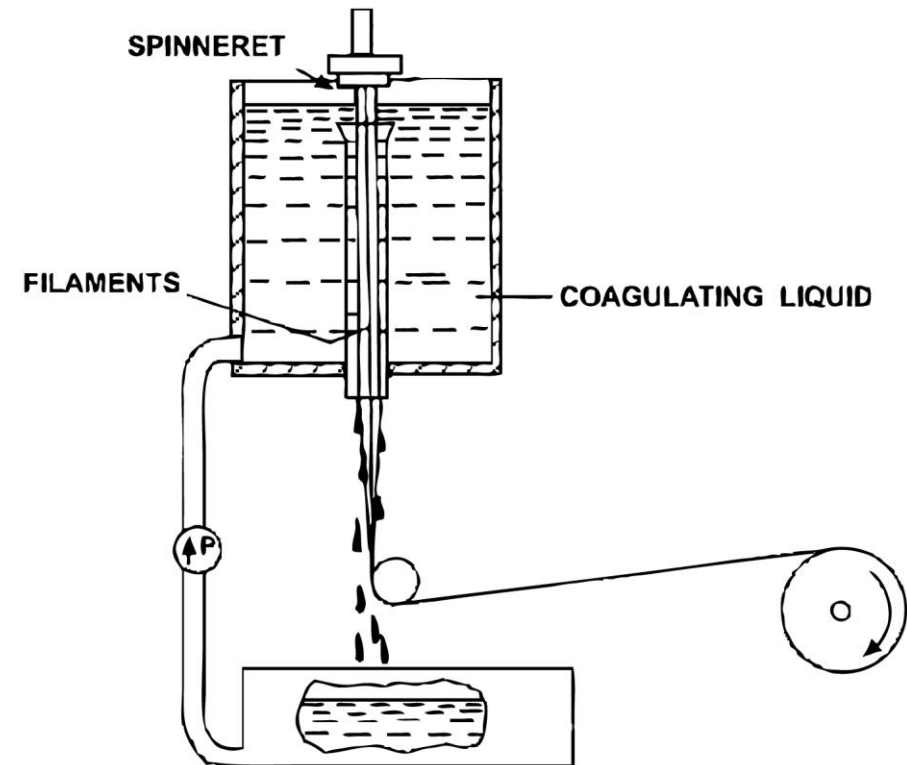


Fibres

Aramid fibres

Aramid fibres are produced from aromatic polyamides.

- The polymer solution is synthesised at low temperature (below -10°C) and then **extruded** (fibrillated and drawn) at a temperature of approximately 200°C .
- By this method, the **molecular chain is aligned**, and an improvement of **mechanical properties** can be achieved.

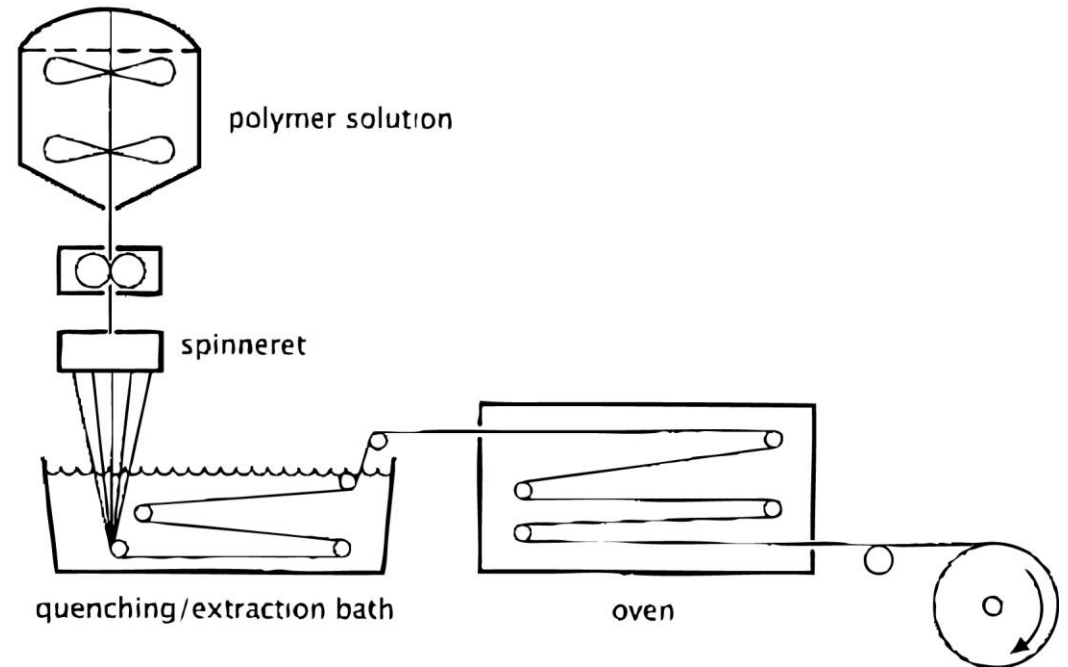


Kelly A. Comprehensive composite materials. ISBN: 0-08-042993-9.

Fibres

Ultra-High Molecular Weight Polyethylene (UHMWPE) fibres

- UHMWPE fibres have excellent toughness, **outstanding high velocity impact resistance**, and high tensile strength due to highly oriented molecular chains.
- However, UHMWPE fibres they have **poor compression strength**.
- UHMWPE fibres are used in armour, in particular personal armour and many other applications where impact/tension loadings are involved.

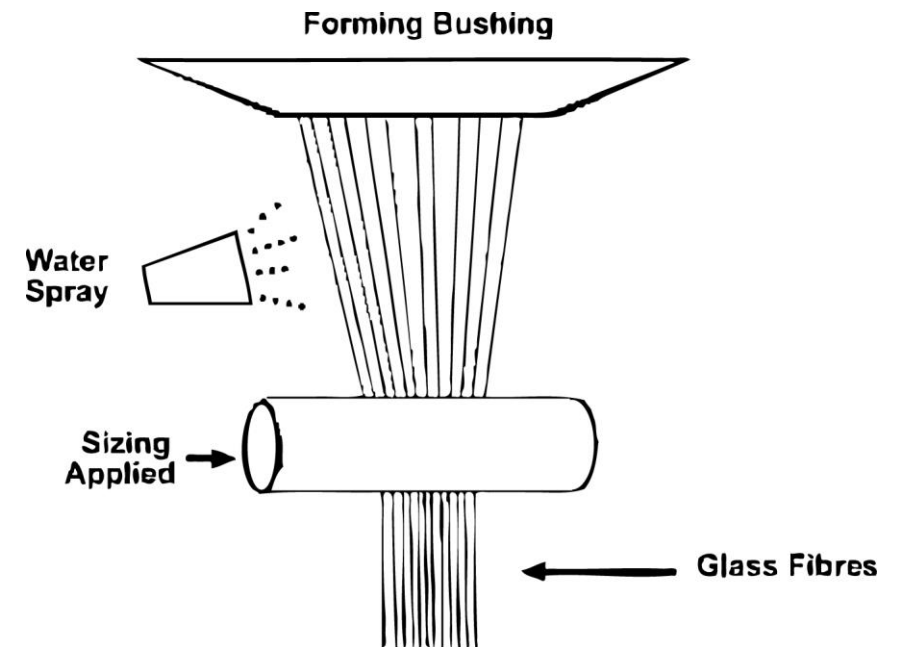


Kelly A. Comprehensive composite materials. ISBN: 0-08-042993-9.

Fibres

Glass fibres

- Most widely used reinforcement;
- Produced by stretching the melted glass (silica - SiO_2 - with sodium carbonate and calcium carbonate; melting temperature of $\approx 1260^\circ\text{C}$) through a die made of rhodium-platinum alloy with very fine and precise orifices;
- Some oxides are added to increase performance.
- A textile coating is applied to produce fabrics without the risk of fibre damage.



Kelly A. Comprehensive composite materials. ISBN: 0-08-042993-9.

Fibres

Other types of fibres

Flax fibres

- Natural fibres.
- Compare favourably with glass fibre composites in terms of specific stiffness and strength and in terms of cost.
- The two drawbacks of most concern to composites manufacturers: its hydrophilic nature, and its poor bonding properties with polymers are being addressed by pre-treatment of fibres before moulding and application of a sizing, respectively.
- Applications include load bearing and outdoor applications such as automotive exterior underfloor panelling, sports equipment and marine structures.

Fibres

Other types of fibres

Ceramic fibres

- Obtained by chemical vapor phase deposition (CVD).
- Combine high mechanical resistance and high modulus of elasticity with resistance to high temperatures.
- Normally produced in the form of small whiskers. Various materials, such as metals, oxides, carbides and organic compounds can be prepared in the form of whiskers.

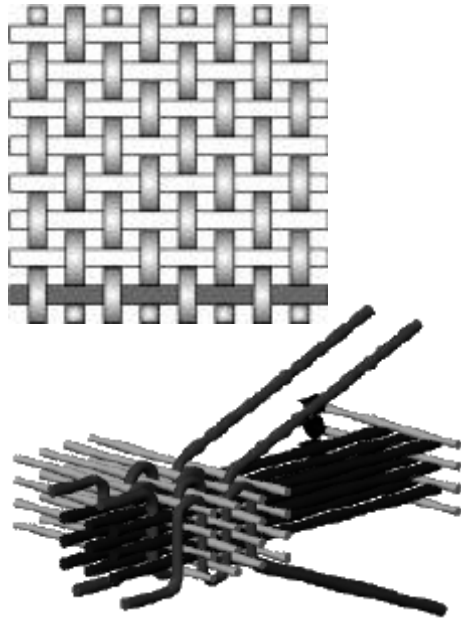
Reinforcements configurations



Roving

Continuous filaments wrapped helically on coils (bobbins). Usually, the roving is destined to the production of short fibres (for example for spray-up moulding), fabrics, or can be processed to produce mats, braids, knits or hybrids.

Reinforcements configurations



Woven fabrics

Fabrics can be of 2D or 3D formats, produced from interlocking bundles of long carbon, aramid, glass fibres or a combination of these, for applications requiring good formability, good impregnation and high damage resistance.

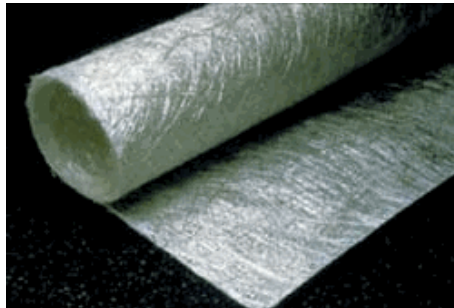
- **2D fabrics** have less undulation, exhibiting higher mould conformability (property known as *drapability*).
- **3D fabrics** are distinguished by their interlaminar strength, due to the fibres in the thickness direction.

Reinforcements configurations



Short fibres

Short fibres are used in felts, mats (CSM), preforms and injection moulding.



Chopped Strand Mat & Continuous Random Mat

Distinct types of mats with randomly distributed fibres include:

- **Chopped Strand Mats (CSM)** - mats with short fibres;
- **Continuous Random Mats (CRM)** - mats of continuous filaments;
- Surface mats.

Reinforcements configurations



Preforms

A **preform** consists of conforming one or several layers of dry reinforcement to the approximate final shape of the component.

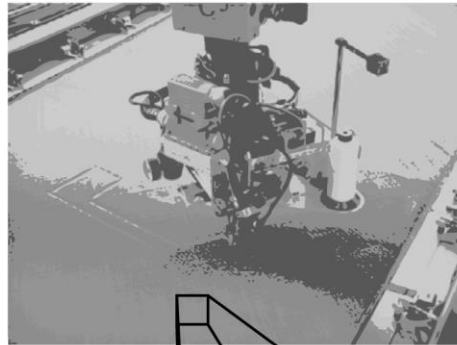
Preforms are produced with different shapes, including **bi-** or **tri-dimensional short or continuous fibres**:

- **Short fibre preforms** may result from cutting and overlapping short fibre mats, or from manual or spray fibres and binder deposition on a mould.
- **Continuous fibre preforms** have a thermoplastic binder which, after heating, can be conformed with a mould and counter mould in a press.



Reinforcements configurations

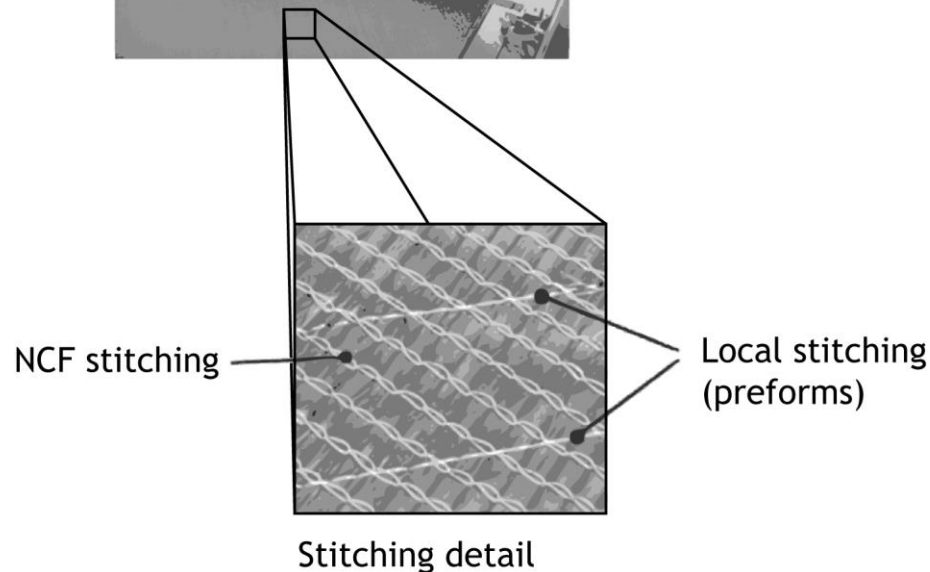
Sewing machine



Non-crimp fabrics (NCFs)

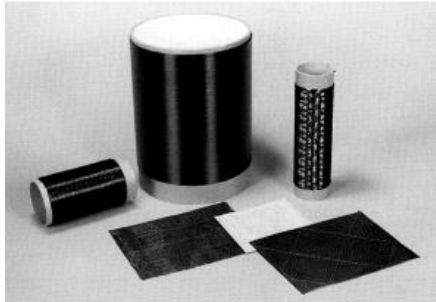
NCFs, or (multi-axial) multiply ward-knitted fabrics, arose from the challenge to create reinforcements that combine unidirectional fibres with integrity, ease of handling, and drape of textile fabrics.

NCFs are an advanced type of textile fabrics that consist of one to several plies of unidirectional fibres with varying fibre orientations that are stacked and knitted together.



S. Bel. Mechanical behaviour of non-crimp fabric (NCF) preforms in composite materials manufacturing. In: Advances in Composites Manufacturing and Process Design. <http://dx.doi.org/10.1016/B978-1-78242-307-2.00012-9> Elsevier, 2015.

Reinforcements configurations



Prepregs (pre-impregnated fibres)

Prepregs can have unidirectional (tape), woven, mat, or roving formats.



- Widely used in the industry, especially with epoxy resins, but also pre-impregnated with thermoplastic matrices.
- Unidirectional *prepregs* (tapes) are used in either manual or automated moulding.
- After lamination, *prepregs* typically cured or consolidated in the presence of pressure and temperature.

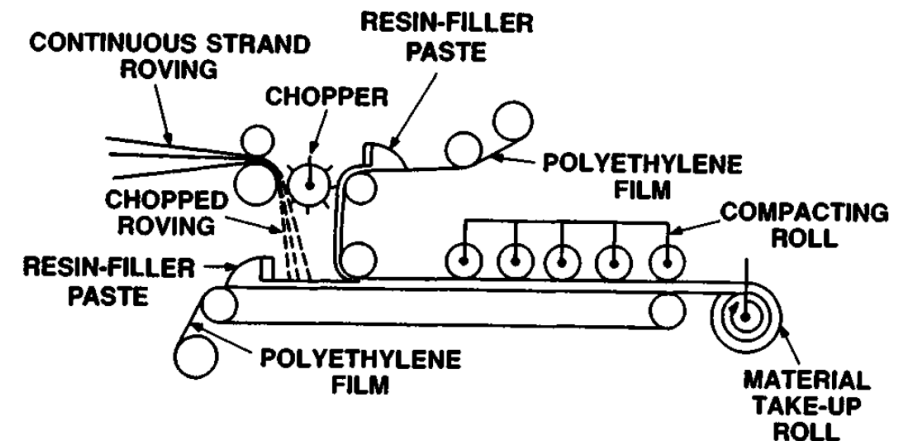
Reinforcements configurations



<https://www.compositesworld.com/news/hexcel-molding-compound-enables-high-volume-zero-waste-process>

Sheet moulding compound (SMC)

- SMC consists of randomly oriented chopped fibres in a matrix of resin and filler or thermoplastic. SMC is produced in a continuous manner. A film can be used to protect the roller.
- SMC rolls are used in **compression moulding** to create large parts, especially for cars and trucks construction.



Matrix materials

Fibres are of little use unless they are bonded together to take the form of a structural element that can carry loads. The binder material is usually called a *matrix*.

The role of the **matrix** is:

- To bind the fibres together
- To transfer external loads to the fibres
- To protect the fibres
- To give the composite material its surface appearance

- **Good fibre/matrix bond**
- **Mechanical properties**
- **Environmental properties**
- **Easily shaped/moulded**

Matrix materials

Epoxy

- Due to its excellent mechanical properties, epoxy is the ideal companion of carbon fibres to form composite materials for highly structural applications.
- On the other hand, it is the only resin which bonds well with aramid fibres.
- Glass/epoxy composites are also common in structural/low cost applications such as wind turbine blades.

Matrix materials

Polyester

- **Styrene** is the cross-linking agent.
- Polyester resins emit strong smelling styrene fumes, which are an inhalation hazard, therefore requires special precautions when processing.
- **An initiator, usually a peroxide, is required to start the reaction between the polyester and the styrene.** Consequently, processing fibreglass-reinforced polyester is quite straightforward.
- The high curing shrinkage is a major drawback.
- Moreover, the **limited range of working times** (a few minutes) makes the impregnation/compaction difficult.

Matrix materials

Vinyl ester

- Vinyl ester resins, like polyester resins, are **dissolved in styrene monomers**, which **reduces their viscosity**.
- A unique characteristic of the vinyl ester molecule is that it **contains OH** (hydroxyl) groups along its length. These OH groups can form hydrogen bonds with similar groups on a fibreglass surface resulting in **excellent wet-out and good adhesion with fibreglass**.

Matrix materials

Phenolic

- Semi-structural parts, subject to **fire, flammability and smoke requirements** (train and aircraft interior applications).
- They may be used as well to produce carbon-carbon composites, where the phenolic resin is pyrolyzed to generate a carbon matrix.

Cyanate Ester

- Low dielectric resins (antennas, radomes, etc.) - limited market due to high cost.
- Low moisture absorption (0.6% - 2.5%).
- Tough resin, due to the moderate cross link density.

Matrix materials

Bismaleimide (BMI)

- Used for high-temperature and high-toughness applications.
- Can be processed at the same temperature - 180°C - and pressure - 0.7 MPa - as epoxy.
- Tack and drape are quite good due to the liquid nature of the reactants.

Polyimide

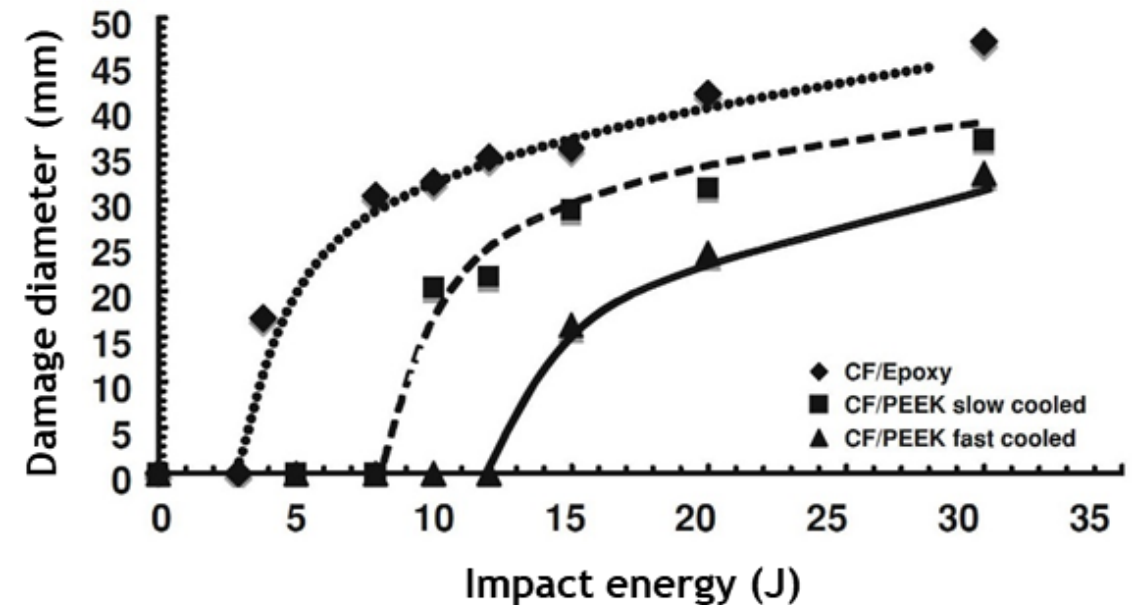
- Unique combination of high-thermal stability, good chemical and solvent resistance, as well as excellent retention of mechanical properties at high temperature.
- Poor tack and drape, difficulty to produce thick laminates.
- Space and aeronautics applications are the most common for this resin due to its characteristics and high cost.

Matrix materials

Thermoplastics

FRTPs are characterised by:

- High strain to failure.
- High fracture toughness and damage tolerance.
- Longer shelf life.
- Ability to reshape and reuse/recycle.



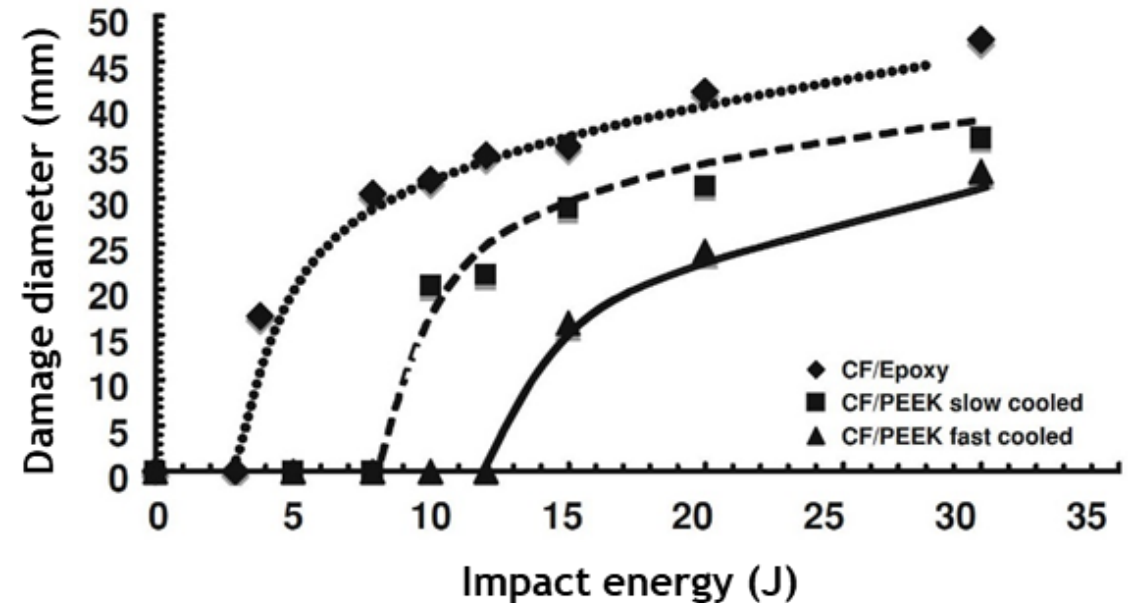
Halpin. In: Nicolais et al. (Eds.). Springer: London, 2011. p. 51-67.

Matrix materials

Thermoplastics

But their use in structural applications is limited due to:

- Reduced performance/cost ratio.
- Manufacturing difficulties - thermoplastic matrices have very high viscosities at processing temperatures, which may result in a large void content due to inadequate impregnation.



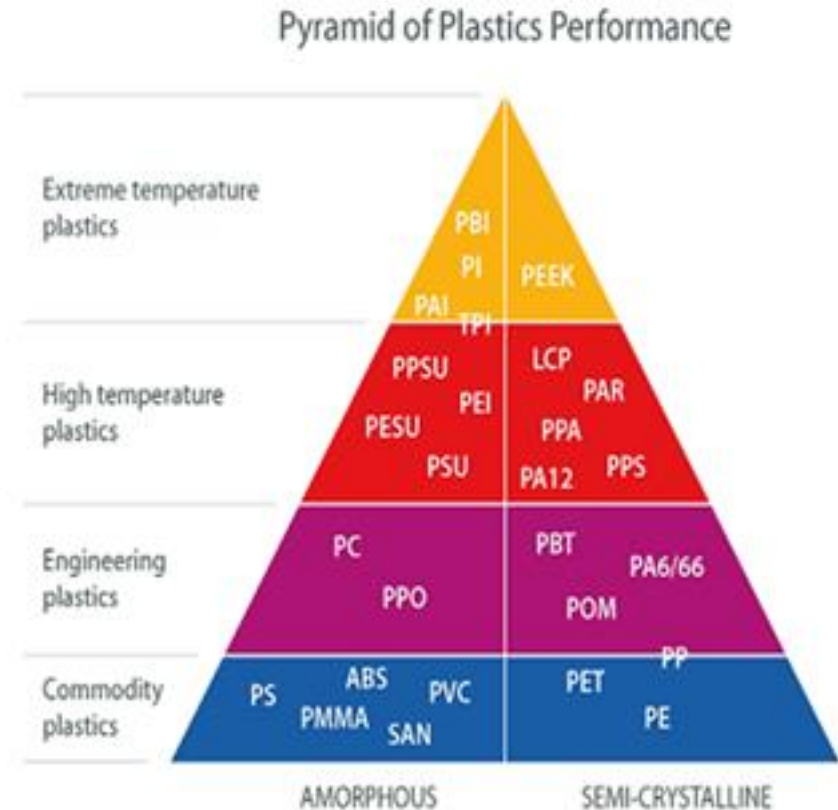
Halpin. In: Nicolais et al. (Eds.). Springer: London, 2011. p. 51-67.

Matrix materials

Thermoplastics

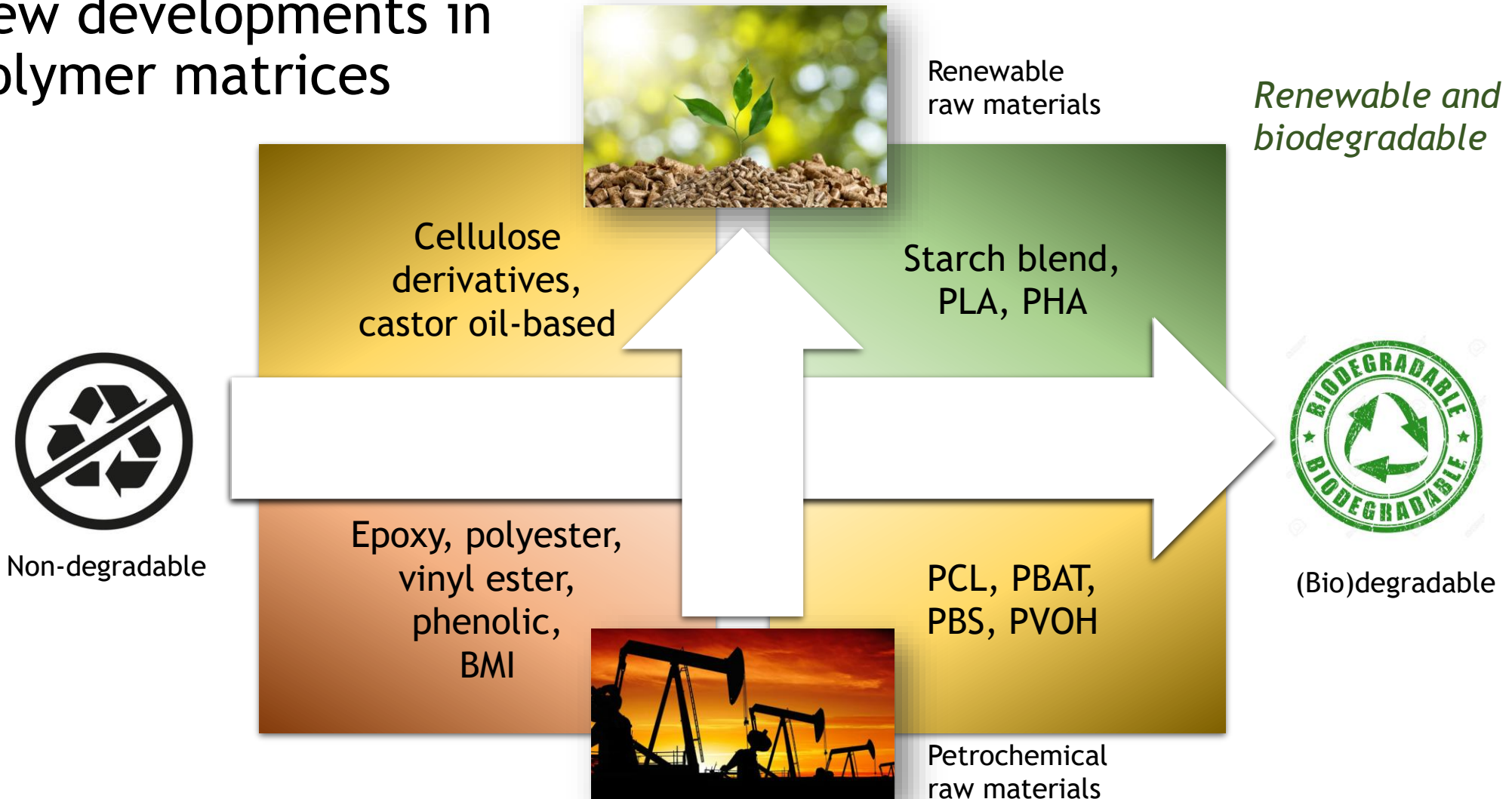
But their use in structural applications is limited due to:

- Reduced performance/cost ratio.
- Manufacturing difficulties - thermoplastic matrices have very high viscosities at processing temperatures, which may result in a large void content due to inadequate impregnation.



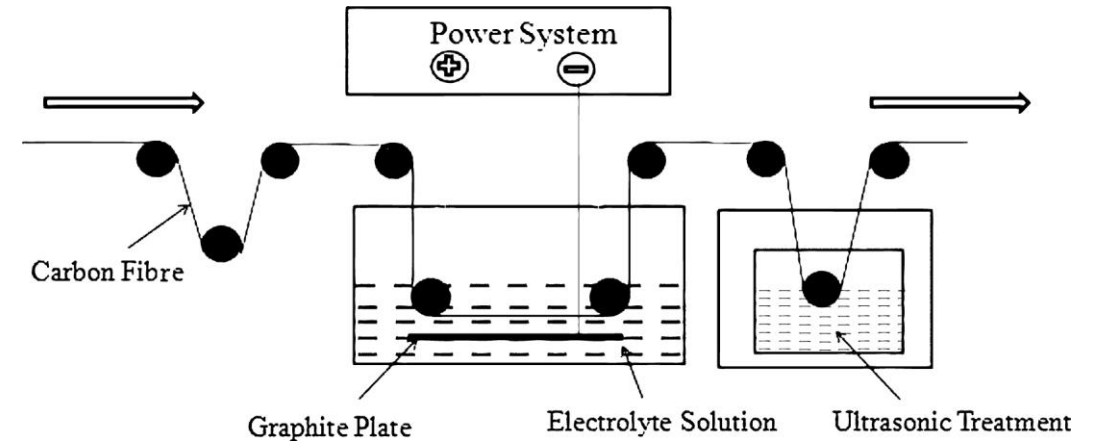
https://omnexus.specialchem.com/selection-guide/high-temperature-thermoplastics?lr=som2016jun&li=100243877&m_i=PnkqATwT0rV%2B3F8urwy3KFPilbrlbmD0Ly6L0tdIVQmW6ppsNG6fUsYJTU8OAZ1vYIUg57YIOPQXGY6YTLrwL1cl3eRPPg#utm_source=NL&utm_medium=EML&utm_campaign=som2016jun

New developments in polymer matrices



Surface treatment and sizing of carbon fibres

- **Oxidation in electrolyte salt solution.**
Oxygen in contact with the carbon fibre surface generates COOH (carboxyl) functional groups and increases the carbon fibre surface roughness
- An **epoxy-based sizing** is afterwards deposited on the carbon fibre surface increasing the number of functional groups.
- **Covalent bonds** between the carboxyl groups and the matrix lead to a very good interface.
- The gradual increase of surface roughness on treated fibres promotes more mechanical **interlocking** as well as carboxyl functional groups.



Surface treatment and sizing of aramid fibres

- Before treatment, the one-dimensional structure of the chain and the already weak bonds between adjacent chains and planes point to the absence of reactive functional groups.
- After spinning, aramid fibres are exposed to a high temperature (230°C) epoxy treatment, **generating -NH₂ functional groups (amines)** and a higher surface roughness.
- **Covalent bonds** between the amine groups and the matrix lead to a very good interface.
- **Interlocking** between the aramid surface and the matrix also enhances the fibre/matrix bond.

Sizing of glass fibres

Application of a **film former** and a **coupling agent**.

- The **film former** is designed to **protect** and lubricate the fibre and hold fibres together prior to moulding. Film formers are usually **chemically similar to the matrix resin** for which the sizing is designed.
- The **coupling agent**, usually an **alkoxysilane** compound, serves primarily to bond the fibre to the matrix. The glass fibre, which is hydrophilic (bonds easily to water), bonds to a resin that is hydrophobic (insoluble in water and does not bond well to it). **Silanes have a silicon end that bonds well to glass, and an opposing organic end that bonds well to resins.**

Silanes (sizing) act as efficient bridges between glass fibres and thermoset matrices by means of covalent bonds.

Constituents selection

Design flexibility

High specific stiffness

High specific strength

Damping capacity

Low thermal expansion coefficient

Durability

Constituents selection

Specific stiffness and strength

Vertical stabilizers and rudder: F-15



Wing covers for F-18



Vertical stabilizers and rudder: F-16



Stabilizers and external fuselage of AV-8B



Constituents selection

Specific stiffness and strength

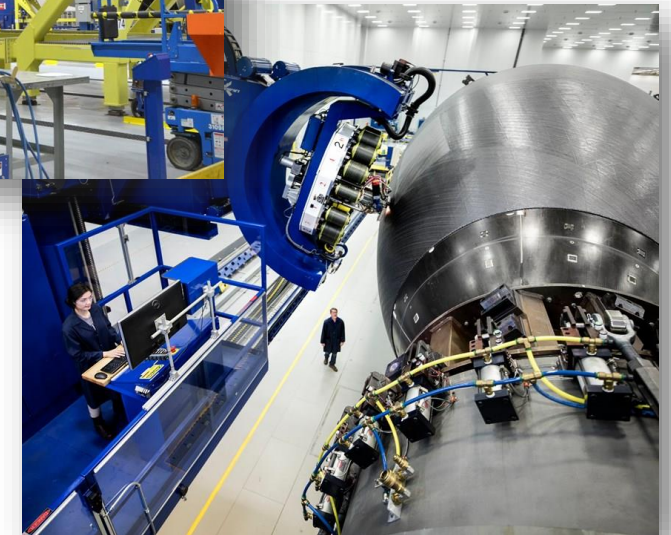


Helicopter Bell 430 uses composite systems in the blades and the fork that holds them

M-309 civil utility aircraft demonstrator has an airframe largely built of carbon fibre composite materials



Boeing 787's Section 41
[The first composite fuselage section for the first composite commercial jet | CompositesWorld](#)



Constituents selection

Specific stiffness and strength



Maclaren MP4-1, 1981

High-pressure resin transfer moulding (HP-RTM) production of composite leaf spring for Volvo's multi-model SPA global platform.
May 2017 CompositesWorld



Fibreglass composite structure used in the 1953 Chevrolet Corvette.



Constituents selection

Zero thermal expansion

- Once the space structures are in orbit, it is critical that all their components remain in the same relative position to each other despite extreme temperature changes.
- The negative coefficient of thermal expansion (CTE) of **carbon** is due to the high crystalline alignment in carbon fibres.



Canadarm2 robotic arm

https://www.esa.int/ESA_Multimedia/Images/2020/04/Canadarm2_robotic_arm

Constituents selection

Crashworthiness

- Crashworthiness is concerned with the absorption of energy through controlled failure mechanisms and modes that enable the maintenance of a gradual decay in the load profile during absorption.
- While metals collapse under crush by buckling and/or folding in accordion mode, **composites** fail through a sequence of fracture mechanisms involving fibre fracture, matrix crazing and cracking, fibre/matrix debonding, delamination and inter-ply separation.

2012 Belgian F1 GP crash

<https://www.essentiallysports.com/lewis-hamilton-romain-grosjean-2012-belgian-gp-crash-slow-mo-reveals-the-severity-of-the-crash/>



Constituents selection

Transparency to electromagnetic waves

- Glass fibres are not widely used in aeronautics due to their relatively low stiffness-to-weight ratio.
- However, radomes are usually made of **glass fibres** due to the low requirements in terms of stiffness and the strict specifications in terms of transparency to electromagnetic waves, property which is related to the electrical conductivity of the material.



https://www.defenseworld.net/news/17801/Jenoptik_To_Supply_28_Protective_Domes_To_BAE_Systems_For_Eurofighter_Typhoon#.X4OHT-17mHs

Questions?

Constituent materials and semi-products

SASCOM

Introductory course on composite materials 2021

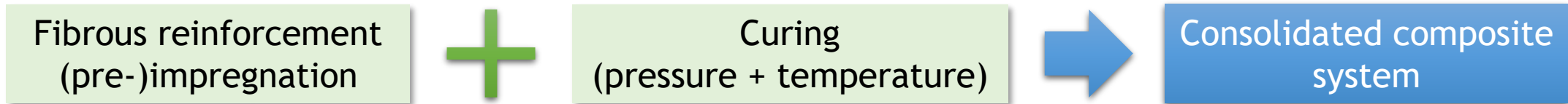
Manufacturing processes

References

Miravete A. Materials, Composites Design Workshop XXI, Stanford University, July 2021.
Marques AT. Composite Systems: Design and Manufacture for Durability, University of Porto, September 2019.
Gay D, Hoa SV, Tsai SW. Composite Materials Design and Applications. CRC Press LLC, 2003.

Manufacturing processes for thermoset matrix composites

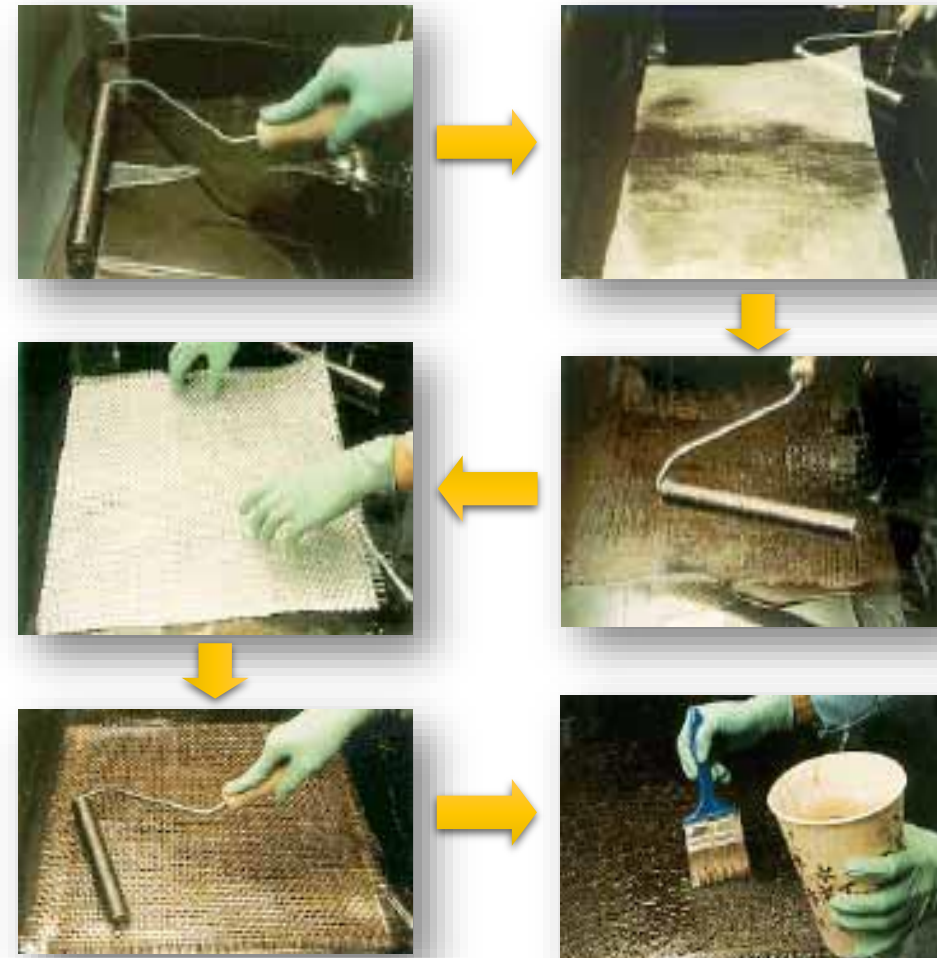
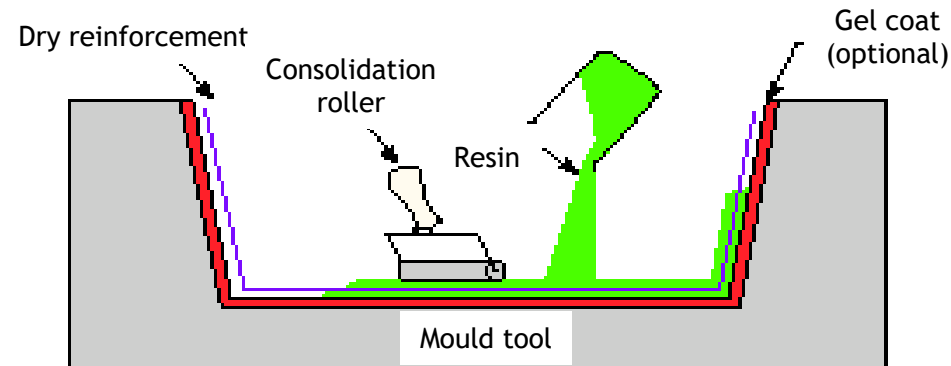
Thermoset matrices are currently the most used for structural applications.



Pressure and temperature are applied to optimise the structural performance of the composite.

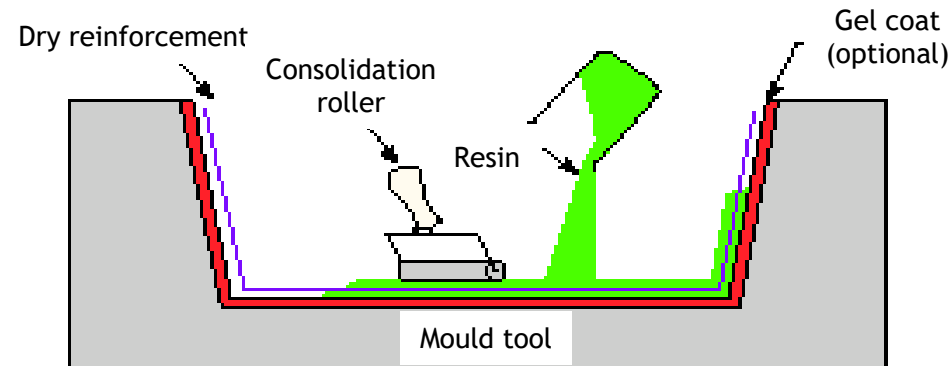
Manufacturing processes for thermoset matrix composites

Hand lay-up (contact moulding) process



Manufacturing processes for thermoset matrix composites

Hand lay-up (contact moulding) process



Mould preparation and selection and careful application of release systems are essential to have a good product.

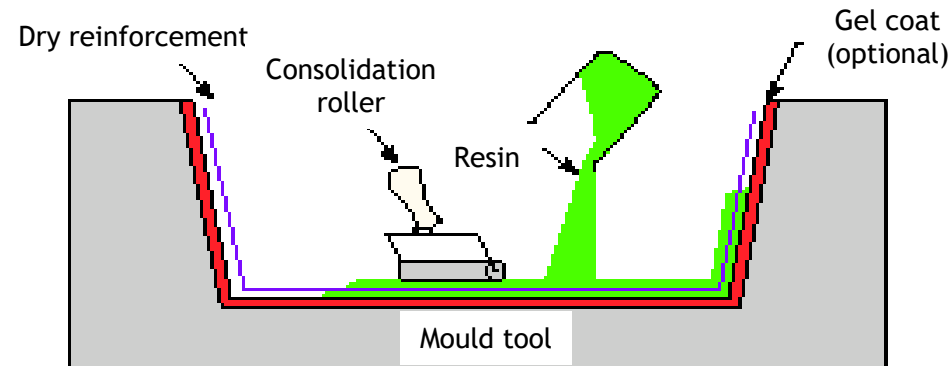
Compaction is done using a roller to squeeze out the air pockets.

The duration for resin setting varies, depending on the amount of accelerator, from a few minutes to a few hours.

Parts of large dimensions can be obtained at the rate of about 2 to 4 parts per day per mould.

Manufacturing processes for thermoset matrix composites

Hand lay-up (contact moulding) process

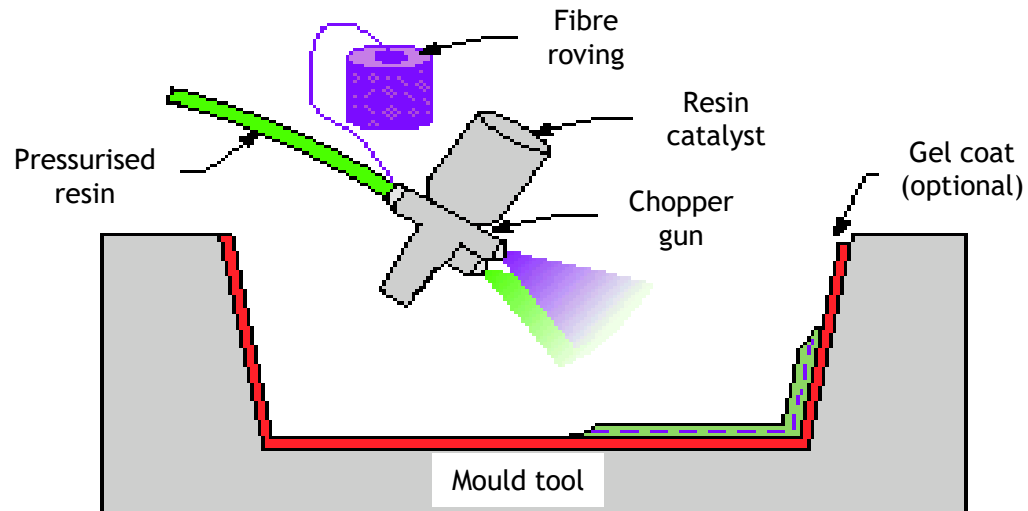


Processing steps

1. **Mould preparation**
2. **Application of release systems** (several layers of a release agent may be necessary)
3. **Application of gel-coat** (resin-rich layer, or just resin layer, normally pigmented)
4. **Mixture of the cure system with the resin**
5. **Lay-up and impregnate individual reinforcement layers, sequentially**
6. **Curing** and, eventually, post-curing according to the instructions of the resin supplier
7. **Demoulding**

Manufacturing processes for thermoset matrix composites

Spray-up process



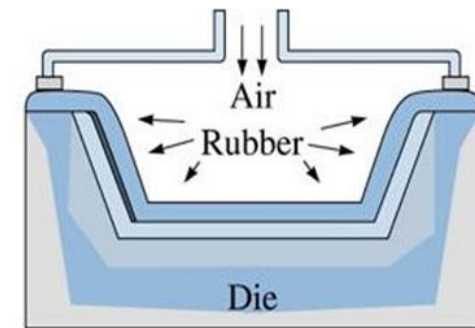
Manufacturing processes for thermoset matrix composites

Compression moulding



- A counter-mould closes the mould after the impregnated reinforcements have been placed on the mould.
- The whole assembly is placed in a press, and polymerisation takes place either at ambient temperature or higher.
- The process is good for average volume production: dozen parts per day, up to 200 with heating.
- Widely used in automotive parts.

Pressure bag moulding



Manufacturing processes for thermoset matrix composites

Compression moulding

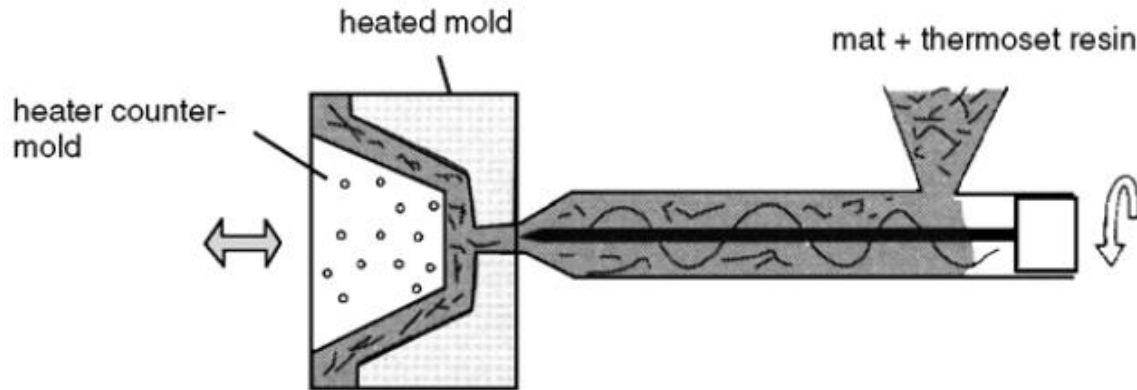


<https://www.youtube.com/watch?v=-LZxhWEmFLY&app=desktop>

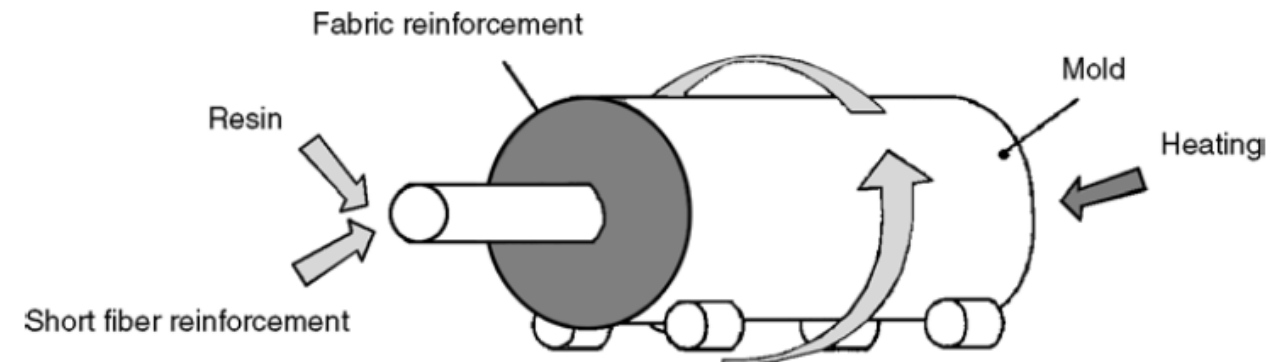
Manufacturing processes for thermoset matrix composites

Injection moulding

(premixed compounds)



Centrifugal moulding



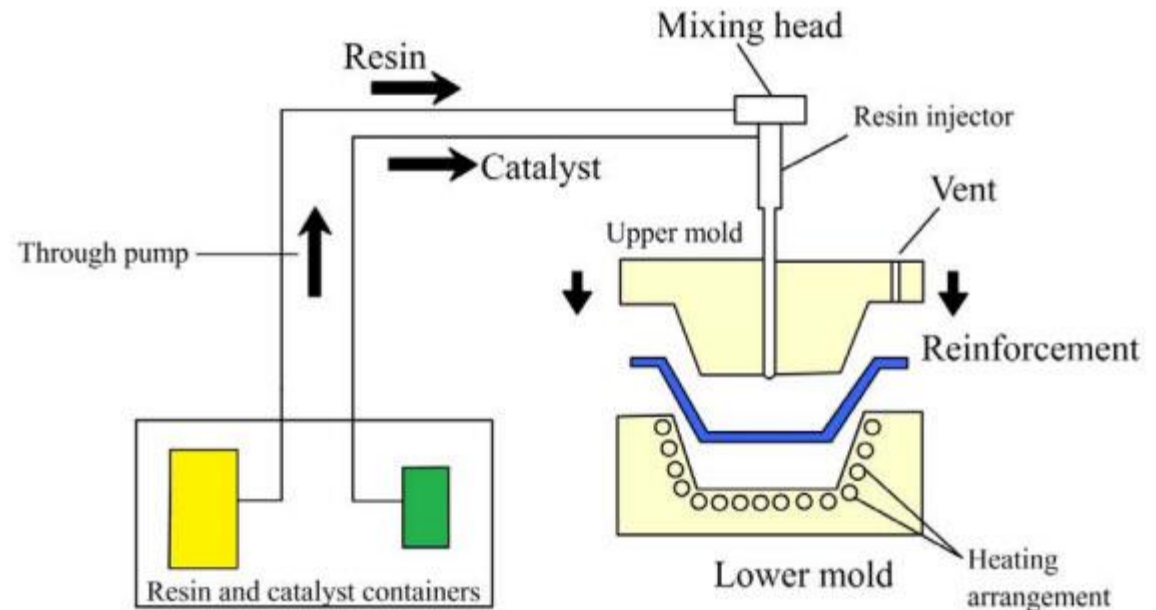
Moulding of **components of revolution** (tubes), allowing homogeneous distribution of resin with good surface conditions, including the internal surface of the tube.

Manufacturing processes for thermoset matrix composites

Resin transfer moulding (RTM)

- Mould and counter-mould
- Viscosity matrix: ≈ 200 cP
- Highly structural
- Injection time: \approx minutes
- Pressure: 4 bar

Centipoise (cP)	Similar to
1	Water
50	Polyester resin
250	Epoxy resin
500	Auto oil
2500	Pancake syrup

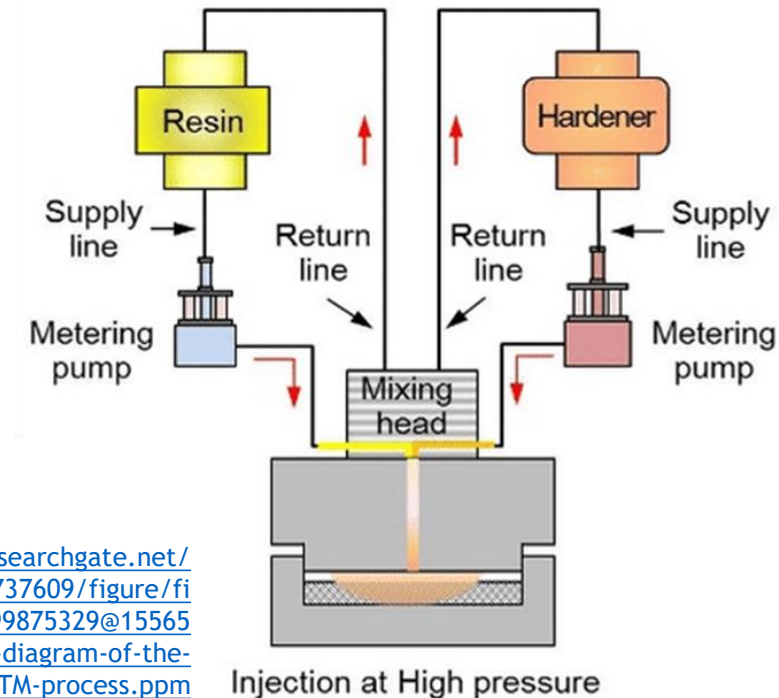


Manufacturing processes for thermoset matrix composites

High-pressure RTM (HP-RTM)

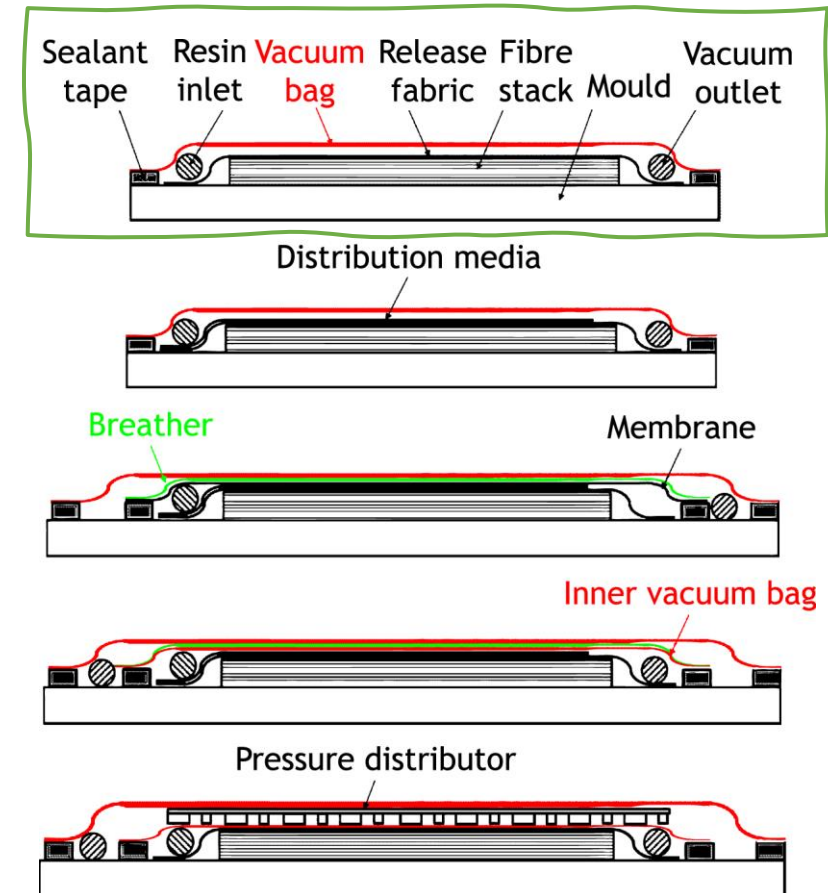
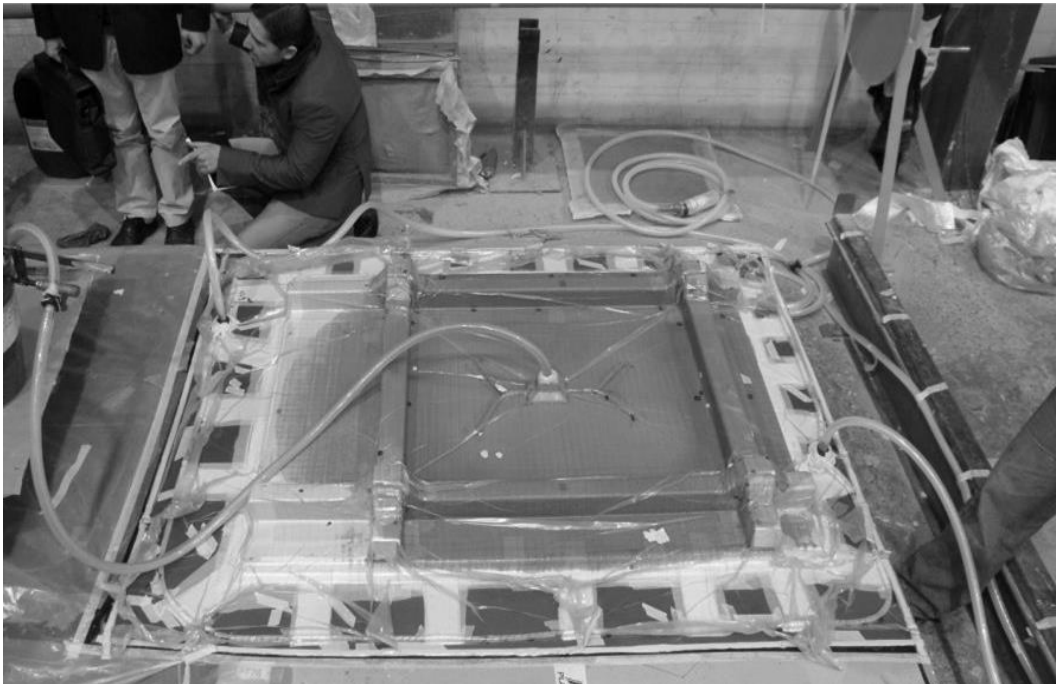
- Mould and counter-mould
- Viscosity matrix: ≈ 40 cP
- Highly structural
- Injection time: \approx seconds
- Pressure: 120 bar

Centipoise (cP)	Similar to
1	Water
50	Polyester resin
250	Epoxy resin
500	Auto oil
2500	Pancake syrup



Manufacturing processes for thermoset matrix composites

Vacuum assisted RTM (VARTM)

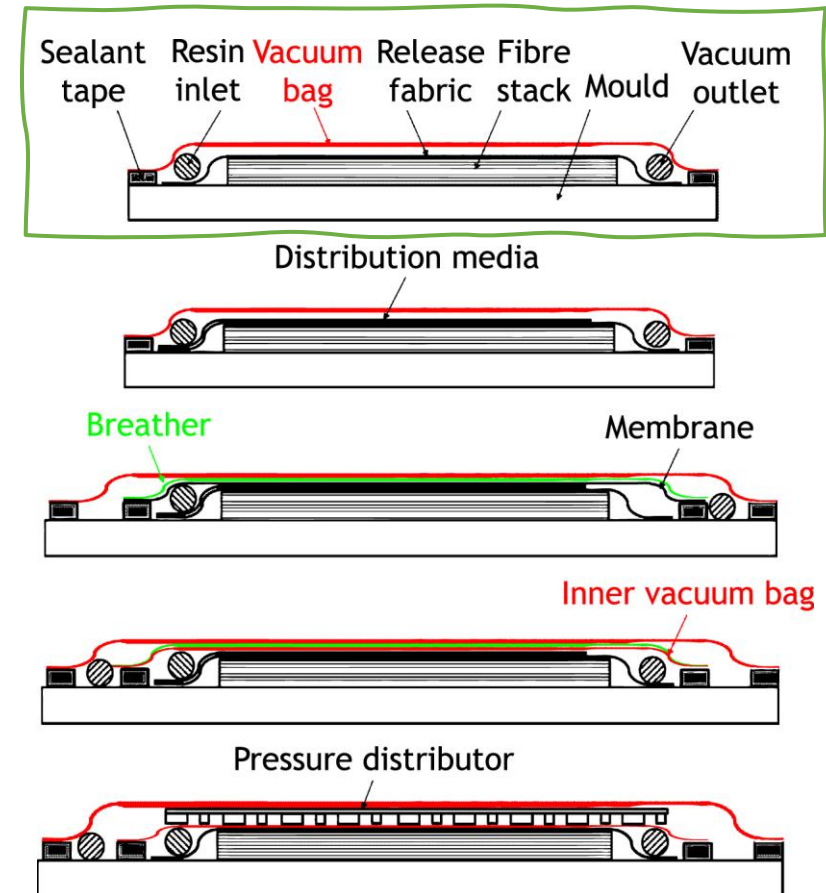


<https://doi.org/10.1016/j.compositesa.2019.105528>

Manufacturing processes for thermoset matrix composites

Vacuum assisted RTM (VARTM)

- Also vacuum resin infusion, it is resin infusion in its most simplified form, first pioneered in the 1950s.
- Fibre impregnation and curing are carried out by the vacuum pressure.
- No resin distribution media to aid wet-out.



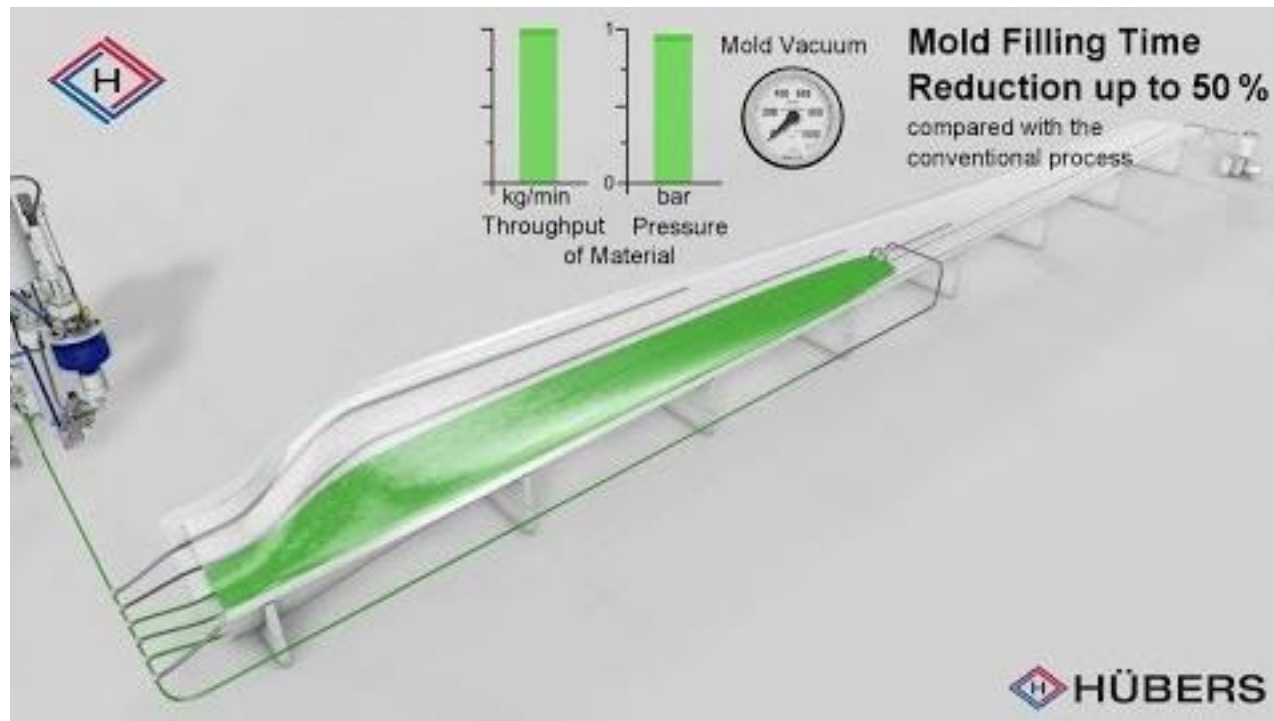
<https://doi.org/10.1016/j.compositesa.2019.105528>

References

Miravete A. Materials, Composites Design Workshop XXI, Stanford University, July 2021.

Manufacturing processes for thermoset matrix composites

Vacuum assisted RTM (VARTM)



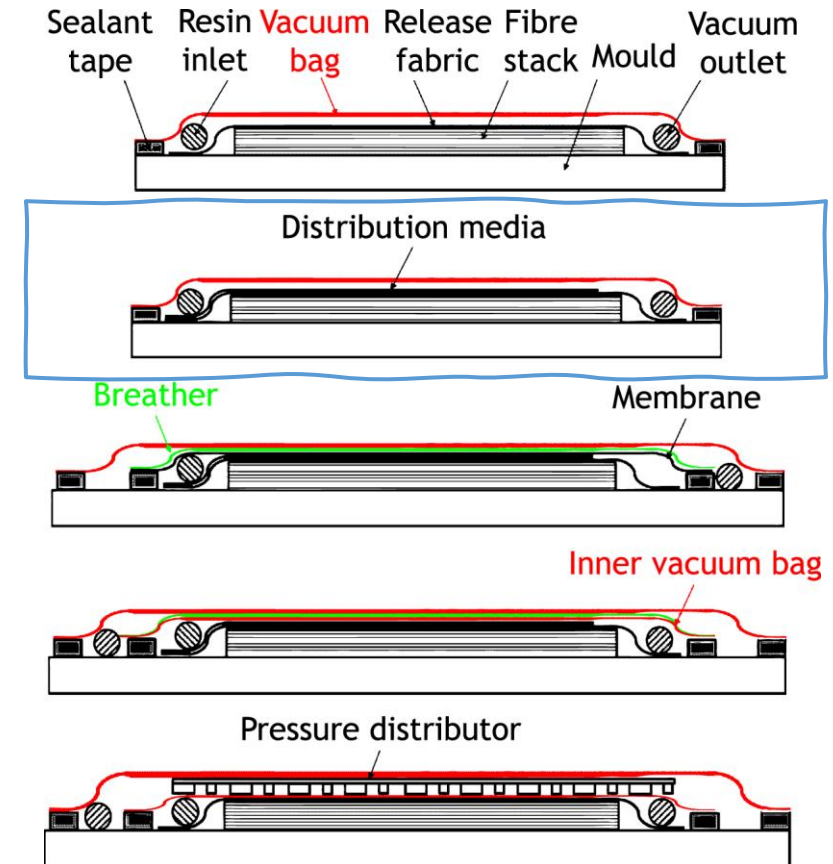
https://www.youtube.com/watch?v=1YXi6zkwEq8&ab_channel=H%C3%9CBERSVerfahrenstechnik

Manufacturing processes for thermoset matrix composites

Other variants of resin infusion

SCRIMP (Seeman's composite resin infusion process) is the most widely used form of resin infusion, first patented by Seemann Composites Inc. in 1990.

- Similar infusion structure to VARTM but introduces a consumable **distribution media** or **flow channels** to aid the flow of resin across the surface of the part and subsequently reduce wet-out time.
- While the distribution media can be positioned below, above or within a reinforcement stack, flow channels are typically included within foam cores used in sandwich structures.



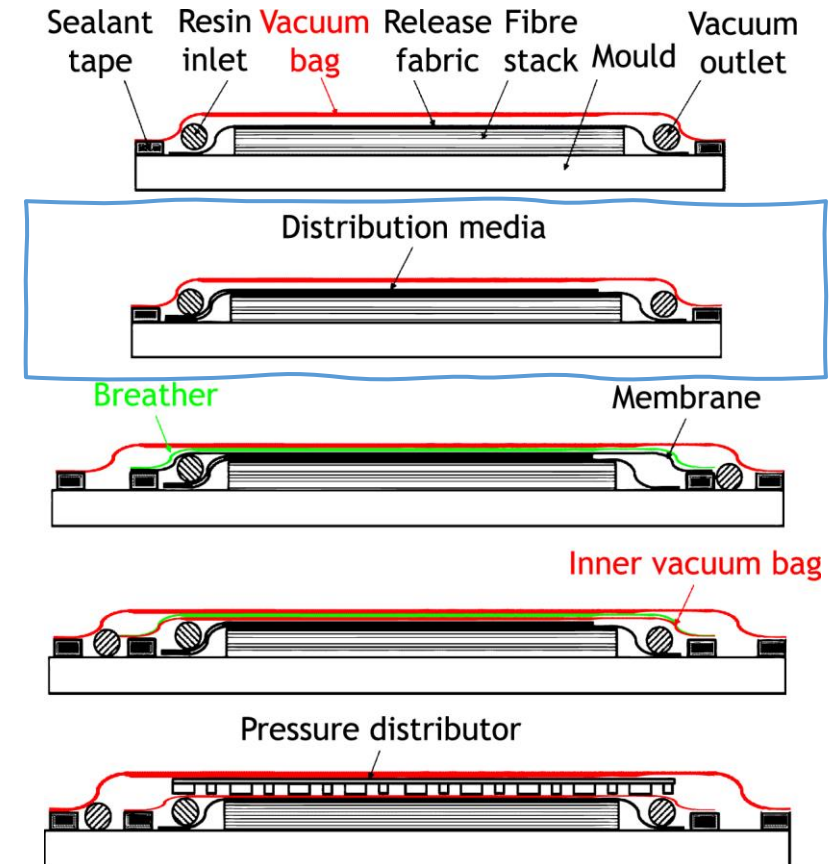
<https://doi.org/10.1016/j.compositesa.2019.105528>

Manufacturing processes for thermoset matrix composites

Other variants of resin infusion

CAPRI (controlled atmospheric pressure resin infusion) is a patented Boeing process.

- Prior to infusion, the fibre layup is cyclically compacted several times (10, 20 or more) by alternating the bag pressure between high levels of vacuum and atmospheric pressure.
- Cyclic compaction increases the amount of fibre nesting in the stack and subsequently decreases the stack thickness and increases the fibre volume fraction that can be achieved at a set vacuum level.
- Reductions in thickness gradients to less than 1% and increases in fibre volume fraction of 5% over SCRIMP have been reported.



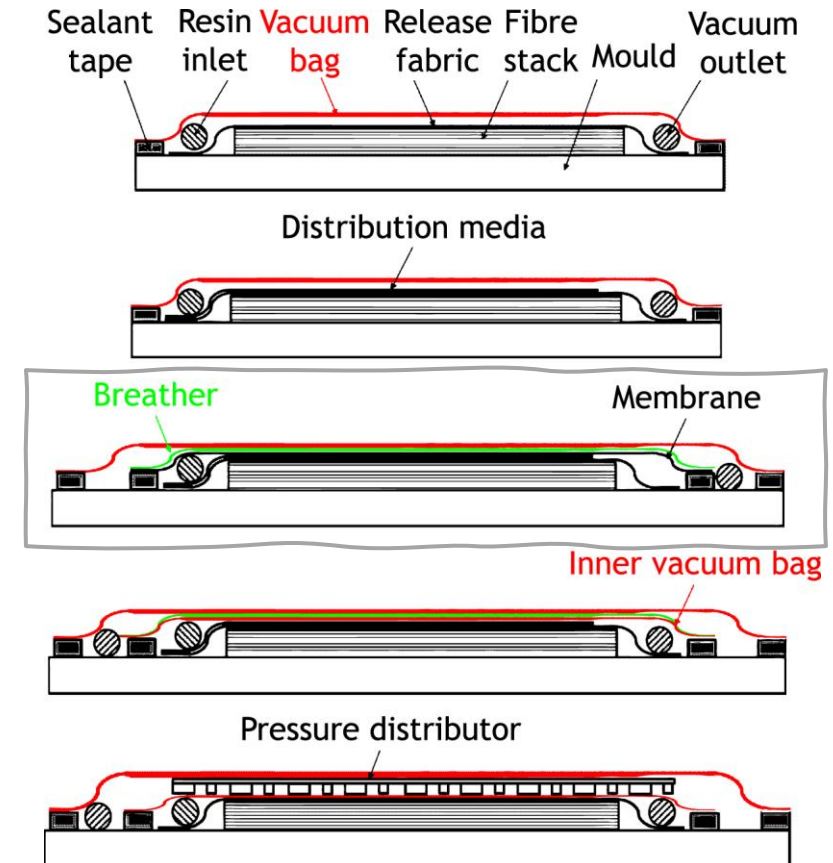
<https://doi.org/10.1016/j.compositesa.2019.105528>

Manufacturing processes for thermoset matrix composites

Other variants of resin infusion

VAP (vacuum assisted process) is an infusion method developed by Airbus that uses a semi-permeable membrane to allow degassing of the infused laminate in the through-thickness direction and reduce the chance of resin lockout and, consequently, dry spots.

- On top of the distribution layer a semi-permeable membrane is placed which is used to divide the infusion setup into two chambers.
- The semi-permeable membrane is sealed over the laminate and resin inlet, with the vacuum outlet being external to this.



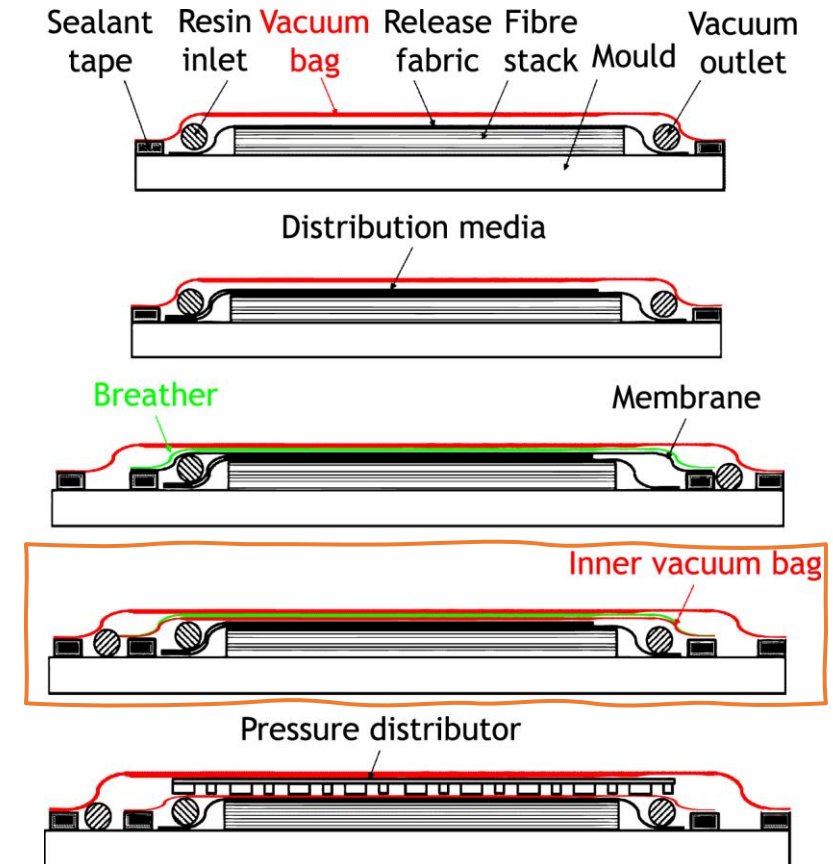
<https://doi.org/10.1016/j.compositesa.2019.105528>

Manufacturing processes for thermoset matrix composites

Other variants of resin infusion

DBVI (double bag vacuum infusion), another Boeing patented process, utilises two vacuum bags to increase vacuum integrity and reduce laminate relaxation.

- The second vacuum bag contains a single vacuum outlet.
- This outer chamber reduces the likelihood of leaks affecting part quality and adds rigidity to the chamber structure to minimise laminate relaxation during infusion.



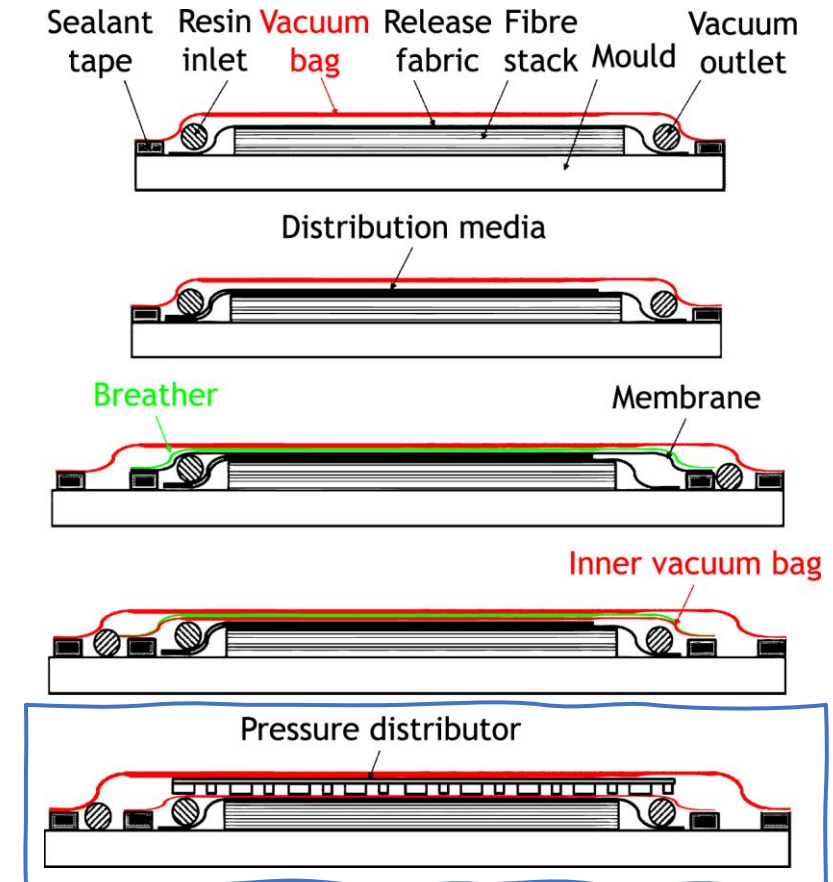
<https://doi.org/10.1016/j.compositesa.2019.105528>

Manufacturing processes for thermoset matrix composites

Other variants of resin infusion

PI (pulsed infusion) is a recently developed method of infusion that utilises a reusable silicon pressure distributor as a resin distribution medium, in conjunction with pressure pulsation to increase laminate mechanical properties and reduce consumable costs.

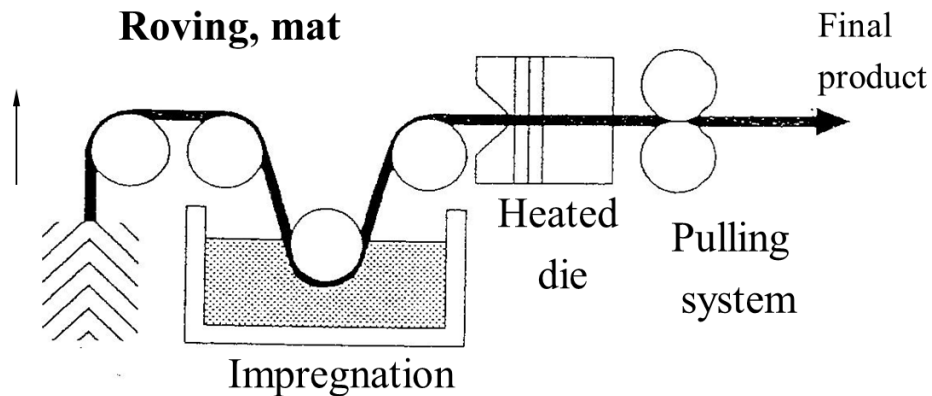
- The method utilises two bags.
- On top of the inner bag, a specially designed silicon pressure mat is placed, with a second vacuum bag covering this entire setup.



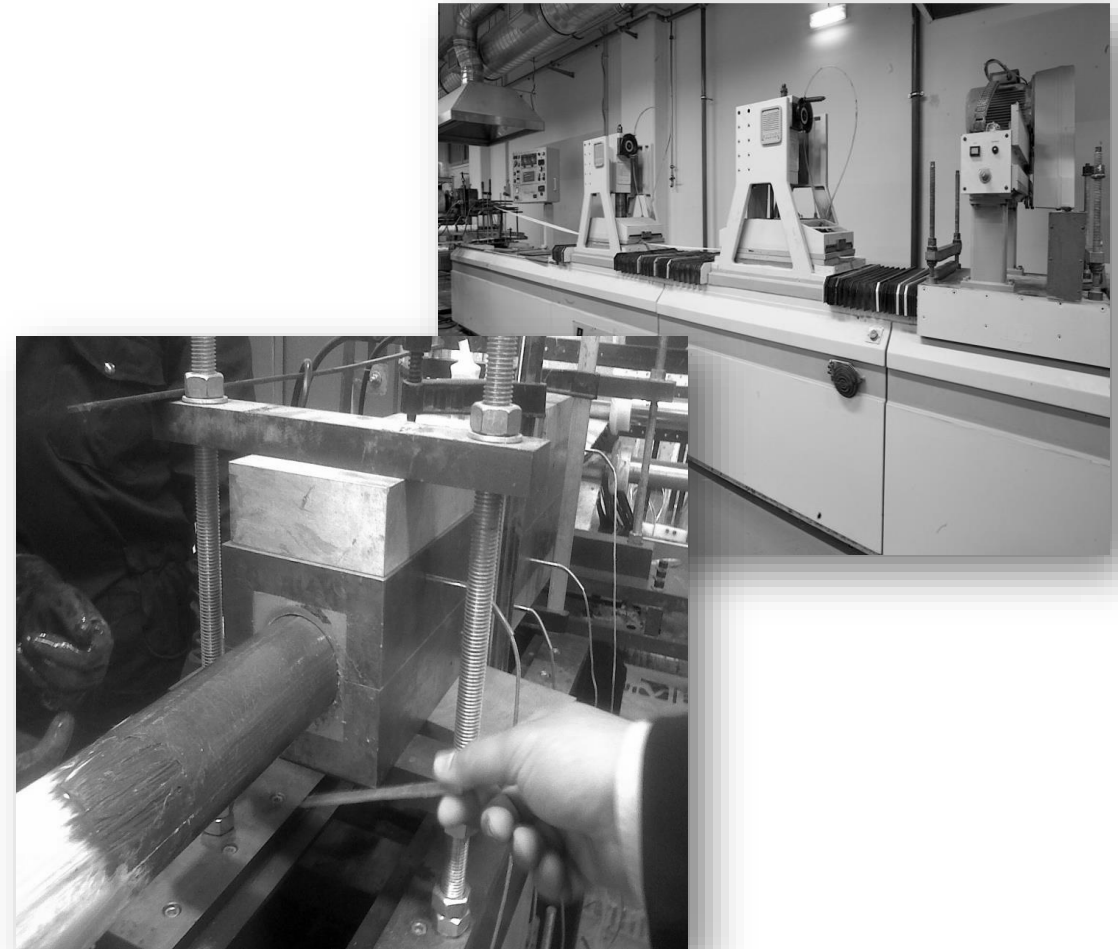
<https://doi.org/10.1016/j.compositesa.2019.105528>

Manufacturing processes for thermoset matrix composites

Pultrusion

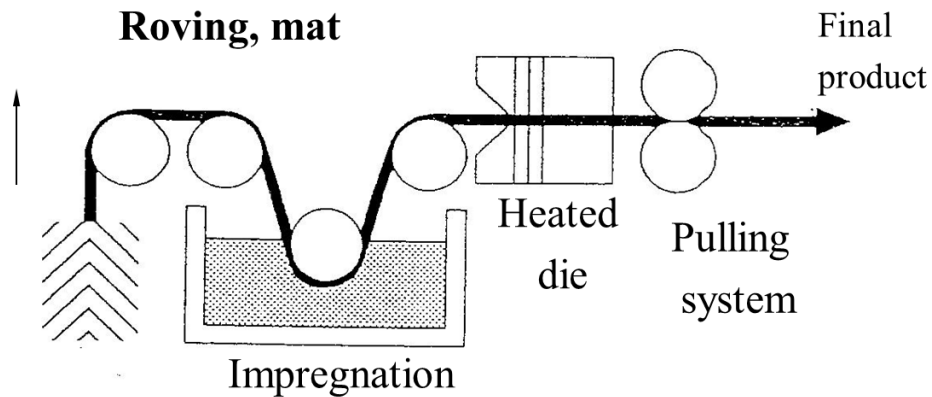


- Typical speeds are 0.6 - 1.2 m/min
- Mould die lengths are 0.6 - 1.5 m
- Fibre volume fractions may reach 65%
- Voids usually range between 1 to 5%
- Pulling forces range between 45 - 90 kN
- Viscosities between 500 - 2,000 cP

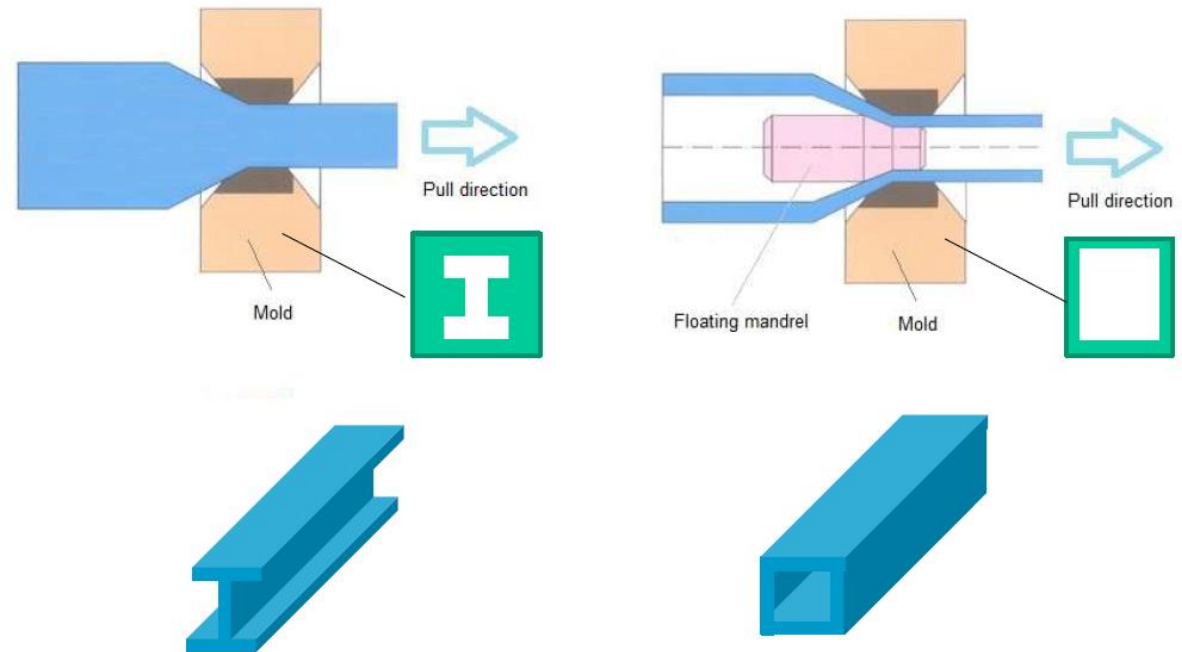


Manufacturing processes for thermoset matrix composites

Pultrusion

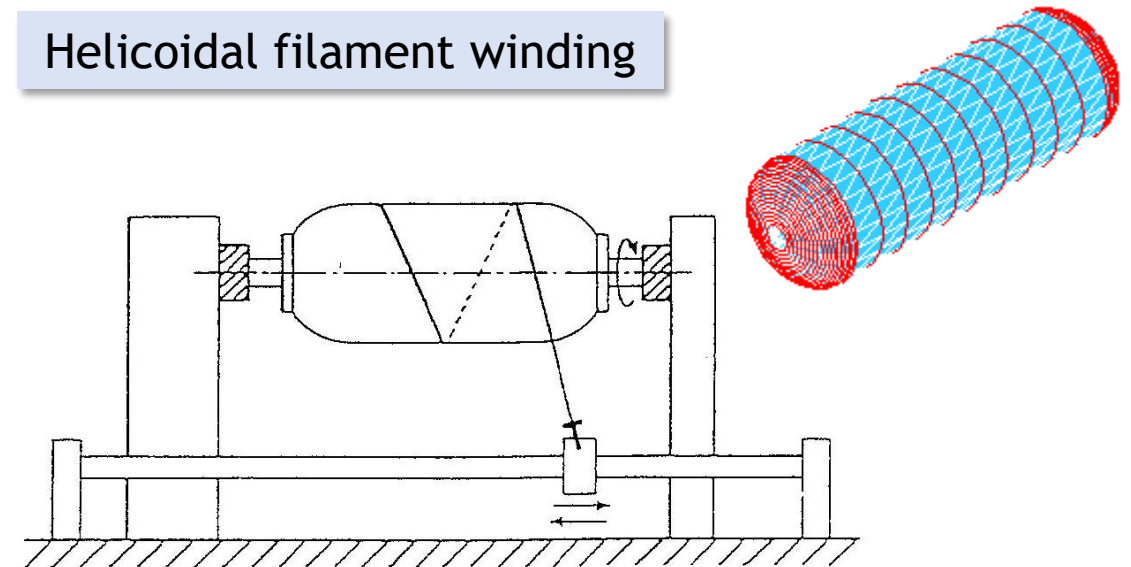
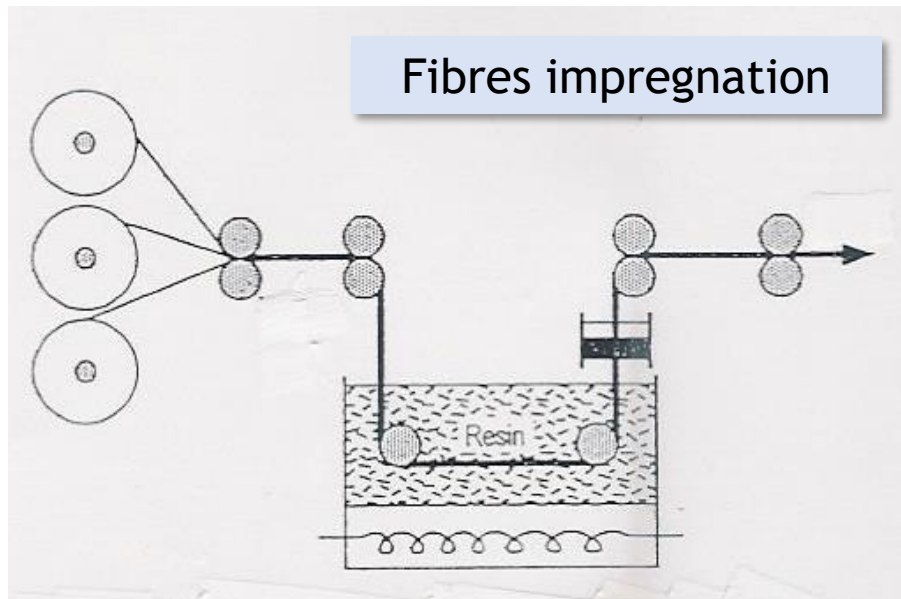


Floating mandrels can be used to make hollow parts



Manufacturing processes for thermoset matrix composites

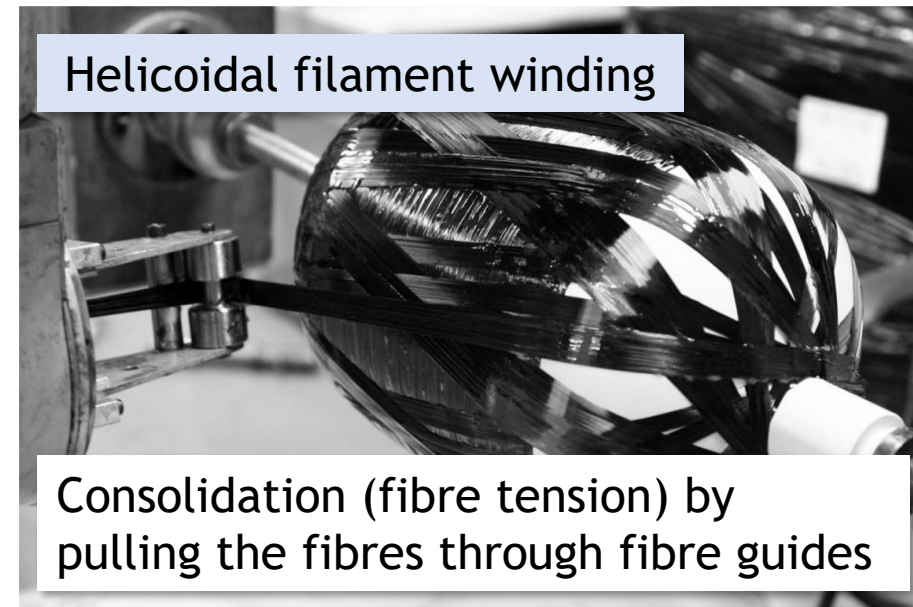
Filament winding



Manufacturing processes for thermoset matrix composites

Filament winding

- High rate process
- Lay-down rates of 136 - 1,360 kg/hr for glass fibre pipes and 5 - 90 kg/hr for carbon fibre aerospace components
- Diameters range between 0.3 - 6 m
- Suitable viscosities range between 350 - 1,000 cP
- Fibres can reach up to 70% volume fraction due to the low viscosity resins

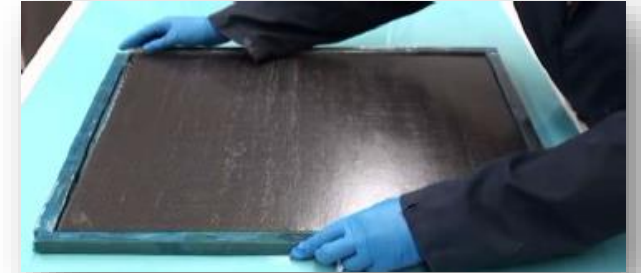


Manufacturing processes for thermoset matrix composites

Vacuum bagging and autoclave curing

Prepreg processing

- In order to get the highest properties, ply thickness and resin distribution are controlled by using a pre-impregnated material (the fibre is already pre-impregnated with the resin - *prepreg* concept).
- The material is placed over a **tool (mould)**, to form the geometric shape of the part.



- Hand lay-up (1 kg/hr)

- Suitable for small parts and complex shapes.
- High labour costs.
- Unidirectional, plain weave, and harness satin weave architectures are used.
- Combinations, such as plain weave and unidirectional, are also utilized.

Manufacturing processes for thermoset matrix composites

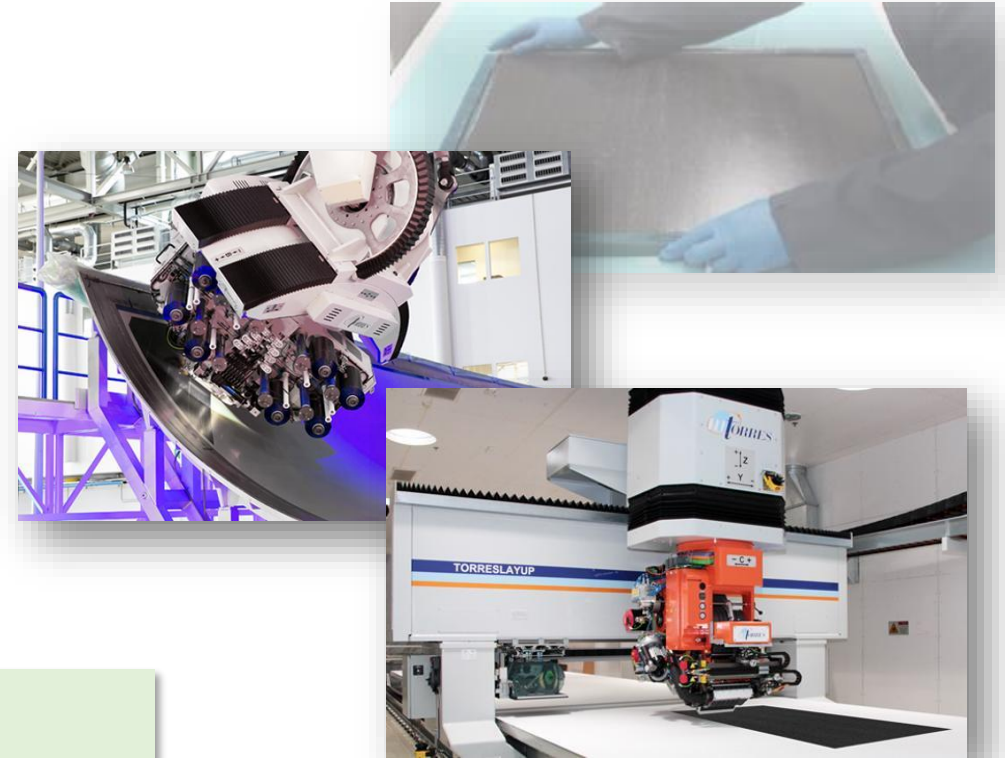
Vacuum bagging and autoclave curing

Prepreg processing

- In order to get the highest properties, ply thickness and resin distribution are controlled by using a pre-impregnated material (the fibre is already pre-impregnated with the resin - *prepreg* concept).
- The material is placed over a **tool (mould)**, to form the geometric shape of the part.

- Hand lay-up (1 kg/hr)

- Automated fibre placement (5 kg/hr)
Tape width from 3.175 mm (1/8") to 12.7mm (1/2")
- Automated tape laying (20 kg/hr)
Tape width up to 300 mm (12")



Manufacturing processes for thermoset matrix composites

Vacuum bagging and autoclave curing

Automated fibre placement (AFP) is an automated process of heating and compacting narrow unidirectional prepreg tapes, suitable for medium to large complex curvature monolithic parts.



https://www.youtube.com/watch?v=_GDqxnahwbk&ab_channel=Aviation%3ABenefitsBeyondBorders



https://www.youtube.com/watch?v=tmmrkswDHP0&ab_channel=MDxmedia

Manufacturing processes for thermoset matrix composites

Vacuum bagging and autoclave curing

Automated tape laying (ATL) allows the rapid deposition of composite *prepreg* tapes to large, low to medium curvature monolithic parts.



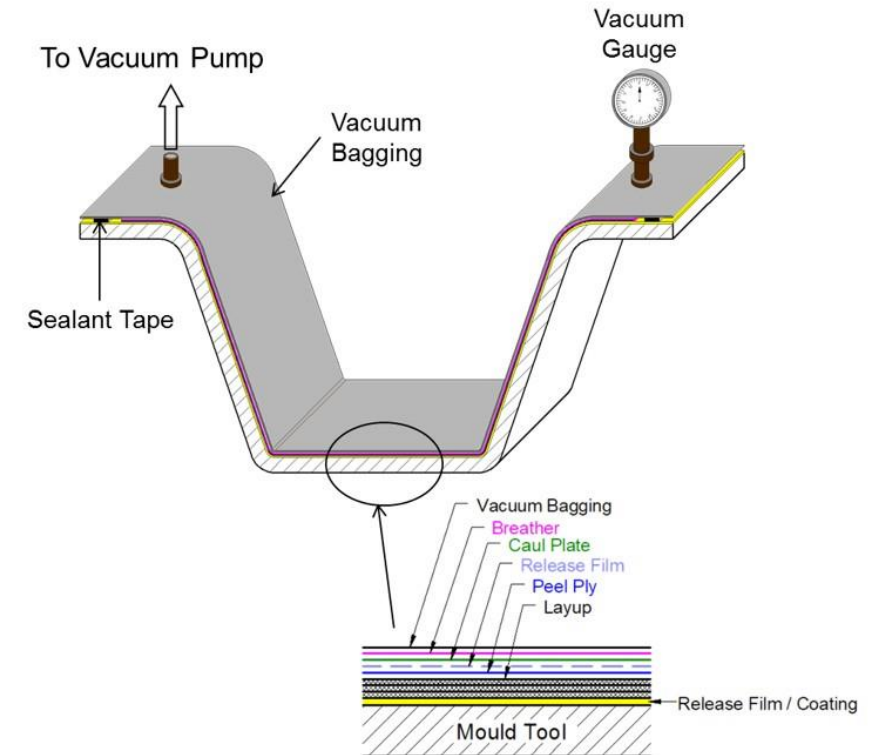
<https://www.youtube.com/watch?v=eDVSLx4S954>

Manufacturing processes for thermoset matrix composites

Vacuum bagging and autoclave curing

Prepreg processing

- In order to get the highest properties, ply thickness and resin distribution are controlled by using a pre-impregnated material (the fibre is already pre-impregnated with the resin - *prepreg* concept).
- The material is placed over a **tool (mould)**, to form the geometric shape of the part.
- The assembly is **vacuum bagged** before transferred to the autoclave (or oven) for curing

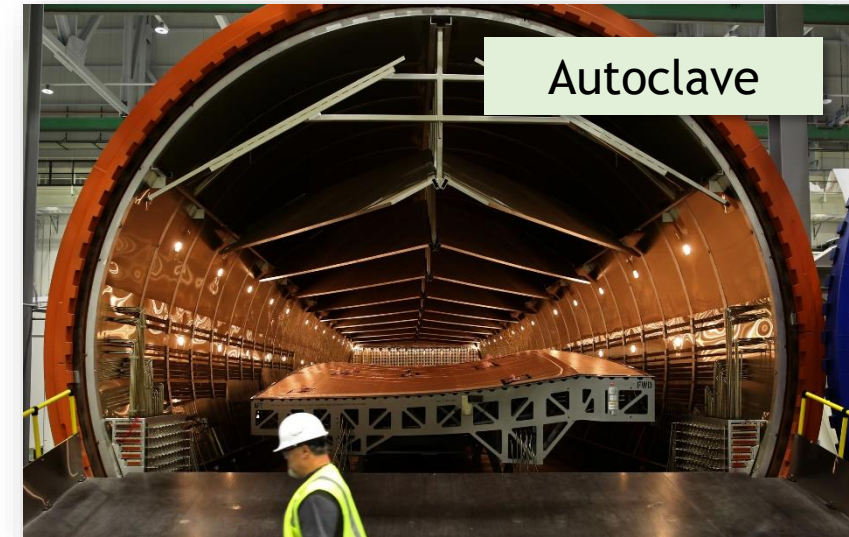


Manufacturing processes for thermoset matrix composites

Vacuum bagging and autoclave curing

Prepreg processing

- To optimise performance, void content should be minimised and therefore, both **temperature** and **pressure** are applied during curing (autoclave).



Manufacturing processes for thermoset matrix composites

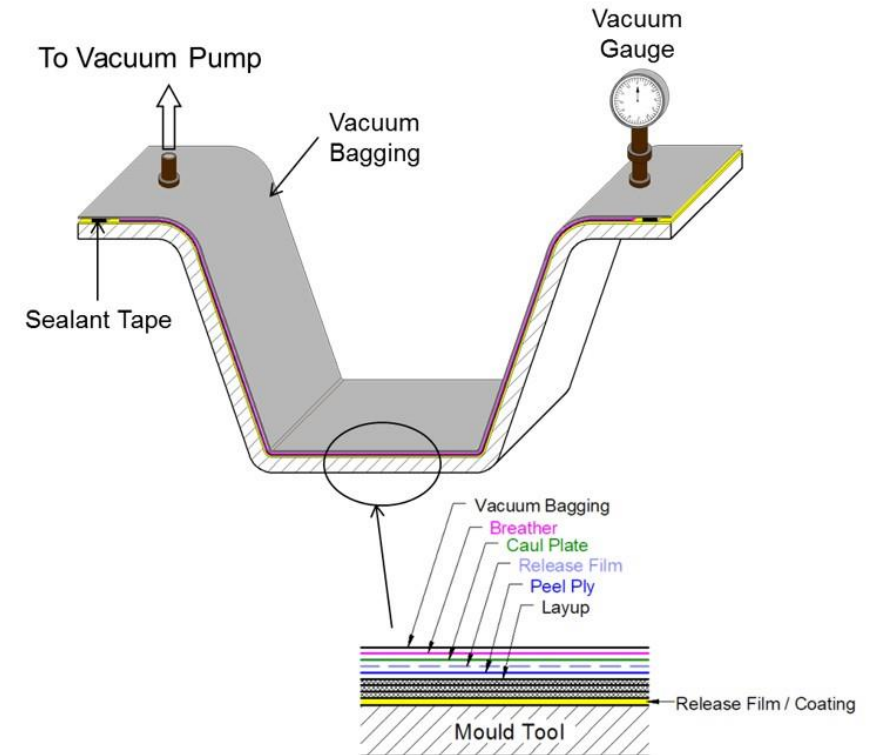
Vacuum bagging and autoclave curing

Fast curing *prepregs*

Curing cycles below 7 min at 120°C and pressures over 5 bar.

Alternative cure cycles can be used.

An oven (only temperature) may also be used - *out-of-autoclave prepregs* - currently still restricted to non-aerospace applications.



Processing of thermoplastic-based composites

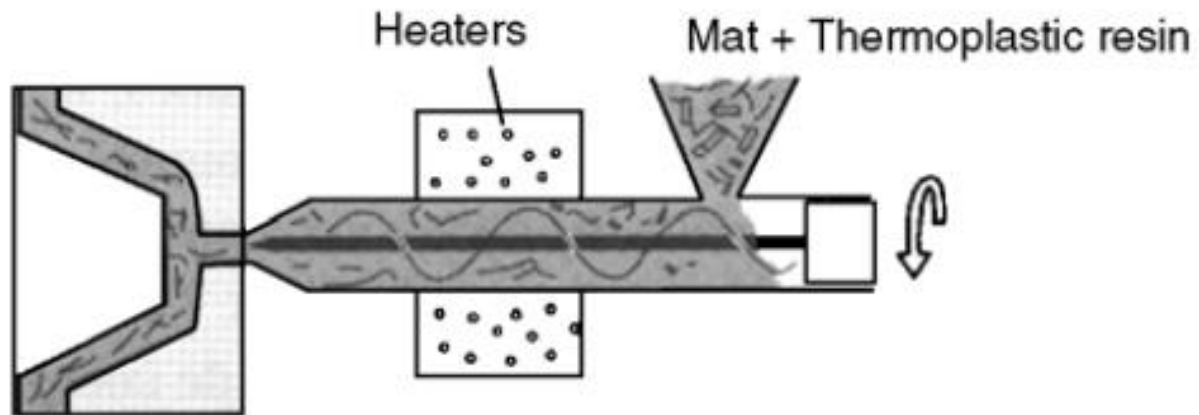
Relevant aspect of thermoplastic composite manufacturing

- Curing is not necessary
- Residual stresses are related with the basic material properties and processing temperatures - usually higher for thermoplastics
- Reduced tendency for delamination
- Fibre movement during “thermoforming” and welding
- Increased tendency for resin rich areas
- Variation in the crystalline morphology due to the difference in the cooling rate within the components leads to variations of the mechanical properties

Processing of thermoplastic-based composites

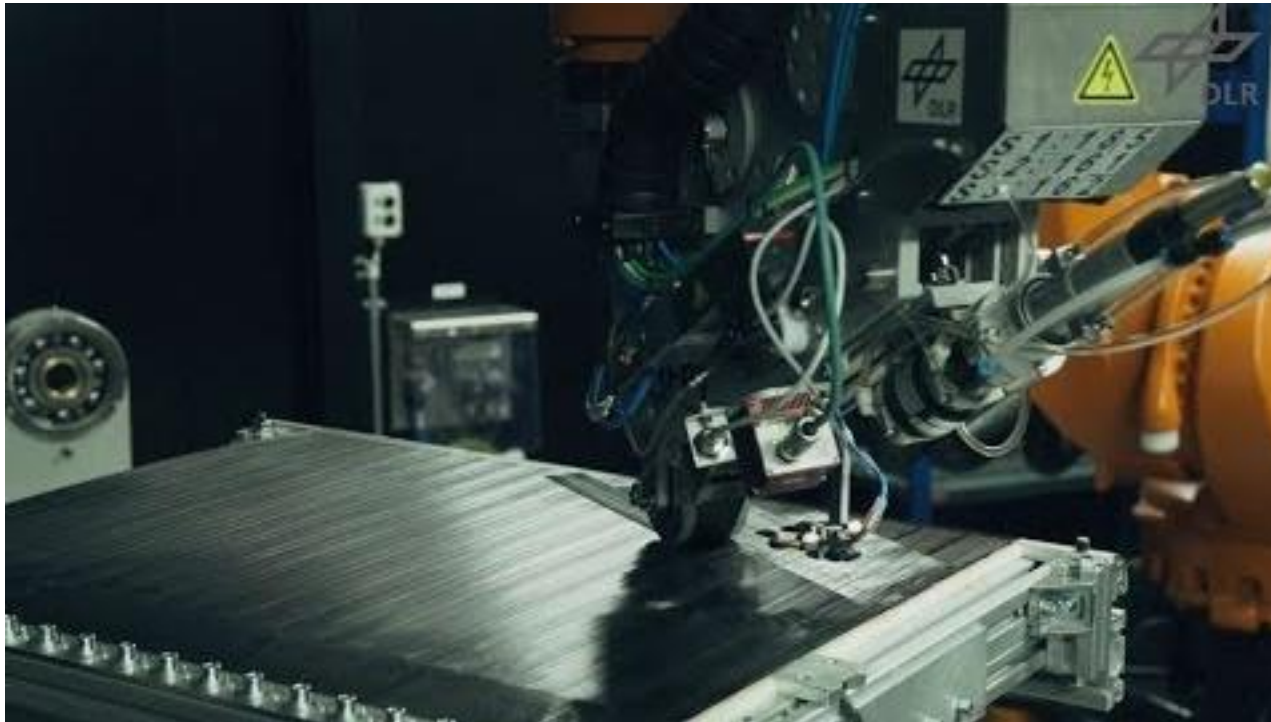
Injection moulding

(premixed compounds)



Processing of thermoplastic-based composites

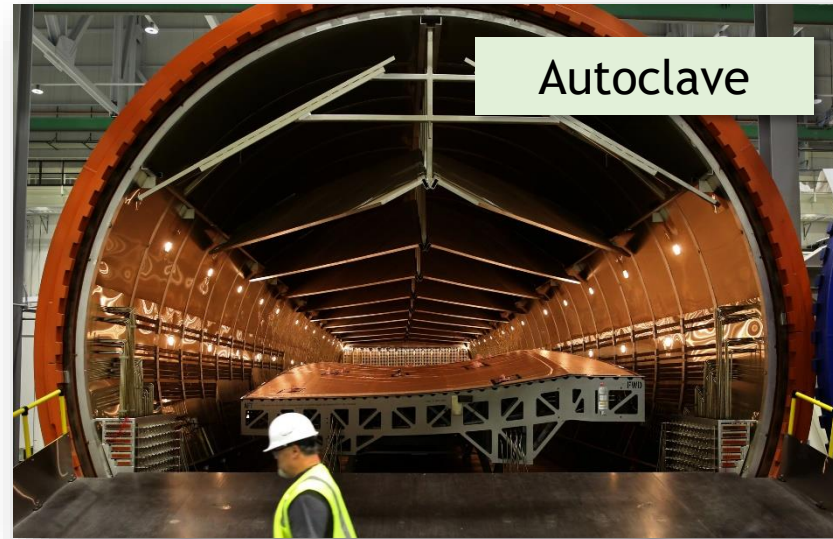
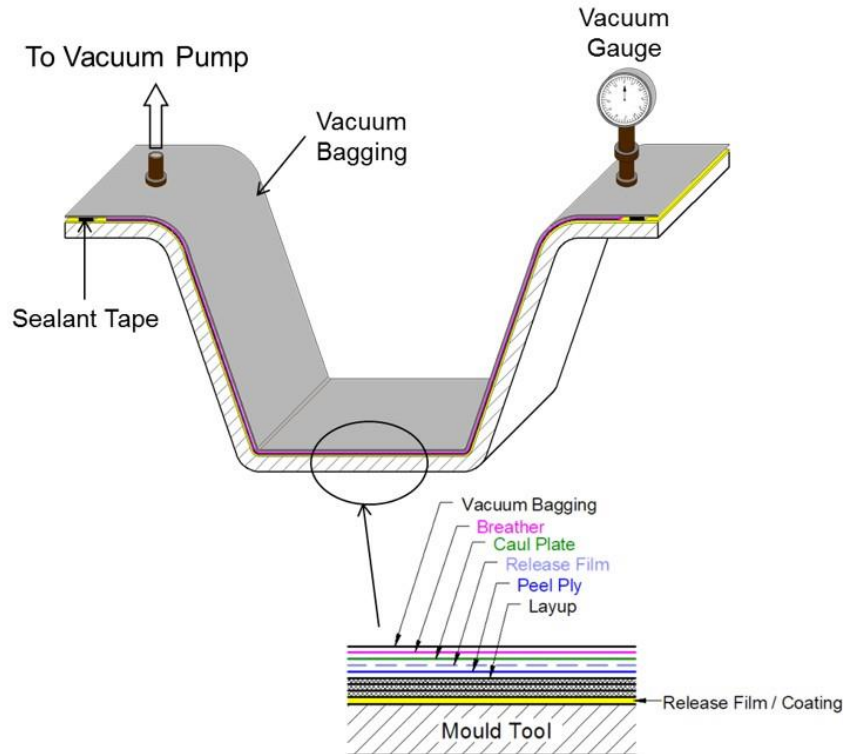
Automated tape laying (ATL) & automated fibre placement (AFP)



<https://www.youtube.com/watch?v=TFxbkFT07Z0>

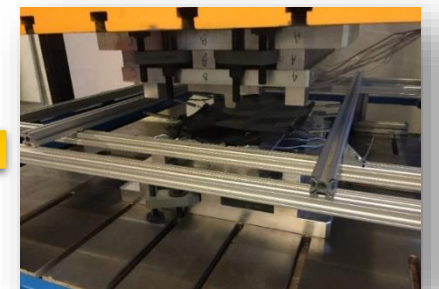
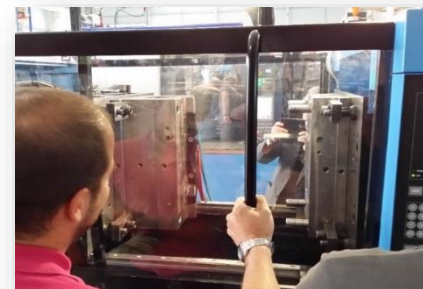
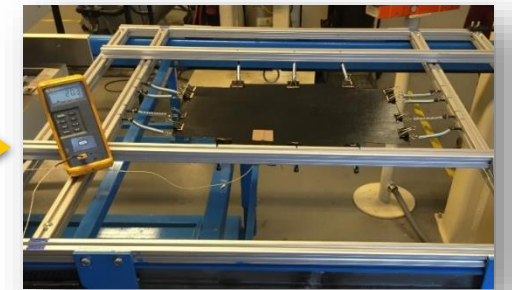
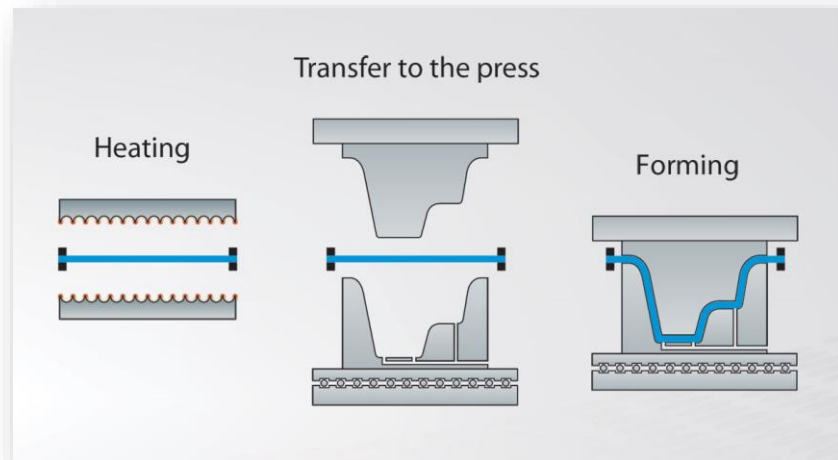
Processing of thermoplastic-based composites

Vacuum bagging and autoclave consolidation



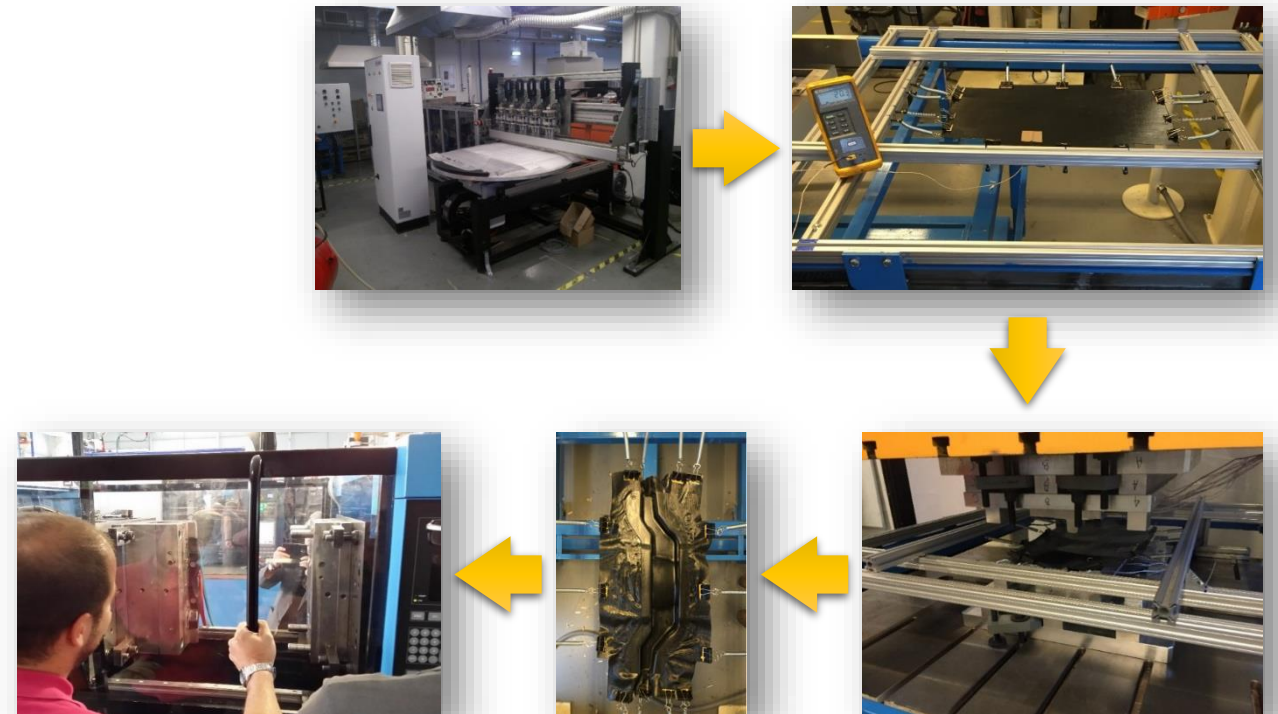
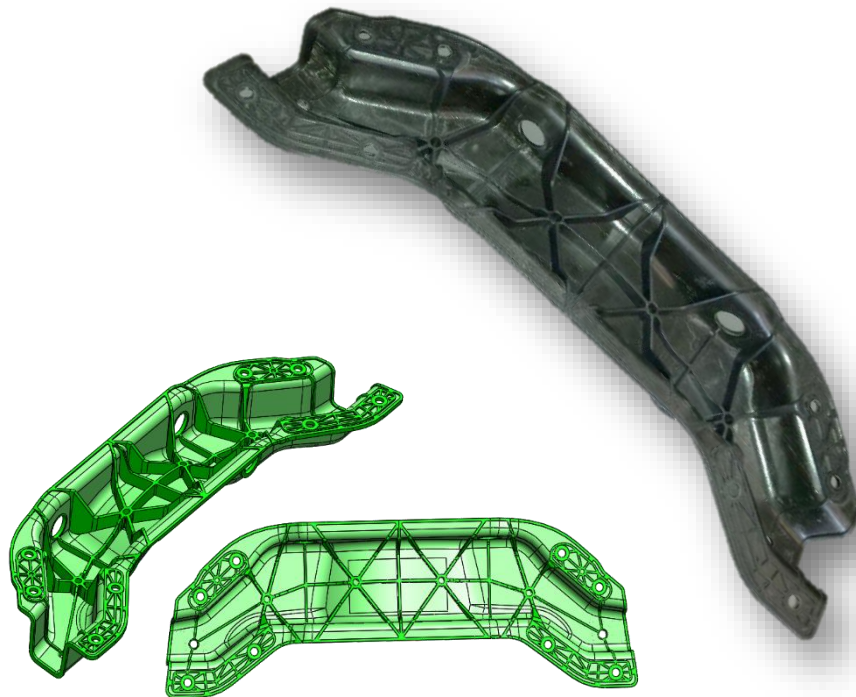
Processing of thermoplastic-based composites

Stamp forming



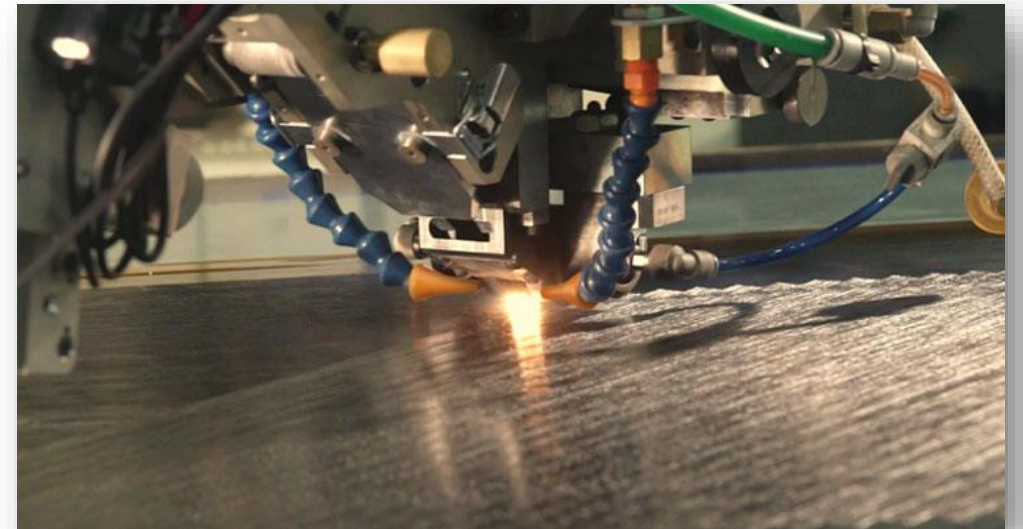
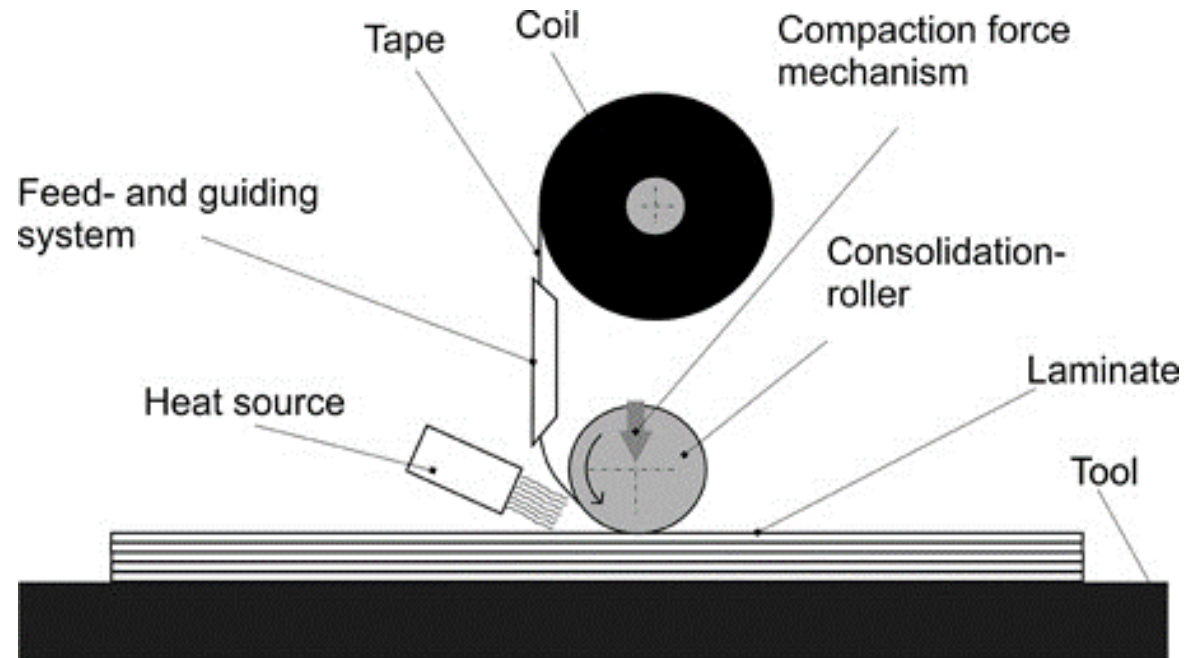
Processing of thermoplastic-based composites

Stamp forming



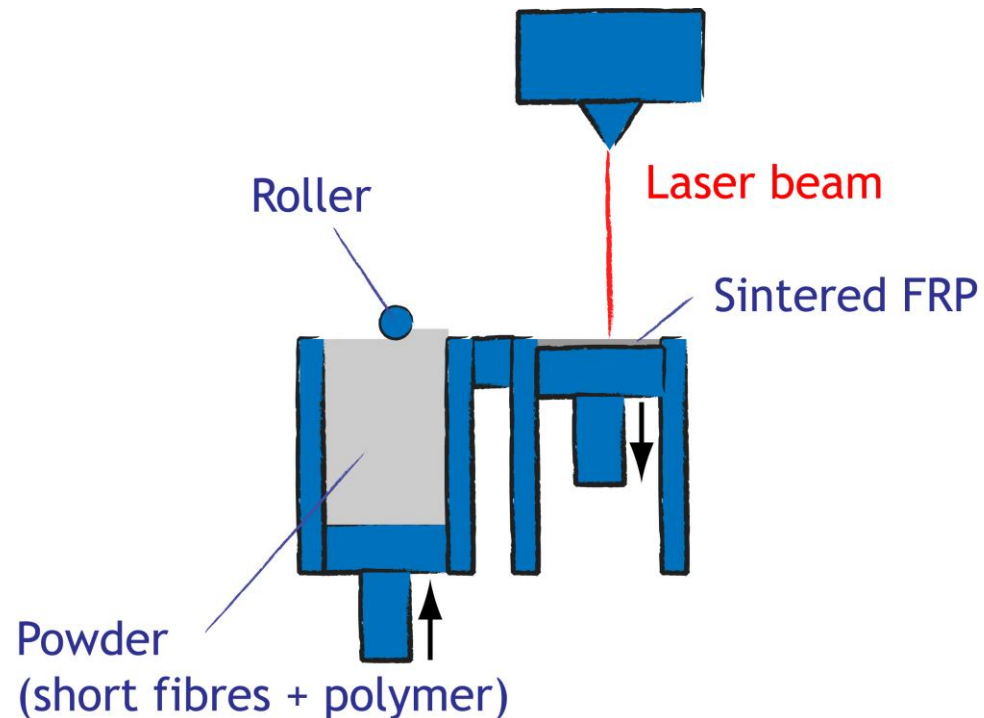
Processing of thermoplastic-based composites

In situ consolidation



Additive manufacturing

Selective Laser Sintering (SLS)



- SLS involves the use of a **high-power laser** to **fuse small particles** of powders into a mass that has a desired three-dimensional shape.
- The laser selectively fuses powdered material by **scanning cross-sections** generated from a 3D digital description of the part on the surface of a powder bed.
- Accelerated ability to take parts **from concept to service**.



Carbon-SLS brake duct bracket

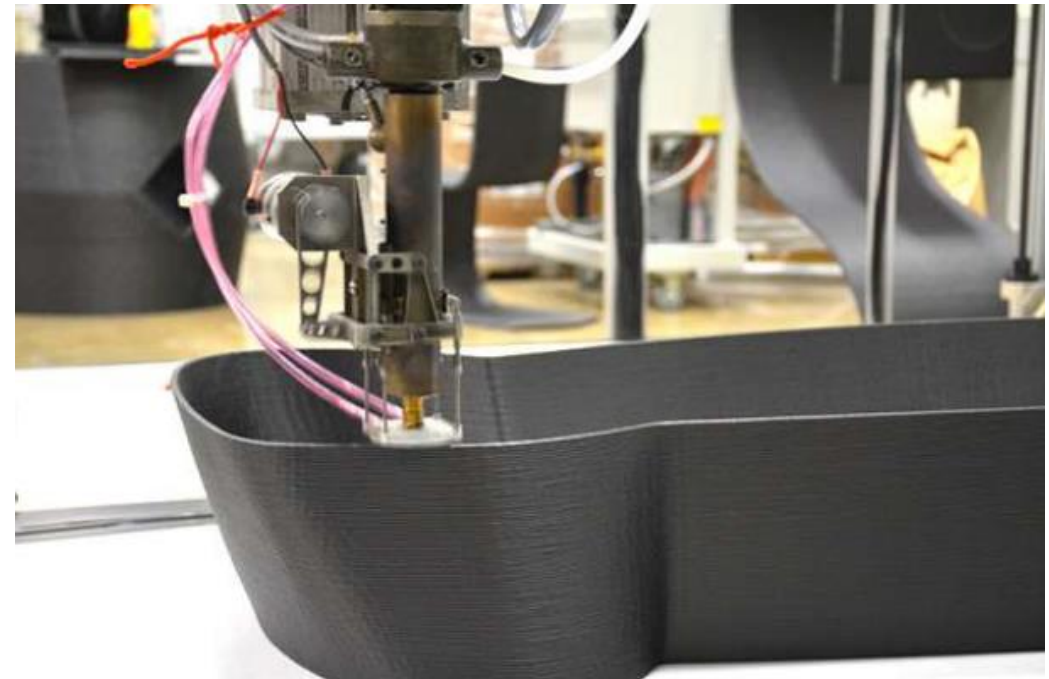


Carbon SLS - duct

Additive manufacturing

Fused Deposition Modelling (FDM)

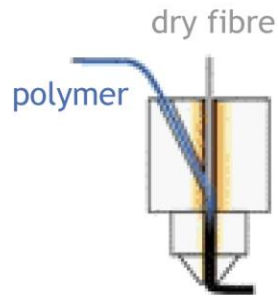
- A thermoplastic filament is unwound from one bobbin and, along with the **chopped carbon fibres**, supplies material to an **extrusion nozzle** which can turn the flow on and off.
- There is typically a worm-drive that pushes the filaments into the nozzle at a controlled rate.
- The nozzle is heated to **melt** the material.
- The thermoplastics are heated above their glass transition temperature and are then deposited along with the carbon fibre by an extrusion head.



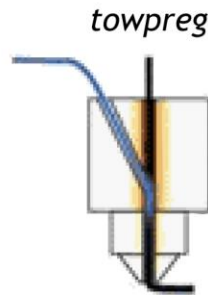
Additive manufacturing

FDM variants

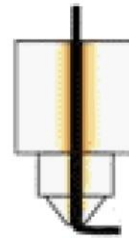
In situ
impregnation



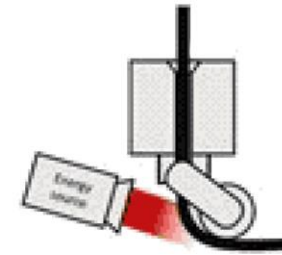
Co-extrusion
with *towpreg*



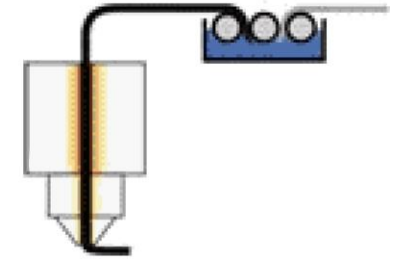
Towpreg
extrusion



In situ
consolidation



In-line
impregnation

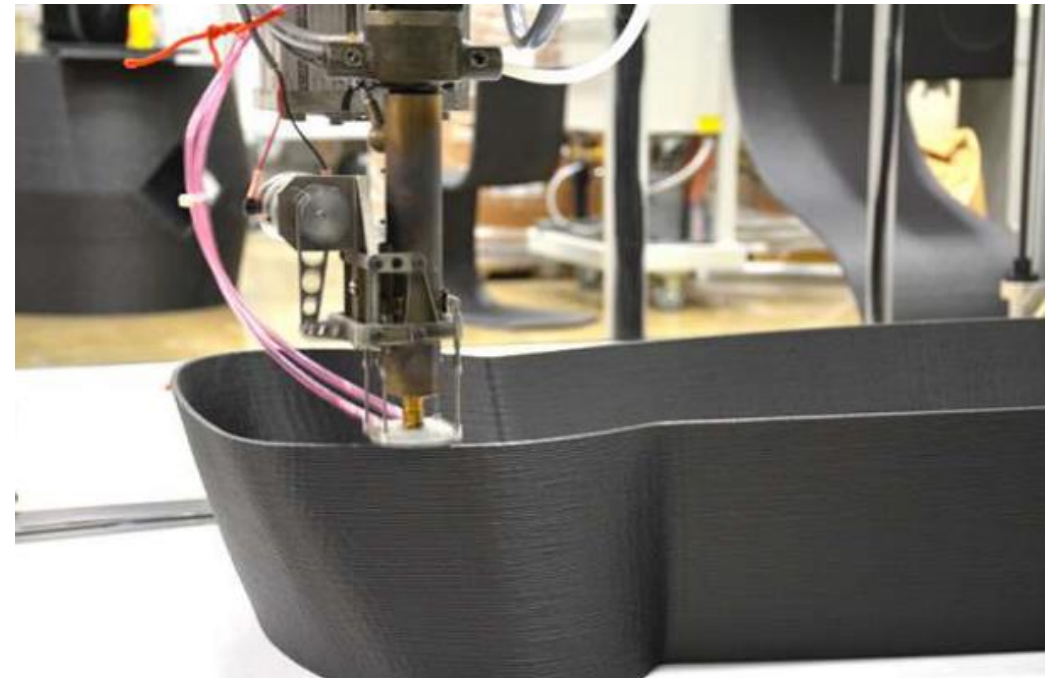
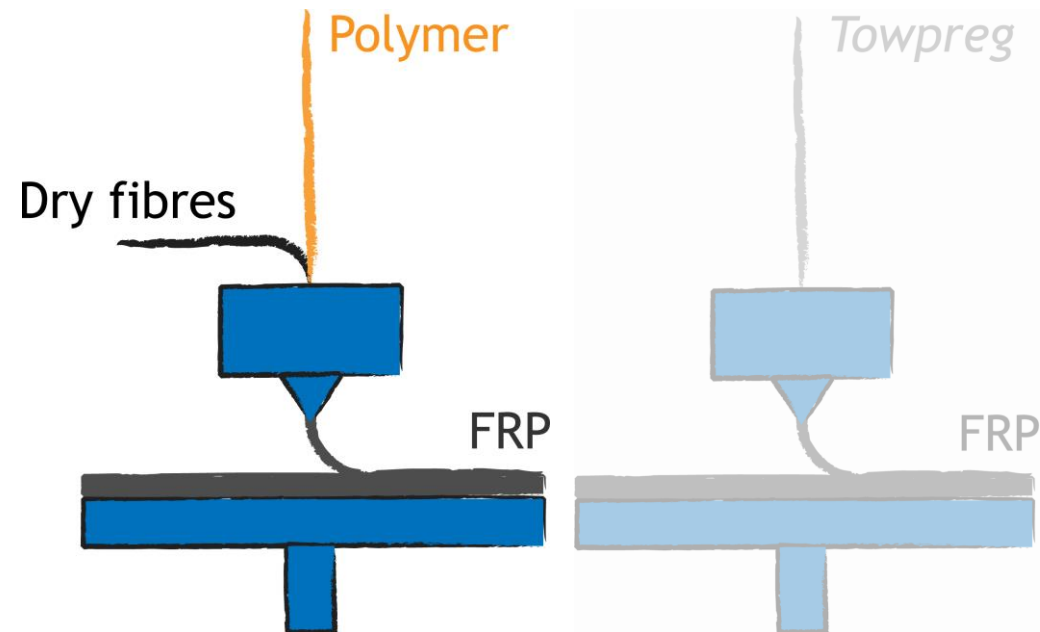


<https://www.compositesworld.com/articles/3d-printing-with-continuous-fiber-a-landscape>

Additive manufacturing

In situ impregnation (FDM variants example)

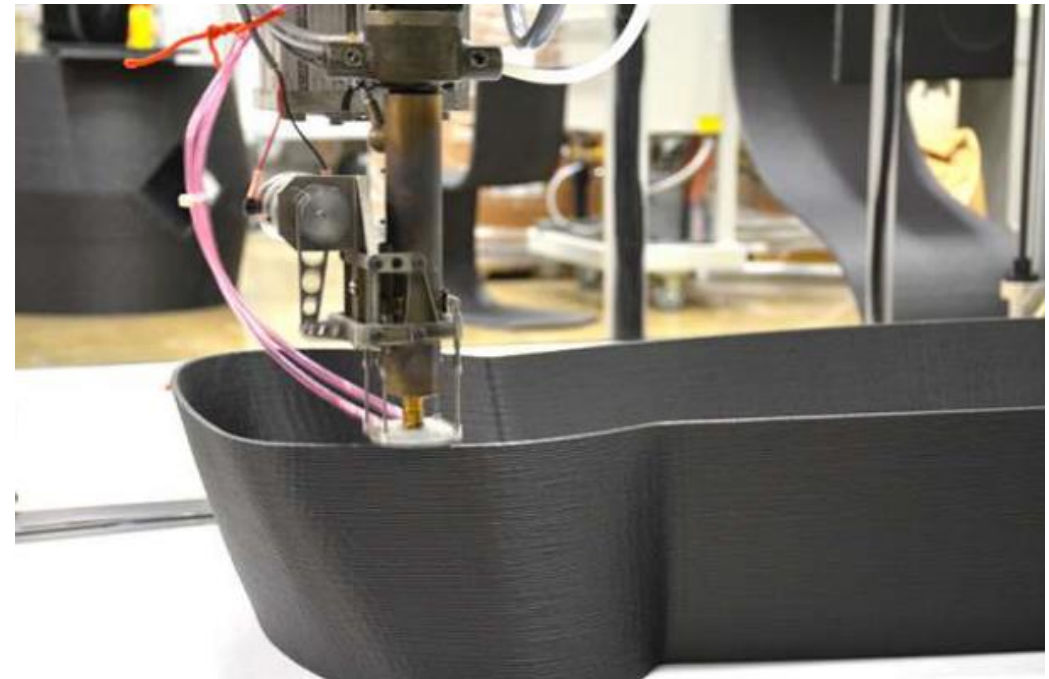
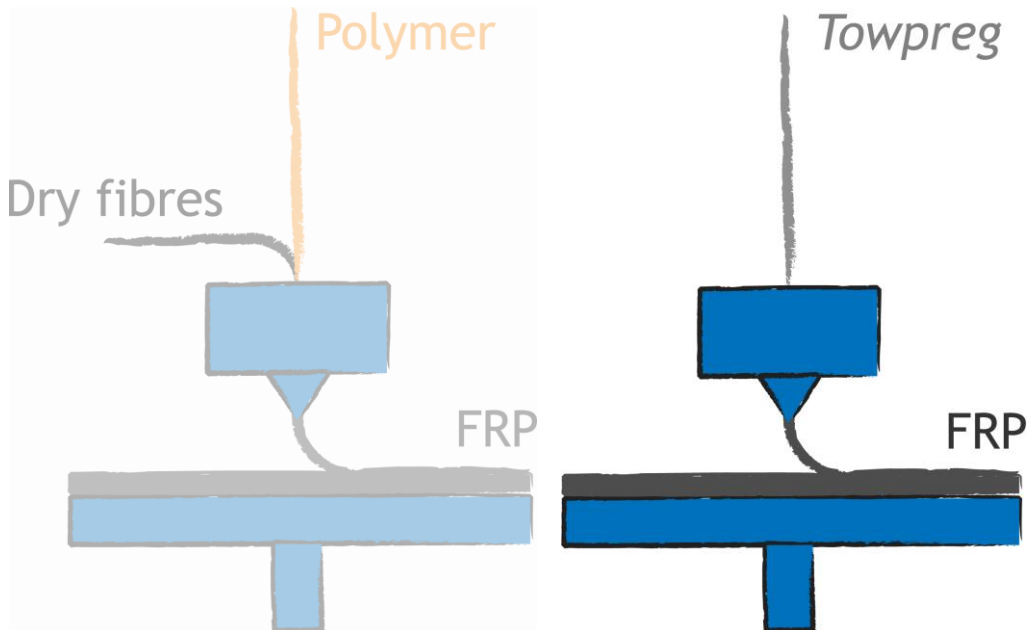
- Carbon fibres and polymer filaments are supplied separately, commingling them in a heated extrusion head.



Additive manufacturing

Towpreg extrusion (FDM variants example)

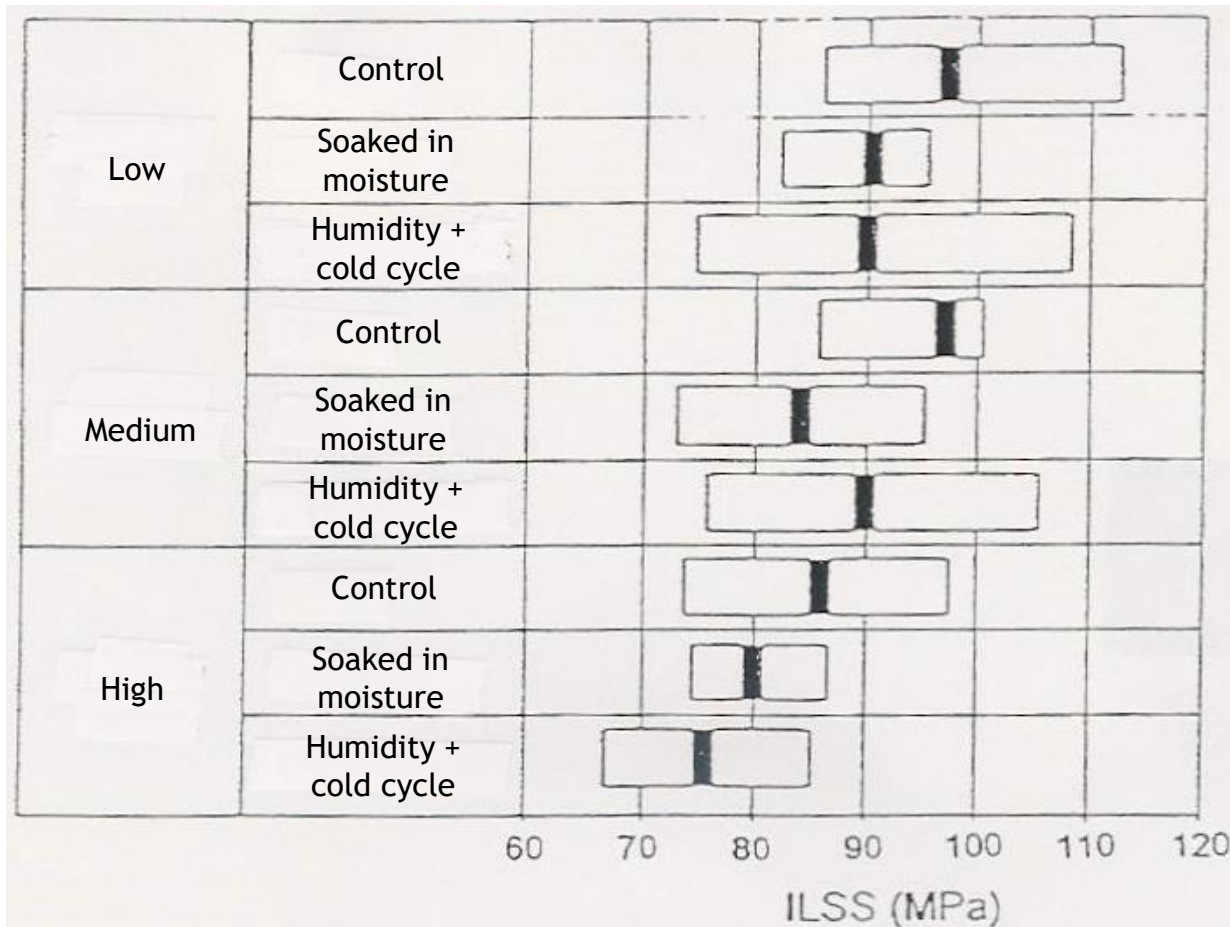
- The *towpreg* input is heated and extruded.



Types of defects in composite systems

- Porosity
- *Prepreg* failures
- Contamination
(by solvent, solids, protector film, ...)
- Fibre misalignment
- Fibre undulation
- Stacking sequence
- Distortion
- Resin degree of cure
- Variations of fibre/resin ratio
- *Prepregs* joints
- Delamination between plies
- Separation between the core and the skin
(sandwich structures)
- Microcracking of the resin
- “Honeycomb” core damaged
(sandwich structures)
- Misplacement of filling compound

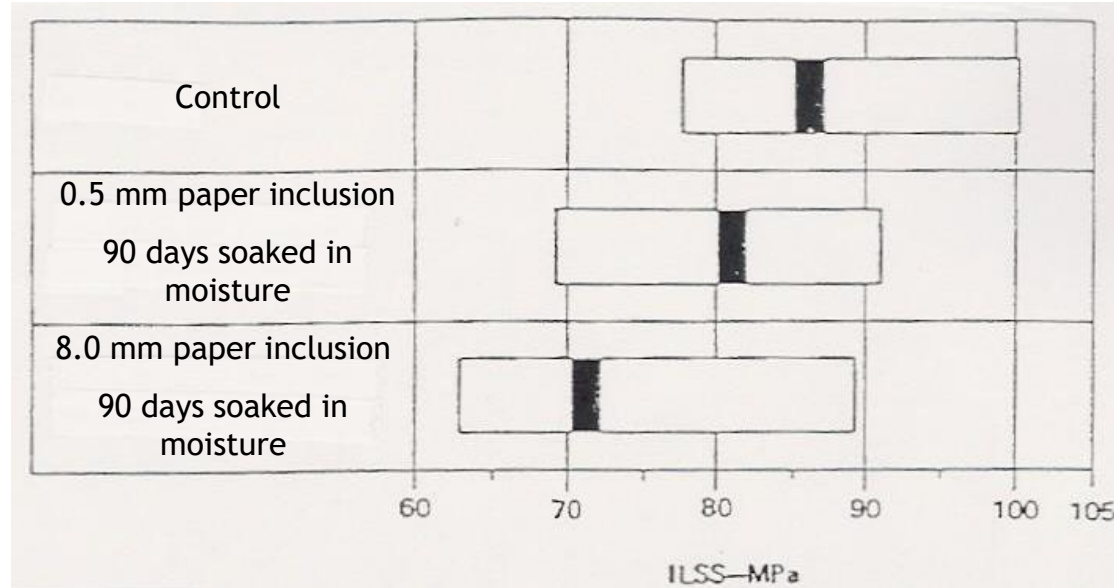
Types of defects in composite systems



Variation of interlaminar shear strength with the void content and preconditioning

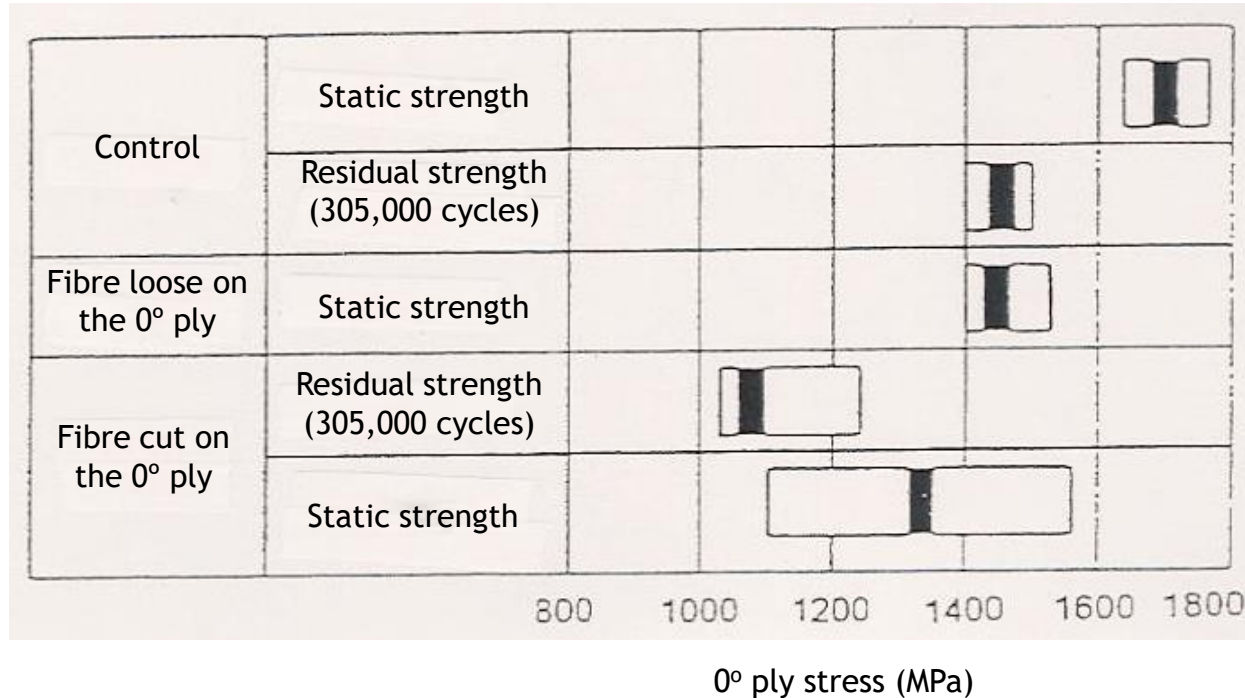
Definition	Void content
Low	< 0.9%
Medium	0.9-3.0%
High	> 3.0%

Types of defects in composite systems



Effect of inclusions, at half thickness, on interlaminar shear strength

Types of defects in composite systems



Effect of defects on the tensile stress of the 0° plies of the skin (0°/45°) of a “sandwich” beam

Questions?

Manufacturing processes

SASCOM

Introductory course on composite materials 2021

Albertino Arteiro & Pedro P. Camanho

INEGI, University of Porto, Porto, Portugal

SASCOM

Introductory course on composite materials 2021

Mechanical behavior and characterization.

Mechanical tests from coupon to sub-component:
Building-block approach. Part 1

References

Marques AT. Composite Systems: Design and Manufacture for Durability, University of Porto, September 2019.

Mechanical behaviour and characterisation

OBJECTIVES

- How to obtain experimentally the **properties** (elastic, strength, toughness, composition, ...) necessary to compare and select materials, and to design structures made therefrom
- Some practical considerations in testing

Mechanical behaviour and characterisation

Different types of tests

- Elastic Properties
- Strength
- Toughness
- Damage tolerance
- Notch sensitivity
- Environmental effects
- ...

Mechanical behaviour and characterisation

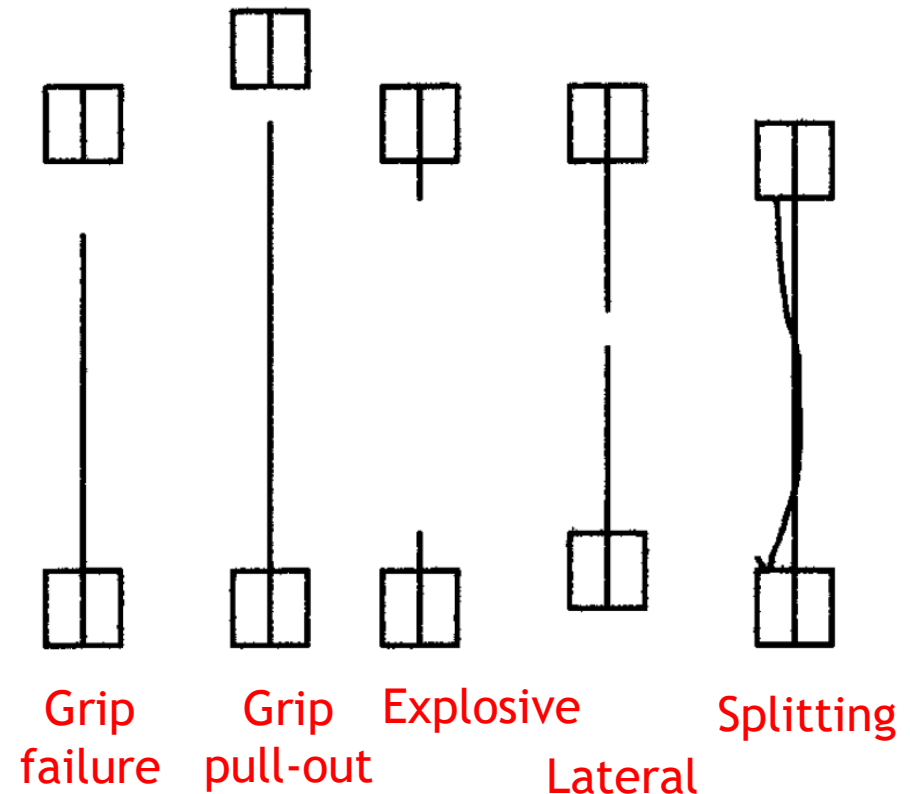
Objectives of different types of tests

- Characterise **fibres and resins**
- Characterise the **elastic behaviour** of the (**anisotropic**) composite system
- Determine the **strength** of the composite system for different failure modes: **longitudinal, transverse, shear, ...**
- Determine the **toughness** of the composite system for different failure modes: **interlaminar mode I (normal), mode II (shear), intralaminar, ...**
- ...

Characterisation of technical fibres and their products

D4018 Test Methods for Properties of Continuous Filament Carbon and Graphite Fiber Tows

- Tensile testing of resin-impregnated and consolidated test specimens made from continuous filament carbon and graphite yarns, rovings, and tows to determine their tensile properties



Characterisation of technical fibres and their products

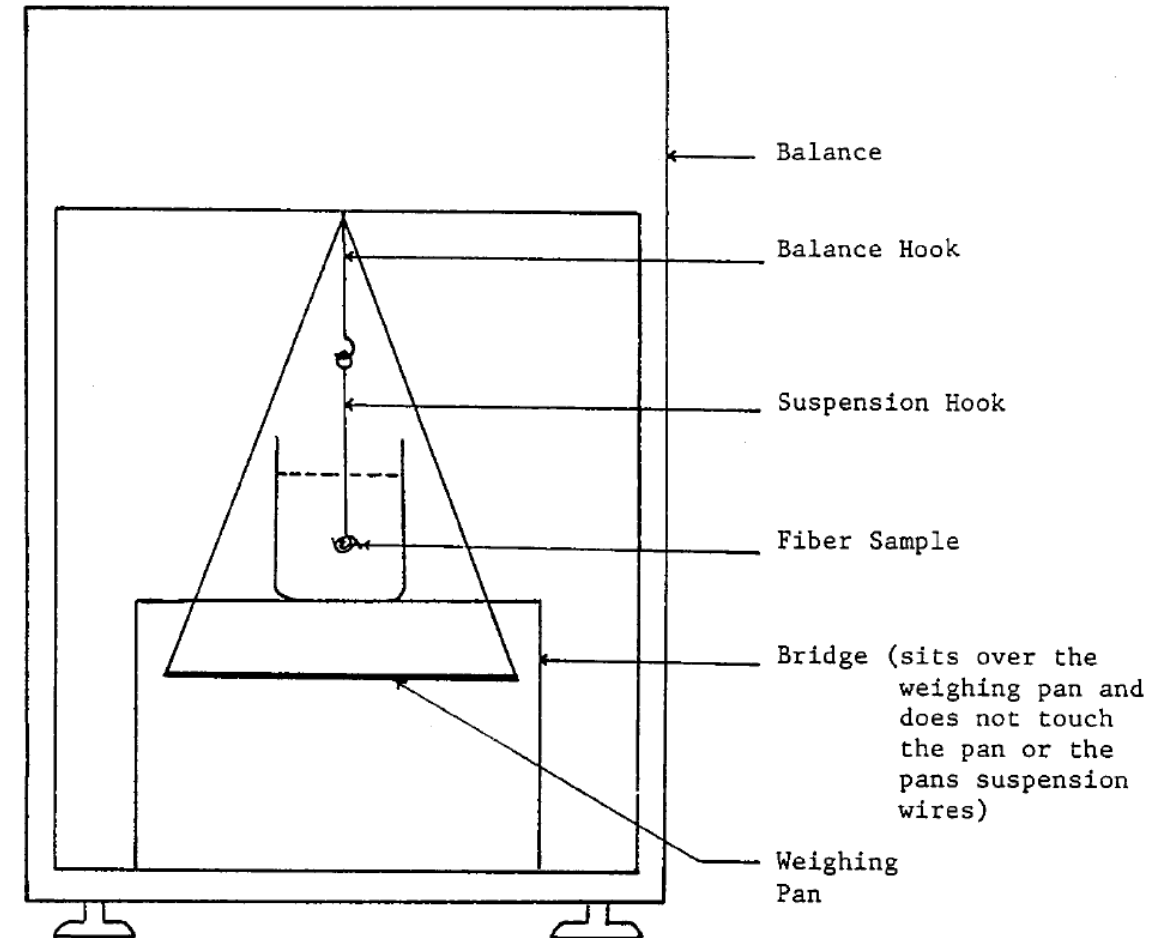
D4102 Test Method for Thermal Oxidative Resistance of Carbon Fibers

- Determination of the weight loss of carbon fibres, exposed to ambient hot air, as a means of characterizing their oxidative resistance

Characterisation of technical fibres and their products

D3800 Test Method for Density of High-Modulus Fibers

- Determination of the density of high-modulus fibres, applicable to both continuous and discontinuous fibres



Characterisation of resins



Viscosimeter



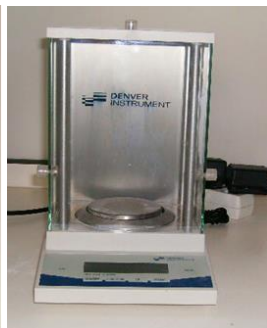
Gel Timer



Ultrasound bath



Mechanical mixer



Scales with different precisions

Characterisation of resins



Hood



Electric oven

Characterisation of resins



DSC Q20 with RCS90 Cooler

Differential Scanning Calorimetry (DSC)

- Measures the difference in the amount of heat required to increase the temperature of a sample and a reference as a function of temperature.

Alternatively:

DTA (Differential Thermal Analysis) measures the differences in temperature between a sample and a reference when the same amount of heat energy is applied to both.

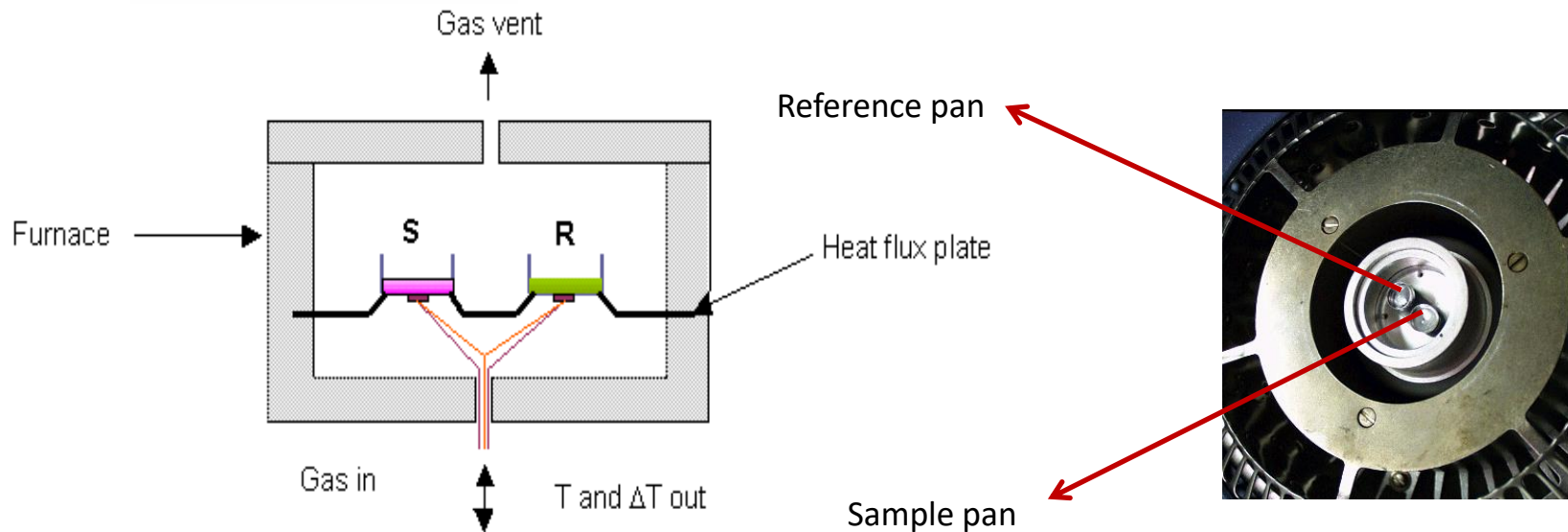
Characterisation of resins



DSC Q20 with RCS90 Cooler

Differential Scanning Calorimetry (DSC)

- Measures the difference in the amount of heat required to increase the temperature of a sample and a reference as a function of temperature.



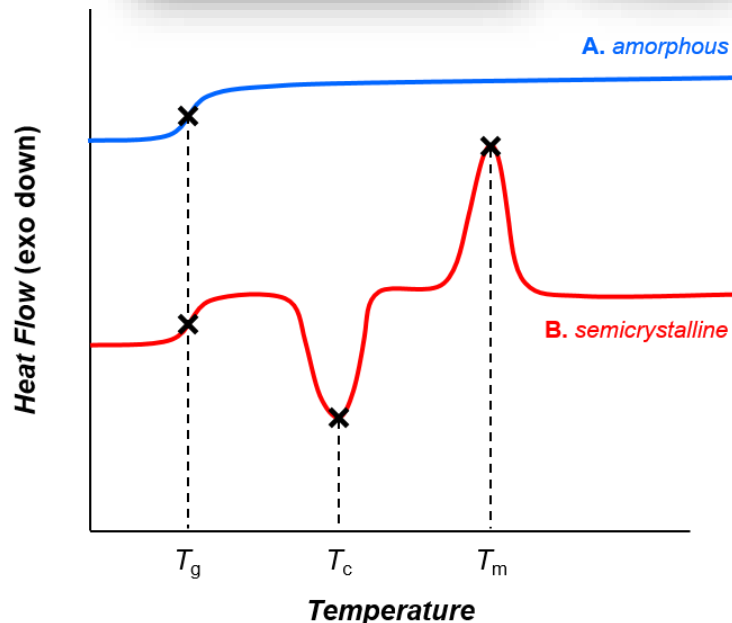
Characterisation of resins



DSC Q20 with RCS90 Cooler

Differential Scanning Calorimetry (DSC)

- Temperature and heat flow associated with material transitions
- Glass transition
- Melting and boiling points



Thermal transitions in (A) amorphous and (B) semicrystalline polymers. As the temperature increases, both amorphous and semicrystalline polymers go through the glass transition (T_g). Amorphous polymers (A) do not exhibit other phase transitions. However, semicrystalline polymers (B) undergo crystallization and melting (at temperatures T_c and T_m , respectively).

Characterisation of resins



DSC Q20 with RCS90 Cooler

Differential Scanning Calorimetry (DSC)

- Rate and degree of cure
- Cure kinetics
- Crystallization time and temperature
- Degree of crystallinity
- Heat of fusion and of reaction
- Specific heat / heat capacity
- Oxidative/thermal stability
- Purity

Characterisation of resins



SDT Q600

Thermal Gravimetric Analysis (TGA) (thermogravimetry)

- Measures the mass change of the sample with a thermo-balance.
- Simultaneous measurement of weight change (TGA) and differential heat flow (DSC)



Rheometer HR1

- Rheology study
- Viscosity measurements
- Loss modulus
- Storage modulus
- Shear strain

Characterisation of resins

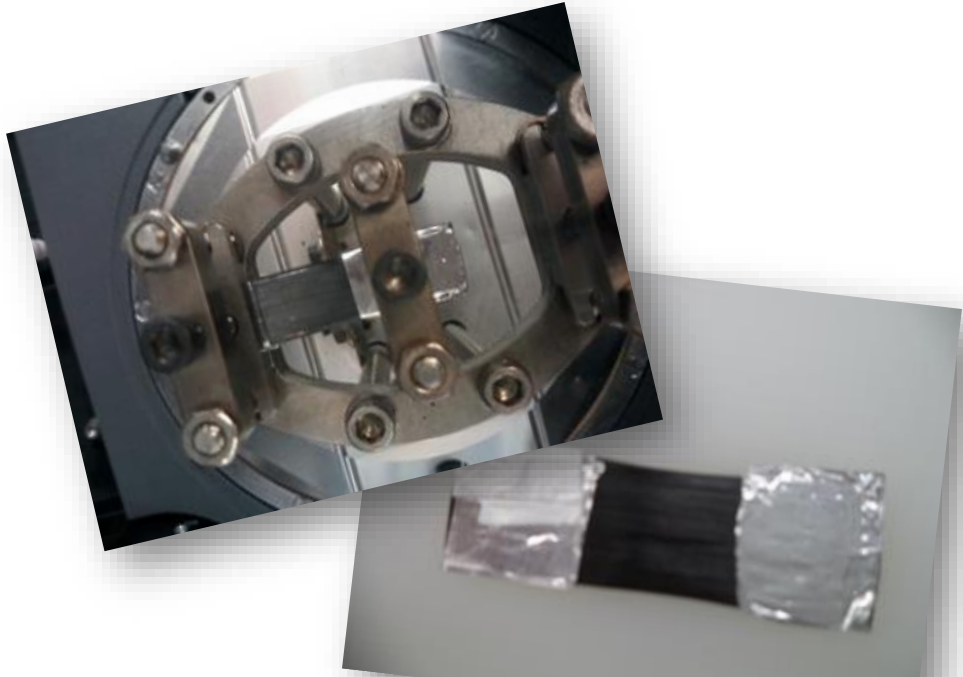


DMA Q800

Dynamic Mechanical Analysis (DMA)

- Measures mechanical properties of materials as a function of time, temperature, and frequency
- Can be used to determine the glass transition temperature of the material
- Dual/single cantilever beam
- 3-point bending
- Tension
- Compression
- Shear

Characterisation of resins

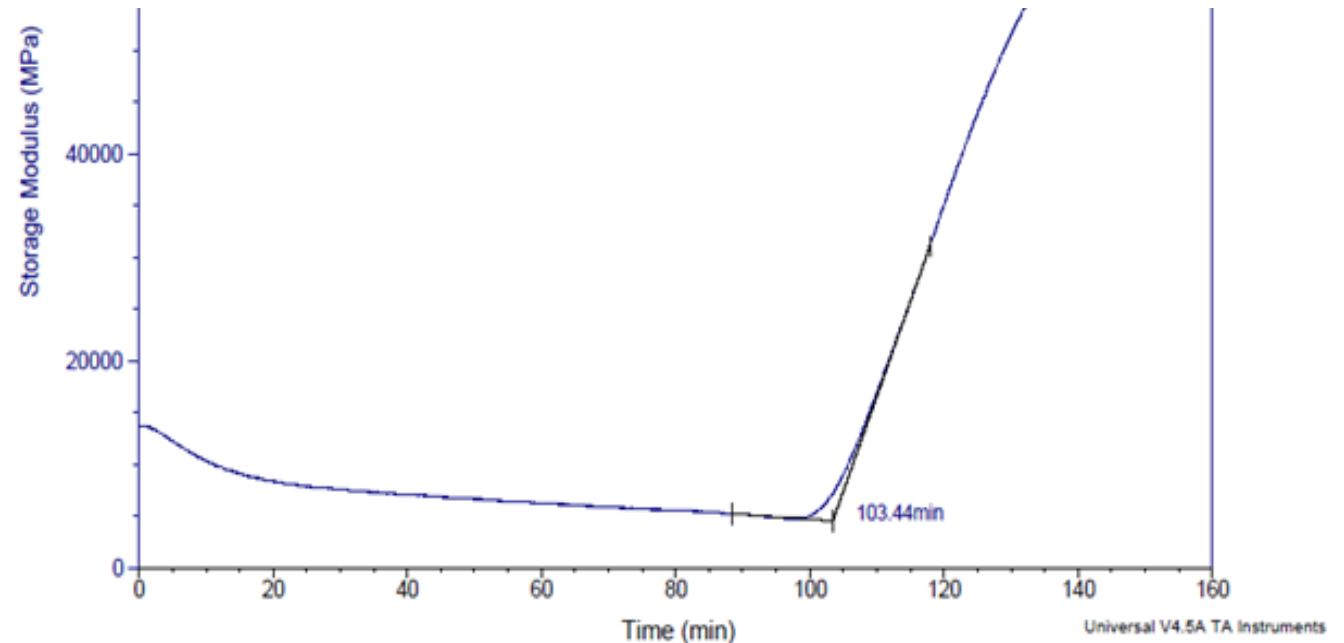


In the isothermal mode the gel time is determined by rapidly heating a sample to the desired temperature. Gelation occurs when the storage modulus starts increasing rapidly.

DMA Q800

Dynamic Mechanical Analysis (DMA)

Gel time determination in carbon fibre *prepreg* materials



Characterisation of resins and *prepregs* (including cure parameters)

D3531 *Test Method for Resin Flow of Carbon Fiber-Epoxy Prepreg*

D3532 *Test Method for Gel Time of Carbon Fiber-Epoxy Prepreg*

D2471 *Practice for Gel Time and Peak Exothermic Temperature of Reacting Thermosetting Resins*

D4473 *Test Method for Plastics: Dynamic Mechanical Properties: Cure Behavior*

Determination of contents (including volatile and solid residues)

C613/C613M Test Method for Constituent Content of Composite Prepreg by Soxhlet Extraction

D3529/D3529M Test Method for Matrix Solids Content and Matrix Content of Composite Prepreg

D3530/D3530M Test Method for Volatiles Content of Composite Material Prepreg

Characterisation of the composition of the composite

- Density: **ASTM D792-91**
- Fibre volume fraction
 - Optical methods
 - Dissolution of the matrix in acid: **ASTM D3171-76**
- Void content (VC): **ASTM D2584-68**
 - Manufacturing quality: VC < 1%
- Humidity: comparison of weight before and after drying.
 - Typical values in polymer matrix composites: 1% to 2%

$$V_f = \frac{\text{Volume of fiber}}{\text{Total volume}}$$

Chemical/solvent resistance

D543 Practices for Evaluating the Resistance of Plastics to Chemical Reagents

D570 Test Method for Water Absorption of Plastics

Thermophysical Properties

Linear thermal expansion Coefficient

- **D696** *Test Method for Coefficient of Linear Thermal Expansion of Plastics Between -30C and 30C with a Vitreous Silica Dilatometer*
- **E228** *Test Method for Linear Thermal Expansion of Solid Materials With a Push-Rod Dilatometer*
- **E289** *Test Method for Linear Thermal Expansion of Rigid Solids with Interferometry*

Thermophysical Properties

Thermal Diffusivity

- **E1461** *Test Method for Thermal Diffusivity by the Flash Method*

Transition Temperatures and Enthalpies, and Specific Heat Capacity by DSC

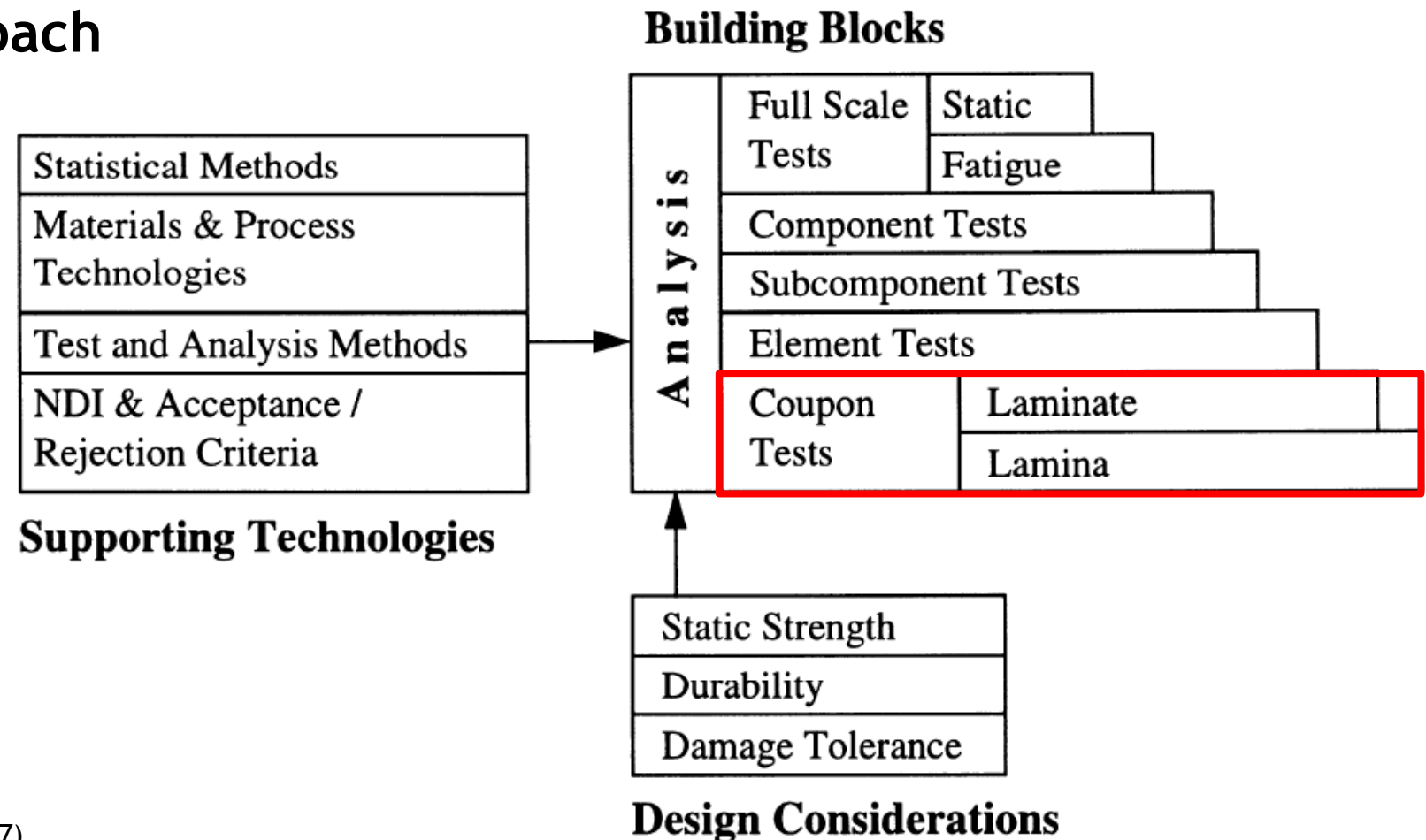
- **D3418** Test Method for Transition Temperatures and Enthalpies of Fusion and Crystallization of Polymers by Differential Scanning Calorimetry
- **E1269** Test Method for Determining Specific Heat Capacity by Differential Scanning Calorimetry

Mechanical Tests

- Tensile tests
- Compression tests
- Shear tests
- Bending tests
- Properties in thickness direction
- Fracture toughness tests
- Low-velocity impact tests
- Compression-after-impact tests
- ...

Mechanical Tests

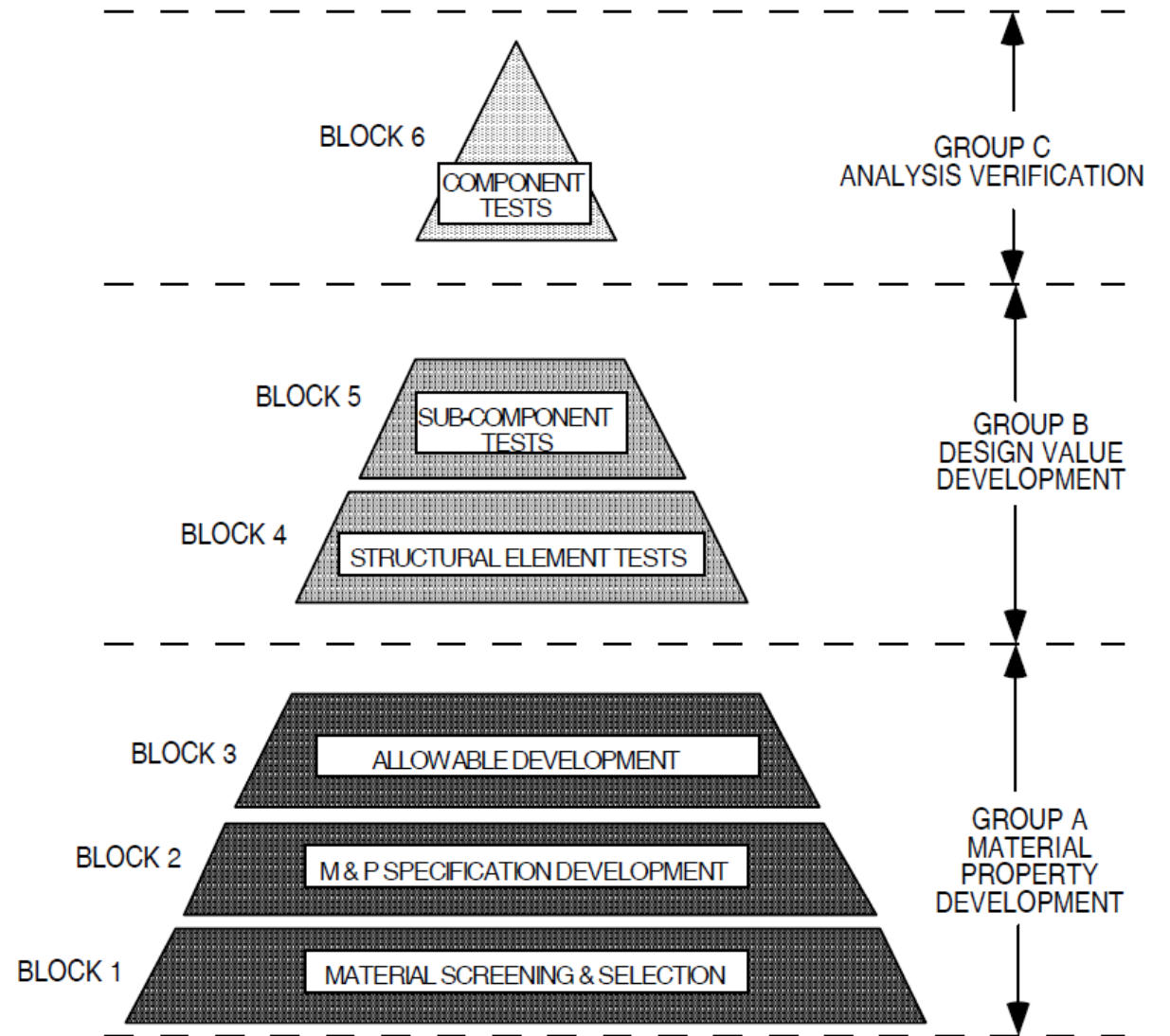
Building block approach



Mechanical Tests

Building block approach

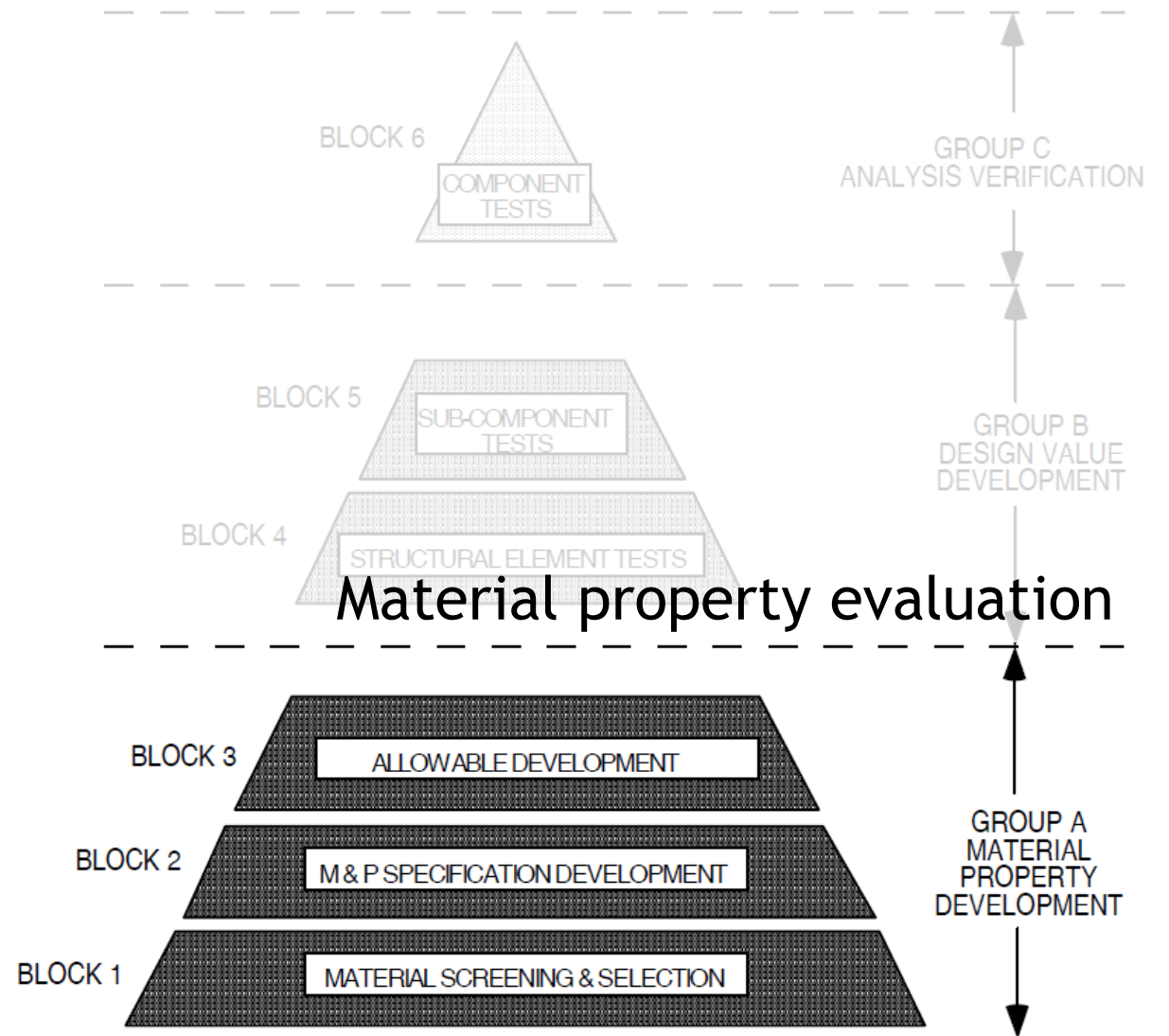
Test pyramid



Mechanical Tests

Building block approach

Test pyramid

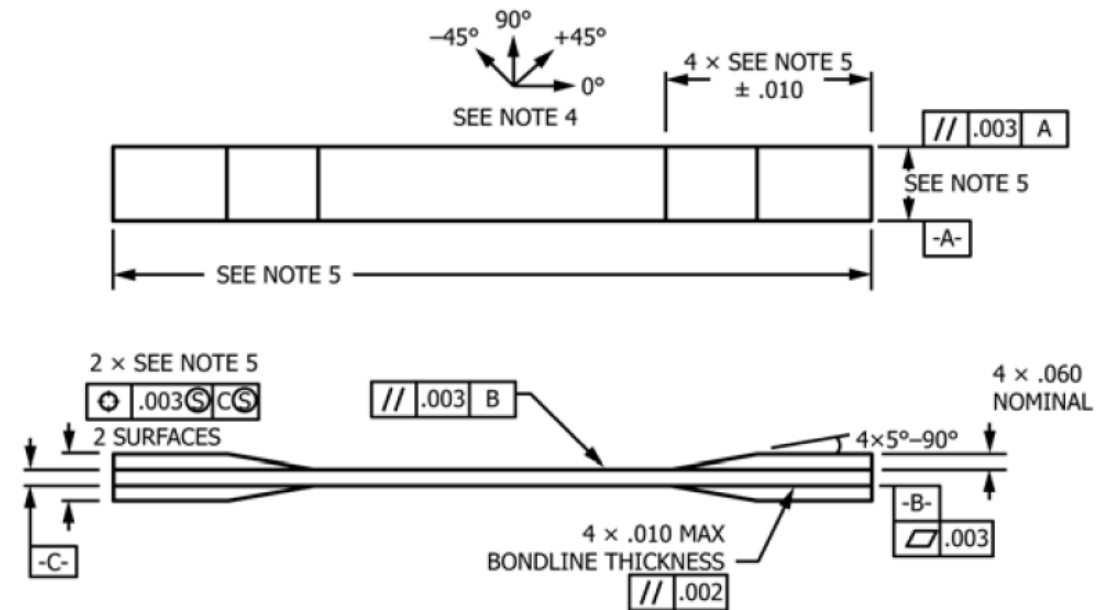


Tensile tests

- Mainly applied to unidirectional $[0^\circ]_n$ and $[90^\circ]_n$ composites.
- The goals are the measurement of E_1 , ν_{12} and X_T in the first case, and E_2 e Y_T in the second.



E_1 , E_2 , ν_{12} (elastic properties)
 X_T , Y_T (strength)



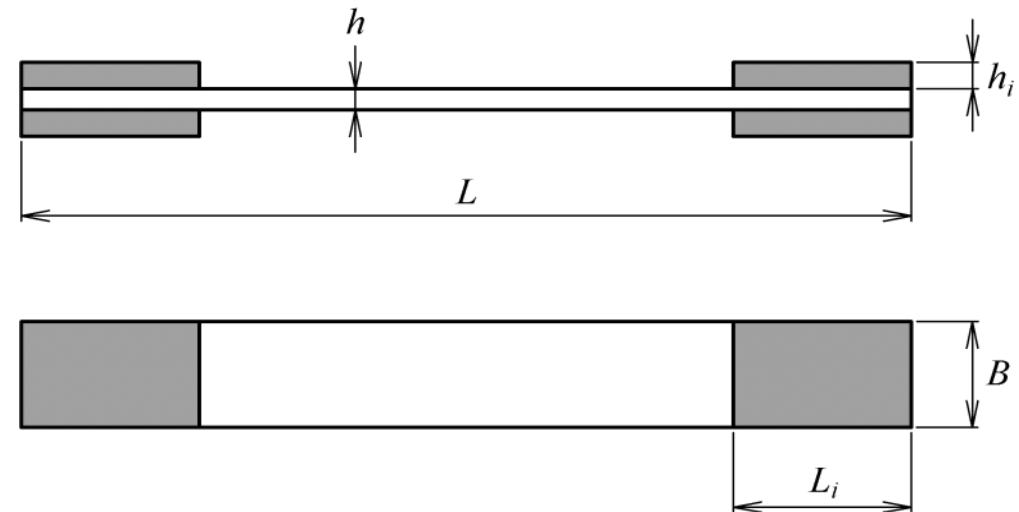
Tensile tests

- Mainly applied to unidirectional $[0^\circ]_n$ and $[90^\circ]_n$ composites.
- The goals are the measurement of E_1 , ν_{12} and X_T in the first case, and E_2 e Y_T in the second.



E_1 , E_2 , ν_{12} (elastic properties)
 X_T , Y_T (strength)

Schematic representation of an example of a tensile test specimen



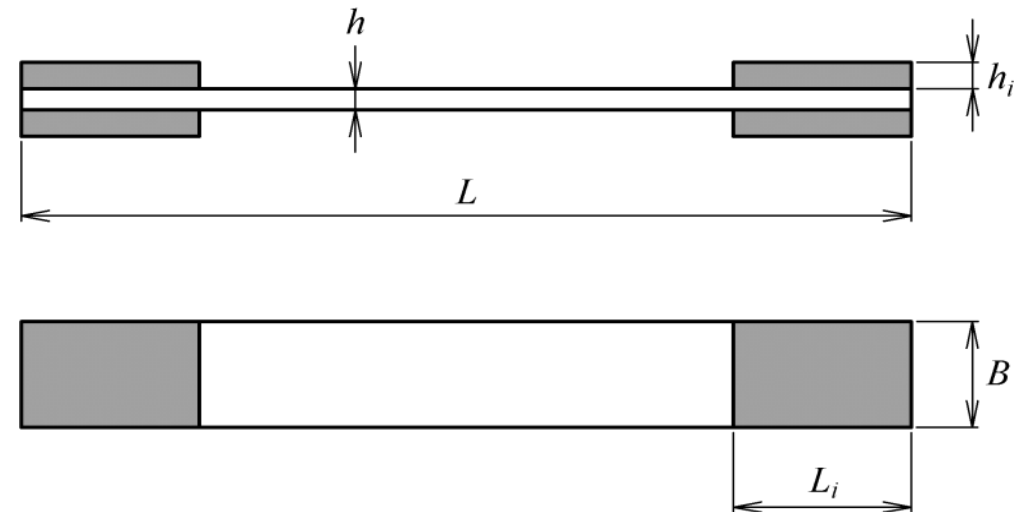
Tensile tests

Strength

- The use of **end tabs** aims to transmit the load from the jaws of the testing machine to the specimen in a more gradual way, as well as prevent premature damage.

Standards

- ASTM D3039
- ISO 527
- BS 2782
- CRAG 300-302



Tensile tests

Strength

- The **end tabs** must be sufficiently resistant to allow achieving the tensile strength of the specimen, which implies the use of structural adhesives for bonding to the composite.
- **Bonding end tabs:** The failure strain of the adhesive needs to be higher than the failure strain of the composite, and the adhesive shear strength should exceed 30 MPa.

Tensile tests

Strength

- The indentation of the **end tabs** by the jaw is important to prevent slipping of the specimen.
- **Aluminium** and $[\pm 45^\circ]_n$ **fibreglass end tabs** are typically used.
- The good alignment of the **tabs** is fundamental to get rigorous results.

Tensile tests

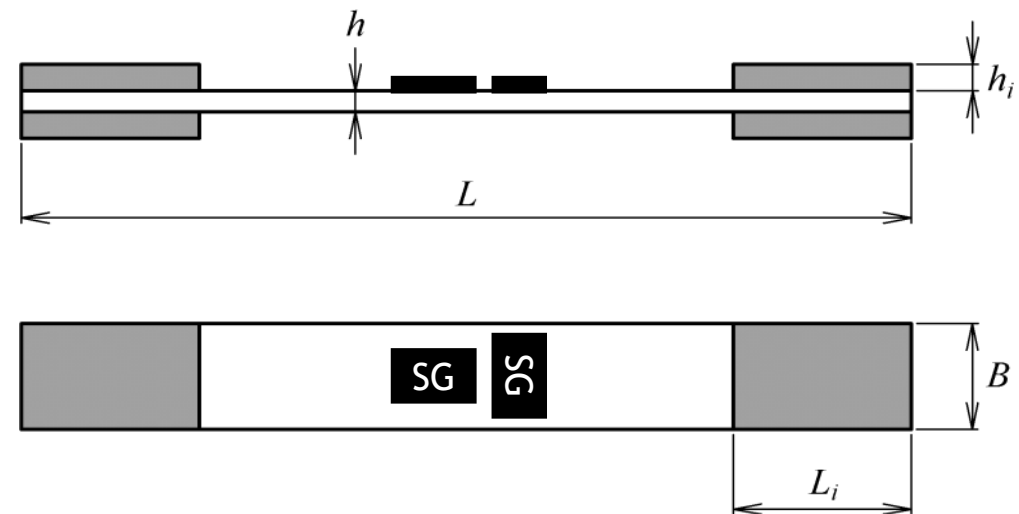
Recommended specimen dimensions according to ASTM, ISO and CRAG

Laminate	Standard	L (mm)	B (mm)	h (mm)	L_i (mm)	h_i (mm)
$[0^\circ]_n$	ASTM D 3039	250	15	1.0	56	1.5
	ISO 527	250	15	1.0	50	0.5 - 2.0
	CRAG 300	200 - 250	10	1.0	50	0.5 - 2.0
$[90^\circ]_n$	ASTM D 3039	175	25	2.0	25	1.5
	ISO 527	250	25	2.0	50	0.5 - 2.0
	CRAG 301	200 - 250	20	2.0	50	0.5 - 2.0
Multidirectional	ASTM D 3039	250	25	2.5	-	-
	ISO 527	≥ 200	12.5 - 25	1.0 - 10.0	45	≥ 3.0
	CRAG 302	≥ 200	$\geq 10h, 20$	1.0 - 4.0	≥ 50	0.5 - 2.0

Tensile tests

Strain gauges

- Ensure **correct alignment**: 2° error in the alignment implies differences of approximately 15% in measured properties
- **Surface preparation and adequate bonding**: the deformation in the strain gauge must be representative of the deformation in the specimen

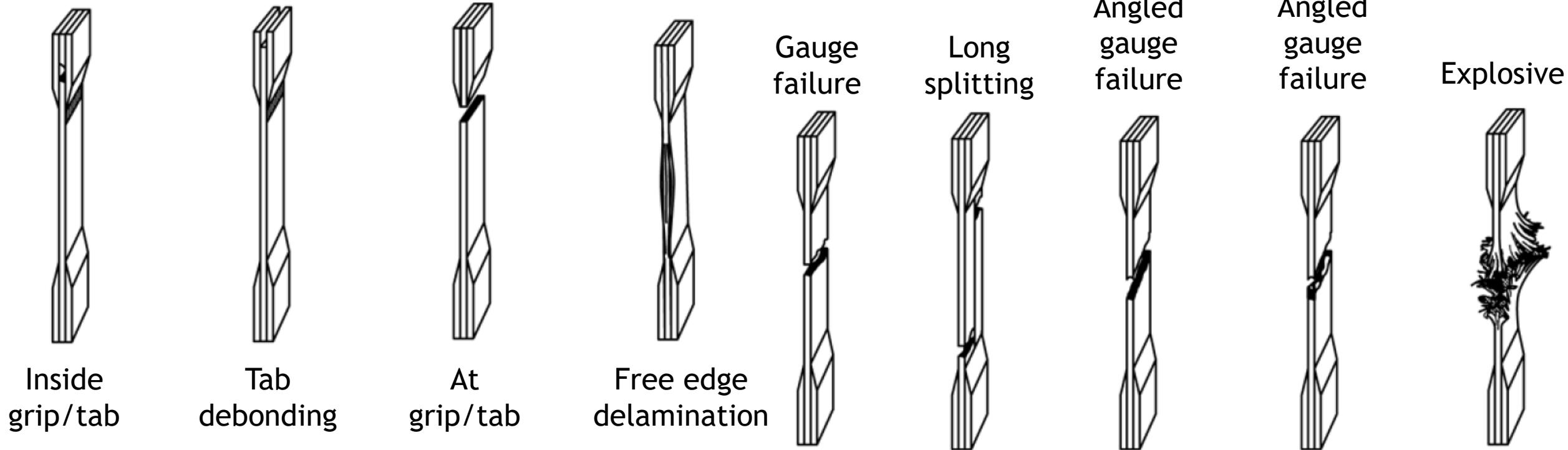


Tensile tests

Preform	Carbon fibers characteristics		
Prepreg	Tow n filaments	E-modulus (GPa)	Tensile strength (MPa)
Epoxy carbon fabric	3k	70	1150
Epoxy carbon fabric	6k	65	850
Epoxy carbon fabric	12k	63	800
Epoxy carbon UD	24k	126	2300
Epoxy carbon UD	50k	130	1900

Tensile tests

- Tensile test typical failure modes



Compression tests

Elastic and Strength Properties

Compression at 0° and 90°

Compression



E_{1c} (E_{2c}) (elastic properties)

X_C , Y_C (strength)

Test methods

- ASTM D695 (not recommended in high-strength composites)
- ASTM D3410 / D3410M
 - Fixing 'Celanese'
 - Fixing IITRI
- Fixing ICSTM
- Imperial College rig

Compression tests

Elastic and Strength Properties

Compression at 0° and 90°

Compression



E_{1c} (E_{2c}) (elastic properties)
 X_C , Y_C (strength)

Care in transferring the load to the specimen

- Avoid buckling.
- Avoid premature crushing at the load introduction regions.

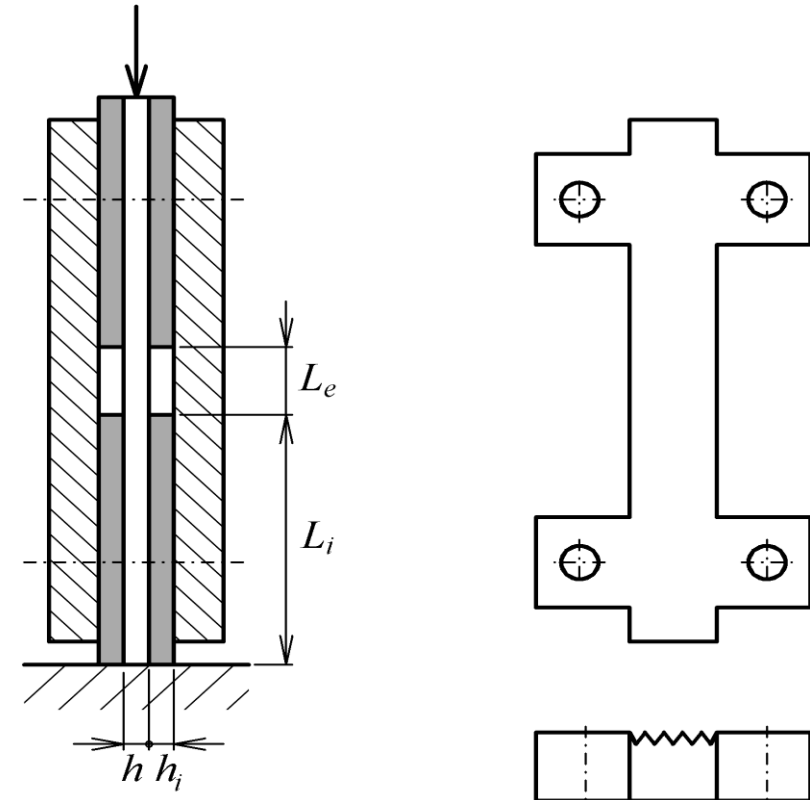
Measurement of longitudinal compressive strength, X_C , has proved to be one of the most complicated issues in the study of composite materials.

The main problem in applying compression loads in $[0^\circ]_n$ specimens is the strong tendency to premature crushing at the load introduction regions

Compression tests

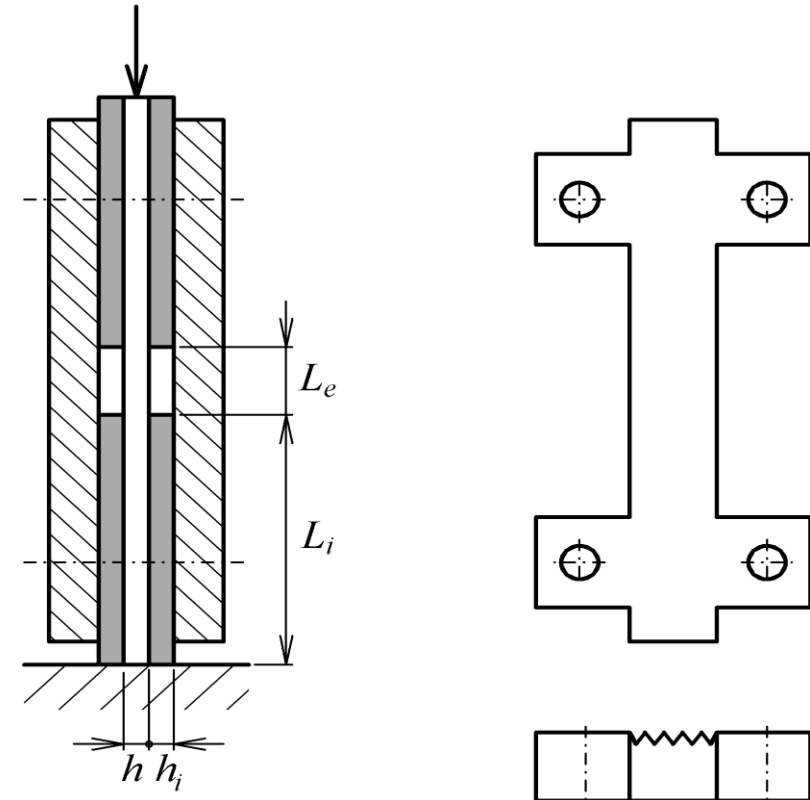
Schematic representation of **ASTM D 695** test (withdrawn 1996), including anti-buckling guides.

Typical dimensions are $h = h_i = 2$ mm,
 $L_i = 35$ mm, $L_e \leq 10$ mm and
width $B \leq 10$ mm.



Compression tests

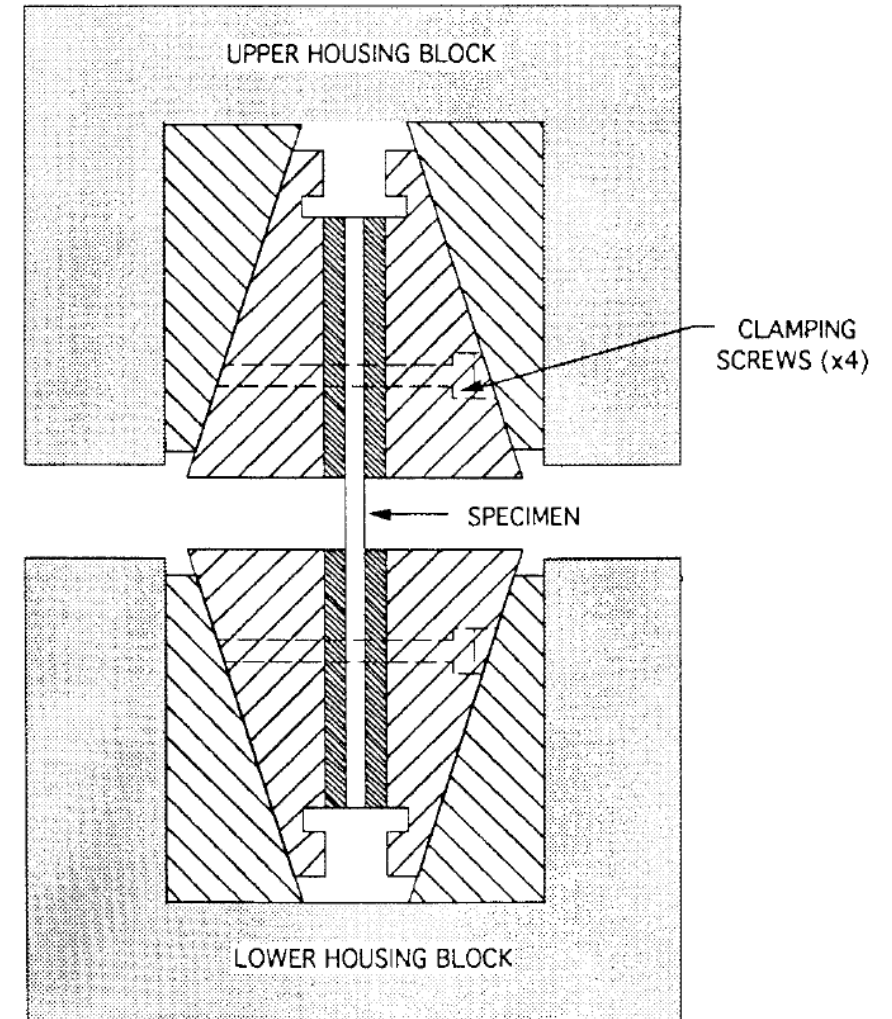
- The practice has shown that this method is **inappropriate for laminates $[0^\circ]_n$** , because the loading mode generates, prematurely, transverse cracks that propagate from the top to the central area of the test piece.
- However, this test **allows measuring Y_C in $[90^\circ]_n$ laminates**. In this case, inserts are not needed, and the specimen is wider (up to $B = 20$ mm).



Compression tests

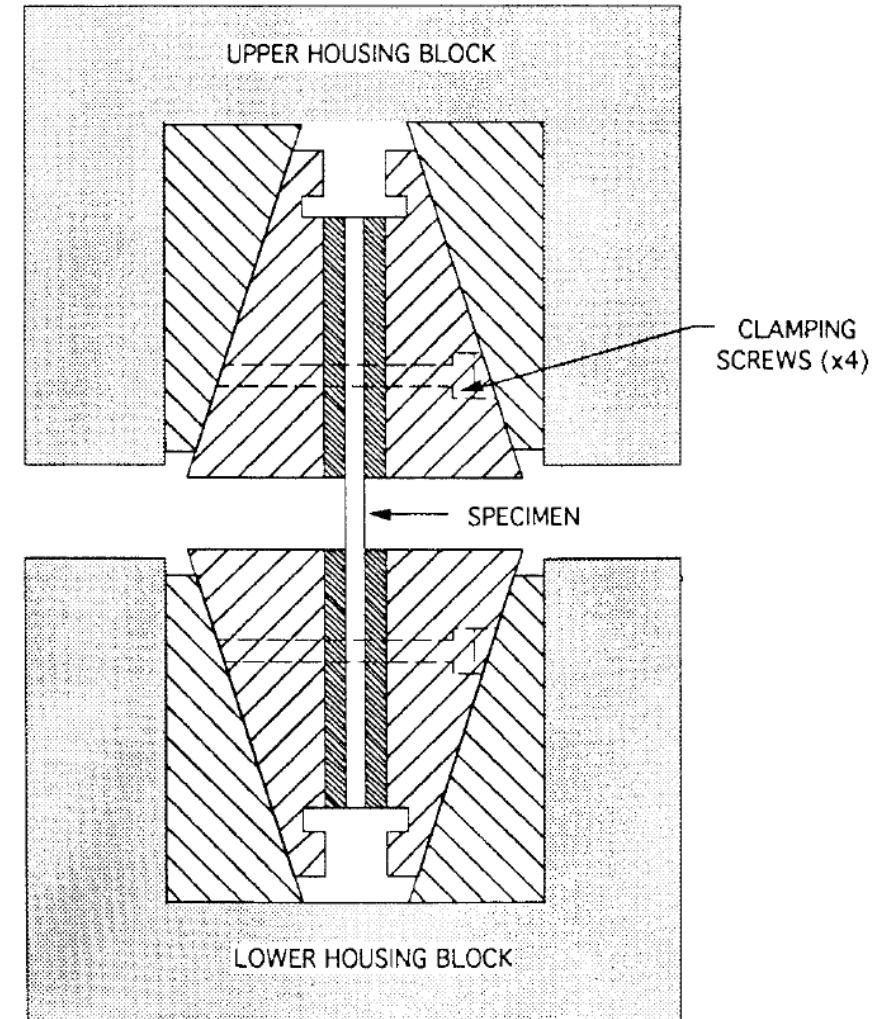
The **ASTM D 3410** standard was developed specifically for $[0^\circ]_n$ specimens, providing load transfer through shear forces, generated in the inserts with the wedges.

The test devices are usually named **Celanese** and **IITRI**.



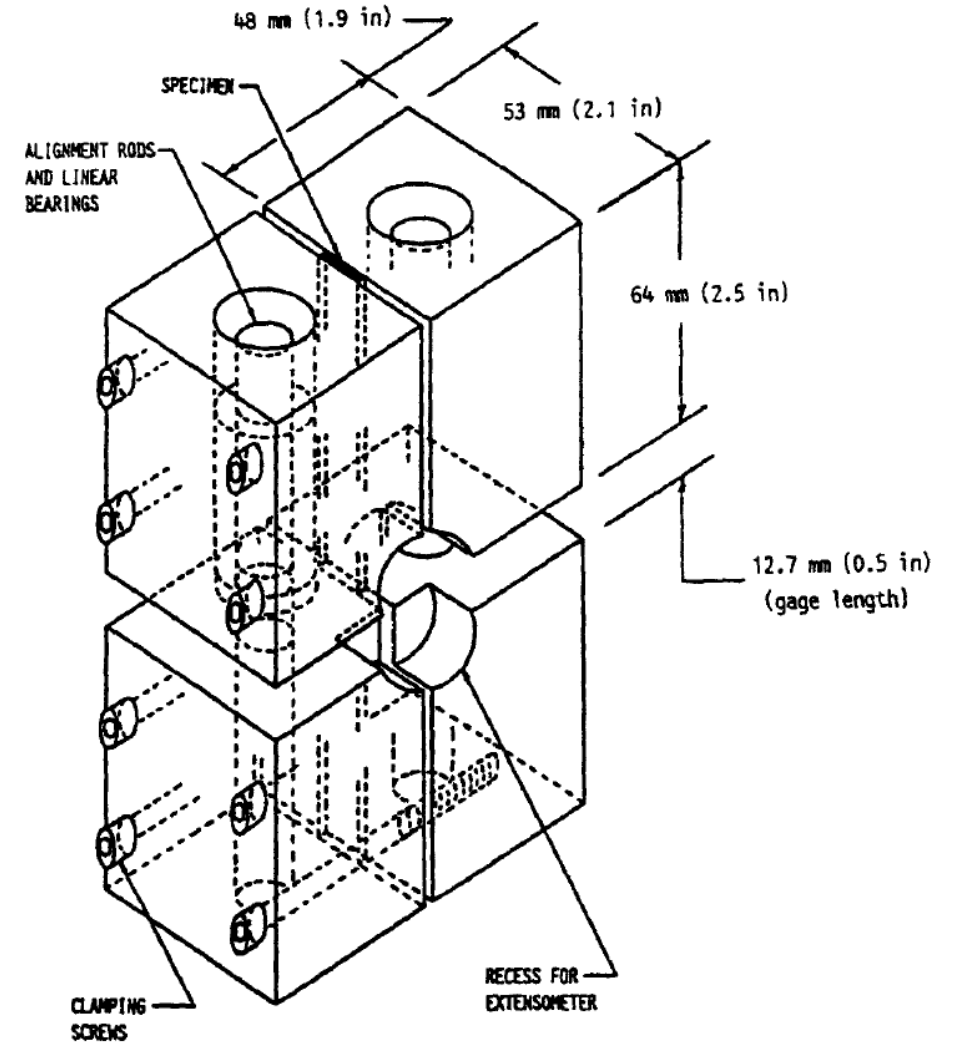
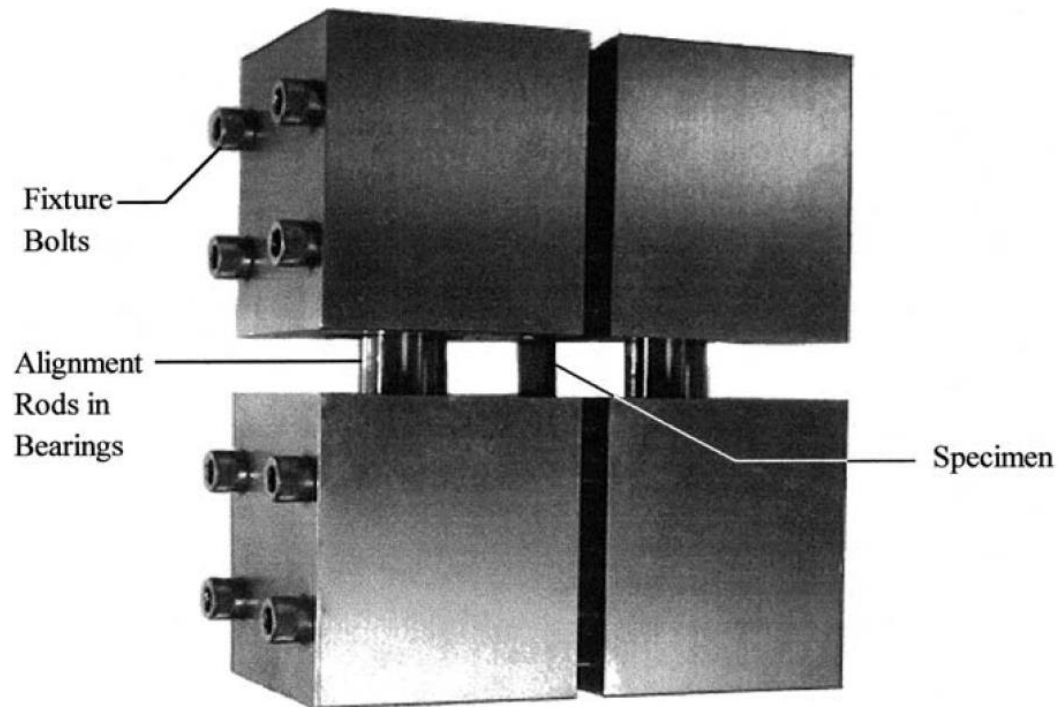
Compression tests

- In the **Celanese** configuration, the **wedges are conical**, being surrounded by a cylindrical outer sleeve for alignment. The load is applied to the external wedges.
- The **IITRI** wedges are housed in the cavities of a **trapezoidal** machined steel block.



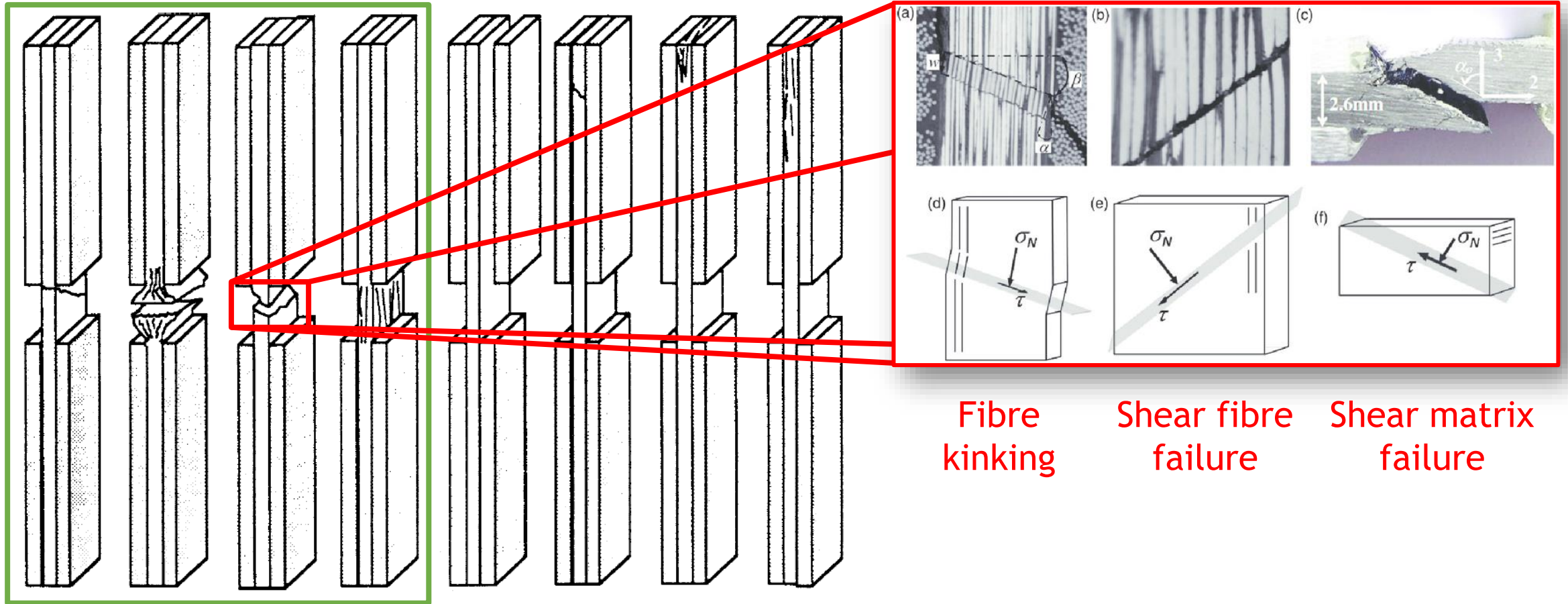
Compression tests

The **ASTM D 6641** standard uses a Combined Loading Compression (CLC) test fixture.



Compression tests

Failure modes



Fibre kinking

Shear fibre failure

Shear matrix failure

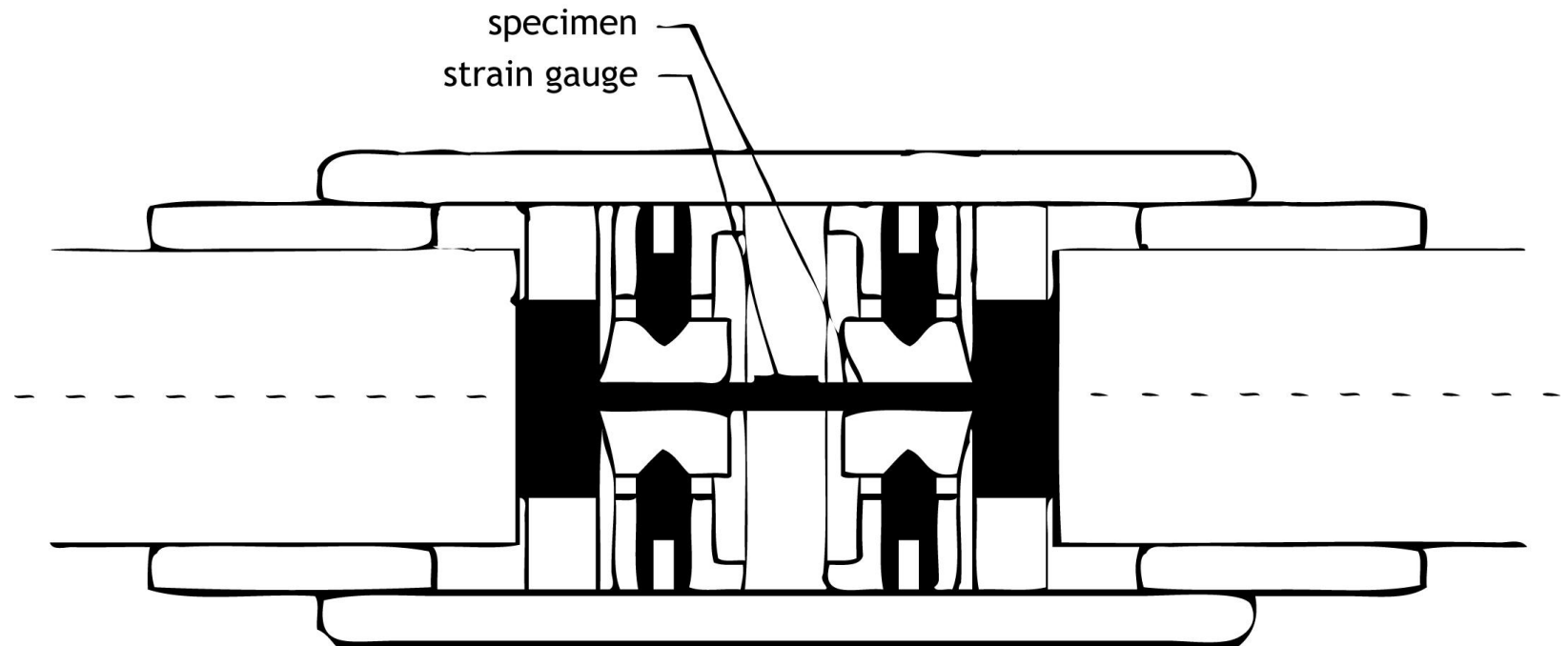
Acceptable failure modes

Unacceptable failure modes

Compression tests

Longitudinal compression

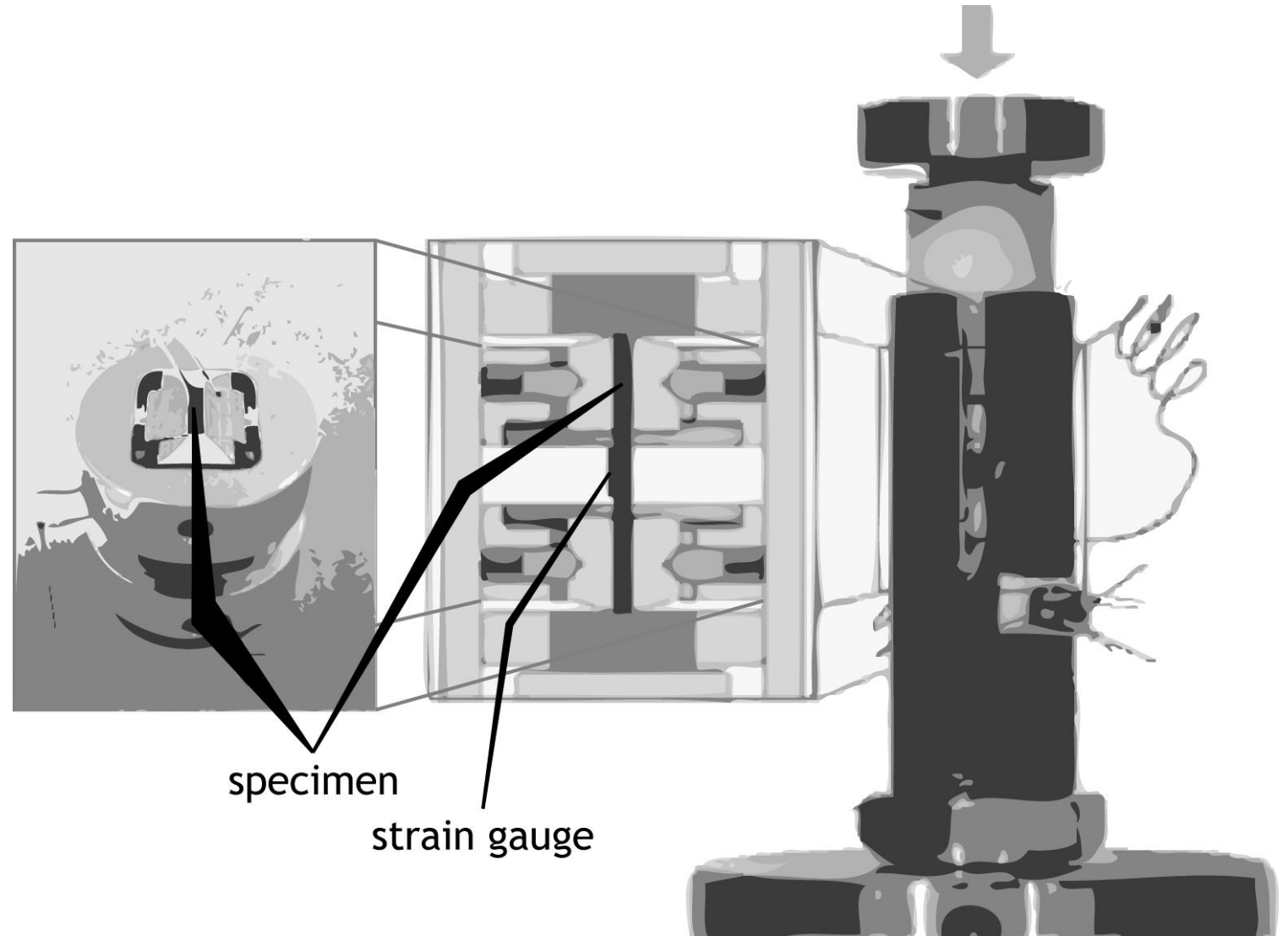
Realistic longitudinal compressive strengths of the 0° ply (X_c) can only be derived from tests on multidirectional laminates.



Compression tests

Longitudinal compression

Realistic longitudinal compressive strengths of the 0° ply (X_c) can only be derived from tests on multidirectional laminates.

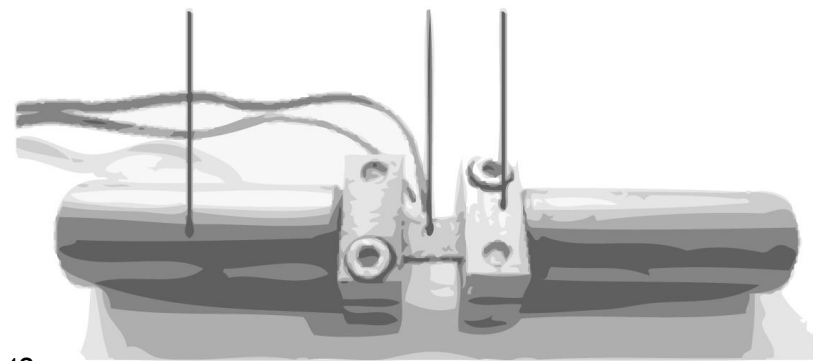
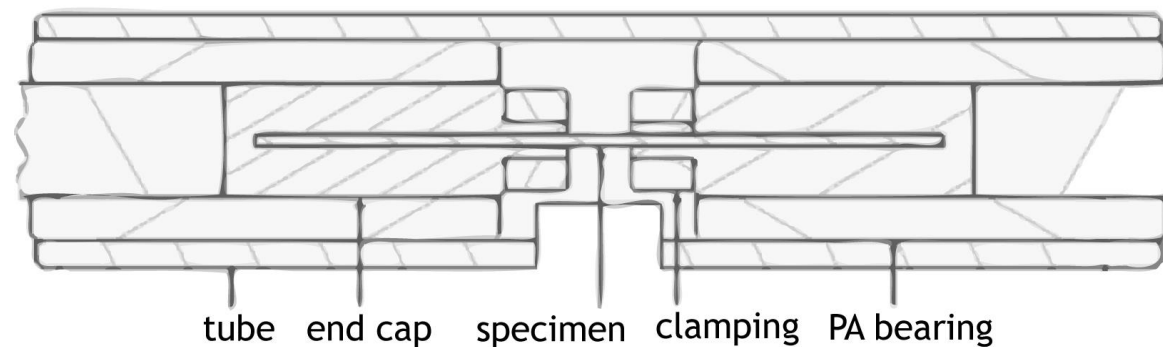


Composites: Part A 42 (2011) 462-470. doi:
10.1016/j.compositesa.2011.01.002

Compression tests

Longitudinal compression

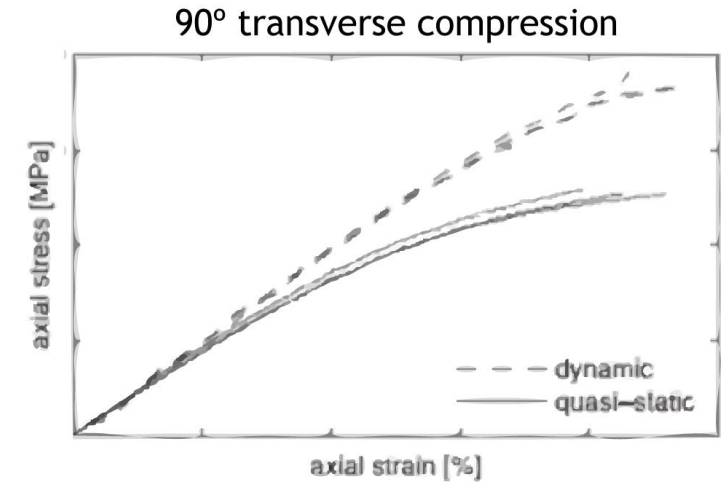
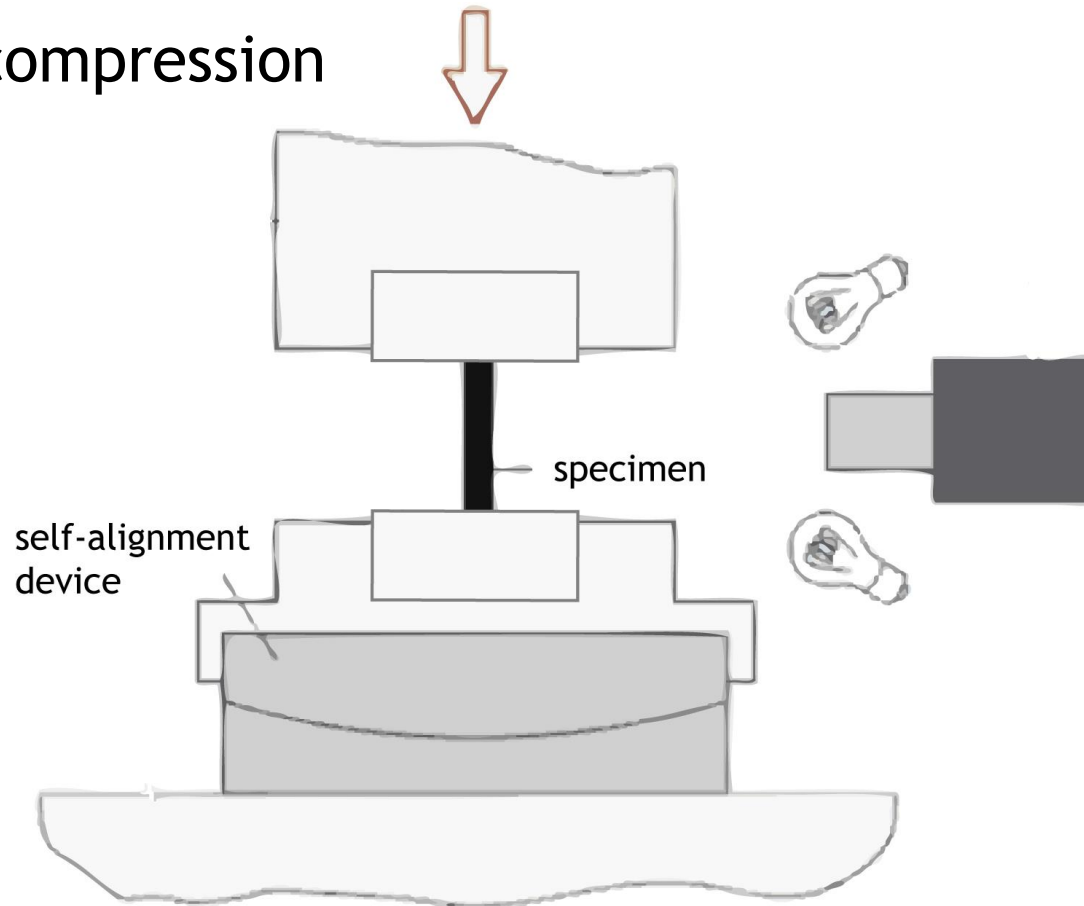
Realistic longitudinal compressive strengths of the 0° ply (X_c) can only be derived from tests on multidirectional laminates.



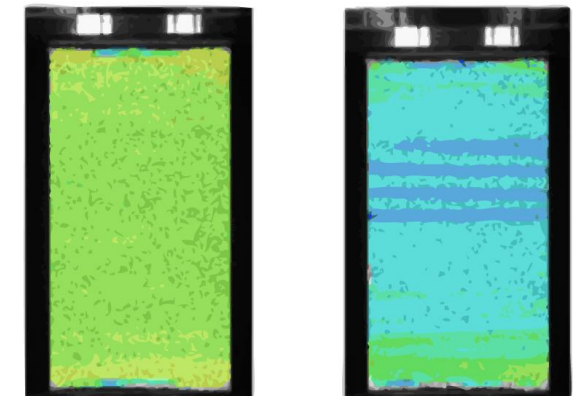
Composite Structures 180 (2017) 429-438.
<http://dx.doi.org/10.1016/j.compstruct.2017.08.048>

Compression tests

Transverse compression



Axial strain fields



Questions?

Mechanical behavior and characterization.

Mechanical tests from coupon to sub-component:
Building-block approach. Part 1

SASCOM

Introductory course on composite materials 2021

Mechanical behavior and characterization.

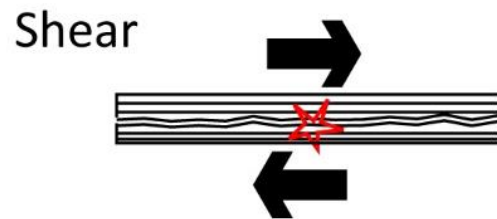
Mechanical tests from coupon to sub-component:
Building-block approach. Part 2

References

Marques AT. Composite Systems: Design and Manufacture for Durability, University of Porto, September 2019.

Shear tests

Elastic and Strength Properties



G_{12} (elastic properties)

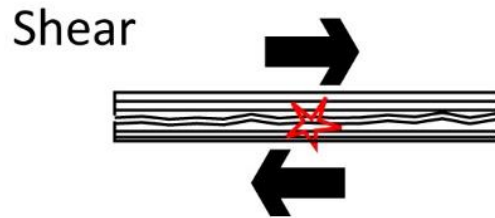
S_L (strength)

Test methods

- Specimen $[\pm 45^\circ]_{ns}$: ASTM D3518
- Specimen 'off-axis' 10° (tension/compression)
- Iosipescu: ASTM D5379
- Two-rail shear test: ASTM D4255
- V-Notched. ASTM D7078
- Torsion test of plates
- Torsion test of thin-walled tubes

Shear tests

Elastic and Strength Properties



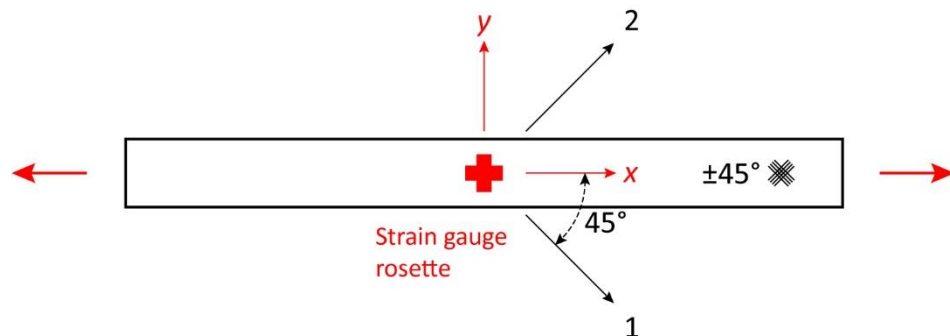
G_{12} (elastic properties)
 S_L (strength)

- The main problem in the characterisation of the shear behaviour is to generate a pure shear state on a volume of material sufficiently representative.
- In general, the tests give satisfactory results for the shear modulus G_{12} , but there are questions about the validity of the values of S_L obtained by some of these test methods.

Shear tests

The **ASTM D 3518** standard is used to characterise the in-plane shear response using $[\pm 45^\circ]_{ns}$ laminates ($4 \leq n \leq 6$).

- The test is usually performed at 2 mm/min. The measurement of G_{12} requires strain gauges in the longitudinal (x) and transverse (y) directions.



$$\tau_{12} = \frac{\sigma_x}{2}$$

$$\gamma_{12} = \varepsilon_x - \varepsilon_y$$

Shear tests

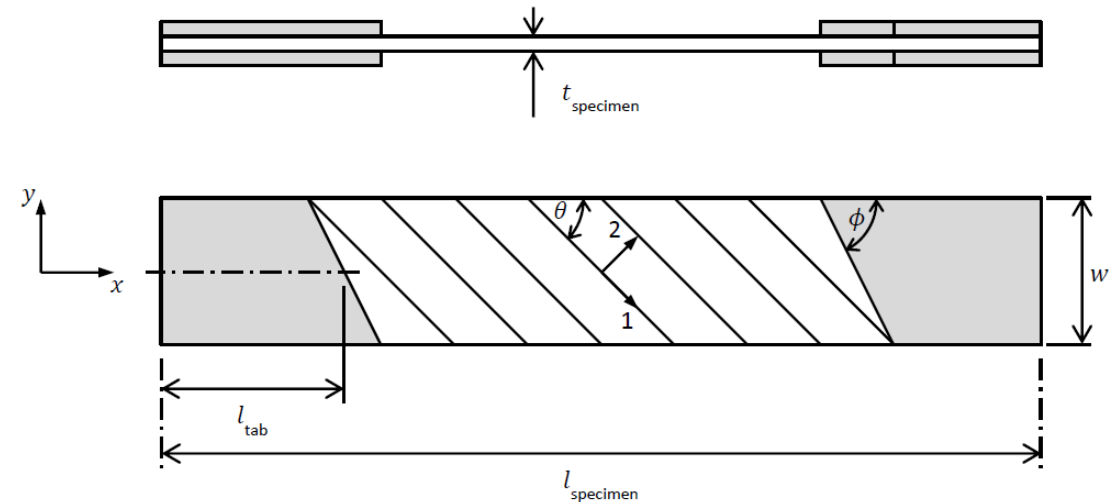
The **ASTM D 3518** standard is used to characterise the in-plane shear response using $[\pm 45^\circ]_{ns}$ laminates ($4 \leq n \leq 6$).

- This test is relatively **easy to perform** and allows expeditiously determination of G_{12} .
- However, the validity of the **measured shear strength is doubtful**, due to a **relatively complex gradual rupture process**, involving the formation of transverse cracks and delaminations, as well as strong geometric and material nonlinearities that cause considerable **fibre rotation**.

Shear tests

Tensile test of 10° off-axis unidirectional laminates

- The specimen is a unidirectional laminate, whose fibres are oriented at 10° with respect to the loading axis x .
- In tension, the jaws of the testing machine prevent rotations, generating additional moments and shear forces close to the grips. Hence, the specimen should be relatively long, and **oblique end tabs** are recommended to prevent premature failure.



Shear tests

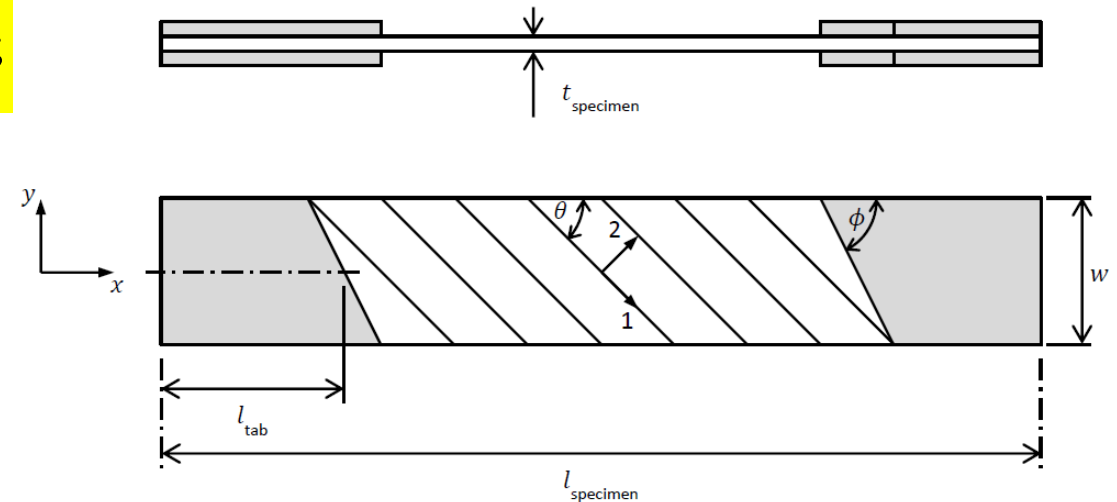
Tensile test of 10° off-axis unidirectional laminates

- The specimen is a unidirectional laminate, whose fibres are oriented at 10° with respect to the loading axis x .

$$\sigma_1 = \sigma_x \cos^2 \theta; \quad \sigma_2 = \sigma_x \sin^2 \theta; \quad \tau_{12} = \frac{\sigma_x}{2} \sin 2\theta;$$

$$\gamma_{12} = (\varepsilon_x - \varepsilon_y) \sin 2\theta + \gamma_{xy} \cos 2\theta$$

The choice of an angle $\theta = 10^\circ$ maximises shear deformation without the risk of fibre failure.



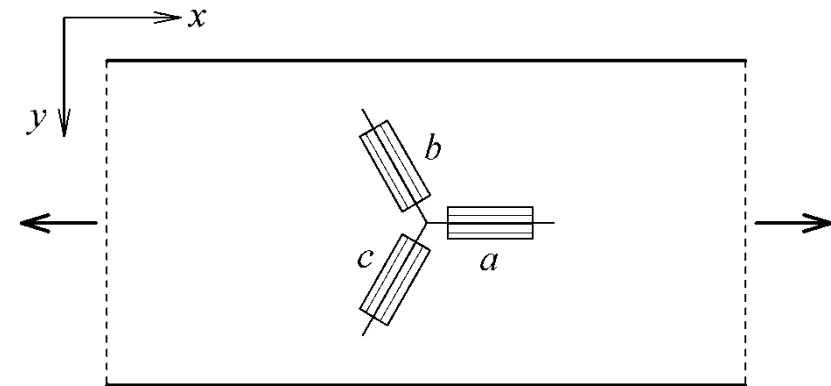
Shear tests

Tensile test of 10° off-axis unidirectional laminates

- The specimen is a unidirectional laminate, whose fibres are oriented at 10° with respect to the loading axis x .

The determination of the shear modulus therefore requires the measurement of deformations in three directions, using for example strain gauge rosettes placed in delta.

$$\varepsilon_x = \varepsilon_a; \quad \varepsilon_y = \frac{2\varepsilon_b + 2\varepsilon_c - \varepsilon_a}{3}; \quad \gamma_{xy} = \frac{2(\varepsilon_c - \varepsilon_b)}{\sqrt{3}};$$



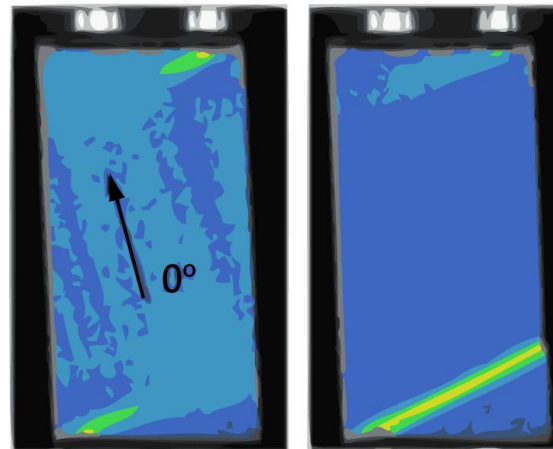
Shear tests

Compressive test of 15° off-axis unidirectional laminates

- The specimen is a unidirectional laminate, whose fibres are oriented at 15° with respect to the loading axis x .

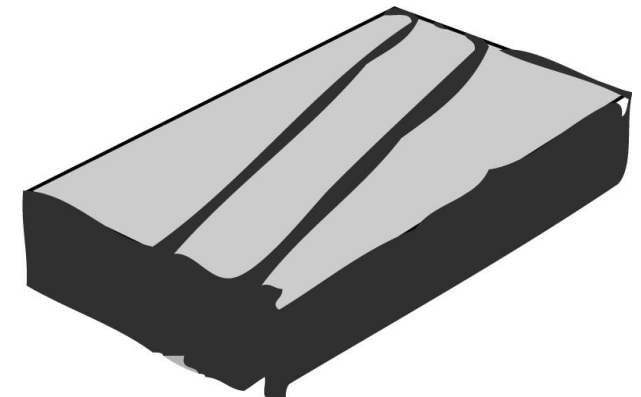
However, end crushing and fibre kinking are not valid failure modes and sometimes difficult to avoid.

Shear angle



Unacceptable failure mode

In-plane shear failure mode



Mechanics of Materials 42 (2010) 1004-1019.
doi: 10.1016/j.mechmat.2010.09.003

Shear tests

Rail shear test

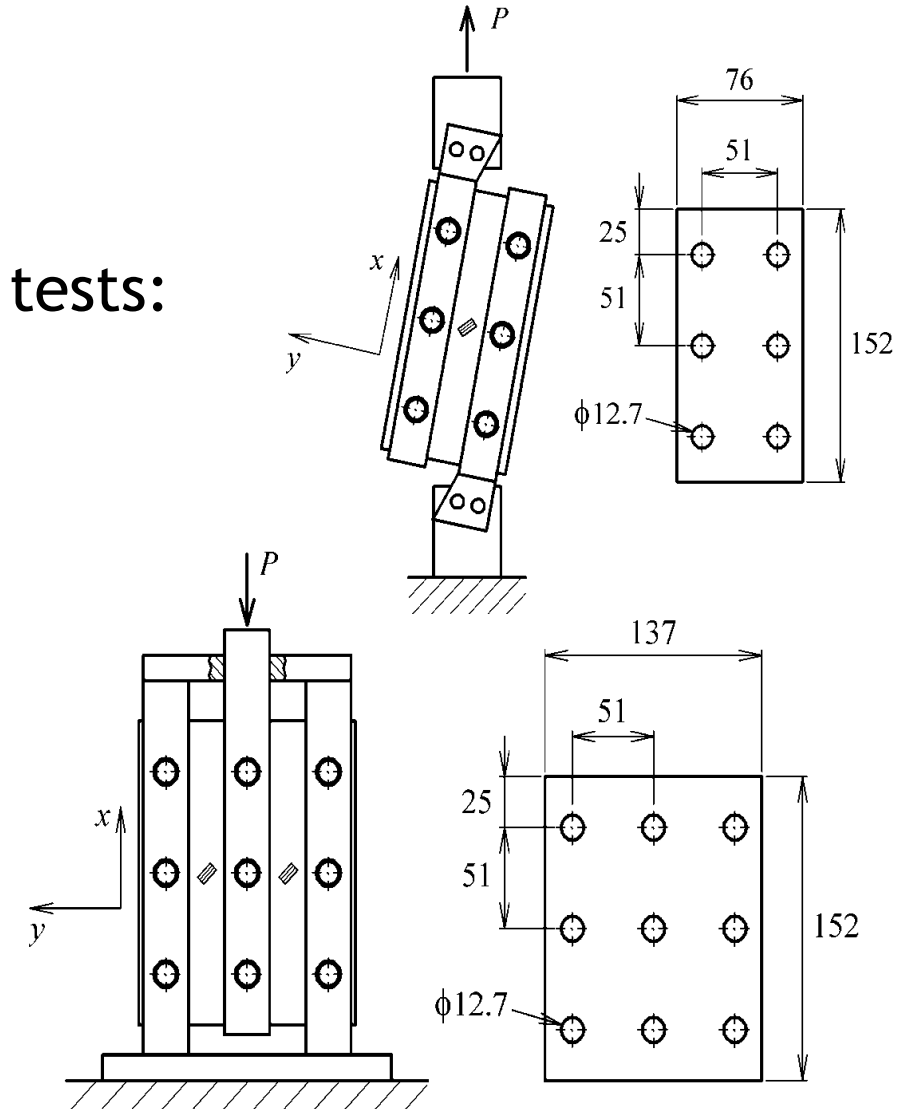
There are two configurations for the rail shear tests:

- Double rail
- Triple rail

In both cases, the loads imposed, P , at the machine head can be tensile or compressive, usually transferred to the laminates through pre-stressed bolted joints.

$$\tau_{xy} = \frac{P}{nLh}$$

$$G_{xy} = \frac{P}{2nLh\varepsilon_e}$$



Shear tests

Rail shear test

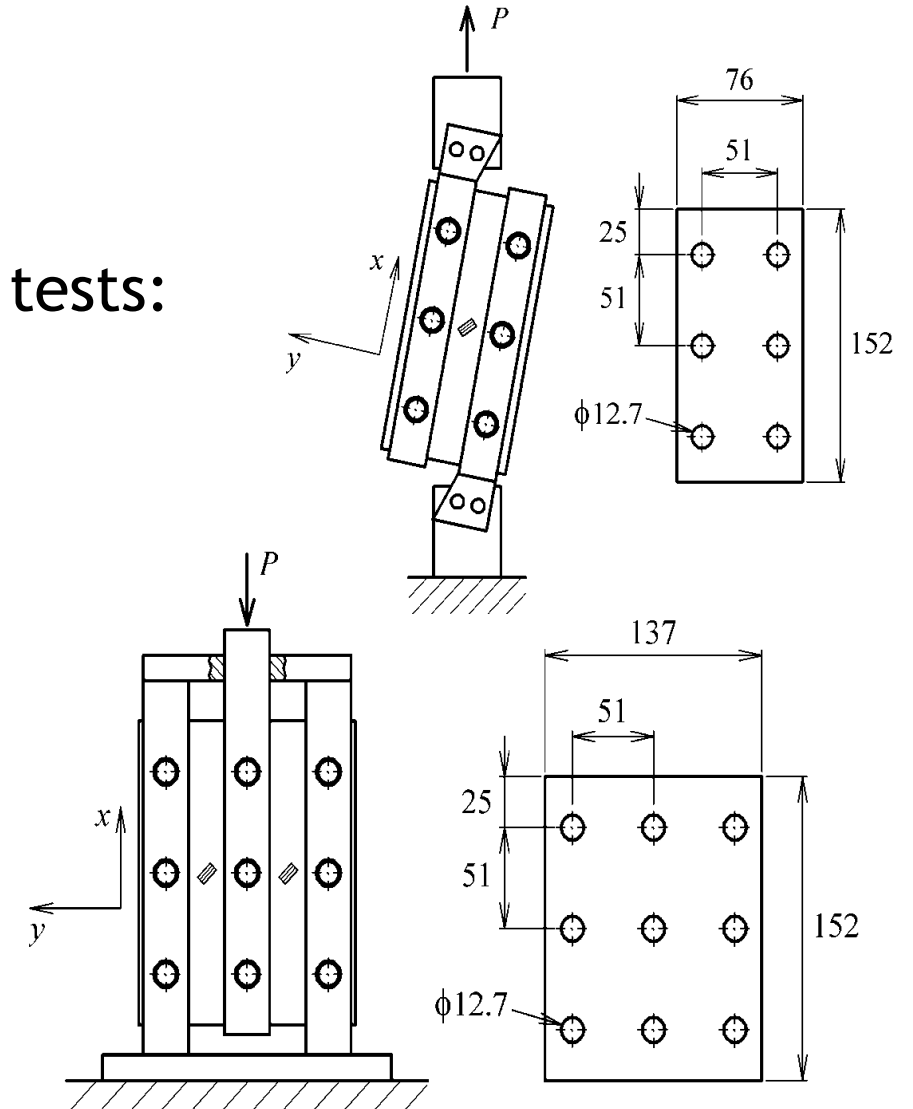
There are two configurations for the rail shear tests:

- Double rail
- Triple rail

For the **triple rail** test, the load applied to the central rail is, generally, compressive, as it avoids a rigid connection to the base.

$$\tau_{xy} = \frac{P}{nLh}$$

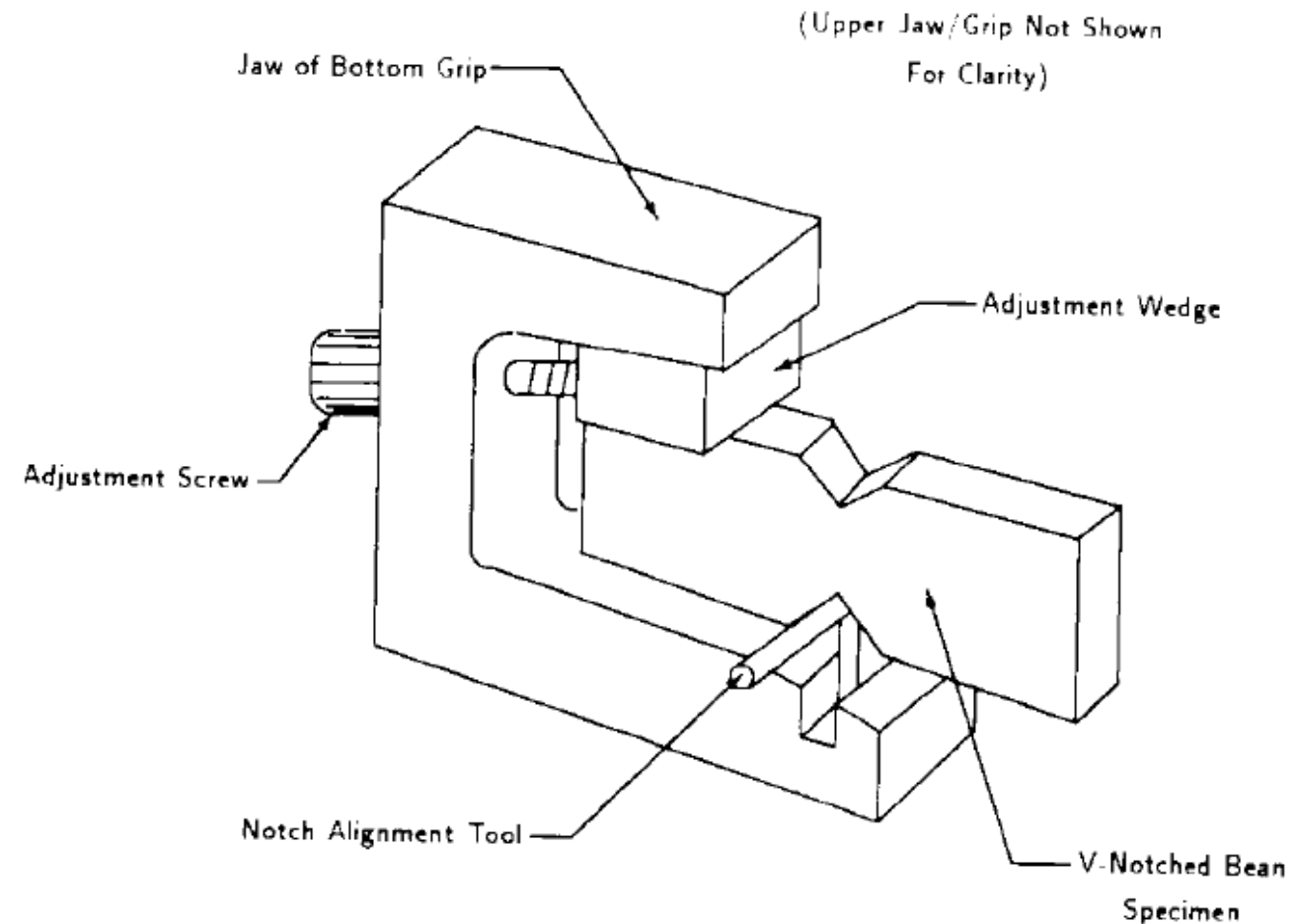
$$G_{xy} = \frac{P}{2nLh\varepsilon_e}$$



Shear tests

Iosipescu test (ASTM D 5379)

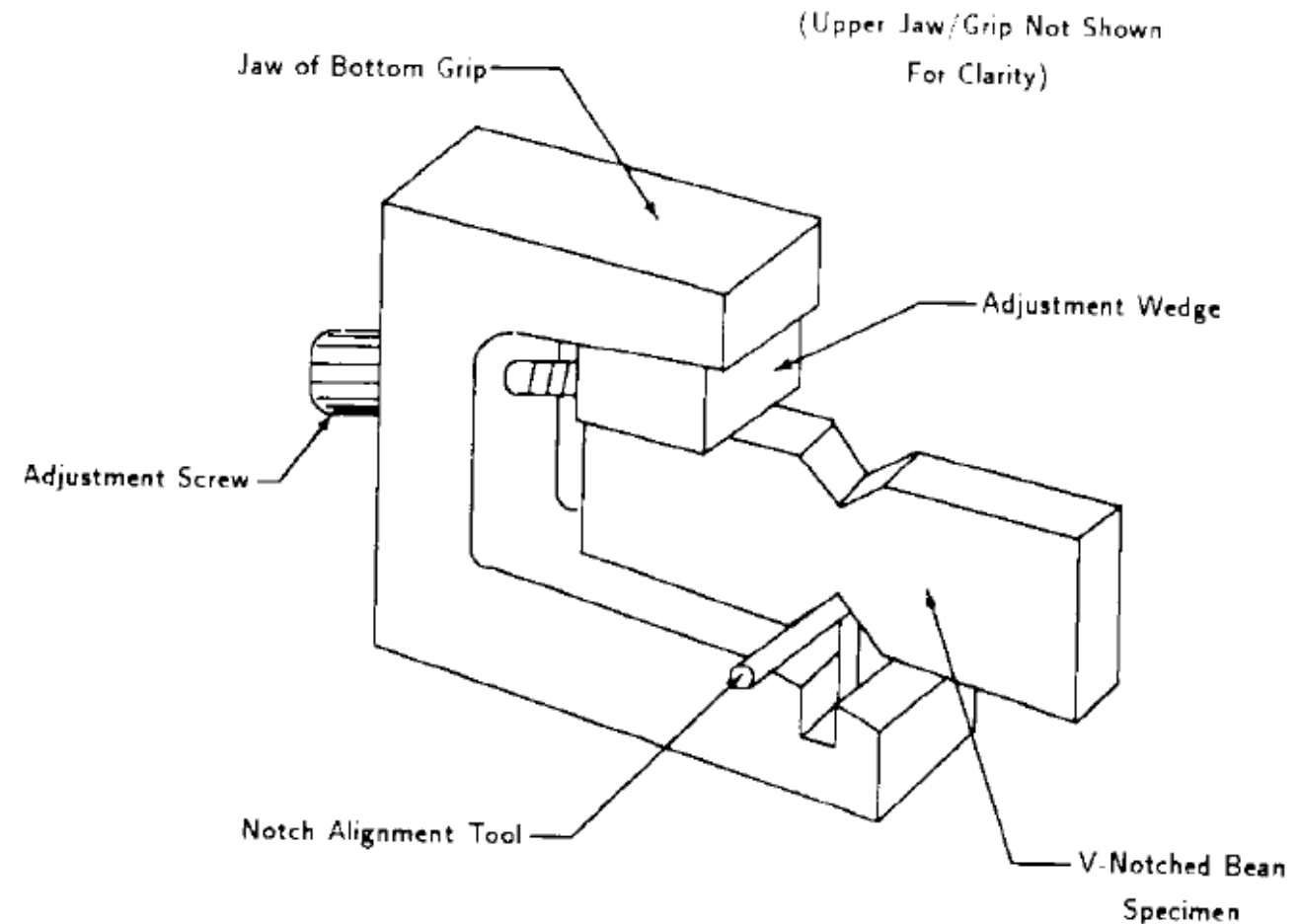
- The method uses a double notched specimen with thickness h between 3 mm and 4 mm.
- This is positioned on the device by means of wedges, being the load transferred to a block sliding on an alignment pin.



Shear tests

Iosipescu test (ASTM D 5379)

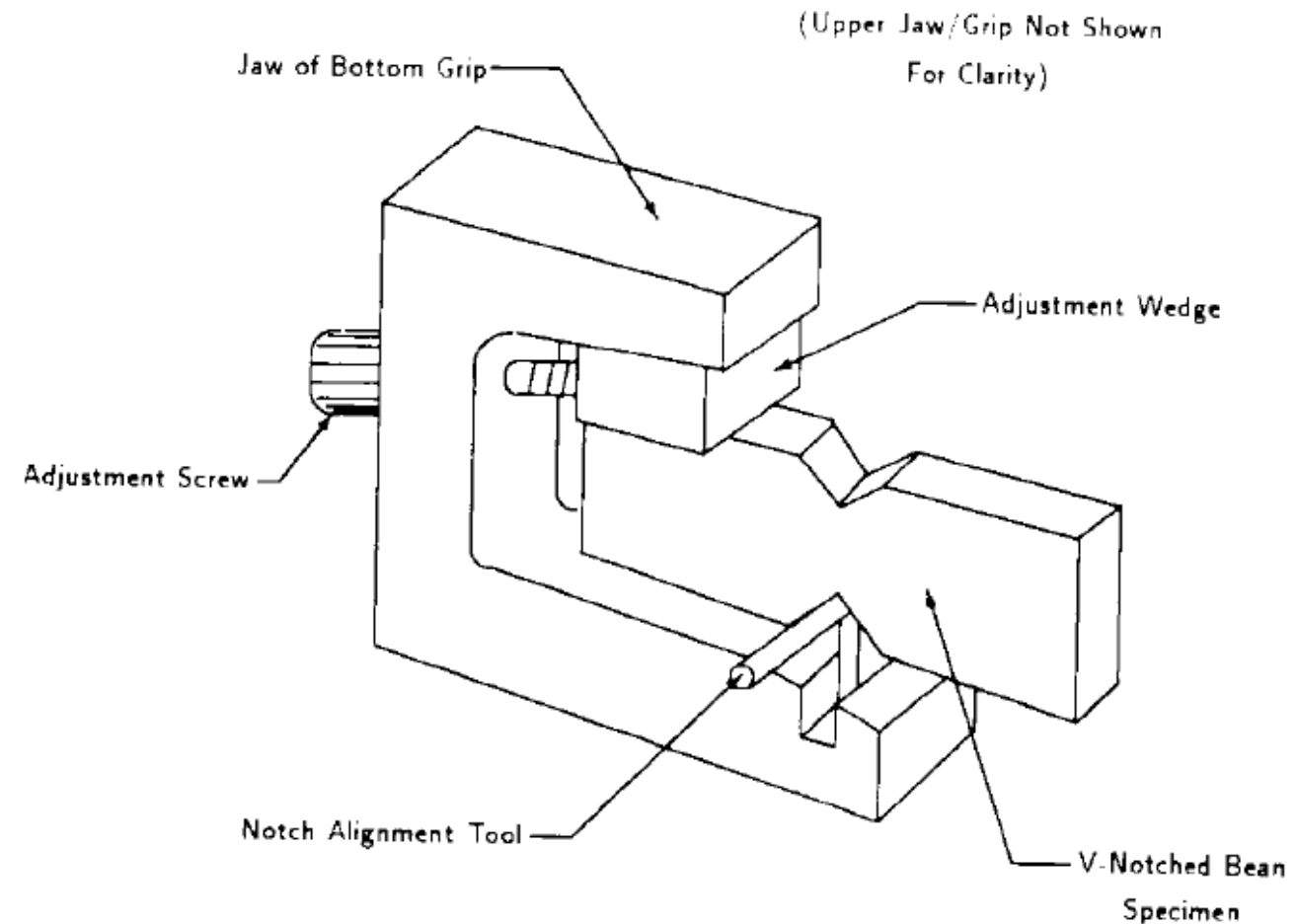
- Except for the highly localised stress concentrations close to the notches, the specimen works as a beam.



Shear tests

Iosipescu test (ASTM D 5379)

- There is an area between the notches subjected to shear stress, where the strain gauges should be bonded at 45° and -45° with the axis of the specimen.
- As this area is too small, the length of the strain gauges grid must not exceed 2 mm.

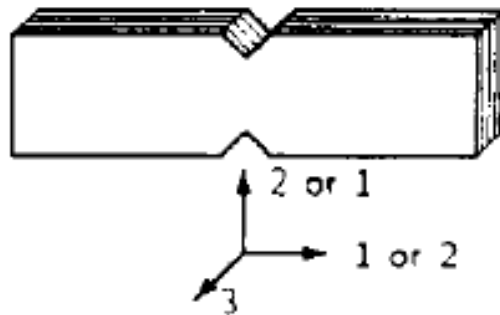


Shear tests

Iosipescu test (ASTM D 5379)

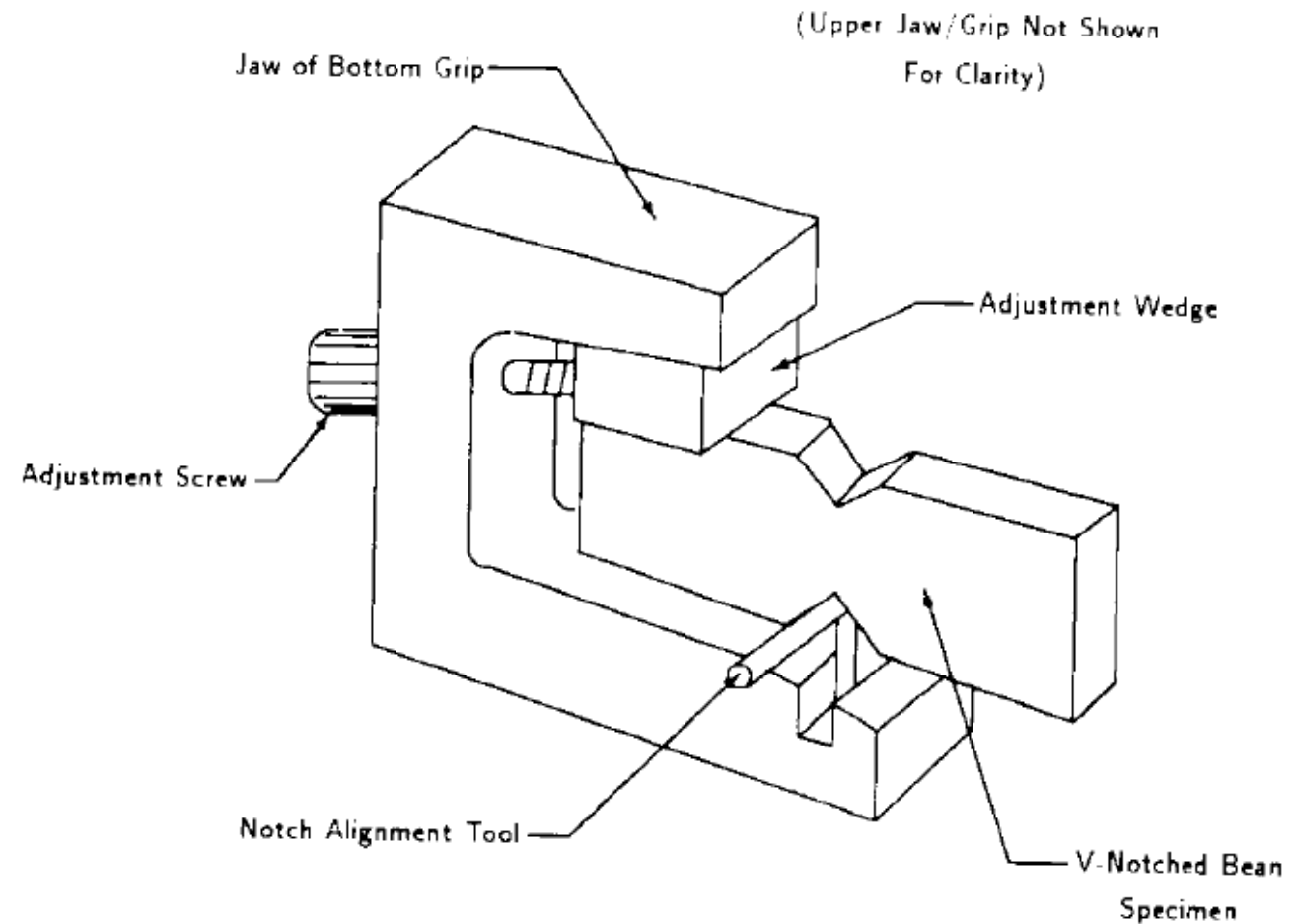
[0/90]_ns or [90/0]_ns Laminates

For $G_{12/21}$



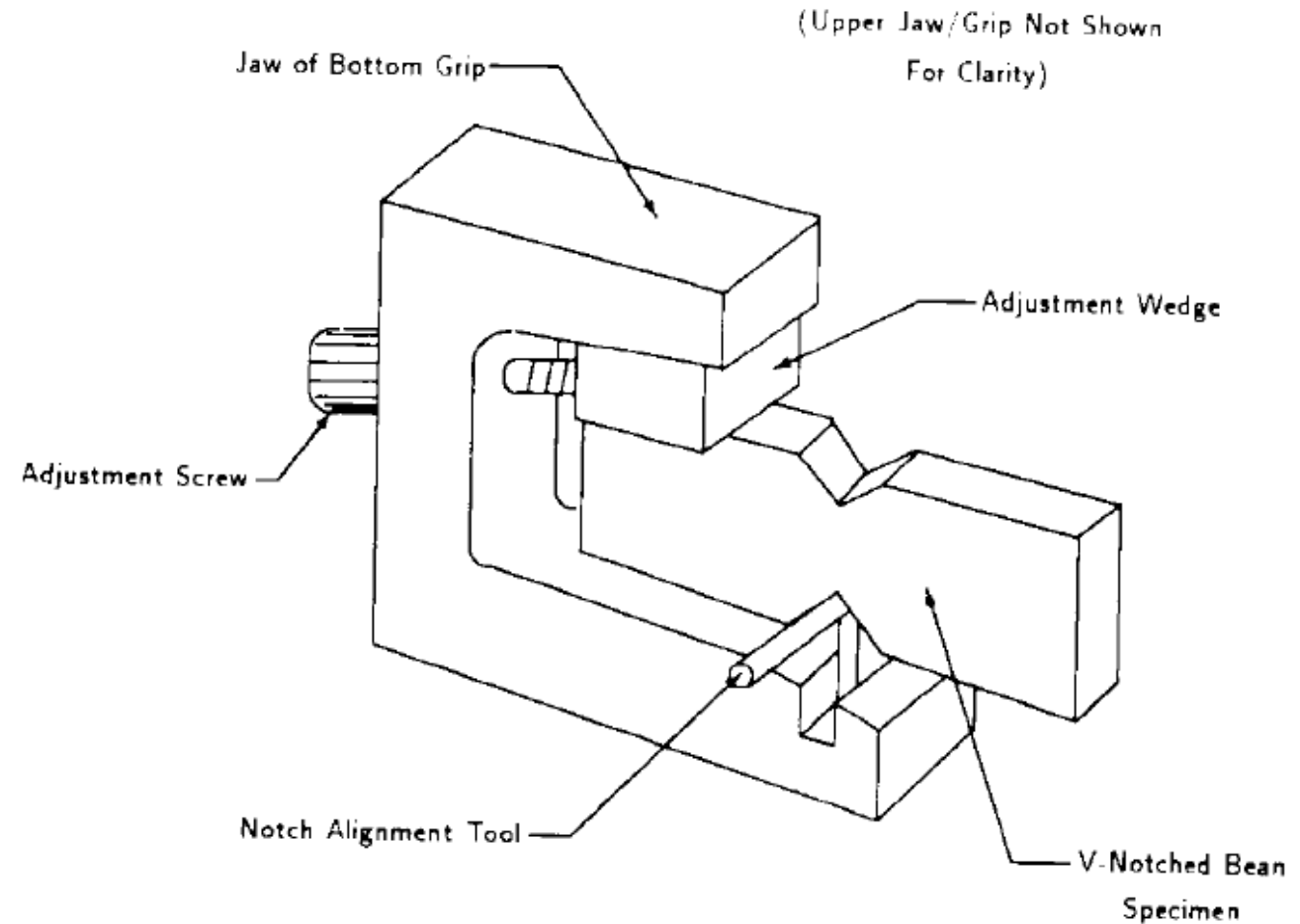
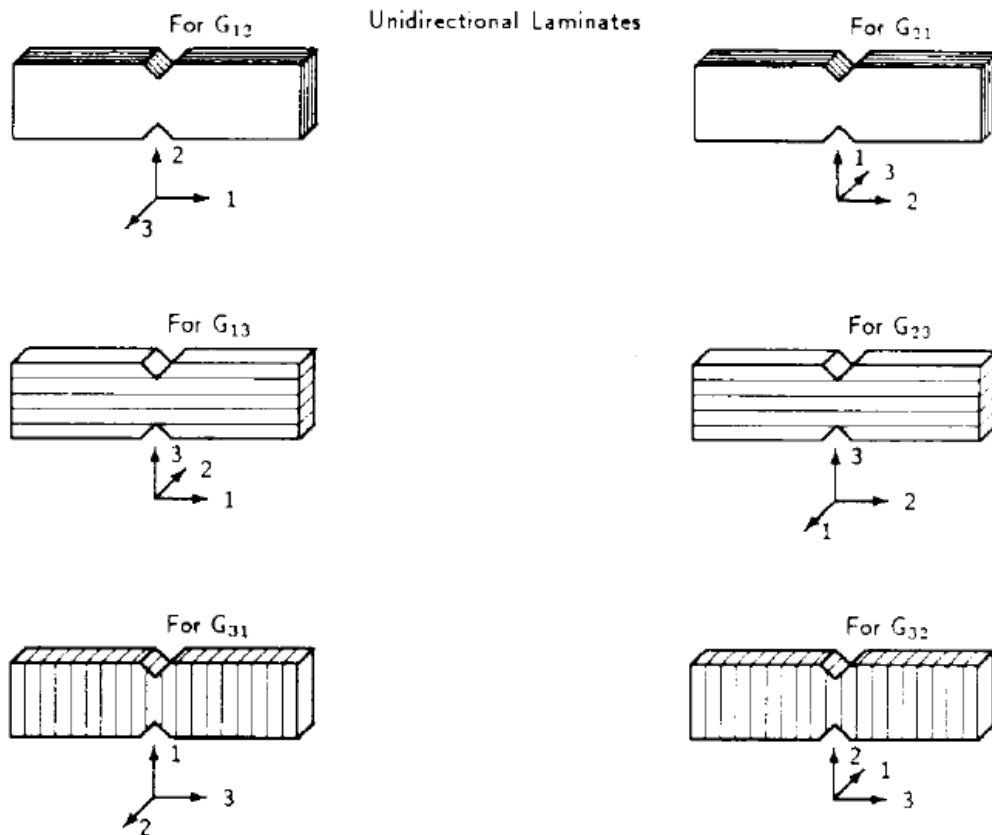
$$\tau_{xy} = \frac{P}{eh}$$

$$G_{xy} = \frac{P}{eh(\epsilon_{45} - \epsilon_{-45})}$$



Shear tests

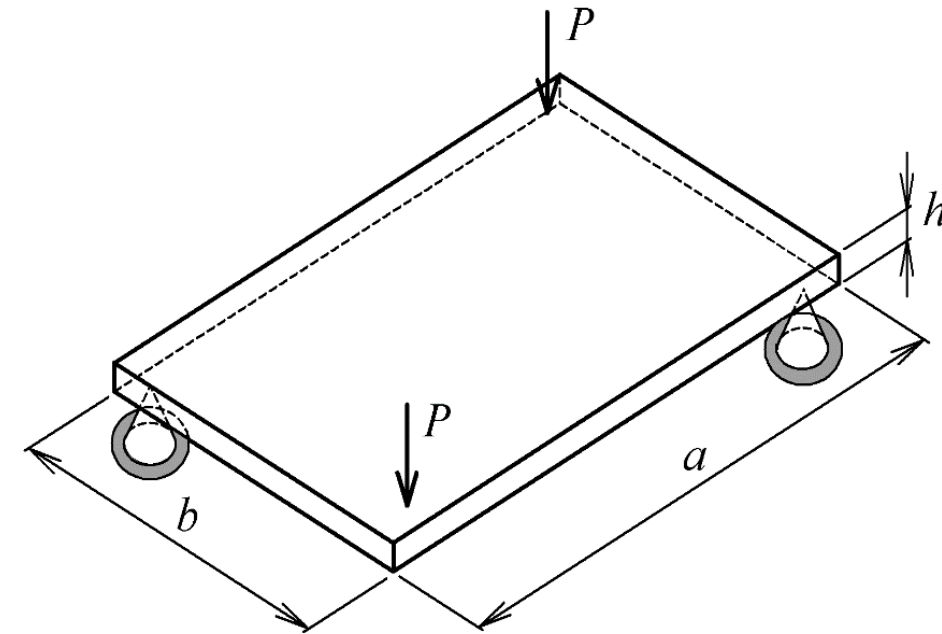
Iosipescu test (ASTM D 5379)



Shear tests

Torsion test of plates

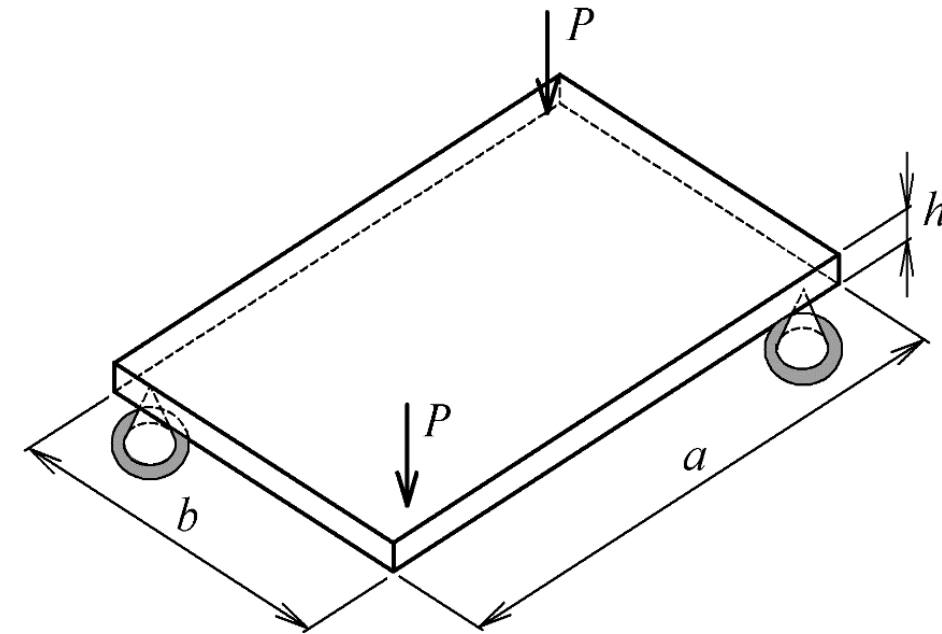
- A rectangular plate supported at two points on a diagonal is subjected to loads applied at two points on the opposite diagonal.
- This loading leads to shear stresses on $[0^\circ]_n$ and $[90^\circ]_n$ unidirectional laminates, but not with other stacking sequences.
- The torsion test of plates is **not adequate** to measure **shear strength**, but gives a simple way to determine **shear modulus**.



Shear tests

Torsion test of plates

- δ is the displacement of the loading points and K is a correction factor in the case the support and loading points are not coincident with the plate vertices.
- This test is easy to perform and requires no strain gauges, as it ensures a uniform state of stress over almost the entire specimen.
- It is therefore considered one of the best methods to measure the shear modulus of composites systems.

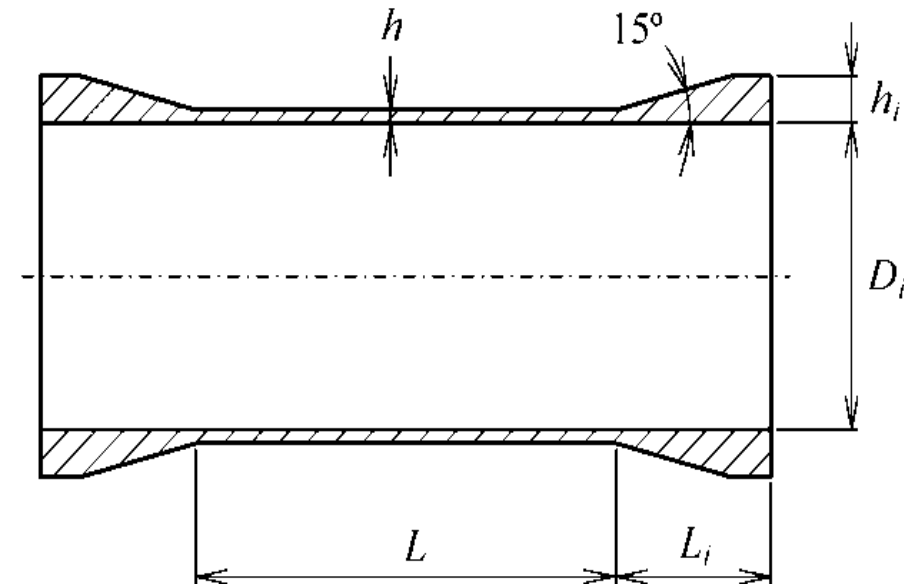


$$G_{12} = K \frac{3Pab}{2\delta h^3}$$

Shear tests

Torsion test of thin-walled tubes (ASTM D 5448)

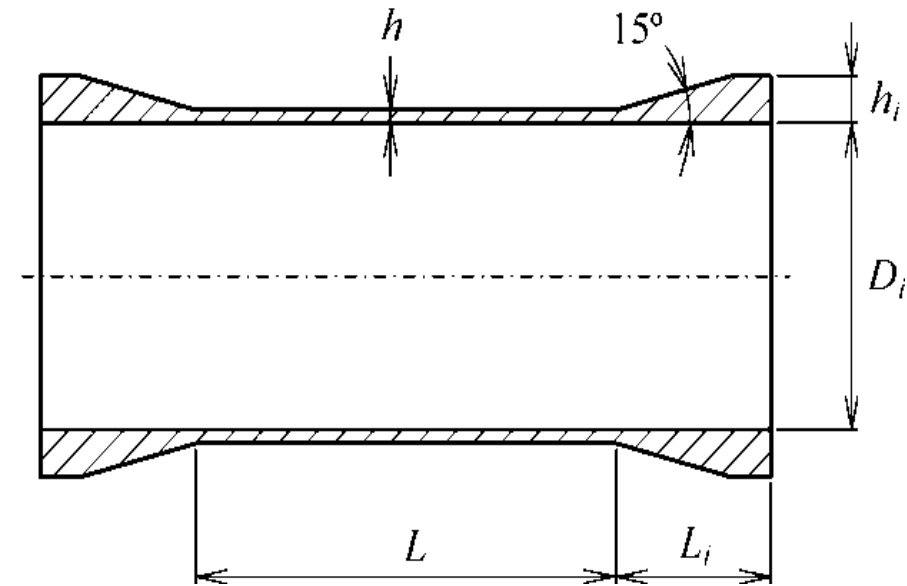
- From the point of view of Mechanics of Materials, the torsion test of thin-walled tubes is the ideal to characterise the shear behaviour, as it ensures a pure shear stress state, and with approximately constant stress through the thin wall thickness.
- In the case of composites of continuous fibres, the pipe to be tested must be manufactured by circumferential filament winding.



Shear tests

Torsion test of thin-walled tubes (ASTM D 5448)

- The shear stress in a thin-walled tube is a function of the applied torsion moment M_t and of the outer and internal diameters D_o and D_i , respectively.
- The ends of the specimen have reinforced winding and are bonded with structural adhesives to the flanges to be fixed to the test machine.
- The test speed is $2^\circ/\text{min}$.



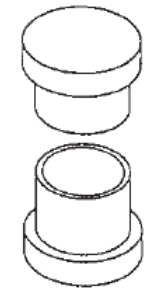
$$G_{xy} = \frac{\tau_{xy}}{\gamma_{xy}} = \frac{\tau_{xy}}{\varepsilon_{45} - \varepsilon_{-45}}$$

$$\tau_{xy} = \frac{32M_t R_o}{\pi(D_o^4 - D_i^4)}$$

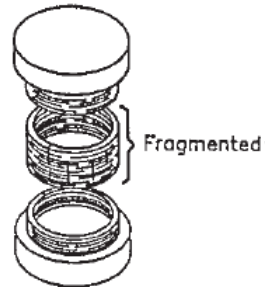
Shear tests

Torsion test of thin-walled tubes (ASTM D 5448)

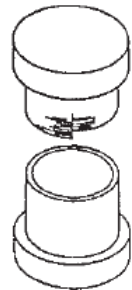
Failure modes



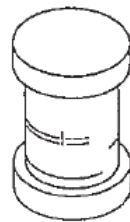
CLASSICAL



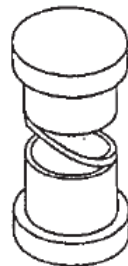
CATASTROPHIC



LOCAL
INSTABILITY



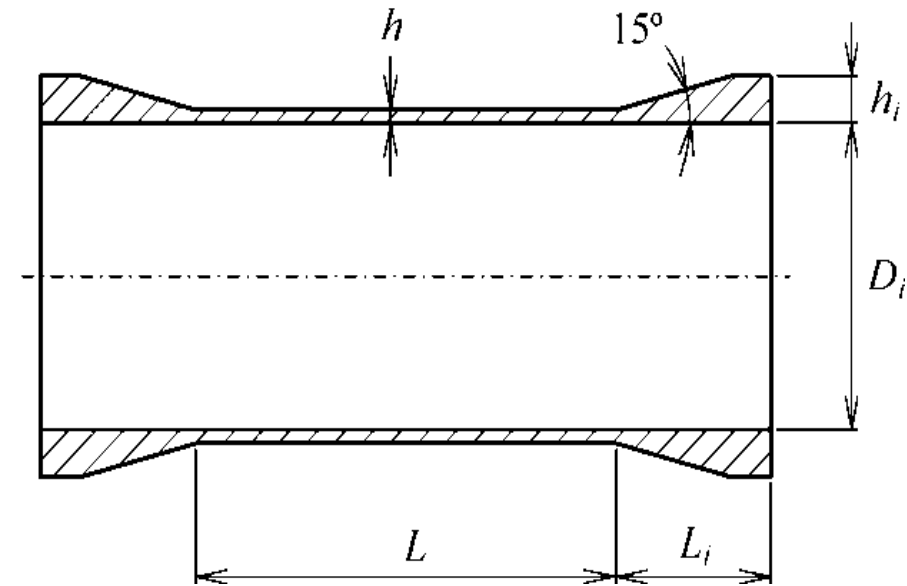
PARTIAL



BAND
SPIRAL



BAND
DETACHMENT



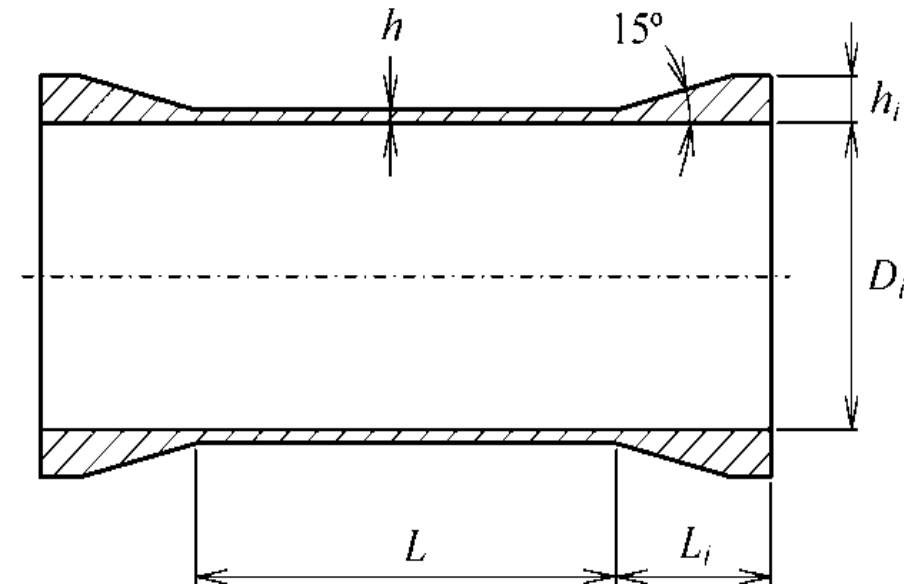
$$G_{xy} = \frac{\tau_{xy}}{\gamma_{xy}} = \frac{\tau_{xy}}{\epsilon_{45} - \epsilon_{-45}}$$

$$\tau_{xy} = \frac{32M_t R_o}{\pi(D_o^4 - D_i^4)}$$

Shear tests

Torsion test of thin-walled tubes (ASTM D 5448)

- Although theoretically ideal, this method is barely used because of the high costs of tubes manufacturing, which are not necessarily representative of the materials to be used in real applications.

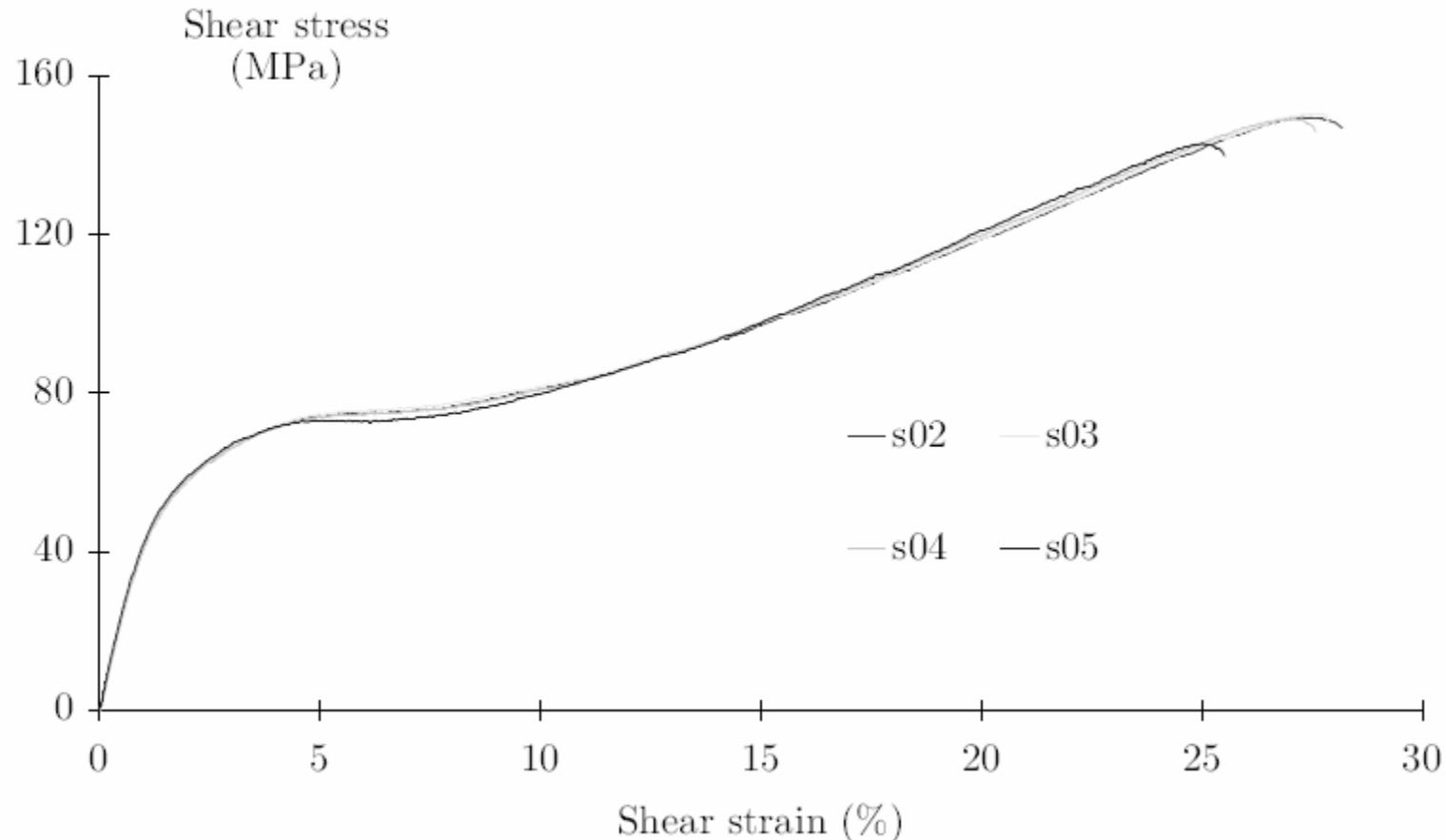


$$G_{xy} = \frac{\tau_{xy}}{\gamma_{xy}} = \frac{\tau_{xy}}{\epsilon_{45} - \epsilon_{-45}}$$

$$\tau_{xy} = \frac{32M_t R_o}{\pi(D_o^4 - D_i^4)}$$

Shear tests

$[\pm 45^\circ]_{ns}$ laminate



Shear tests should be interpreted with caution: the nonlinear shear behaviour is not an intrinsic property of the ply, but it depends on the laminate where the ply is inserted.

Shear tests

Tests

$\pm 45^\circ$ tensile test

Advantages

Shear modulus and strength
 Specimen preparation
 Standard test equipment
 Data reduction
 Can be used for cyclic and environmental conditions
 ASTM and ISO Standards

Disadvantages

Stain limit often required for strength
 Only suitable for continuous aligned fibres
 Special laminate layup required
 Strength dependent on the number of layers
 Strain gauges or extensometers required

10° off-axis test

Shear modulus and strength
 Additional in-plane elastic properties
 Specimen preparation
 Standard test equipment
 Can be used for cyclic and environmental conditions

Only suitable for continuous aligned fibres
 Mixed mode failure
 Three element rosette required
 Data reduction complex
 Sensitive to specimen/strain gauge misalignment
 No existing standard

Shear tests

Tests

Rail shear test

Advantages

Shear modulus and strength
 Compatible with most material types
 Stress state fairly uniform near the specimen centre
 Data reduction
 Can be used for cyclic and environmental conditions

Disadvantages

Large specimen/extensive preparation
 Specimen susceptible to machining defects
 Difficult to bolt/bond specimen to loading rails
 Special test fixture required
 Strain gauges required
 Large scatter in strength data

V-notched beam test

Shear modulus and strength
 Compatible with most material types
 Small quantity of material is required
 Data reduction
 Suitable for use under environmental conditions
 ASTM standard

Accurate specimen machining required
 Special test fixture required
 Strain gauges required
 Non-uniform shear stress state
 ASTM test fixture not completely satisfactory
 Cannot be used under cyclic loading

Shear tests

Tests

Plate twist test

Advantages

Shear modulus only

Compatible with most material types

Stress state fairly uniform

Easy and economic specimen
manufacturing

Easy and economic testing and
data reduction

Can be used for cyclic and
environmental conditions

ISO standard

Disadvantages

Not suitable for strength data

Shear tests

Tests

Torsion of thin
wall tube

Advantages

Shear modulus and strength
Compatible with most material types
Stress state fairly uniform
Data reduction
Can be used for cyclic and
environmental conditions
ASTM standard only

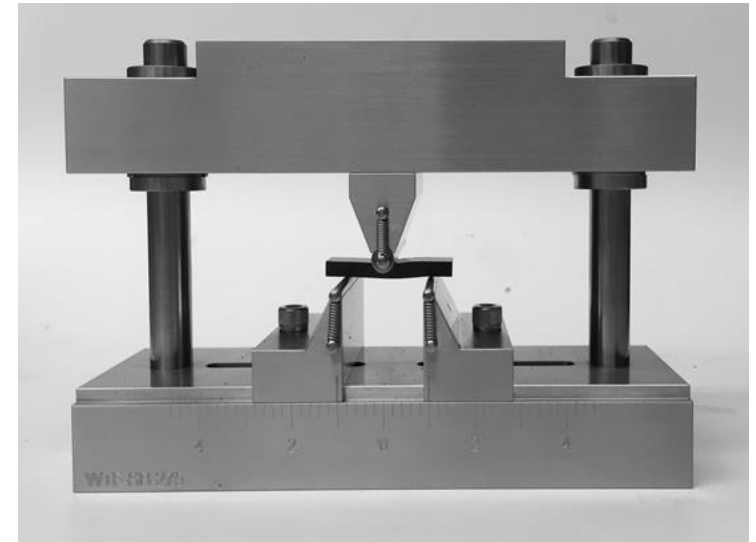
Disadvantages

Large and expensive cylinder specimen
Extensive specimen preparation and testing
Torsion facility and adhesively bonded grips
Alignment fixture for specimen preparation
Strain gauges required
Non-uniform through-thickness shear stress

Interlaminar shear strength (ILSS)

Short-beam shear test ASTM D 2344

- 3-point bending test configuration.
- The distance, L , between supports is deliberately reduced in order to promote an interlaminar shear failure instead of bending failure.
- According to Beam Theory, the shear stress has a parabolic distribution in the thickness direction, becoming zero at the surfaces and having the maximum value in the middle.



$$\tau_{xz}^{\max} = \frac{3P}{4Bh}$$

Bending tests

- Bending tests are required to determine the bending modulus.
- Even if it is considered that the compressive modulus is equal to the tensile modulus, the bending modulus is not necessarily equal to the tensile modulus.

Considering a $[0^\circ]_4$ carbon/epoxy laminate, the laminate Young's modulus determined using a tensile test and bending test, E_{T1} (E_{T2}) and E_{F1} (E_{F2}) respectively, are equal:

$$E_{T1} = E_{F1} = 129 \text{ GPa}$$

$$E_{T2} = E_{F2} = 9.5 \text{ GPa}$$

Bending tests

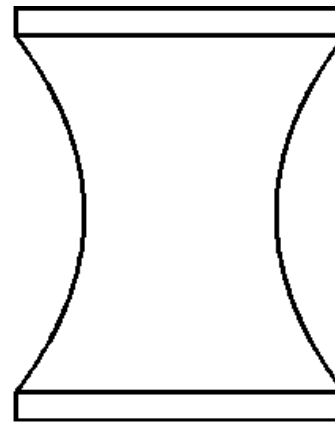
- Bending tests are required to determine the bending modulus.
- Even if it is considered that the compressive modulus is equal to the tensile modulus, the bending modulus is not necessarily equal to the tensile modulus.

If the laminate has two resin-rich layers (RRL), 0.1 mm thick each, $(0^\circ/\text{RRL}/0^\circ)_s$, the Young's modulus determined using tensile and bending tests, E_{T1} (E_{T2}) and E_{F1} (E_{F2}) are different:

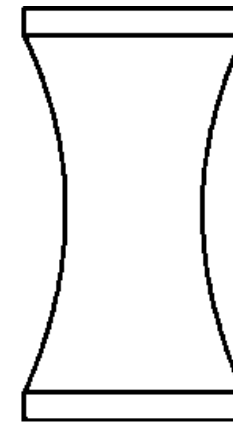
$$E_{T1} = 93.86 \text{ GPa} ; E_{F1} = 101.93 \text{ GPa}$$
$$E_{T2} = 8.75 \text{ GPa} ; E_{F2} = 8.92 \text{ GPa}$$

Properties in the thickness direction

- Require very thick specimens, typically between 15 and 25 mm, which, in addition to be very expensive, can be problematic in view of the exothermic nature of the cure process and the poor thermal conductivity of polymers.
- Examples of specimens used in tensile and compressive tests in the thickness direction:
 - a) Double elliptical curvature
 - b) Rectangular central section



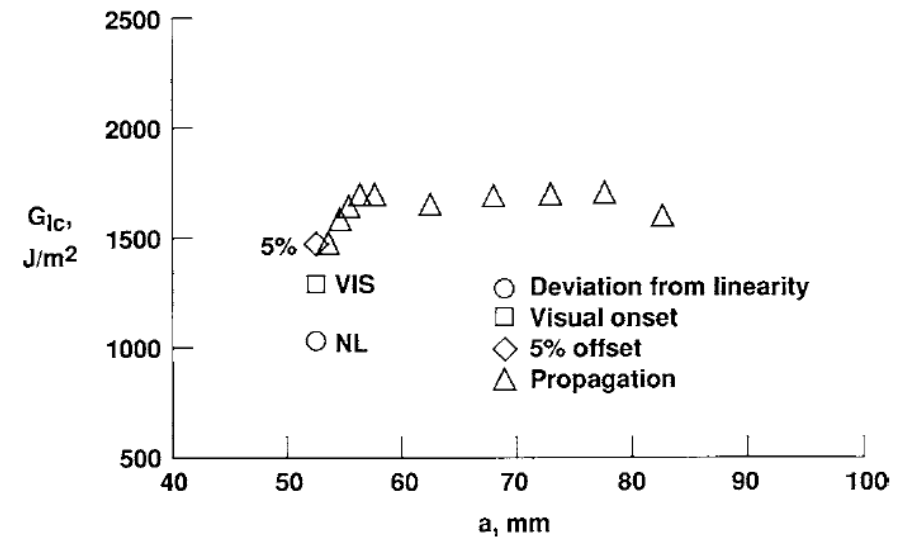
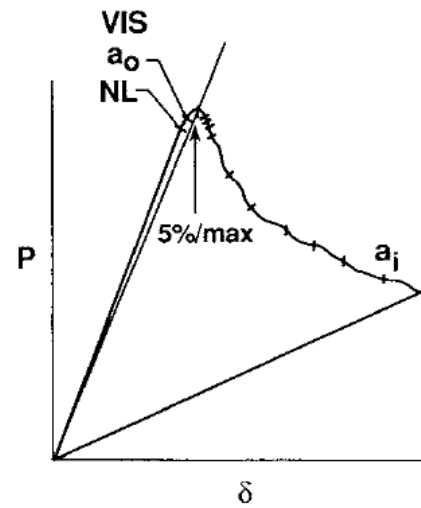
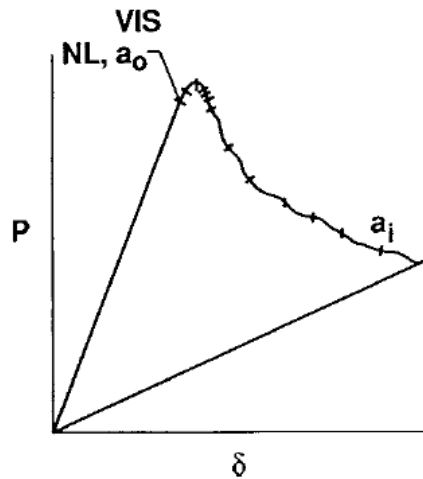
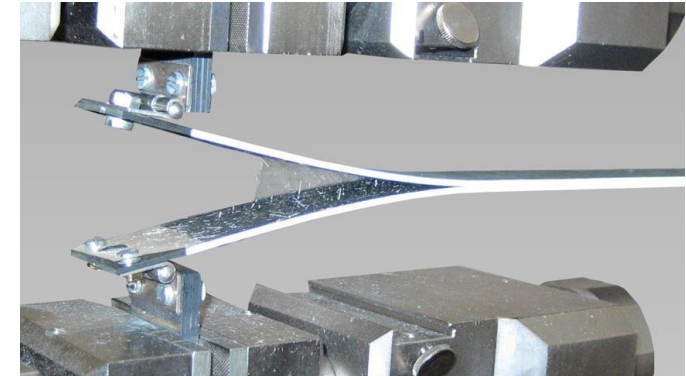
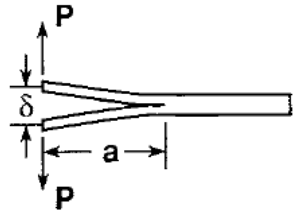
a)



b)

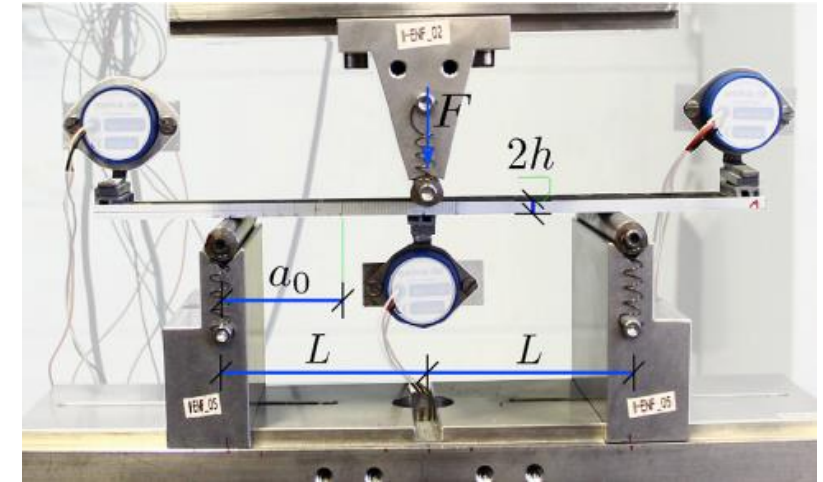
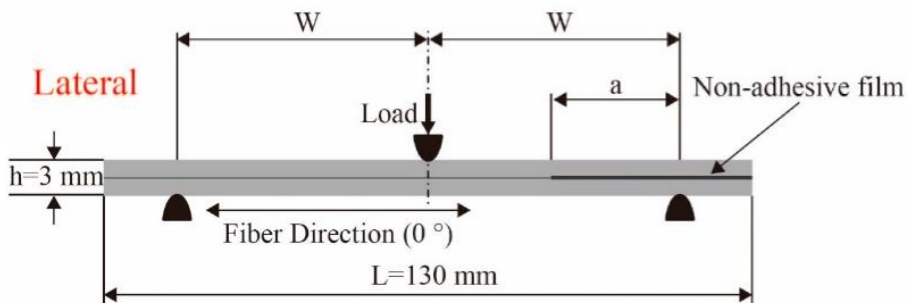
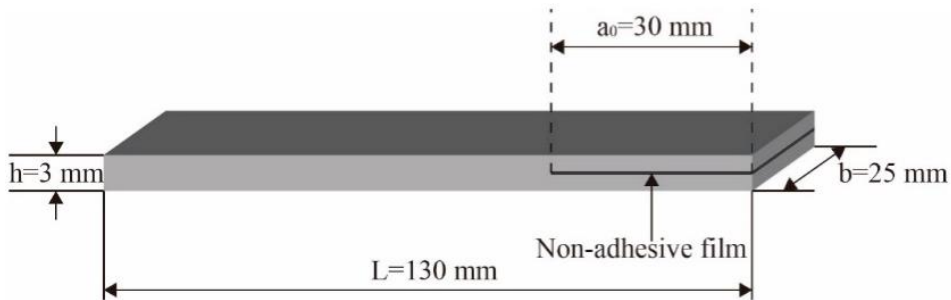
Mode I (opening) interlaminar fracture toughness

Double cantilever beam (DCB) test ASTM D 5528



Mode II (sliding) interlaminar fracture toughness

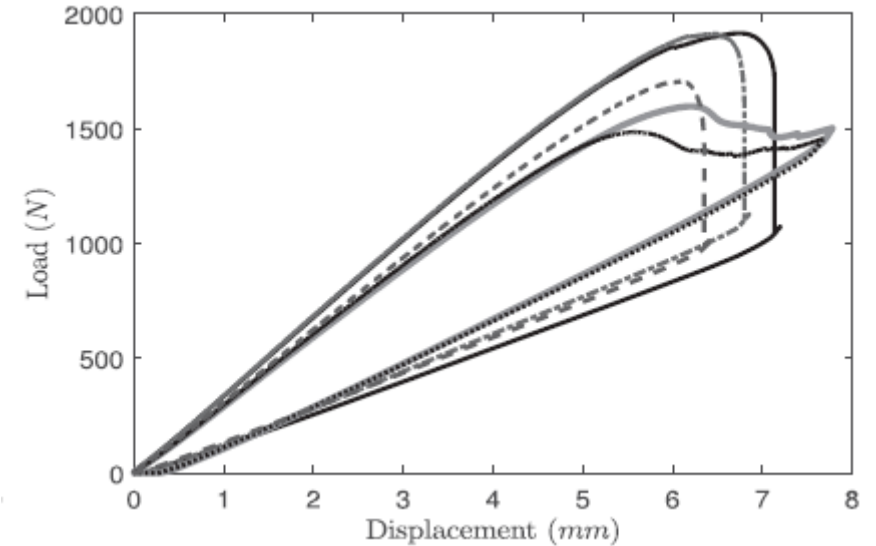
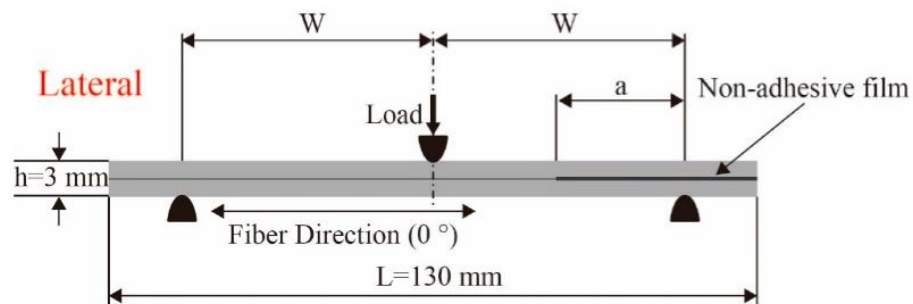
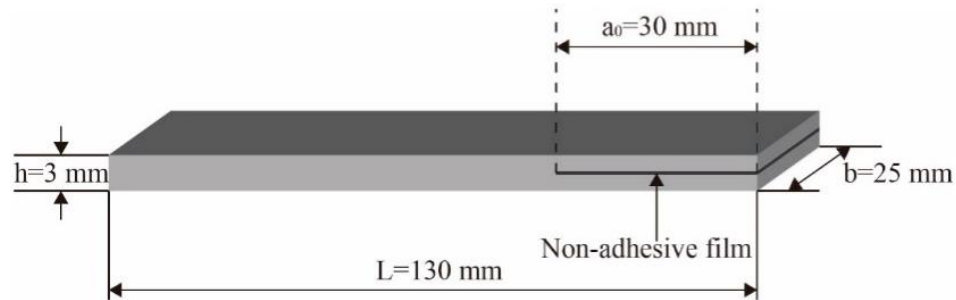
End-notched flexure (ENF) test ASTM D 7905



[S. Abdel-Monsef. A COMPREHENSIVE METHODOLOGY TO ANALYSE BONDED JOINTS SUBJECTED TO DIFFERENT ENVIRONMENTAL CONDITIONS. Doctoral Thesis, Universitat de Girona, 2020. Composite Structures 234 \(2020\) 111689. <https://doi.org/10.1016/j.compstruct.2019.111689>](#)

Mode II (sliding) interlaminar fracture toughness

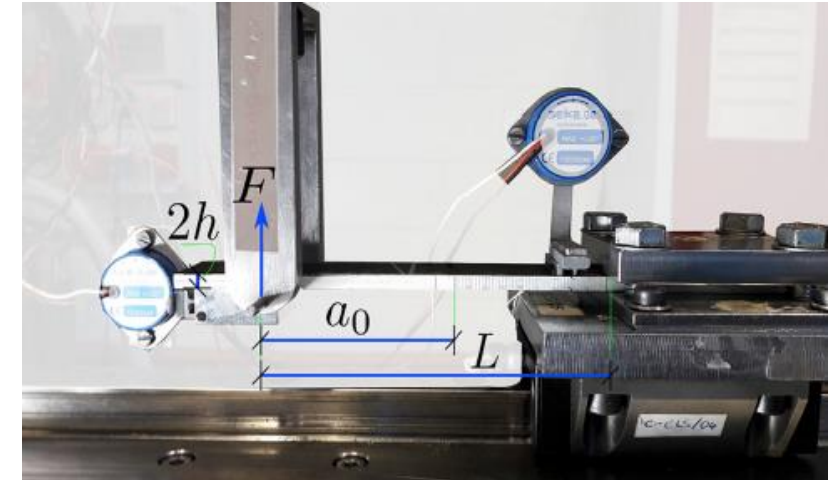
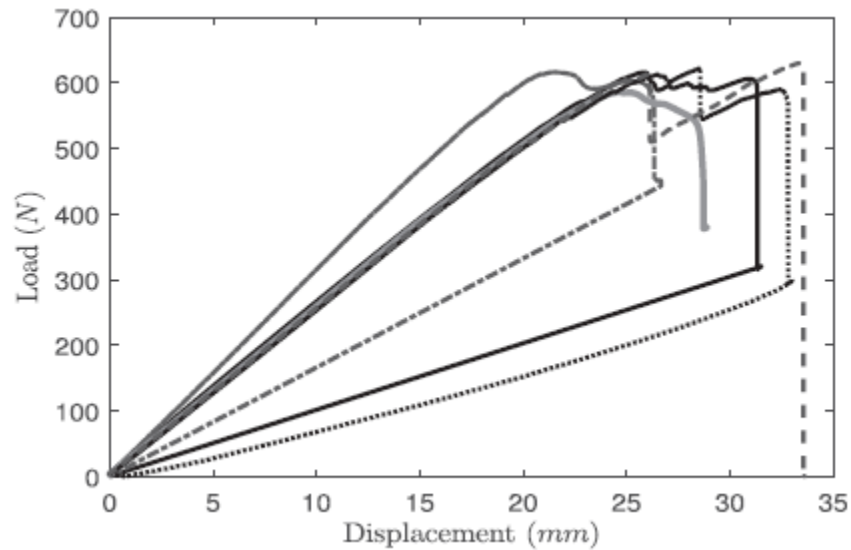
End-notched flexure (ENF) test ASTM D 7905



[S. Abdel-Monsef. A COMPREHENSIVE METHODOLOGY TO ANALYSE BONDED JOINTS SUBJECTED TO DIFFERENT ENVIRONMENTAL CONDITIONS. Doctoral Thesis, Universitat de Girona, 2020. Composite Structures 234 \(2020\) 111689. <https://doi.org/10.1016/j.compstruct.2019.111689>](#)

Mode II (sliding) interlaminar fracture toughness

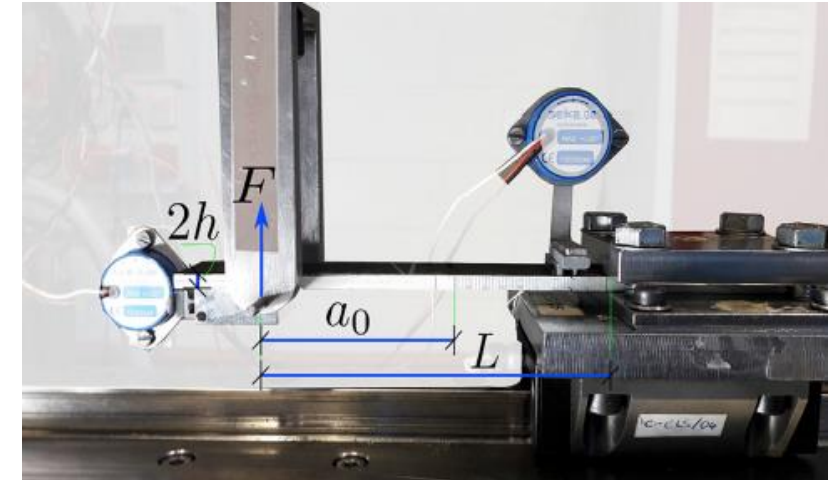
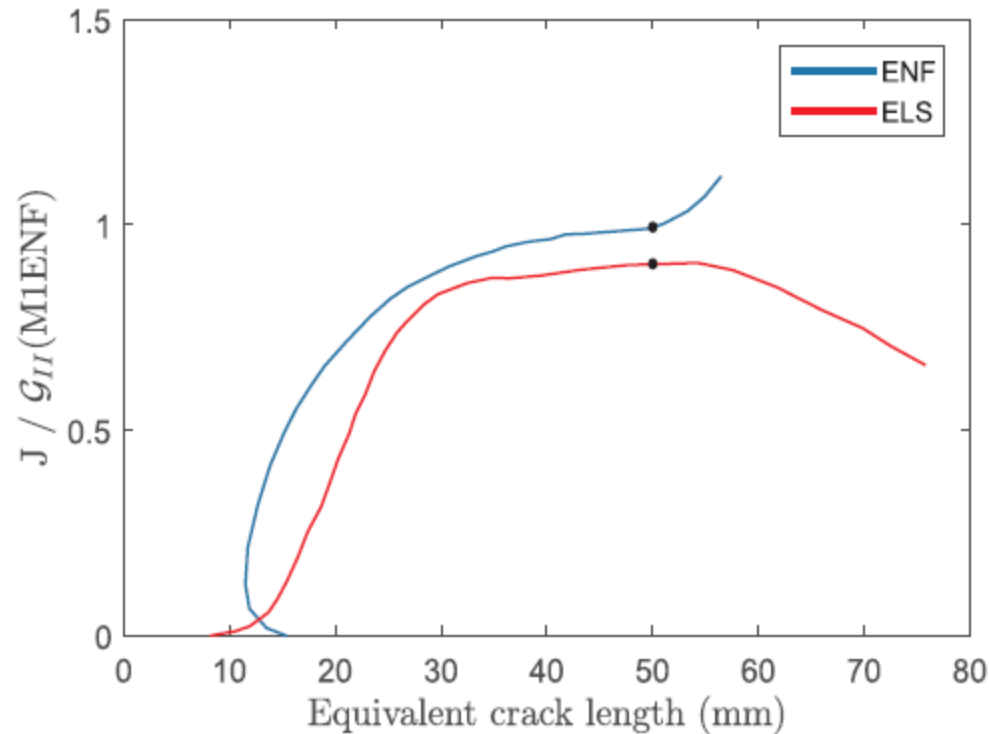
End-load split (ELS) test ISO 15114



[S. Abdel-Monsef. A COMPREHENSIVE METHODOLOGY TO ANALYSE BONDED JOINTS SUBJECTED TO DIFFERENT ENVIRONMENTAL CONDITIONS. Doctoral Thesis, Universitat de Girona, 2020. Composite Structures 234 \(2020\) 111689. <https://doi.org/10.1016/j.compstruct.2019.111689>](#)

Mode II (sliding) interlaminar fracture toughness

End-load split (ELS) test ISO 15114



S. Abdel-Monsef. A COMPREHENSIVE METHODOLOGY TO ANALYSE BONDED JOINTS SUBJECTED TO DIFFERENT ENVIRONMENTAL CONDITIONS. Doctoral Thesis, Universitat de Girona, 2020. Composite Structures 234 (2020) 111689. <https://doi.org/10.1016/j.compstruct.2019.111689>

Mixed mode I-mode II interlaminar fracture toughness

Mixed-mode bending test ASTM D 6671

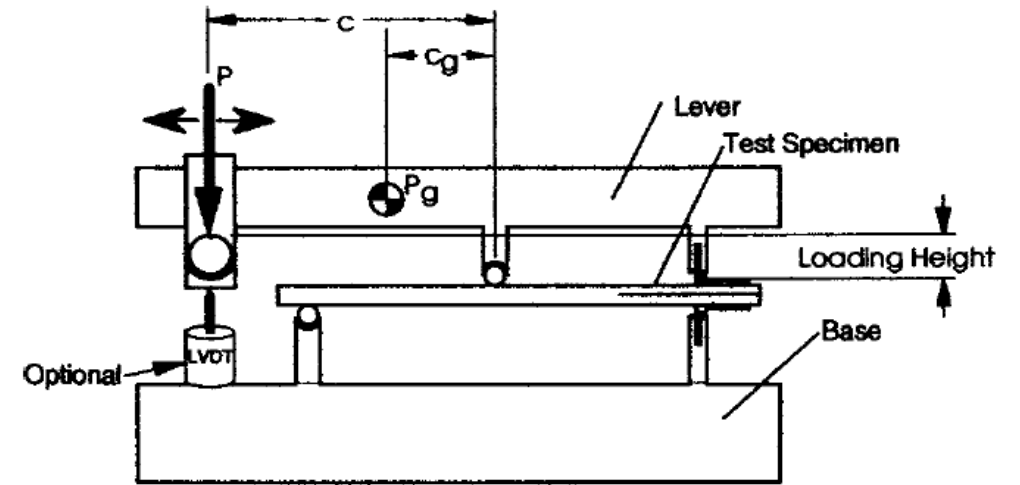
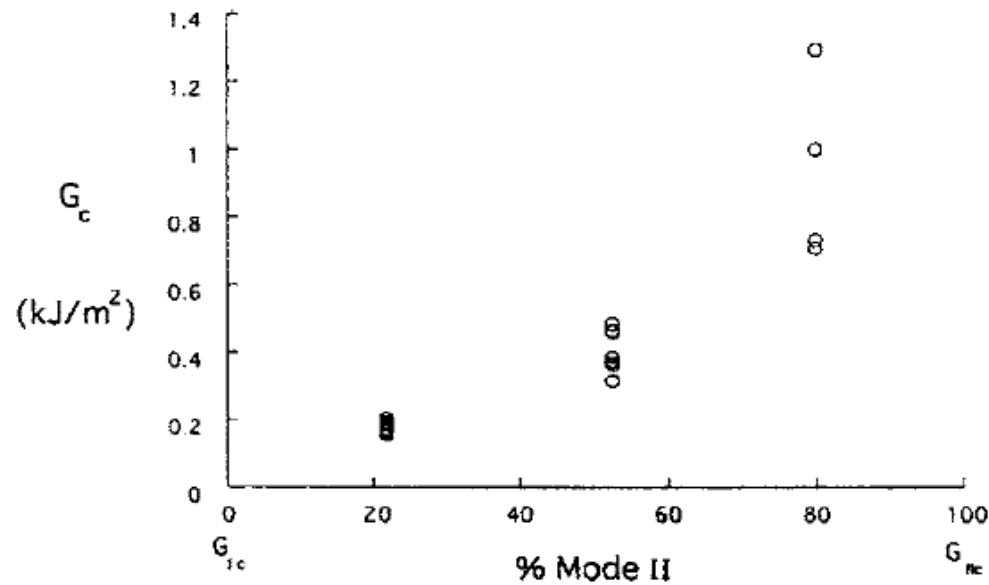
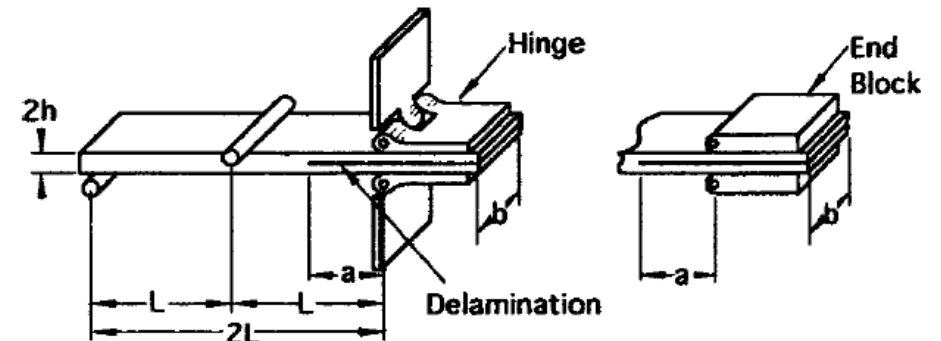
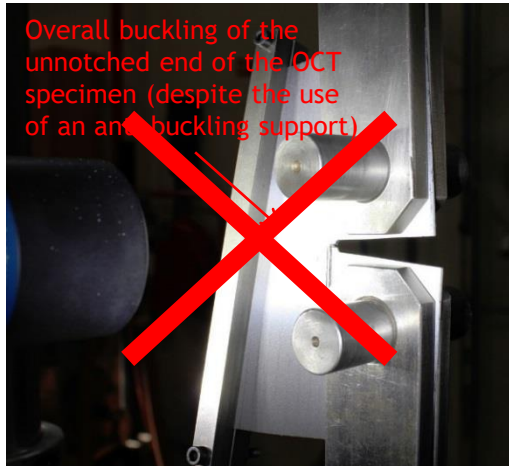


FIG. 1 MMB Apparatus

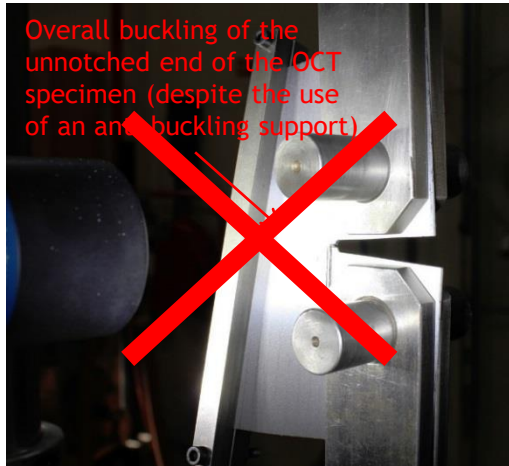


Intralaminar fracture toughness

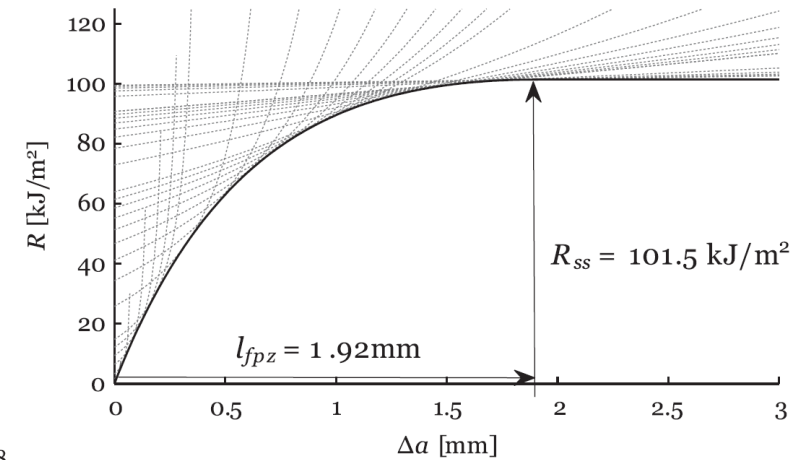
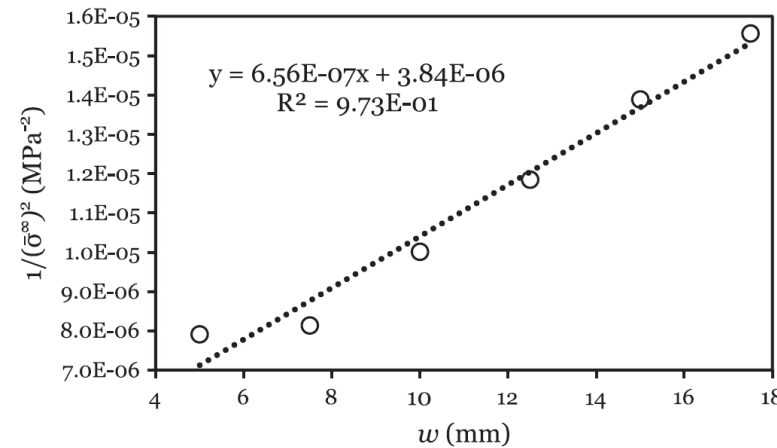
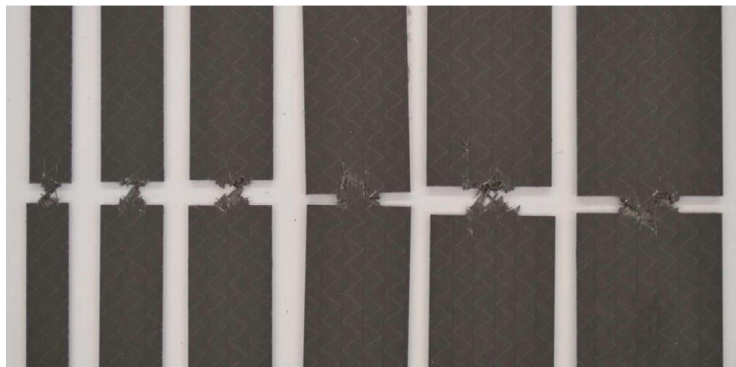


- Proposal of a robust test method to measure the fracture toughness of the 0° plies and of multidirectional laminates in tension and in compression.
- Determination of the mode I crack resistance curve (R-curve) of composite laminates from the *size effect law* of geometrically similar specimens of different sizes with *positive geometry*.

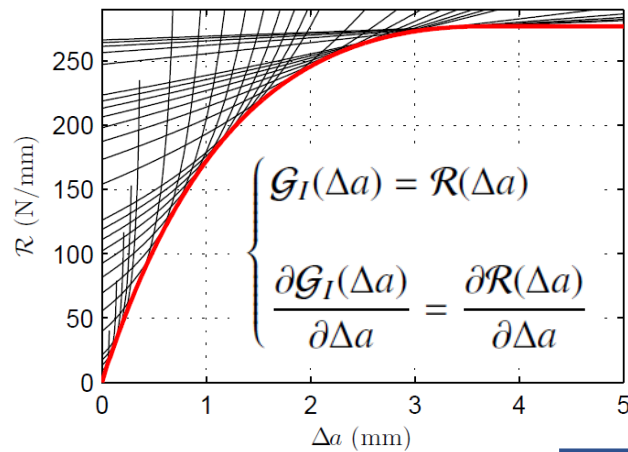
Intralaminar fracture toughness



- Proposal of a robust test method to measure the fracture toughness of the 0° plies and of multidirectional laminates in tension and in compression

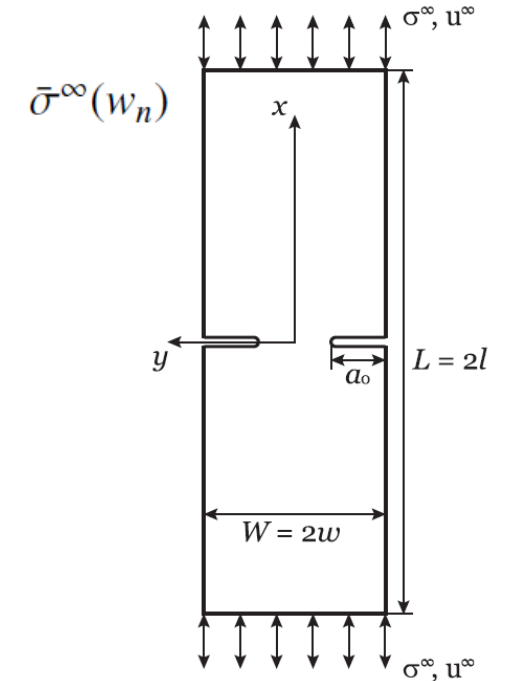


Intralaminar fracture toughness



$$\mathcal{G}_I = \frac{1}{E} \mathcal{K}_I^2$$

$$\begin{aligned} \acute{E} &= \left(\frac{1 + \rho}{2E_x E_y} \right)^{-1/2} \mu^{-1/4} \\ \rho &= \frac{(E_x E_y)^{1/2}}{2G_{xy}} - (v_{xy} v_{yx})^{1/2} \\ \mu &= \frac{E_y}{E_x} \end{aligned}$$



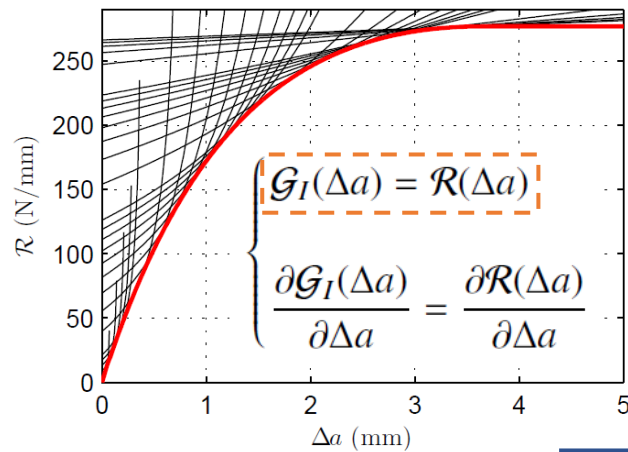
$$\begin{aligned} \alpha &= a/w \\ \varphi &= \mu^{-1/4} w/l \end{aligned}$$

$$\mathcal{G}_I(\Delta a) = \frac{1}{E} w (\sigma^\infty)^2 \kappa^2 \left(\alpha_0 + \frac{\Delta a}{w}, \rho, \varphi \right)$$

References

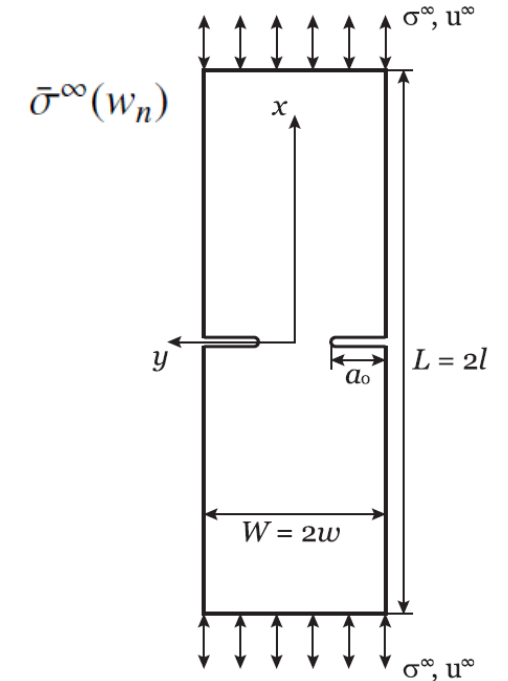
- Catalanotti G, Xavier J, Camanho PP. Measurement of the compressive crack resistance curve of composites using the size effect law. *Compos Part A-Appl S* 2014;56:300-307.
- Catalanotti G, Arteiro A, Hayati M, Camanho PP. Determination of the mode I crack resistance curve of polymer composites using the size-effect law. *Eng Fract Mech* 2014;118:49-65.

Intralaminar fracture toughness



$$G_I = \frac{1}{E} \mathcal{K}_I^2$$

$$\begin{aligned} \dot{E} &= \left(\frac{1 + \rho}{2E_x E_y} \right)^{-1/2} \mu^{-1/4} \\ \rho &= \frac{(E_x E_y)^{1/2}}{2G_{xy}} - (v_{xy} v_{yx})^{1/2} \\ \mu &= \frac{E_y}{E_x} \end{aligned}$$



$$\mathcal{K}_I = \sigma^\infty \sqrt{w} \kappa(\alpha, \rho, \varphi) \quad \begin{cases} \alpha = a/w \\ \varphi = \mu^{-1/4} w/l \end{cases}$$

$$R(\Delta a) = \frac{1}{E} w (\bar{\sigma}^\infty)^2 \kappa^2 \left(\alpha_0 + \frac{\Delta a}{w}, \rho, \varphi \right)$$

↓

$$\bar{\sigma}^\infty = \bar{\sigma}^\infty(w)$$

$$\frac{\partial R}{\partial w} = 0$$

$$\frac{\partial}{\partial w} \left[w (\bar{\sigma}^\infty)^2 \kappa^2 \right] = 0$$

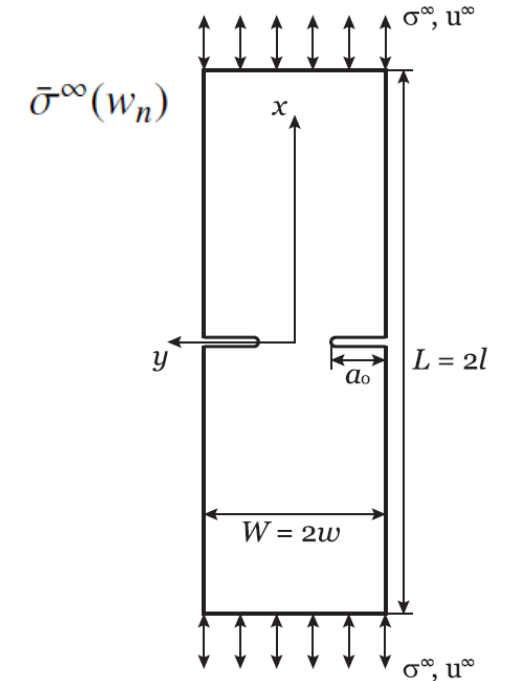
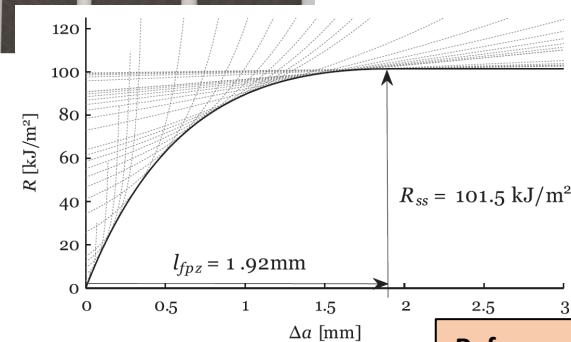
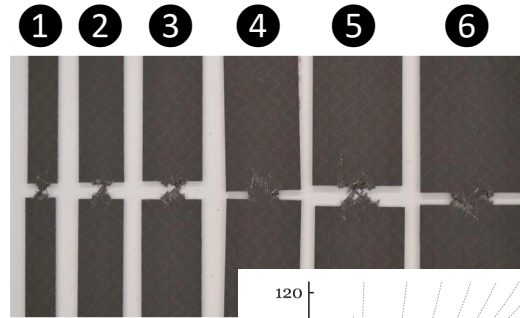
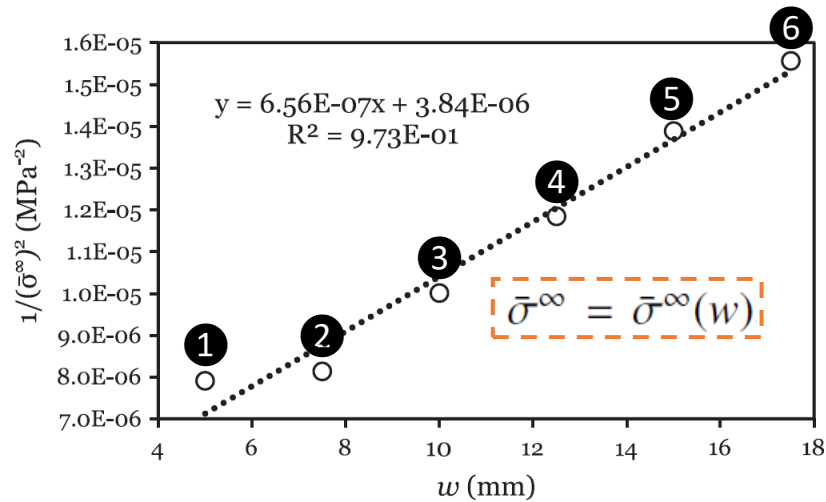
which can be solved for

$$w = w(\Delta a)$$

References

- Catalanotti G, Xavier J, Camanho PP. Measurement of the compressive crack resistance curve of composites using the size effect law. *Compos Part A-Appl S* 2014;56:300-307.
- Catalanotti G, Arteiro A, Hayati M, Camanho PP. Determination of the mode I crack resistance curve of polymer composites using the size-effect law. *Eng Fract Mech* 2014;118:49-65.

Intralaminar fracture toughness



Regressions fit	Formula	Fitting parameters
Bilogarithmic	$\ln \sigma_u = \ln \frac{M}{\sqrt{N+w}}$	M, N
Linear regression I	$\frac{1}{\sigma_u^2} = A w + C$	A, C
Linear regression II	$\frac{1}{w\sigma_u^2} = \hat{A} \frac{1}{w} + \hat{C}$	\hat{A}, \hat{C}

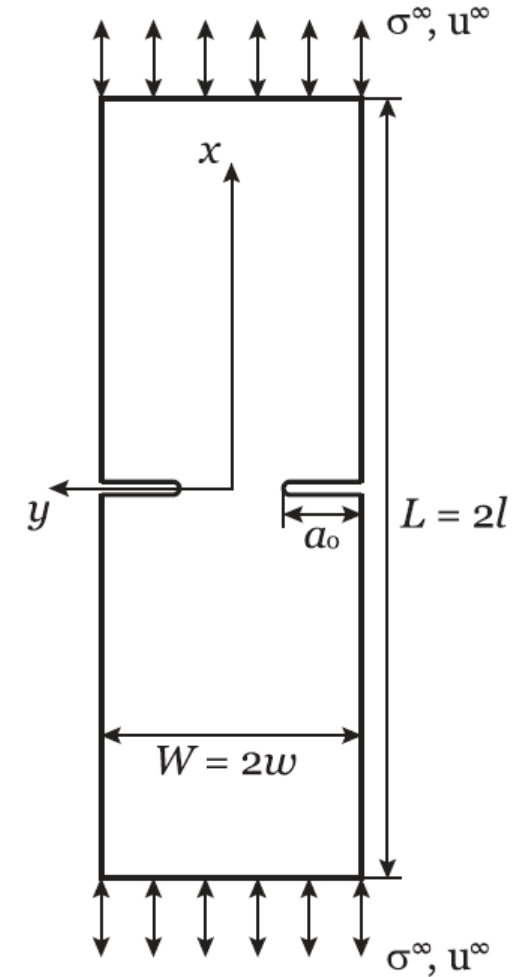
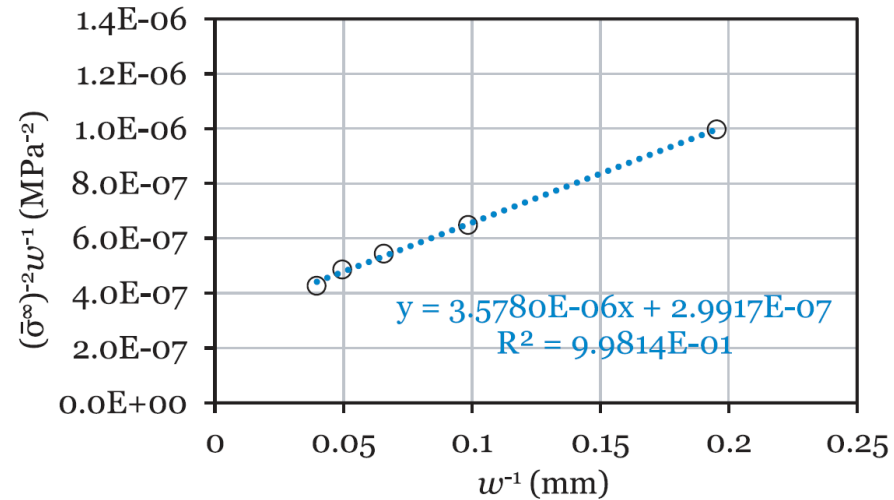
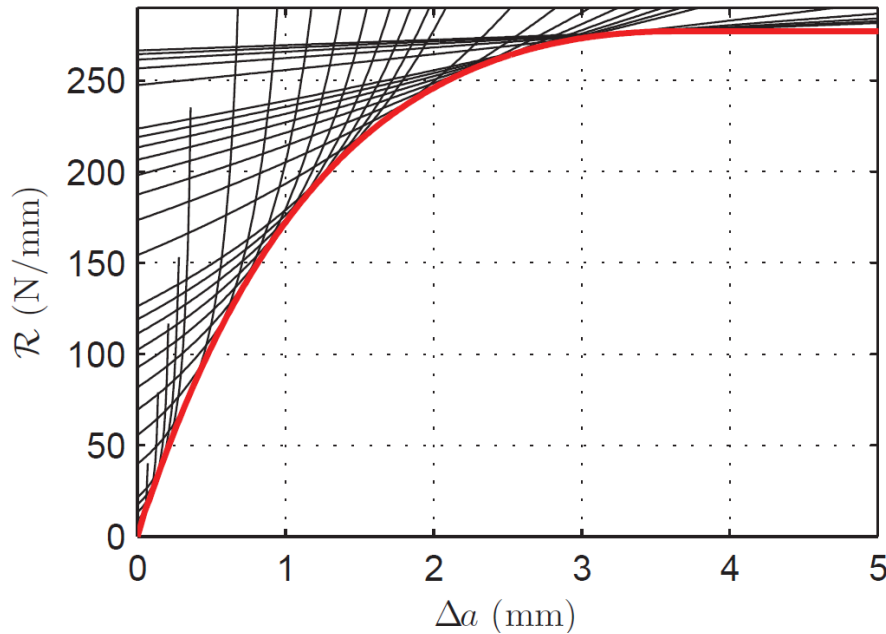
References

Catalanotti G, Xavier J, Camanho PP. Measurement of the compressive crack resistance curve of composites using the size effect law. *Compos Part A-Appl S* 2014;56:300-307.

Catalanotti G, Arteiro A, Hayati M, Camanho PP. Determination of the mode I crack resistance curve of polymer composites using the size-effect law. *Eng Fract Mech* 2014;118:49-65.

Intralaminar fracture toughness

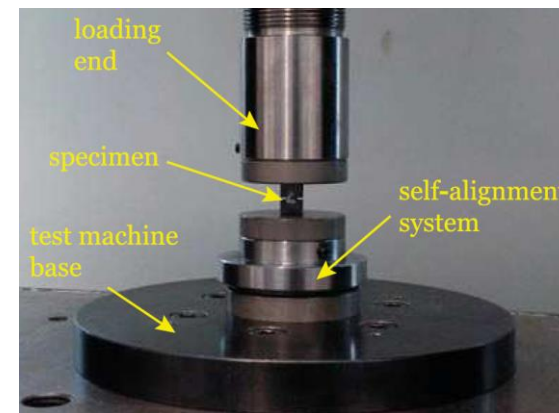
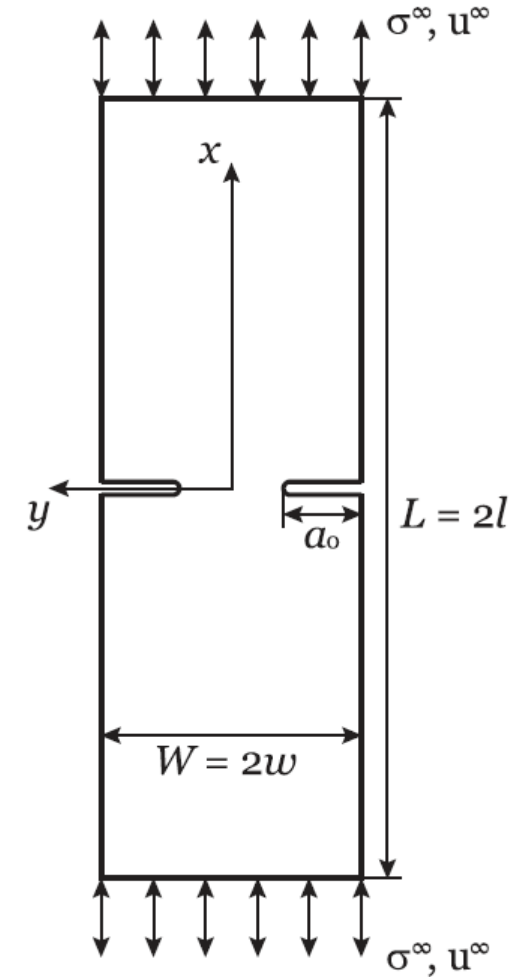
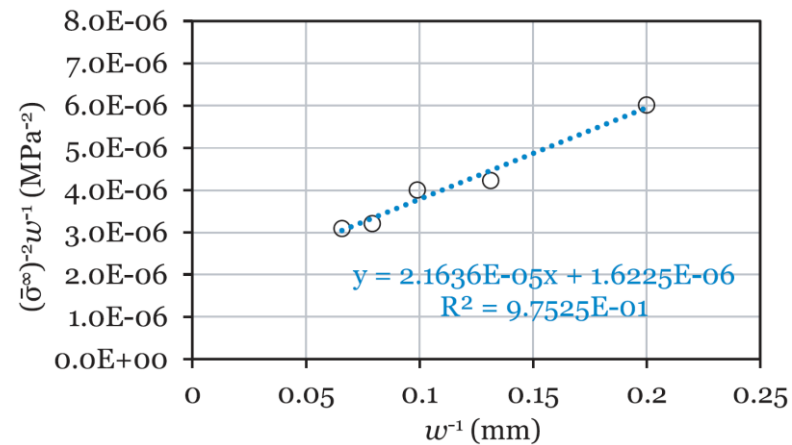
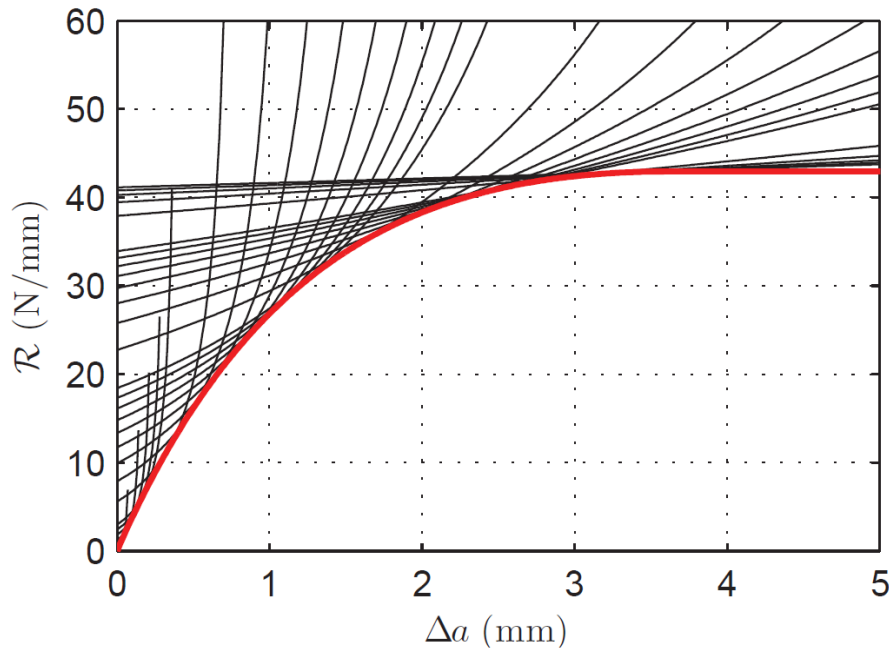
Double edge notch tension size effect law



[A. Arteiro. Structural Mechanics of Thin-Ply Laminated Composites. Universidade do Porto, 2016.](#)

Intralaminar fracture toughness

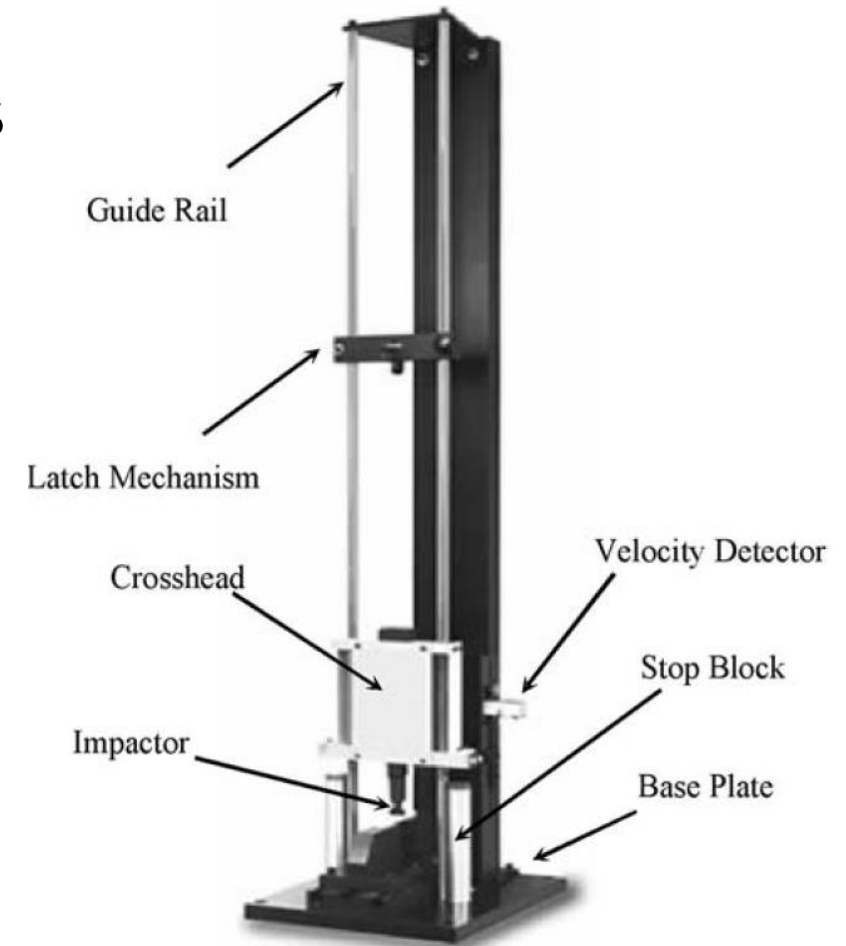
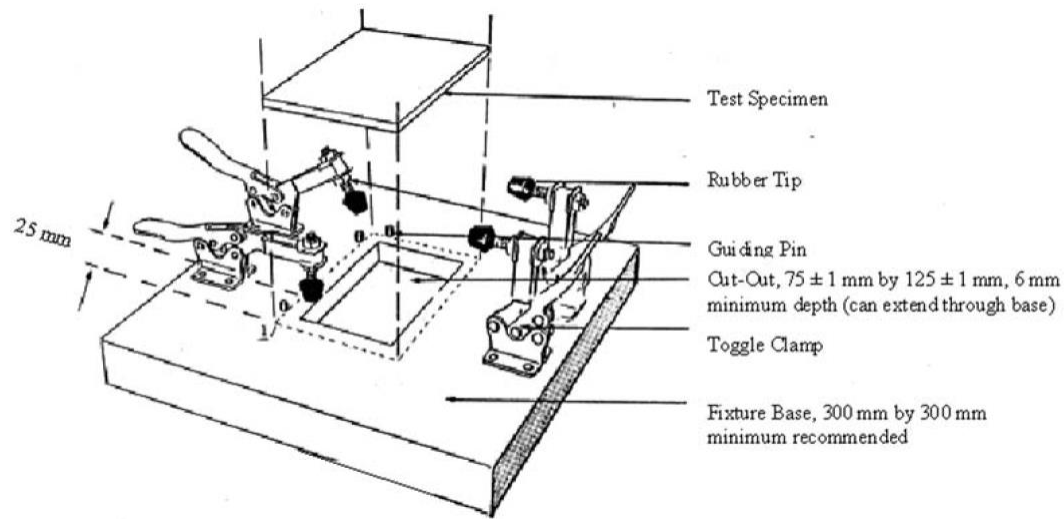
Double edge notch compression size effect law



[A. Arteiro. Structural Mechanics of Thin-Ply Laminated Composites. Universidade do Porto, 2016.](#)

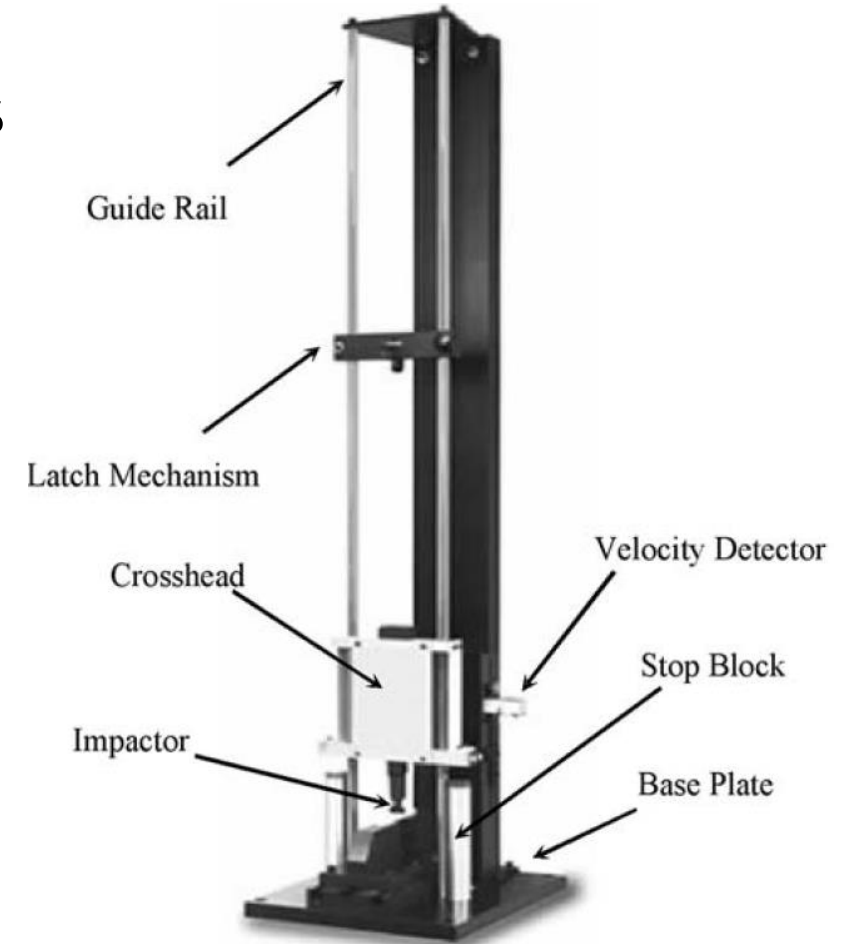
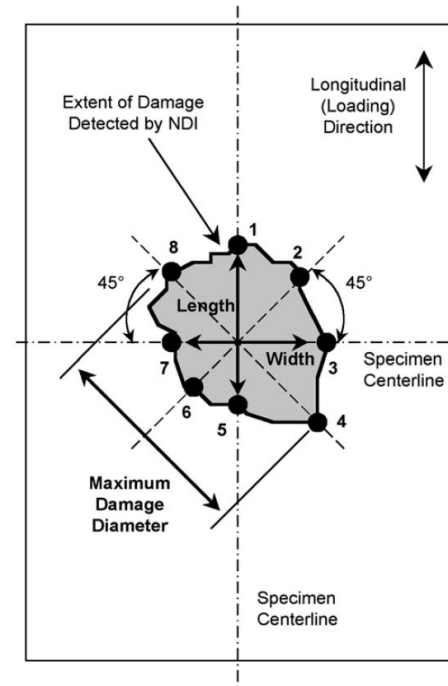
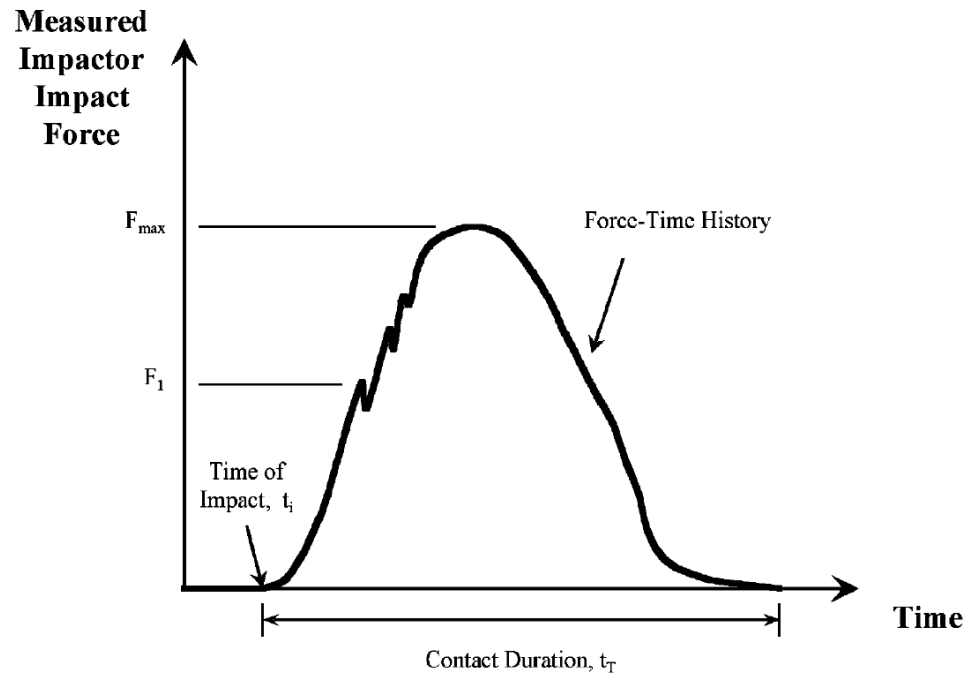
Damage tolerance

ASTM D 7136 Low-Velocity Impact (LVI) and ASTM D 7137 Compression After Impact (CAI) tests



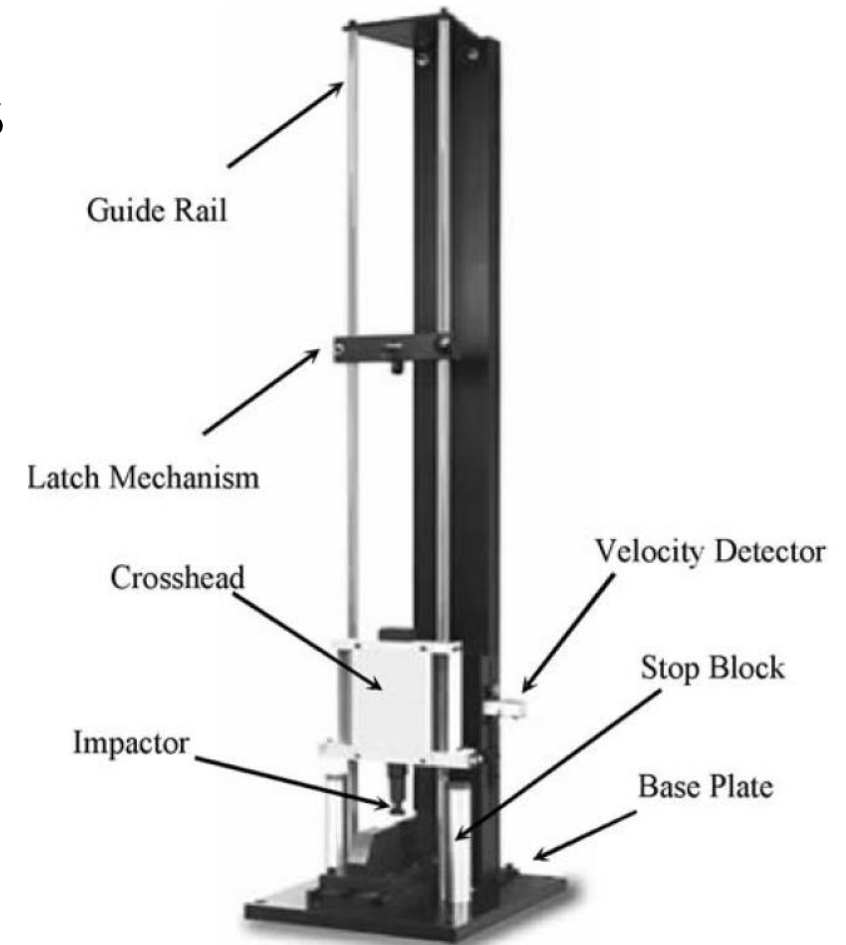
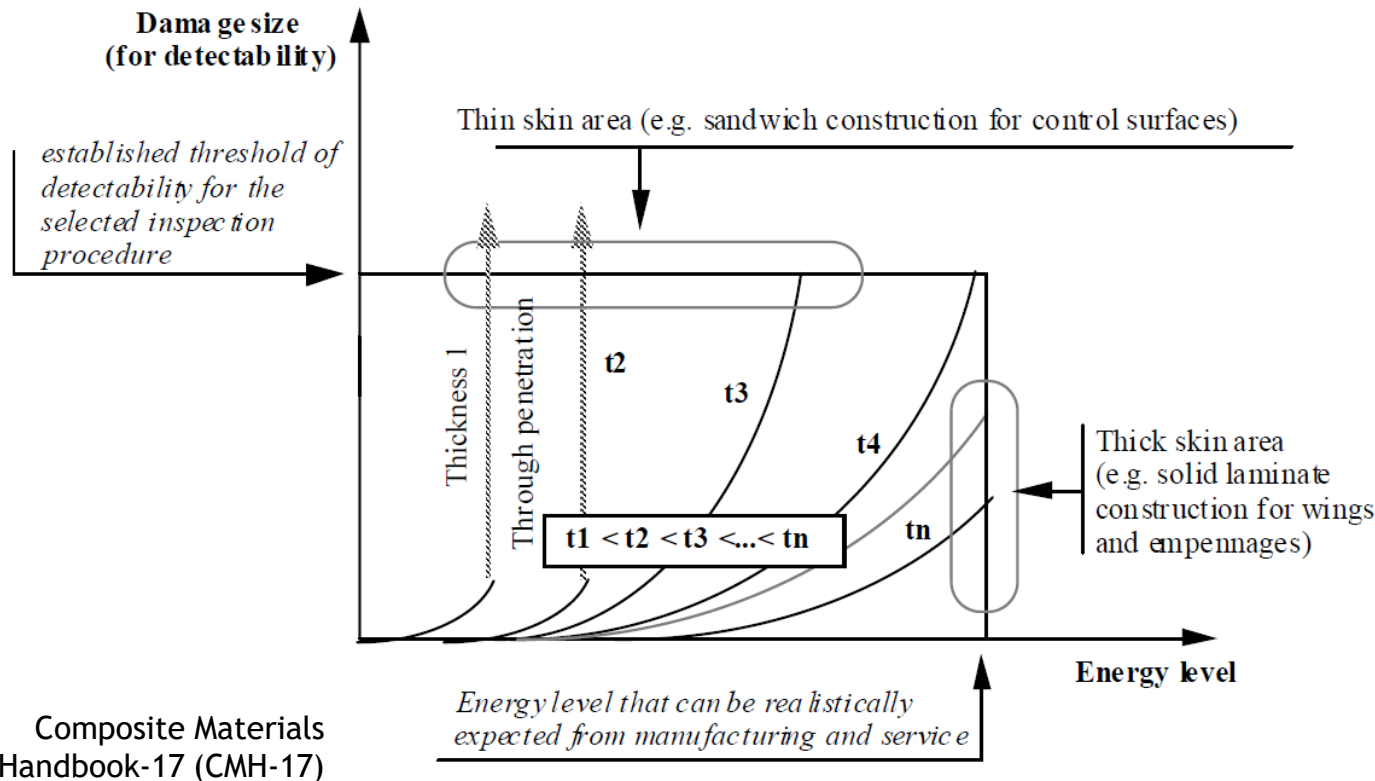
Damage tolerance

ASTM D 7136 Low-Velocity Impact (LVI) and ASTM D 7137 Compression After Impact (CAI) tests



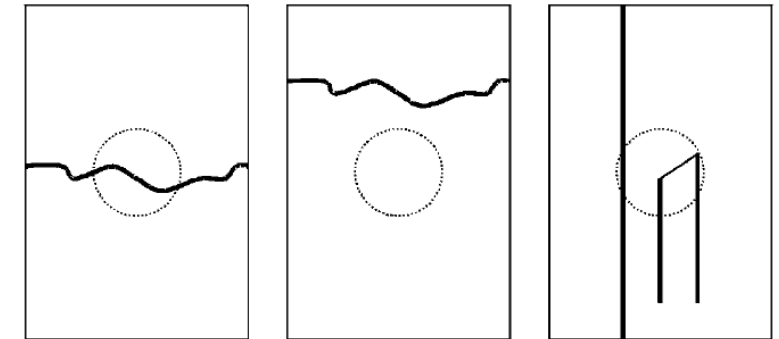
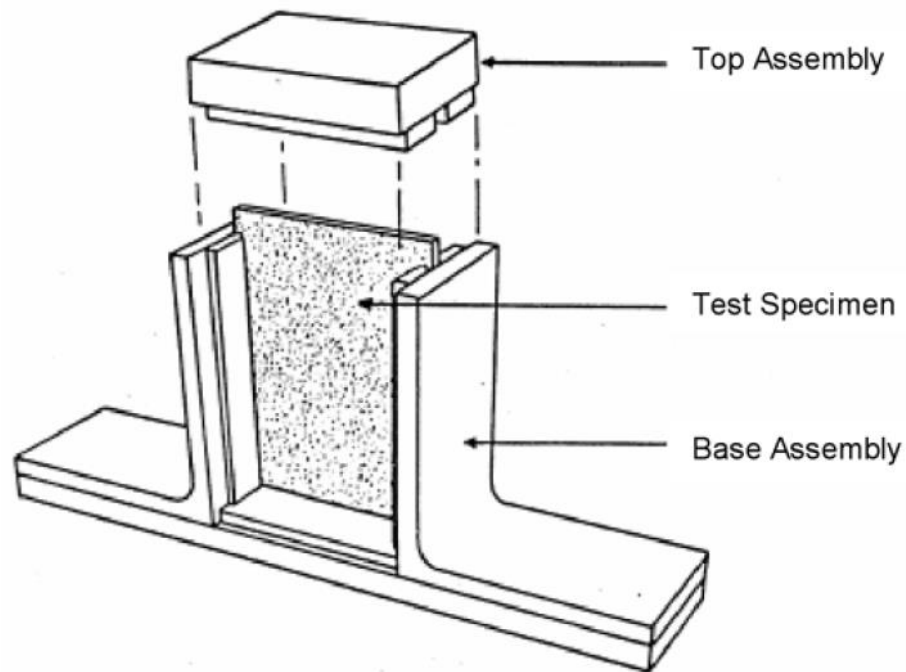
Damage tolerance

ASTM D 7136 Low-Velocity Impact (LVI) and ASTM D 7137 Compression After Impact (CAI) tests



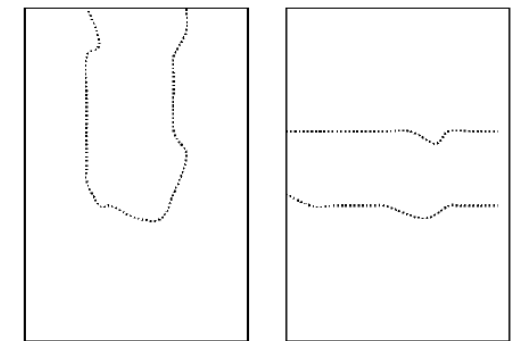
Damage tolerance

ASTM D 7136 Low-Velocity Impact (LVI) and ASTM D 7137 Compression After Impact (CAI) tests



Compression failure

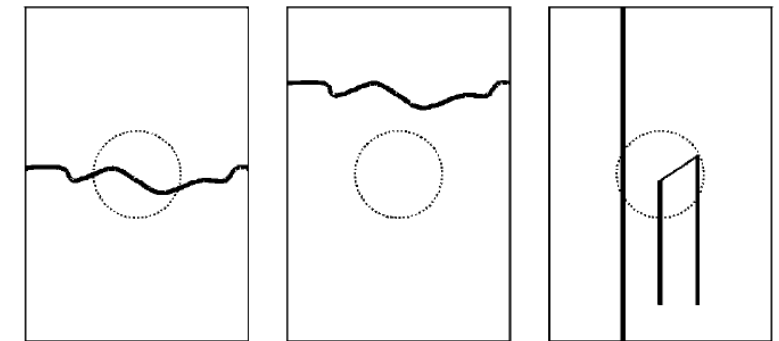
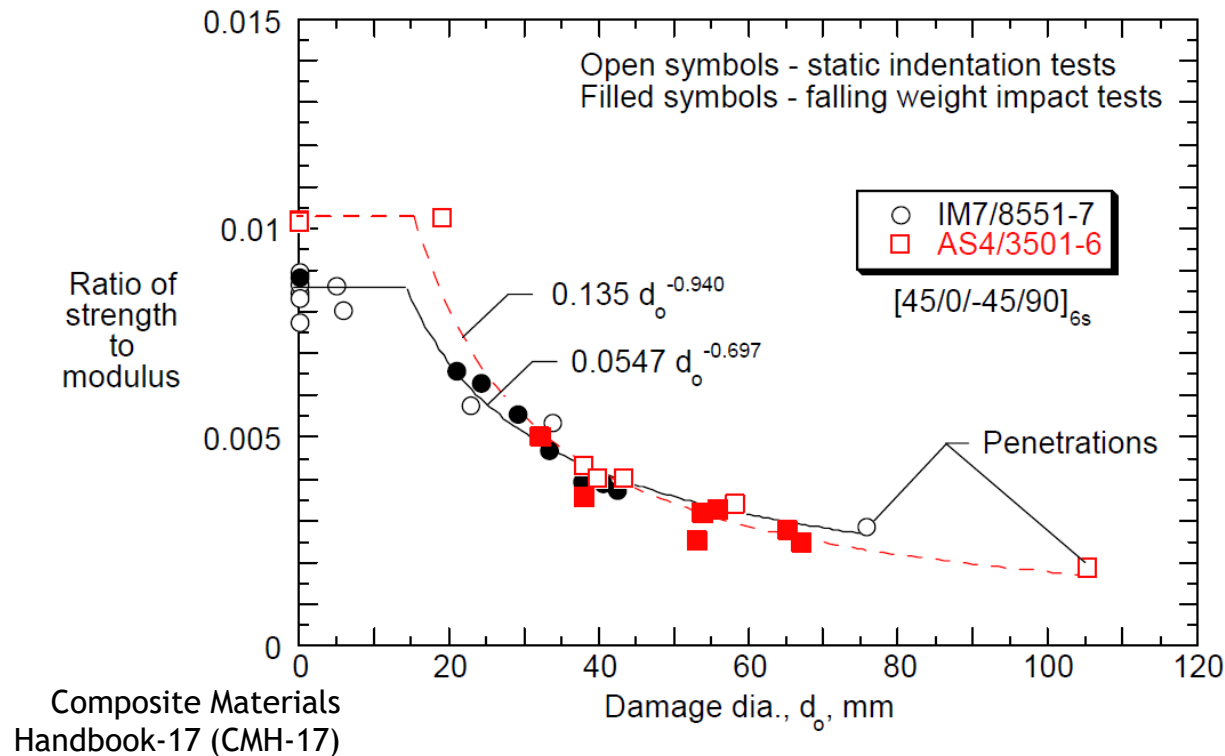
Splitting



Delamination failure

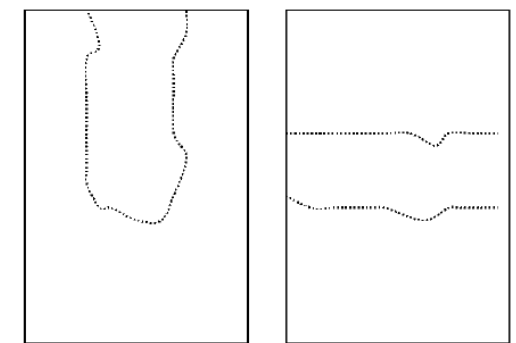
Damage tolerance

ASTM D 7136 Low-Velocity Impact (LVI) and ASTM D 7137 Compression After Impact (CAI) tests



Compression failure

Splitting



Delamination failure

Experimental characterisation

Rubbish in  rubbish out

- Careful production of laminates for specimens
- Careful production of specimens
- Careful individual measurement of each specimen
- Careful installation of strain gauges
- Calibration of equipment (e.g. load cells)

Experimental characterisation

Prevention is better remediation

- Record all data relating to the tests carried out, as well as the manufacture of specimens (dates, temperatures, used equipment, etc.).
- If possible and necessary, use more than one method to register the same measurement (e.g. photogrammetric and optical systems to record a crack length).
- Try to anticipate what can go wrong, and plan how to resolve the situation before it happens, just in case.

Experimental characterisation

Prevention is better remediation

- Try to anticipate what can go wrong, and plan how to resolve the situation before it happens, just in case.
- Example: the first tests are often lost or invalid.
- Start from spare specimens, until all is under control (load application, data acquisition, etc.).

Experimental characterisation

Prevention is better remediation

- Try to anticipate what can go wrong, and plan how to resolve the situation before it happens, just in case.
- Example: sometimes, the results after data reduction do not make sense (e.g. as there was a calibration problem with the equipment).
- After the first formal test, stop, make data reduction and verify if the results make sense. Specially if the tests imply breaking the specimens.

Experimental characterisation

Prevention is better remediation

- Try to anticipate what can go wrong, and plan how to resolve the situation before it happens, just in case.
- Example: Some specimens can be damaged accidentally prior to test.
- Include spare specimens when defining the manufacturing plan and the test matrix.

Health and safety

- Masks, goggles, boots, gloves and ear protection should be used in certain circumstances.
- All equipment and laboratories should have procedures to use, for work and safety, that must be well known and respected.

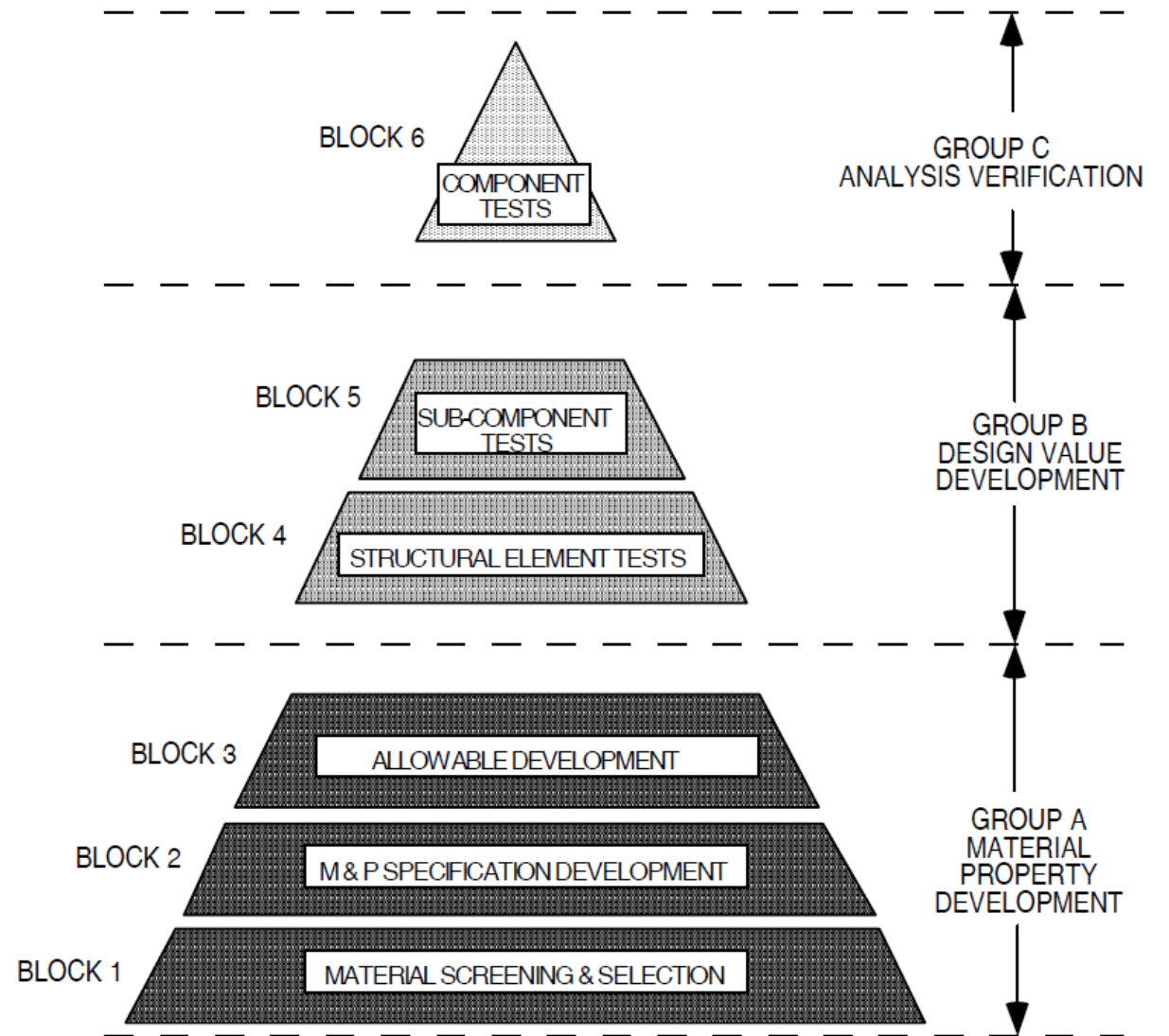
Significance of test results

- The variability of materials properties implies that multiple tests (usually 5 or more, but depending on the type and goal of the test) are needed to characterise each property.
- If possible, use standardised tests.
- If possible, use certified equipment.

Mechanical Tests

Building block approach

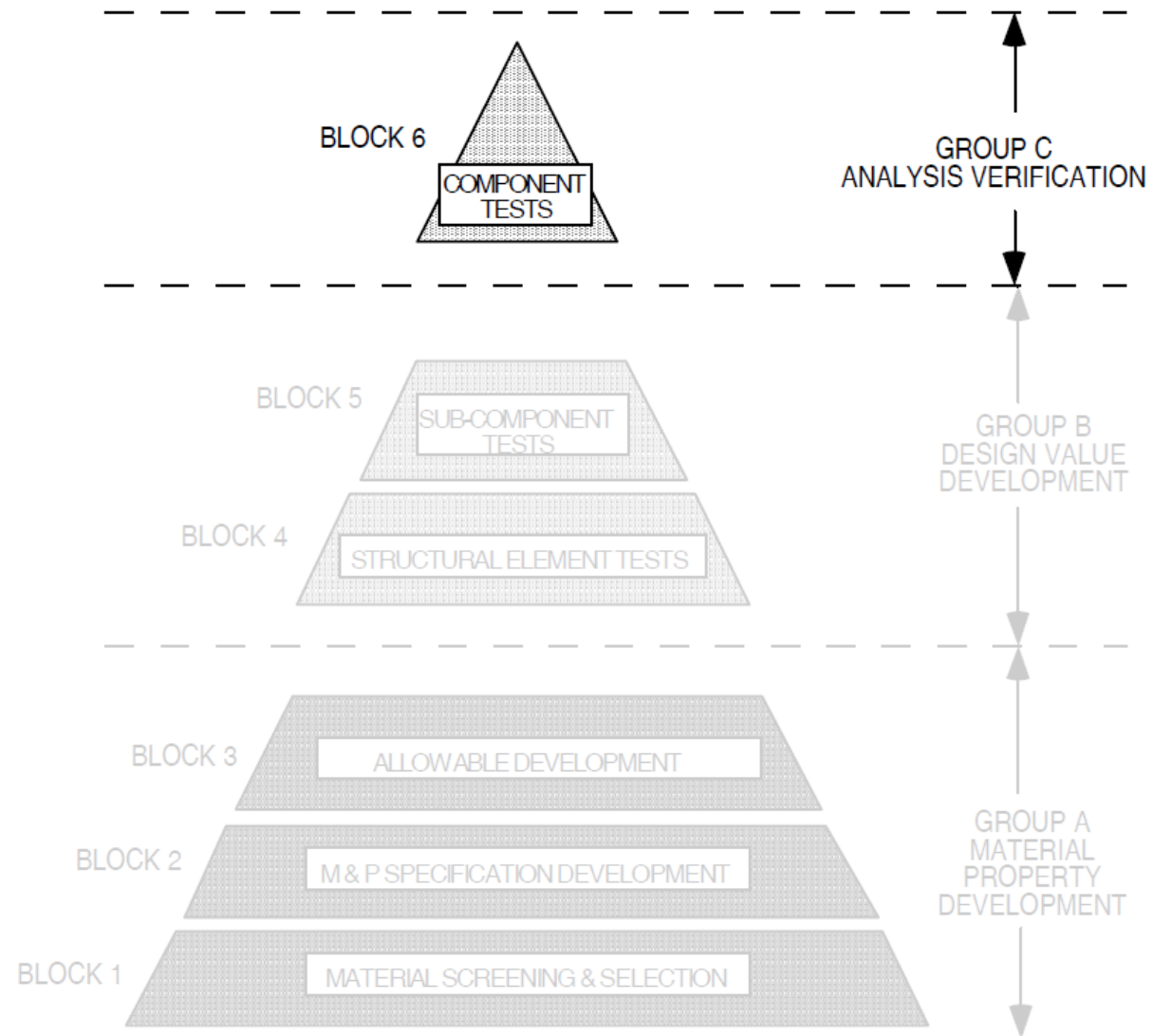
Test pyramid



Mechanical Tests

Building block approach

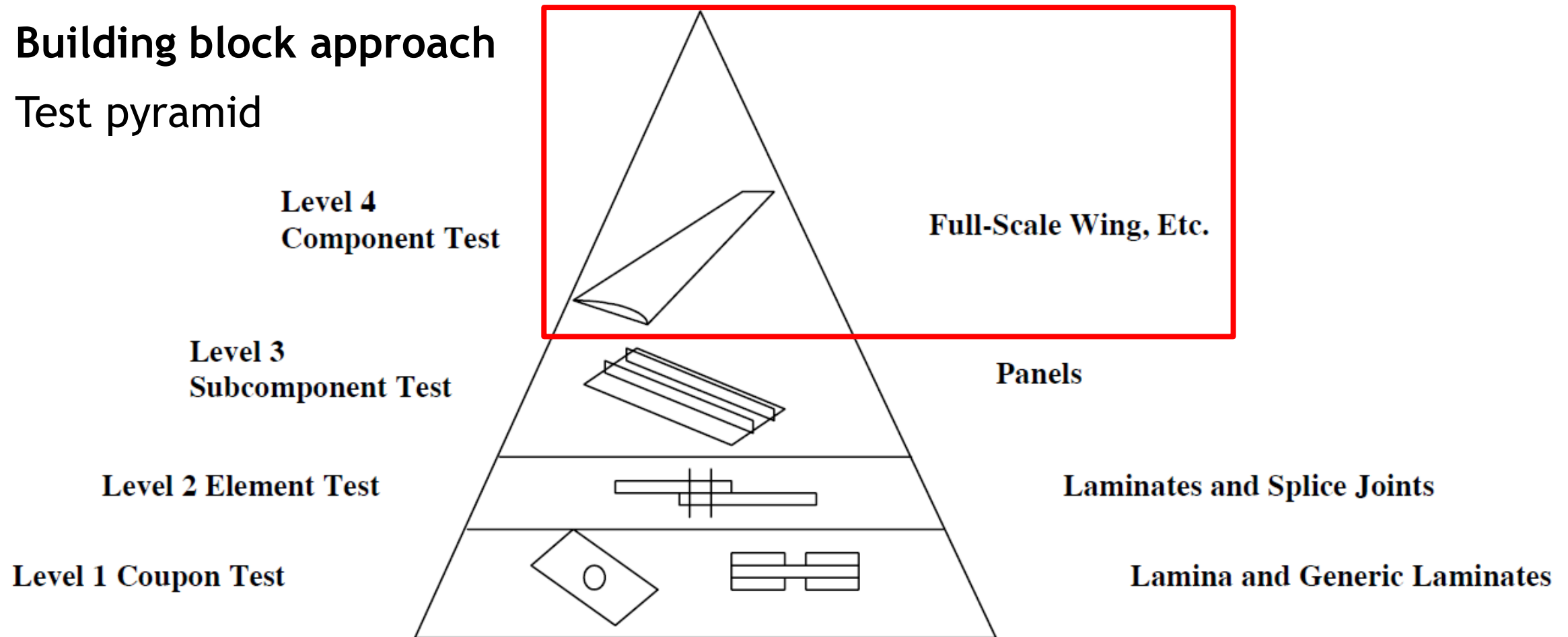
Test pyramid



Mechanical Tests

Building block approach

Test pyramid



Composite Materials Handbook-17 (CMH-17)



Questions?

Mechanical behavior and characterization.

Mechanical tests from coupon to sub-component:
Building-block approach. Part 2

SASCOM

Introductory course on composite materials 2021

Albertino Arteiro & Pedro P. Camanho

INEGI, University of Porto, Porto, Portugal

SASCOM

Introductory course on composite materials 2021

Classical lamination theory

Part 1

References

Tsai SW, Melo JDD. Composite materials design and testing – unlocking mystery with invariants. Stanford: Composites Design Group, Department of Aeronautics and Astronautics, Stanford University, 2015.

Marques AT. Composite Systems: Design and Manufacture for Durability, University of Porto, September 2019.

Jones RM. Mechanics of composite materials. New York: Taylor & Francis, 1999.

Tsai SW, Melo JDD, Sihm S, Arteiro A, Rainsberger R. Composite Laminates – Theory and practice of analysis, design and automated layup. Stanford: Composites Design Group, Department of Aeronautics and Astronautics, Stanford University, 2017.

Tsai SW. Strength & Life of Composites. Stanford: Composites Design Group, Department of Aeronautics and Astronautics, Stanford University, 2008.

Anisotropic strain-stress relations

The stress/strain relationship for an anisotropic material reads:

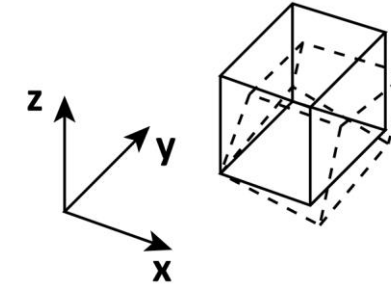
$$\epsilon_{ij} = S_{ijkl} \sigma_{kl}$$

where:

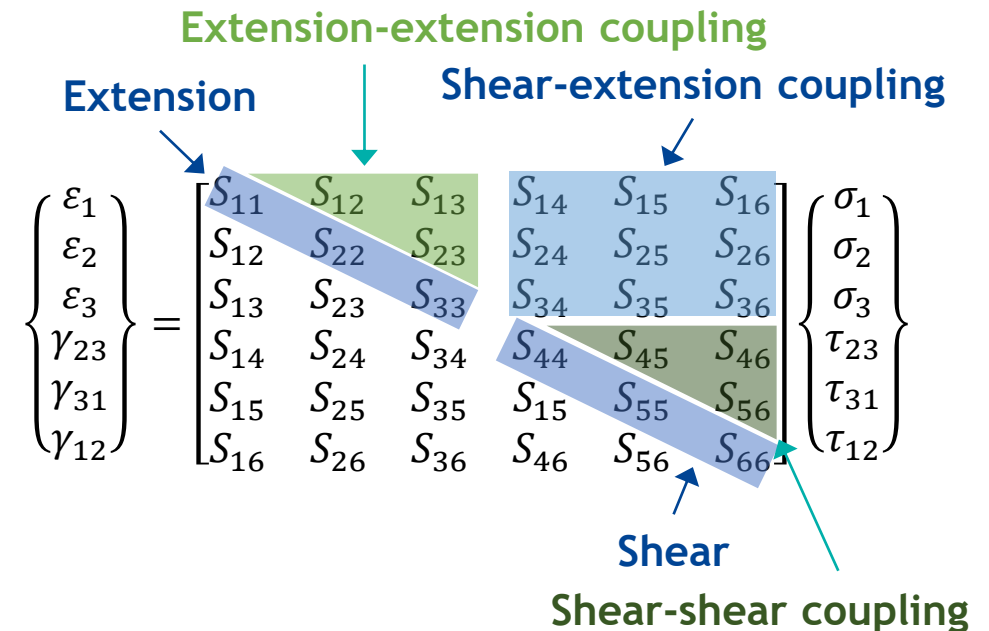
ϵ_{ij} - 2nd order Strain Tensor

σ_{kl} - 2nd order Stress Tensor

S_{ijkl} - 4th order Compliance Tensor



Deformation of an anisotropic cube under σ_z



Anisotropic strain-stress relations

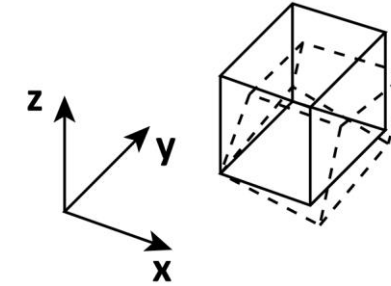
The stress/strain relationship for an anisotropic material reads:

$$\epsilon_{ij} = S_{ijkl} \sigma_{kl}$$

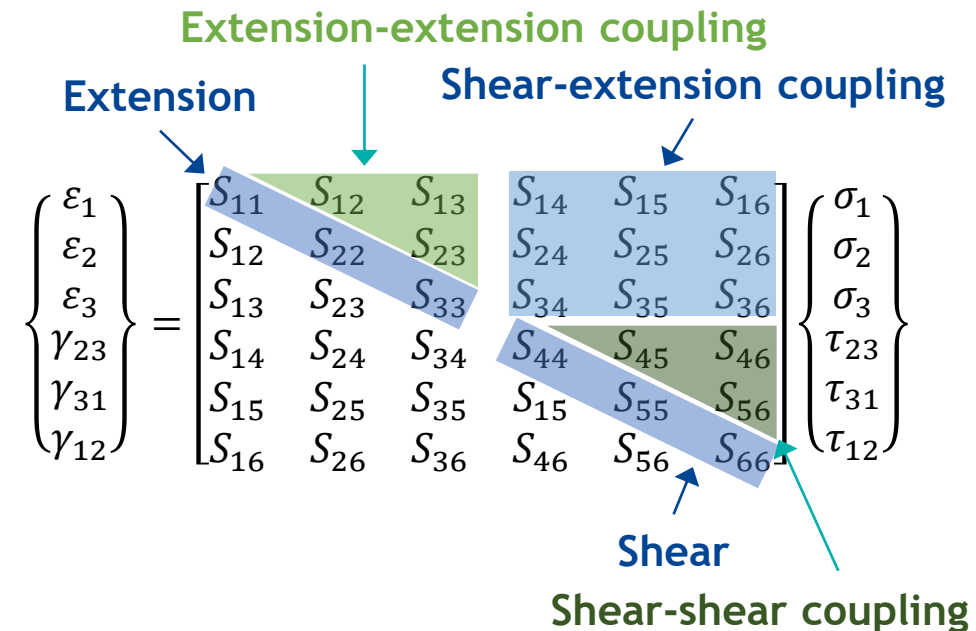
Stress Reciprocity - $S_{ijkl} = S_{ijlk}$

Strain Reciprocity - $S_{ijkl} = S_{jikl}$

Symmetry of the terms S_{ijkl} - $S_{ijkl} = S_{klij}$



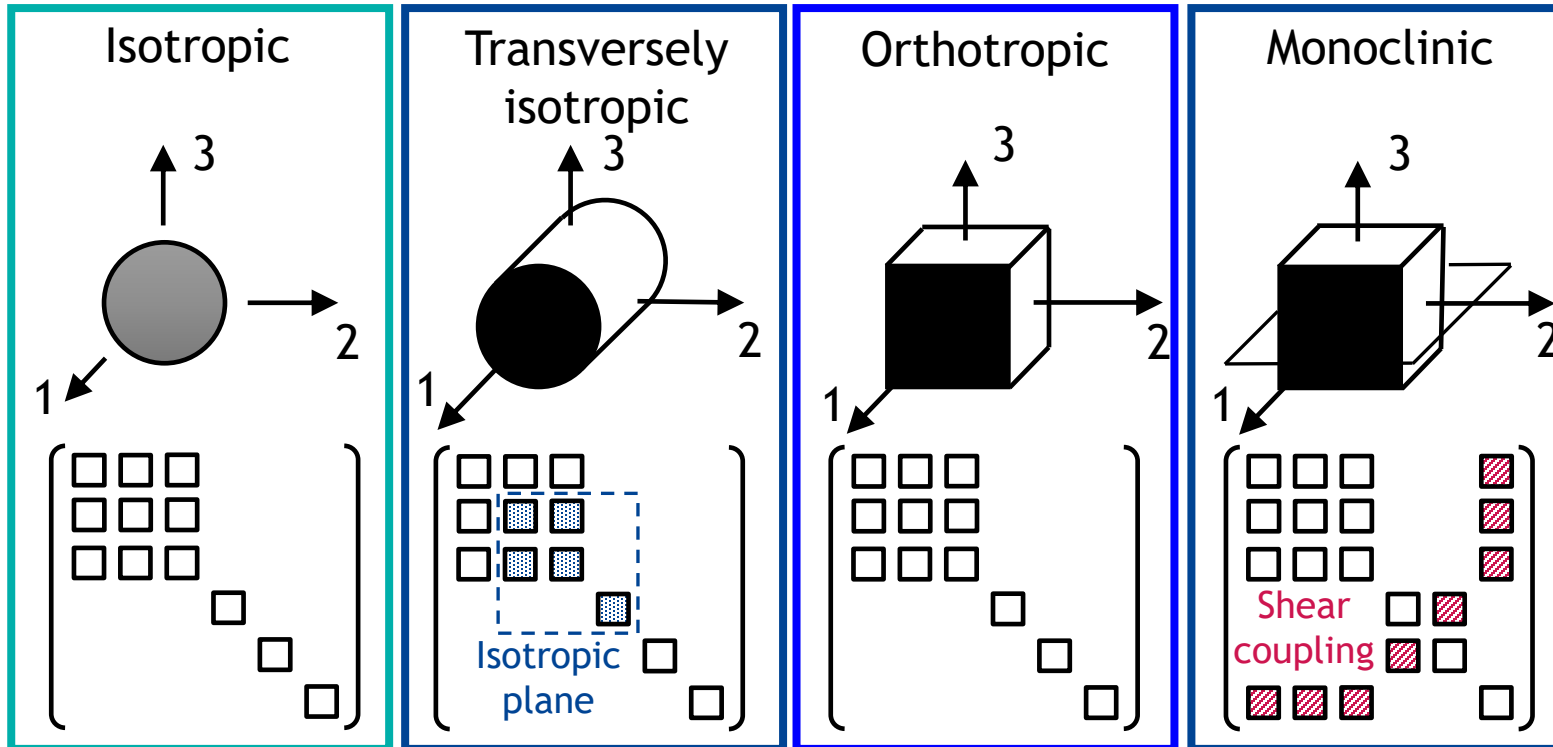
Deformation of an anisotropic cube under σ_z



Materials symmetries

Metals

[0]  [θ]



Orthotropic materials

Two orthogonal symmetry planes

9 independent engineering constants:
 E_1, E_2, E_3 Young's moduli
 G_{23}, G_{13}, G_{12} shear moduli
 $\nu_{12}, \nu_{13}, \nu_{23}$ Poisson's ratios

Materials symmetries

Given the symmetry of the compliance matrix, the following relationships hold:

$$\begin{aligned} \nu_{21}/E_2 &= \nu_{12}/E_1 \\ \nu_{31}/E_3 &= \nu_{13}/E_1 \\ \nu_{32}/E_3 &= \nu_{23}/E_2 \end{aligned}$$

$$\begin{Bmatrix} \varepsilon_{11} \\ \varepsilon_{22} \\ \varepsilon_{33} \\ \gamma_{23} \\ \gamma_{13} \\ \gamma_{12} \end{Bmatrix} = \begin{bmatrix} \frac{1}{E_1} & -\frac{\nu_{21}}{E_2} & -\frac{\nu_{31}}{E_3} & 0 & 0 & 0 \\ -\frac{\nu_{12}}{E_1} & \frac{1}{E_1} & -\frac{\nu_{32}}{E_3} & 0 & 0 & 0 \\ -\frac{\nu_{13}}{E_1} & -\frac{\nu_{23}}{E_2} & \frac{1}{E_3} & 0 & 0 & 0 \\ 0 & 0 & 0 & \frac{1}{G_{23}} & 0 & 0 \\ 0 & 0 & 0 & 0 & \frac{1}{G_{13}} & 0 \\ 0 & 0 & 0 & 0 & 0 & \frac{1}{G_{12}} \end{bmatrix} \begin{Bmatrix} \sigma_{11} \\ \sigma_{22} \\ \sigma_{33} \\ \tau_{23} \\ \tau_{13} \\ \tau_{12} \end{Bmatrix}$$

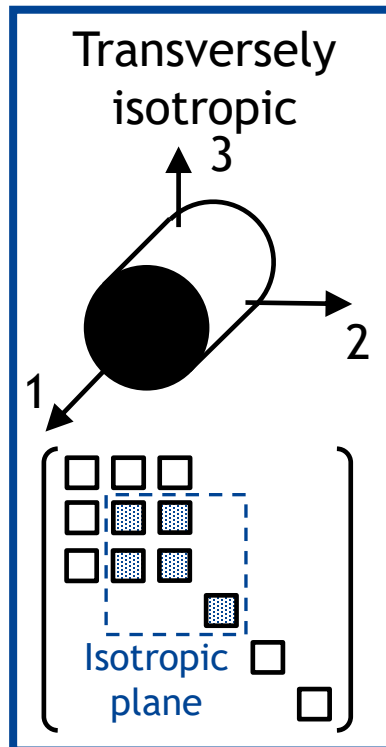
Orthotropic materials

Two orthogonal symmetry planes

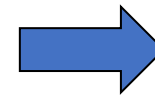
9 independent engineering constants:
 E_1, E_2, E_3 Young's moduli
 G_{23}, G_{13}, G_{12} shear moduli
 $\nu_{12}, \nu_{13}, \nu_{23}$ Poisson's ratios

Stiffness and compliance matrices

[0]



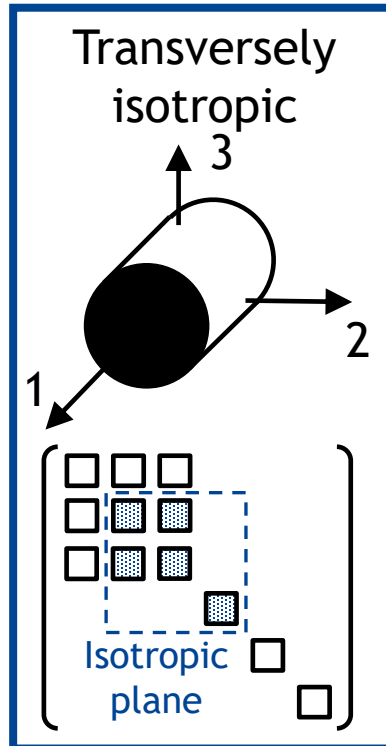
$$\begin{bmatrix}
 C_{11} & C_{12} & C_{13} & 0 & 0 & 0 \\
 C_{21} & C_{22} & C_{23} & 0 & 0 & 0 \\
 C_{21} & C_{32} & C_{22} & 0 & 0 & 0 \\
 0 & 0 & 0 & \frac{C_{22} - C_{23}}{2} & 0 & 0 \\
 0 & 0 & 0 & 0 & C_{66} & 0 \\
 0 & 0 & 0 & 0 & 0 & C_{66}
 \end{bmatrix}
 \quad
 \begin{bmatrix}
 S_{11} & S_{12} & S_{13} & 0 & 0 & 0 \\
 S_{21} & S_{22} & S_{23} & 0 & 0 & 0 \\
 S_{21} & S_{32} & S_{22} & 0 & 0 & 0 \\
 0 & 0 & 0 & \frac{S_{22} - S_{23}}{1/2} & 0 & 0 \\
 0 & 0 & 0 & 0 & S_{66} & 0 \\
 0 & 0 & 0 & 0 & 0 & S_{66}
 \end{bmatrix}$$



Matrix inversion

Stiffness and compliance matrices

[0]



$$\begin{bmatrix} C_{11} & C_{12} & C_{13} & 0 & 0 & 0 \\ C_{21} & C_{22} & C_{23} & 0 & 0 & 0 \\ C_{21} & C_{32} & C_{22} & 0 & 0 & 0 \\ 0 & 0 & 0 & \frac{C_{22} - C_{23}}{2} & 0 & 0 \\ 0 & 0 & 0 & 0 & C_{66} & 0 \\ 0 & 0 & 0 & 0 & 0 & C_{66} \end{bmatrix}$$

$$\begin{bmatrix} S_{11} & S_{12} & S_{13} & 0 & 0 & 0 \\ S_{21} & S_{22} & S_{23} & 0 & 0 & 0 \\ S_{21} & S_{32} & S_{22} & 0 & 0 & 0 \\ 0 & 0 & 0 & \frac{S_{22} - S_{23}}{1/2} & 0 & 0 \\ 0 & 0 & 0 & 0 & S_{66} & 0 \\ 0 & 0 & 0 & 0 & 0 & S_{66} \end{bmatrix}$$

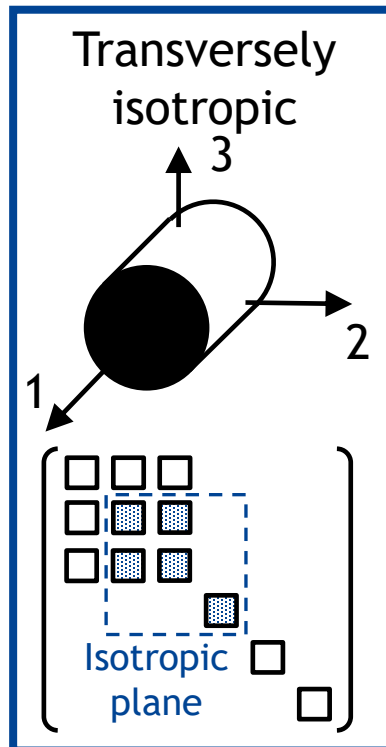


Isotropic plane
(2 constants)



Stiffness and compliance matrices

[0]



$$\begin{bmatrix} C_{11} & C_{12} & C_{13} & 0 & 0 & 0 \\ C_{21} & C_{22} & C_{23} & 0 & 0 & 0 \\ C_{21} & C_{32} & C_{22} & 0 & 0 & 0 \\ 0 & 0 & 0 & \frac{C_{22} - C_{23}}{2} & 0 & 0 \\ 0 & 0 & 0 & 0 & C_{66} & 0 \\ 0 & 0 & 0 & 0 & 0 & C_{66} \end{bmatrix}$$

$$\begin{bmatrix} S_{11} & S_{12} & S_{13} & 0 & 0 & 0 \\ S_{21} & S_{22} & S_{23} & 0 & 0 & 0 \\ S_{21} & S_{32} & S_{22} & 0 & 0 & 0 \\ 0 & 0 & 0 & \frac{S_{22} - S_{23}}{1/2} & 0 & 0 \\ 0 & 0 & 0 & 0 & S_{66} & 0 \\ 0 & 0 & 0 & 0 & 0 & S_{66} \end{bmatrix}$$



Engineering constants
 $E_1 = 1/S_{11}, \dots E_6 = 1/S_{66}$

Plane stress stiffness [Q]

$$\sigma_1 = C_{11}\varepsilon_1 + C_{12}\varepsilon_2 + C_{13}\varepsilon_3 + C_{16}\varepsilon_6$$

$$\sigma_2 = C_{21}\varepsilon_1 + C_{22}\varepsilon_2 + C_{23}\varepsilon_3 + C_{26}\varepsilon_6$$

$$\sigma_6 = C_{61}\varepsilon_1 + C_{62}\varepsilon_2 + C_{63}\varepsilon_3 + C_{66}\varepsilon_6$$

$$\sigma_3 = C_{31}\varepsilon_1 + C_{32}\varepsilon_2 + C_{33}\varepsilon_3 + C_{36}\varepsilon_6 = 0, \sigma_4 = 0, \sigma_5 = 0$$



Assuming plane-stress conditions

The normal strain in the 3-direction can be eliminated as a dependent variable:

$$\varepsilon_3 = -\frac{C_{31}\varepsilon_1 + C_{32}\varepsilon_2 + C_{36}\varepsilon_6}{C_{33}}$$

$$\{\sigma\} = [Q]\{\varepsilon\}, \text{ or } \sigma_i = Q_{ij}\varepsilon_j, \quad i, j = 1, 2, 6$$

$$\text{where } Q_{ij} = \frac{C_{ij} - C_{i3}C_{j3}}{C_{33}}$$

Plane stress stiffness [Q]

Matrix inversion

$$\{S\} = [Q]^{-1}$$

$$S_{11} = \frac{Q_{22}Q_{66} - Q_{26}^2}{|Q|}$$

$$S_{22} = \frac{Q_{11}Q_{66} - Q_{16}^2}{|Q|}$$

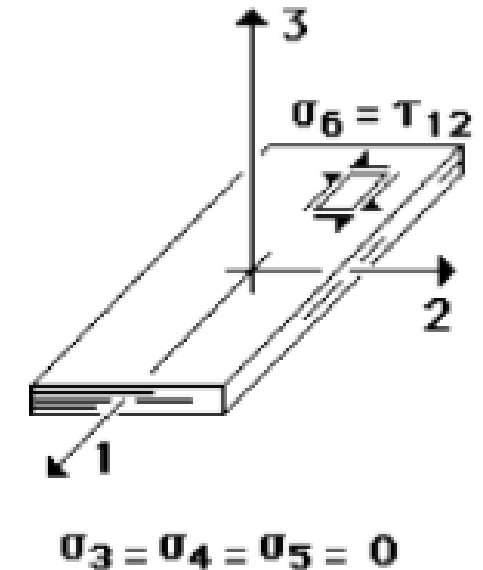
$$S_{12} = \frac{-Q_{12}Q_{66} + Q_{12}Q_{66}}{|Q|}$$

$$S_{66} = \frac{Q_{11}Q_{22} - Q_{12}^2}{|Q|}$$

$$S_{16} = \frac{Q_{12}Q_{26} - Q_{22}Q_{16}}{|Q|}$$

$$S_{26} = \frac{Q_{12}Q_{16} - Q_{11}Q_{26}}{|Q|}$$

$$|Q| = (Q_{11}Q_{22} - Q_{12}^2)Q_{66} + 2Q_{12}Q_{26}Q_{16} - Q_{11}Q_{26}^2 - Q_{22}Q_{16}^2$$



Plane stress stiffness [Q]

Engineering constants

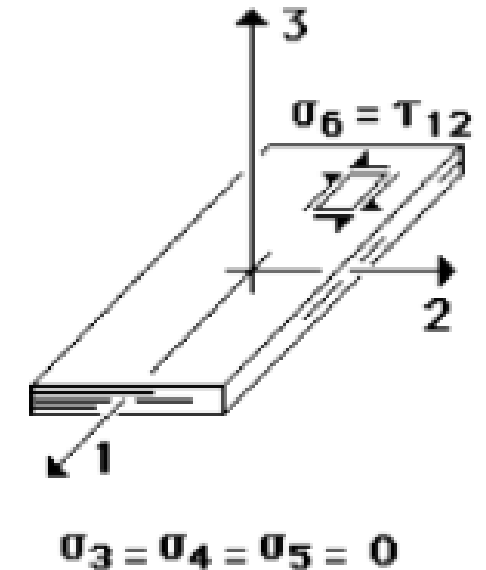
$$E_1 = \frac{1}{S_{11}}, \quad E_2 = \frac{1}{S_{22}}, \quad E_6 = G_{12} = \frac{1}{S_{66}}$$

$$\nu_{21} = -\frac{S_{21}}{S_{22}}, \quad \nu_{12} = -\frac{S_{12}}{S_{11}}$$

$$\nu_{61} = \frac{S_{61}}{S_{66}}, \quad \nu_{16} = \frac{S_{16}}{S_{11}}, \quad \nu_{62} = -\frac{S_{62}}{S_{66}}, \quad \nu_{26} = -\frac{S_{26}}{S_{22}}$$

$$\frac{\nu_{12}}{\nu_{21}} = \frac{S_{22}}{S_{11}} = \frac{E_1}{E_2}, \quad \frac{\nu_{16}}{\nu_{61}} = \frac{S_{66}}{S_{11}} = \frac{E_1}{E_6} = \frac{E_1}{G_{12}}$$

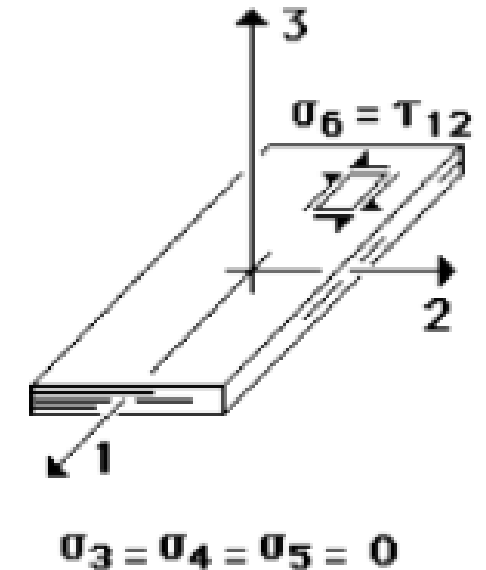
→ Reciprocal relations



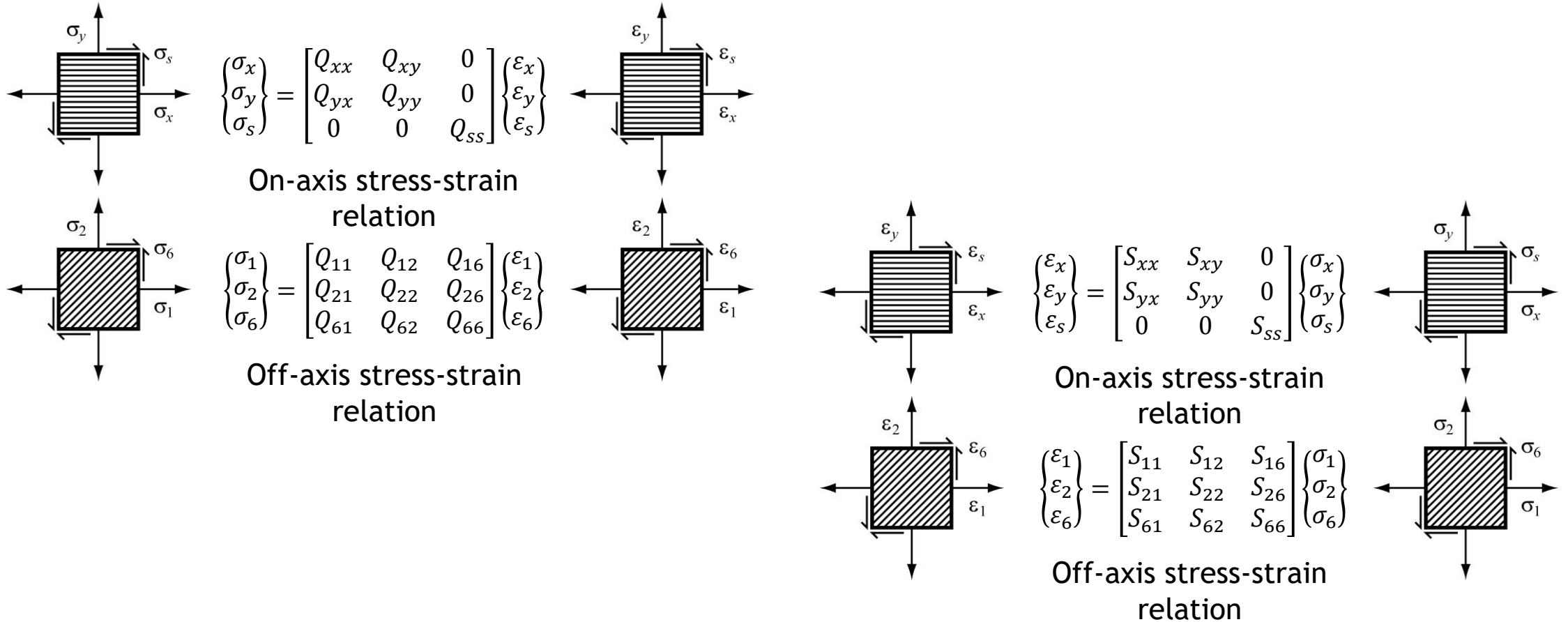
Plane stress stiffness and compliance

$$[Q] = \begin{bmatrix} \frac{E_1}{1 - \nu_{12}\nu_{21}} & \frac{\nu_{12}E_2}{1 - \nu_{12}\nu_{21}} & 0 \\ \frac{\nu_{21}E_1}{1 - \nu_{12}\nu_{21}} & \frac{E_2}{1 - \nu_{12}\nu_{21}} & 0 \\ 0 & 0 & G_{12} \end{bmatrix}$$

$$[S] = \begin{bmatrix} \frac{1}{E_1} & -\frac{\nu_{21}}{E_2} & 0 \\ -\frac{\nu_{12}}{E_1} & \frac{1}{E_2} & 0 \\ 0 & 0 & \frac{1}{G_{12}} \end{bmatrix}$$

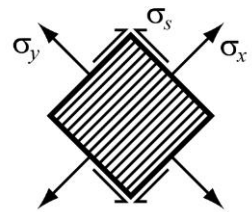


Plane stress-strain relations

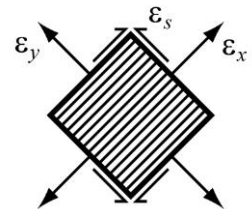
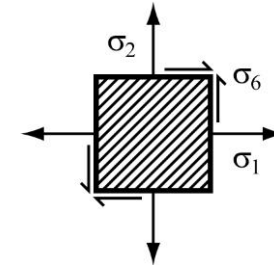


Stress and strain transformation

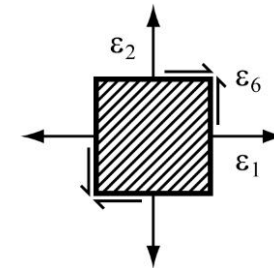
$$(m = \cos \theta, n = \sin \theta)$$



$$\begin{Bmatrix} \sigma_x \\ \sigma_y \\ \sigma_s \end{Bmatrix} = \begin{bmatrix} m^2 & n^2 & 2mn \\ n^2 & m^2 & -2mn \\ -mn & mn & (m^2 - n^2) \end{bmatrix} \begin{Bmatrix} \sigma_1 \\ \sigma_2 \\ \sigma_6 \end{Bmatrix}$$

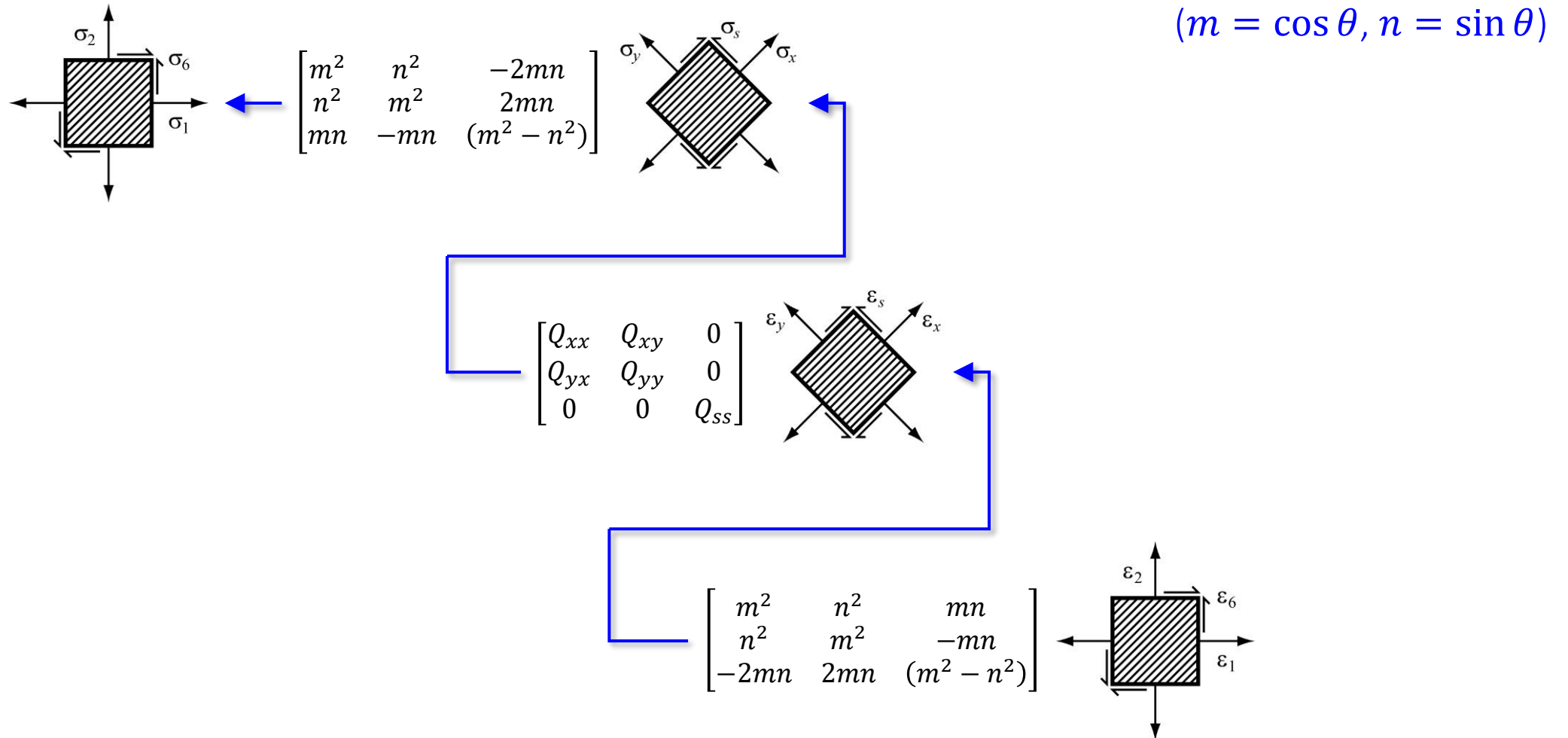


$$\begin{Bmatrix} \epsilon_x \\ \epsilon_y \\ \epsilon_s \end{Bmatrix} = \begin{bmatrix} m^2 & n^2 & mn \\ n^2 & m^2 & -mn \\ -2mn & 2mn & (m^2 - n^2) \end{bmatrix} \begin{Bmatrix} \epsilon_1 \\ \epsilon_2 \\ \epsilon_6 \end{Bmatrix}$$



Counter-clockwise (positive) rotation from the laminate to the material coordinate system

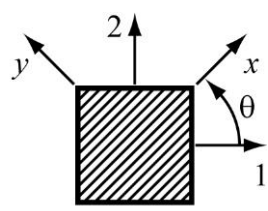
Derivation of stiffness transformation



Plane stress stiffness transformation

$$(m = \cos \theta, n = \sin \theta)$$

Independent of rotation sign (+/- θ)



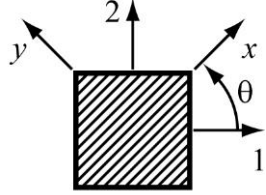
$$\begin{Bmatrix} Q_{11} \\ Q_{22} \\ Q_{12} \\ Q_{66} \\ Q_{16} \\ Q_{26} \end{Bmatrix} = \begin{bmatrix} m^4 & n^4 & 2m^2n^2 & 4m^2n^2 \\ n^4 & m^4 & 2m^2n^2 & 4m^2n^2 \\ m^2n^2 & m^2n^2 & m^4 + n^4 & -4m^2n^2 \\ m^2n^2 & m^2n^2 & -2m^2n^2 & (m^2 - n^2)^2 \\ m^3n & -mn^3 & mn^3 - m^3n & 2(mn^3 - m^3n) \\ mn^3 & -m^3n & m^3n - mn^3 & 2(m^3n - mn^3) \end{bmatrix} \begin{Bmatrix} Q_{xx} \\ Q_{yy} \\ Q_{xy} \\ Q_{ss} \end{Bmatrix}$$

Note: above the blue line
the exponents are even;
below the exponents are odd.

$$Q_{11} = m^4Q_{xx} + n^4Q_{yy} + 2m^2n^2Q_{xy} + 4m^2n^2Q_{ss}$$

Plane stress stiffness transformation

$$(m = \cos \theta, n = \sin \theta)$$



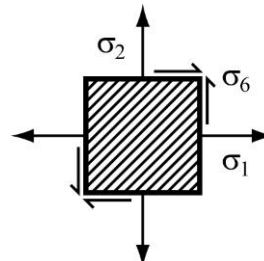
$$\begin{Bmatrix} Q_{11} \\ Q_{22} \\ Q_{12} \\ Q_{66} \\ Q_{16} \\ Q_{26} \end{Bmatrix} = \begin{bmatrix} m^4 & n^4 & 2m^2n^2 & 4m^2n^2 \\ n^4 & m^4 & 2m^2n^2 & 4m^2n^2 \\ m^2n^2 & m^2n^2 & m^4 + n^4 & -4m^2n^2 \\ m^2n^2 & m^2n^2 & -2m^2n^2 & (m^2 - n^2)^2 \\ m^3n & -mn^3 & mn^3 - m^3n & 2(mn^3 - m^3n) \\ mn^3 & -m^3n & m^3n - mn^3 & 2(m^3n - mn^3) \end{bmatrix} \begin{Bmatrix} Q_{xx} \\ Q_{yy} \\ Q_{xy} \\ Q_{ss} \end{Bmatrix}$$

Dependent of rotation sign (+/-θ)

$$Q_{11} = m^4Q_{xx} + n^4Q_{yy} + 2m^2n^2Q_{xy} + 4m^2n^2Q_{ss}$$

Note: above the blue line
the exponents are even;
below the exponents are odd.

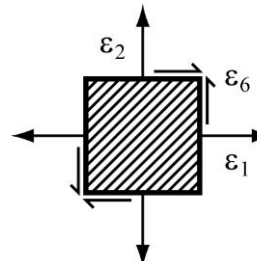
Off-axis stiffness/compliance relation

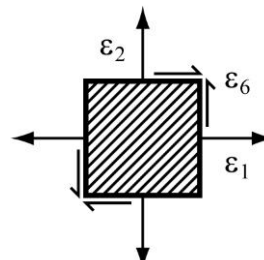


Non-zero components

$$\begin{Bmatrix} \sigma_1 \\ \sigma_2 \\ \sigma_6 \end{Bmatrix} = \begin{bmatrix} Q_{11} & Q_{12} & Q_{16} \\ Q_{21} & Q_{22} & Q_{26} \\ Q_{61} & Q_{62} & Q_{66} \end{bmatrix} \begin{Bmatrix} \varepsilon_1 \\ \varepsilon_2 \\ \varepsilon_6 \end{Bmatrix}$$

Off-axis stress-strain relation

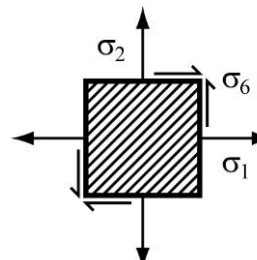




Non-zero components

$$\begin{Bmatrix} \varepsilon_1 \\ \varepsilon_2 \\ \varepsilon_6 \end{Bmatrix} = \begin{bmatrix} S_{11} & S_{12} & S_{16} \\ S_{21} & S_{22} & S_{26} \\ S_{61} & S_{62} & S_{66} \end{bmatrix} \begin{Bmatrix} \sigma_1 \\ \sigma_2 \\ \sigma_6 \end{Bmatrix}$$

Off-axis stress-strain relation



Trace of [Q] - Tsai's modulus

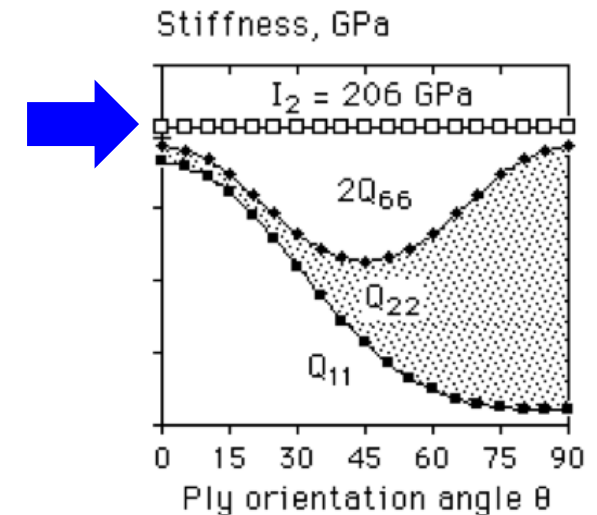
$$I_1 = Q_{xx} + Q_{yy} + 2Q_{xy} = Q_{11} + Q_{22} + 2Q_{12}$$

$$I_2 = Q_{xx} + Q_{yy} + \underline{2Q_{ss}} = Q_{11} + Q_{22} + 2Q_{66} = \text{Trace} = \text{Tsai's modulus} = \text{Tr}$$

$$\begin{Bmatrix} \sigma_1 \\ \sigma_2 \\ \sigma_6 \end{Bmatrix} = \begin{bmatrix} Q_{11} & Q_{12} & 2Q_{16} \\ Q_{21} & Q_{22} & 2Q_{26} \\ Q_{61} & Q_{62} & 2Q_{66} \end{bmatrix} \begin{Bmatrix} \varepsilon_1 \\ \varepsilon_2 \\ \varepsilon_{12} \end{Bmatrix}$$

(Tensorial strain)

Tsai's modulus remains constant



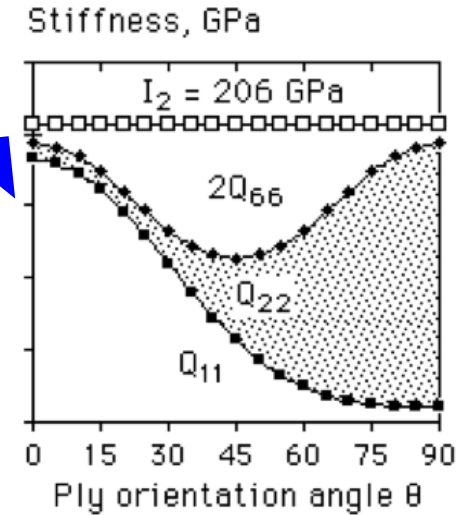
<https://doi.org/10.1016/j.compstruct.2020.112683>

Master ply defined as $Q_{ij}^* = Q_{ij} / Tr$

Tsai-normalised plane stress stiffness [Q]

Material	Q_{xx}^*	Q_{yy}^*	Q_{ss}^*	Tr, GPa	Trace*
IM7/977-3	0.883	0.0459	0.0358	218	1.000
T800/Cytec	0.896	0.0498	0.0274	183	1.000
T700 C-Ply	0.876	0.0579	0.0338	139	1.001
AS4/3501	0.857	0.0556	0.0438	162	1.000
IM6/epoxy	0.880	0.0486	0.0362	232	1.001
AS4/F937	0.886	0.0578	0.0271	168	0.998
T300/N5208	0.883	0.0502	0.0348	206	1.002
Median	0.883	0.0502	0.0348	183	1.000
Coeff var	1.2%	0.48%	0.57%		0.13%

Tsai's modulus remains constant



$$Trace^* = Q_{xx}^* + Q_{yy}^* + 2Q_{ss}^*$$

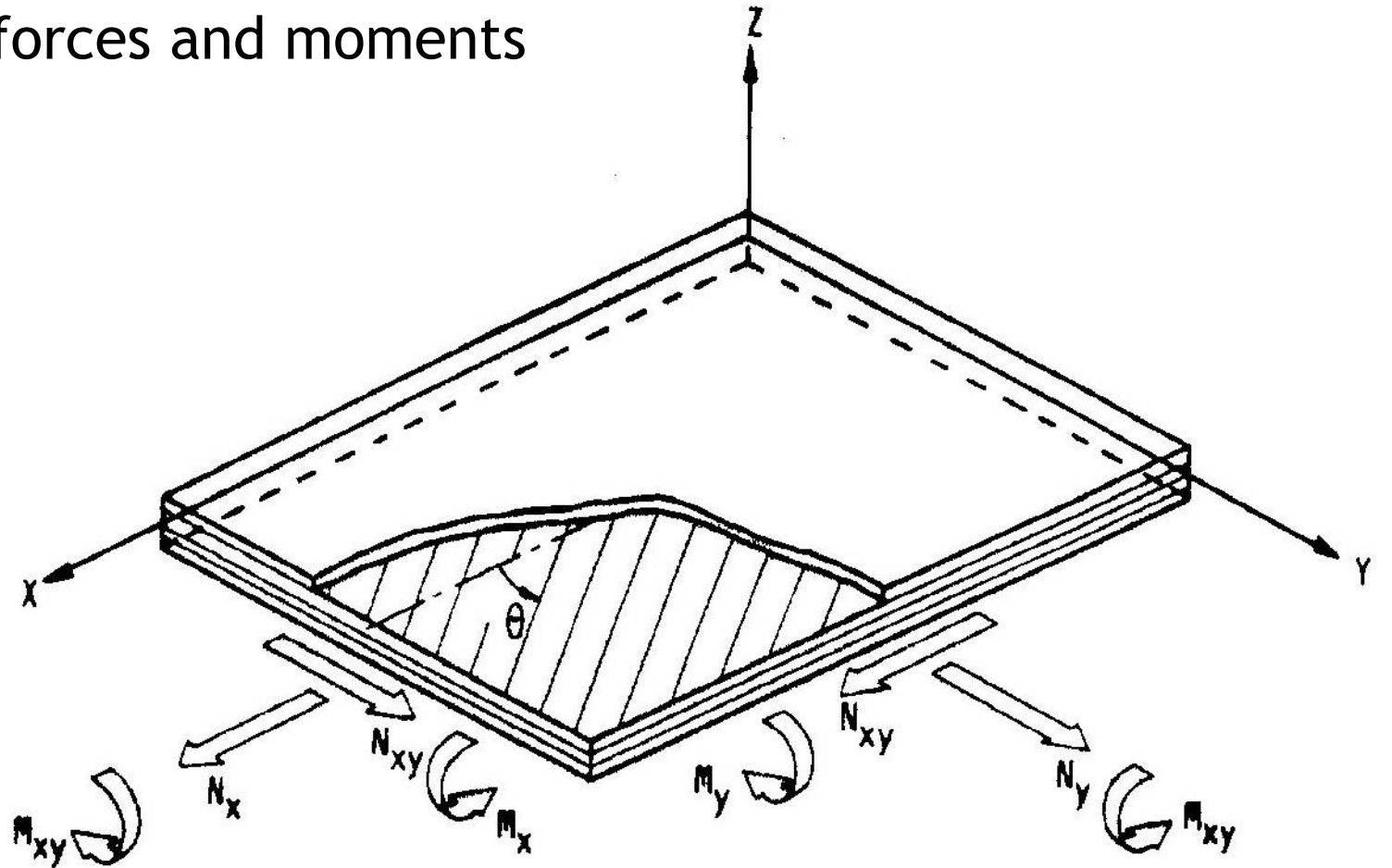
From: Tsai SW. Composites Design Workshop. Stanford: Composites Design Group, Department of Aeronautics and Astronautics, Stanford University.

Classical laminated plate theory

- ✓ Based on Kirchhoff hypotheses: $\gamma_{xz}, \gamma_{yz} = 0$
- ✓ Displacements $u, v = f(z)$ (linear function)
- ✓ $\epsilon_z = 0$
- ✓ Displacements $u, v, w \ll$ thickness
- ✓ $\epsilon_x, \epsilon_y, \gamma_{xy} \ll 1$ (linear elasticity)
- ✓ Applies the generalised Hooke's law for each ply

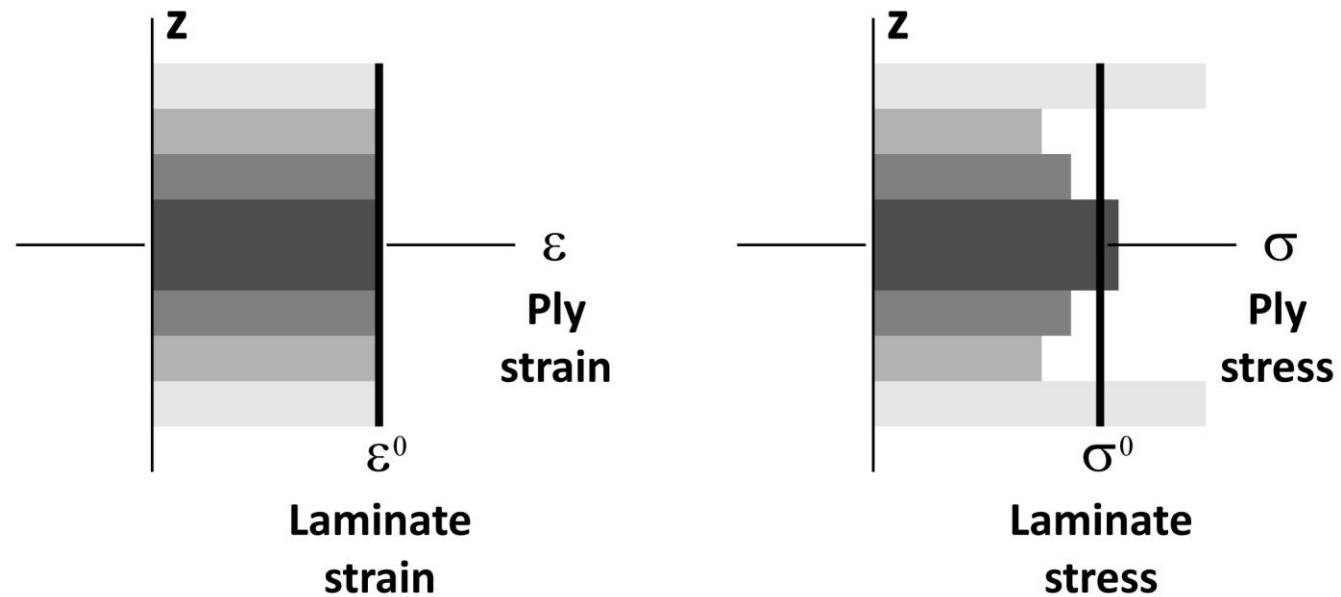
Classical laminated plate theory

- Laminate and applied forces and moments

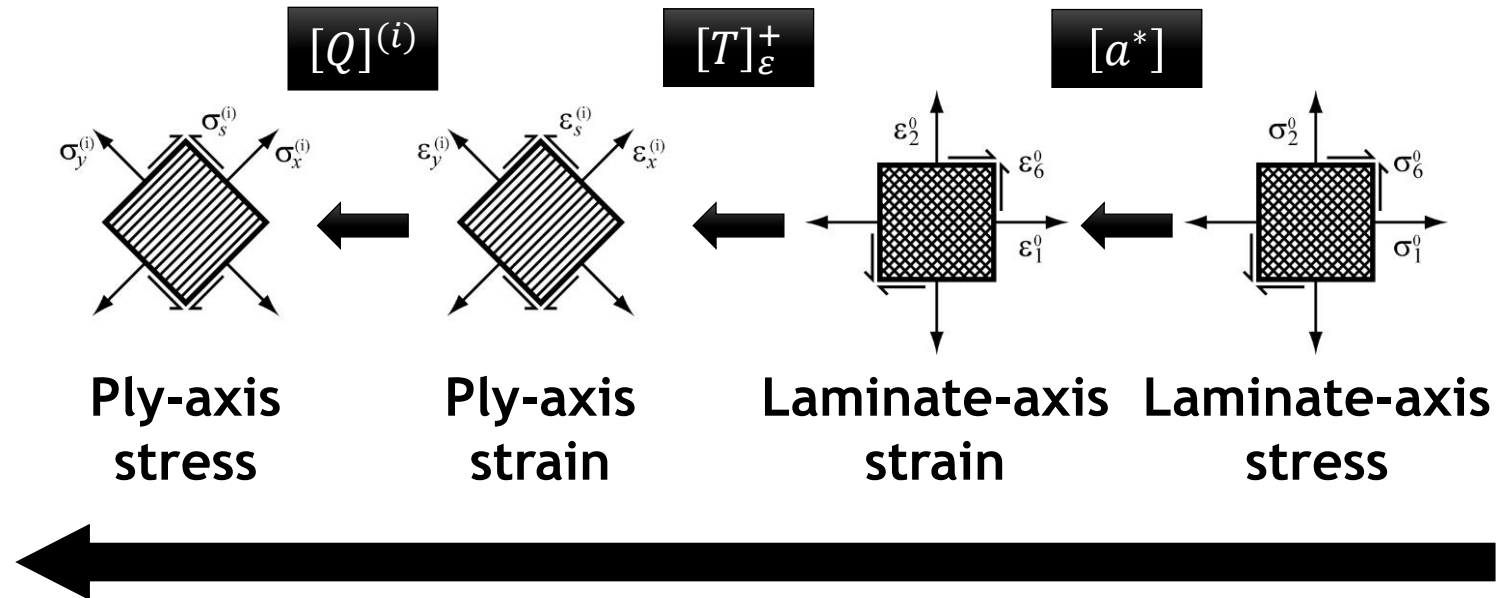


Classical laminated plate theory

Equal laminate and ply strains



Ply stress from laminate stress



In-plane stress-strain relations

$$\{\boldsymbol{\varepsilon}\} = \{\boldsymbol{\varepsilon}^0\}, \varepsilon_i = \varepsilon_i^0, i = 1, 2, 6$$

$$\{N\} = \int_{-h/2}^{h/2} \{\boldsymbol{\sigma}\} dz = \int_{-h/2}^{h/2} [Q]\{\boldsymbol{\varepsilon}\} dz = \left[\int_{-h/2}^{h/2} [Q] dz \right] \{\boldsymbol{\varepsilon}^0\} = [A]\{\boldsymbol{\varepsilon}^0\}$$

Stress resultants

Laminate in-plane stiffness $[A]$ and compliance $[a]$

$$[A] = \int_{-h/2}^{h/2} [Q] dz, [A^*] = \frac{1}{h}[A], \text{ in Pa}; [a] = [A]^{-1}, [a^*] = h[a]$$

$$\{\boldsymbol{\sigma}^0\} = \frac{1}{h}\{N\} = [A^*]\{\boldsymbol{\varepsilon}^0\}; \{\boldsymbol{\varepsilon}^0\} = [a]\{N\} = [a^*]\{\boldsymbol{\sigma}^0\}$$

In-plane stress

In-plane stress-strain relations

$$\{\boldsymbol{\varepsilon}\} = \{\boldsymbol{\varepsilon}^0\}, \varepsilon_i = \varepsilon_i^0, i = 1, 2, 6$$

$$\{N\} = \int_{-h/2}^{h/2} \{\boldsymbol{\sigma}\} dz = \int_{-h/2}^{h/2} [Q]\{\boldsymbol{\varepsilon}\} dz = \left[\int_{-h/2}^{h/2} [Q] dz \right] \{\boldsymbol{\varepsilon}^0\} = [A]\{\boldsymbol{\varepsilon}^0\}$$

Stress resultants

Laminate in-plane stiffness $[A]$ and compliance $[a]$

$$[A] = \sum_{i=1}^m [Q']^{(i)}, [A^*] = \frac{1}{h} [A], \text{ in Pa}; [a] = [A]^{-1}, [a^*] = h[a]$$

$$\{\boldsymbol{\sigma}^0\} = \frac{1}{h} \{N\} = [A^*]\{\boldsymbol{\varepsilon}^0\}; \{\boldsymbol{\varepsilon}^0\} = [a]\{N\} = [a^*]\{\boldsymbol{\sigma}^0\}$$

In-plane stress



Normalisation of stiffness $[A^*]$ and compliance $[a^*]$ are useful to compare with other laminates, UD plies or metals

Off-axis stiffness/compliance relation

Shear-extension coupling

$$\begin{Bmatrix} \sigma_1^0 \\ \sigma_2^0 \\ \sigma_6^0 \end{Bmatrix} = \begin{bmatrix} A_{11}^* & A_{12}^* & A_{16}^* \\ A_{21}^* & A_{22}^* & A_{26}^* \\ A_{61}^* & A_{62}^* & A_{66}^* \end{bmatrix} \begin{Bmatrix} \varepsilon_1^0 \\ \varepsilon_2^0 \\ \varepsilon_6^0 \end{Bmatrix}$$

$$\begin{Bmatrix} \varepsilon_1^0 \\ \varepsilon_2^0 \\ \varepsilon_6^0 \end{Bmatrix} = \begin{bmatrix} a_{11}^* & a_{12}^* & a_{16}^* \\ a_{21}^* & a_{22}^* & a_{26}^* \\ a_{61}^* & a_{62}^* & a_{66}^* \end{bmatrix} \begin{Bmatrix} \sigma_1^0 \\ \sigma_2^0 \\ \sigma_6^0 \end{Bmatrix}$$

Normalised stiffness and compliance are easier to use and to compare ([Q] and [A*] have the same units)

Unbalanced laminates:
different number of off-axis (+/-θ) plies

Rule to avoid shear-extension coupling:
Balanced laminates with same number of (+/-θ) plies

Questions?

Classical lamination theory

Part 1

SASCOM

Introductory course on composite materials 2021

Classical lamination theory

Part 2

References

Tsai SW, Melo JDD. Composite materials design and testing – unlocking mystery with invariants. Stanford: Composites Design Group, Department of Aeronautics and Astronautics, Stanford University, 2015.

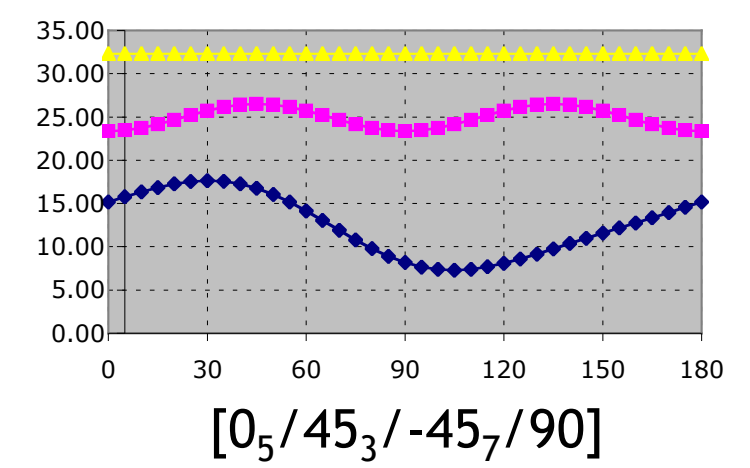
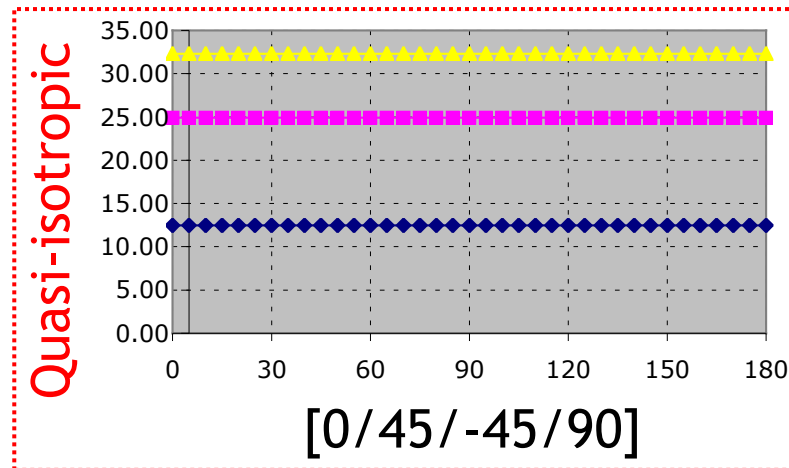
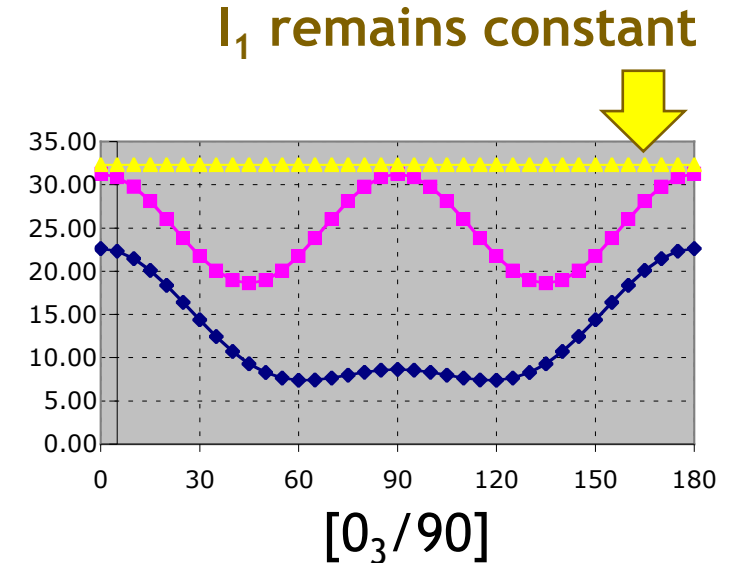
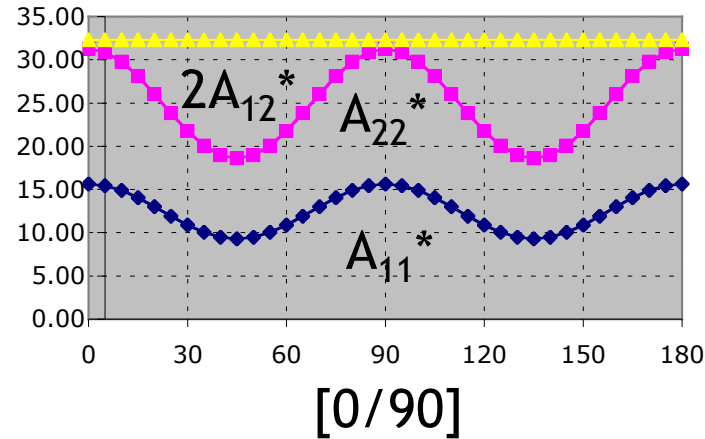
Marques AT. Composite Systems: Design and Manufacture for Durability, University of Porto, September 2019.

Tsai SW, Melo JDD, Sihm S, Arteiro A, Rainsberger R. Composite Laminates – Theory and practice of analysis, design and automated layup. Stanford: Composites Design Group, Department of Aeronautics and Astronautics, Stanford University, 2017.

Tsai SW. Strength & Life of Composites. Stanford: Composites Design Group, Department of Aeronautics and Astronautics, Stanford University, 2008.

Linear combinations: A_{ij}^* , I_1

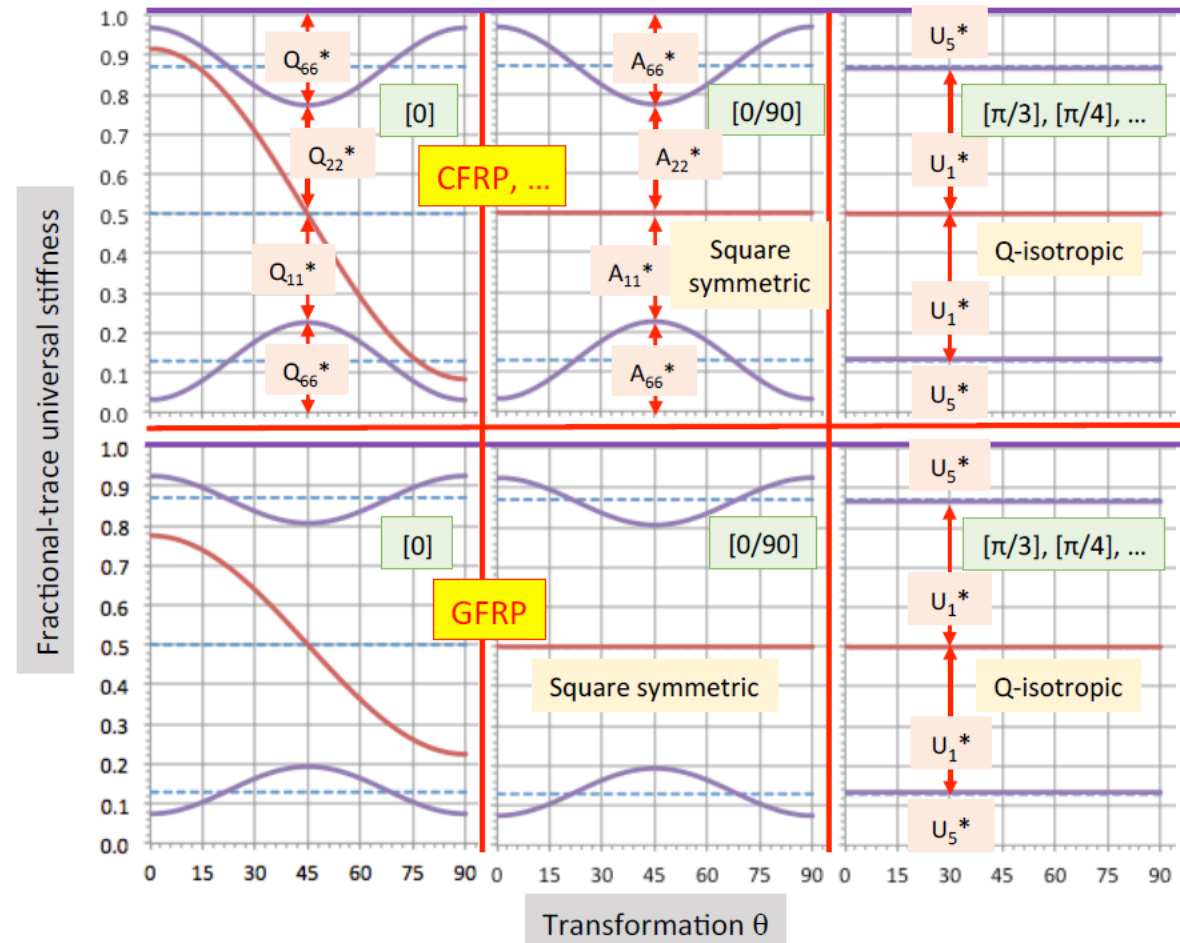
$$I_1 = A_{11}^* + A_{22}^* + 2A_{12}^*$$



From: Tsai SW. *Composites Design Workshop*.
Stanford: *Composites Design Group*,
Department of Aeronautics and Astronautics,
Stanford University.

Linear combinations: A_{ij}^* , Tr (Tsai's modulus)

$$Tr = A_{11}^* + A_{22}^* + 2A_{66}^*$$



From: Tsai SW. *Composites Design Workshop*.
Stanford: *Composites Design Group*,
Department of Aeronautics and Astronautics,
Stanford University.

Invariant approach to stiffness

Tsai-normalised UD stiffness components of several CFRPs are approximately the same.

- The Tsai-normalised longitudinal Young's modulus for 15 different CFRPs has a coefficient of variation of only 1.5%.

A **Master Ply** can be defined using the median values of the Tsai-normalised stiffness properties.

$$Tr = Q_{xx} + Q_{yy} + 2Q_{ss}$$

	E_1^0/Tr	E_2^0/Tr	G_{12}^0/Tr	ν_{12}^0
Universal [0]	0.880	0.052	0.031	0.320
[0/90]	0.468	0.468	0.031	0.036
[\(\pi/4\)]	0.336	0.336	0.129	0.308
[0 ₇ /±45/90]	0.662	0.175	0.070	0.310
[0 ₅ /±45 ₂ /90]	0.518	0.208	0.109	0.423
[0 ₂ /±45/90]	0.445	0.289	0.109	0.308
[0/±45 ₄ /90]	0.217	0.217	0.187	0.552
[0/±45]	0.370	0.155	0.161	0.734
[0/±45/0]	0.499	0.141	0.129	0.701
[0/±30]	0.510	0.074	0.129	1.220
[0/±30/0]	0.611	0.072	0.104	1.079
[±12.5]	0.764	0.053	0.066	0.913

Invariant approach to stiffness

Because E_x accounts for 88% of the value of Tsai's modulus, it is possible to determine the Tsai's modulus using only the longitudinal Young's modulus E_x - the transverse and shear moduli do not need to be measured.

Knowing E_x , the Master Ply concept can be used to determine the Tsai's modulus.

$$Tr = Q_{xx} + Q_{yy} + 2Q_{ss}$$

	E_1^0/Tr	E_2^0/Tr	G_{12}^0/Tr	ν_{12}^0
Universal [0]	0.880	0.052	0.031	0.320
[0/90]	0.468	0.468	0.031	0.036
$[\pi/4]$	0.336	0.336	0.129	0.308
$[0_7/\pm 45_2/90]$	0.662	0.175	0.070	0.310
$[0_5/\pm 45_2/90]$	0.518	0.208	0.109	0.423
$[0_2/\pm 45/90]$	0.445	0.289	0.109	0.308
$[0/\pm 45_4/90]$	0.217	0.217	0.187	0.552
$[0/\pm 45]$	0.370	0.155	0.161	0.734
$[0/\pm 45/0]$	0.499	0.141	0.129	0.701
$[0/\pm 30]$	0.510	0.074	0.129	1.220
$[0/\pm 30/0]$	0.611	0.072	0.104	1.079
$[\pm 12.5]$	0.764	0.053	0.066	0.913

$$Tr = E_1 / 0.880$$

Invariant approach to stiffness

Classical laminated plate theory can be used to generate **Tsai-normalised (Universal) Laminate Factors** for the stiffness components of multidirectional laminates using the **Master Ply**.

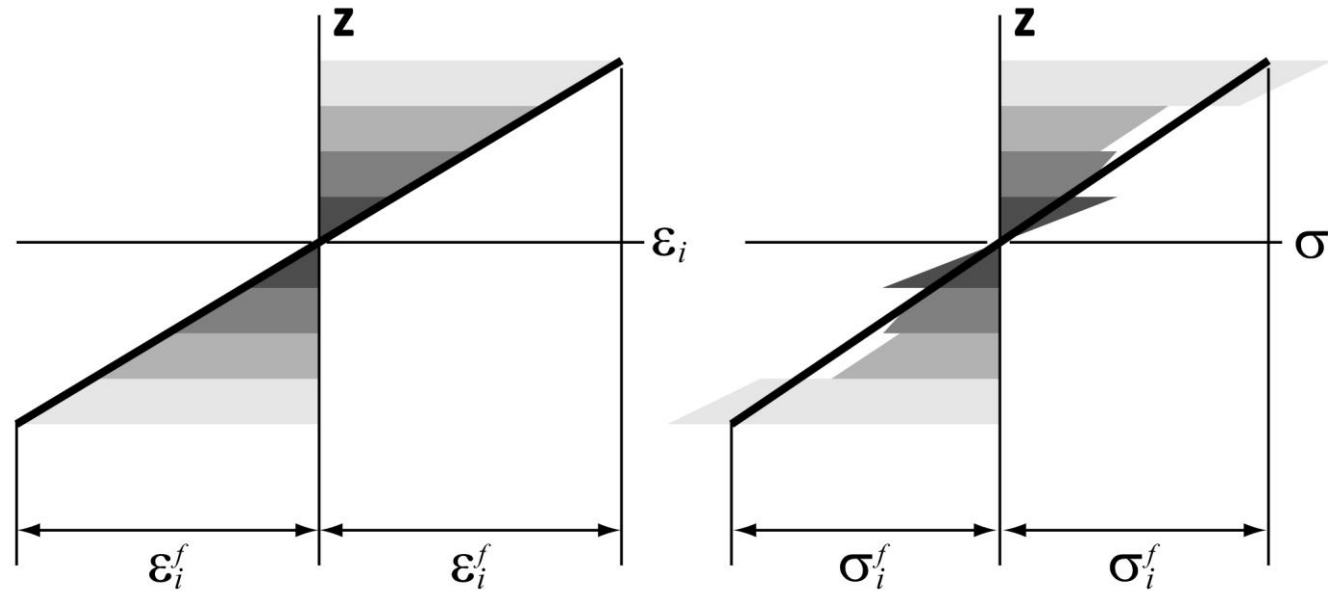
From **Tsai's modulus**, and using the **Tsai-normalised Laminate Factors**, the laminate elastic properties E_1 , E_2 , G_{12} and ν_{12} can be easily obtained.

$$Tr = Q_{xx} + Q_{yy} + 2Q_{ss}$$

	E_1^0/Tr	E_2^0/Tr	G_{12}^0/Tr	ν_{12}^0
Universal [0]	0.880	0.052	0.031	0.320
[0/90]	0.468	0.468	0.031	0.036
$[\pi/4]$	0.336	0.336	0.129	0.308
$[0_7/\pm 45_9/90]$	0.662	0.175	0.070	0.310
$[0_5/\pm 45_2/90]$	0.518	0.208	0.109	0.423
$[0_2/\pm 45/90]$	0.445	0.289	0.109	0.308
$[0/\pm 45_4/90]$	0.217	0.217	0.187	0.552
$[0/\pm 45]$	0.370	0.155	0.161	0.734
$[0/\pm 45/0]$	0.499	0.141	0.129	0.701
$[0/\pm 30]$	0.510	0.074	0.129	1.220
$[0/\pm 30/0]$	0.611	0.072	0.104	1.079
$[\pm 12.5]$	0.764	0.053	0.066	0.913

$$Tr = E_1 / 0.880$$

Flexural stress and strain (symmetric laminates)



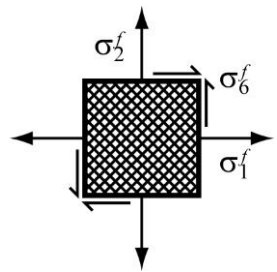
A laminate has **midplane symmetry**, i.e. it is symmetric, when the stacking sequence on both sides starting from the middle plane is identical.

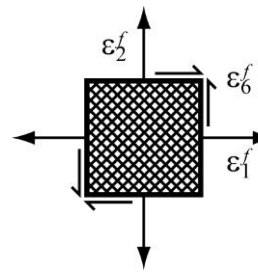
Flexural stress-strain relations

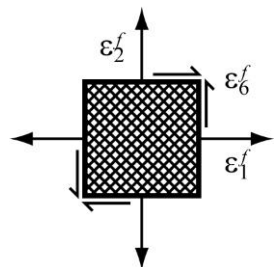
Normalised flexural stiffness

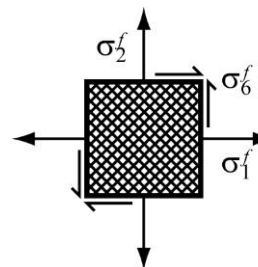
$$[D] = \int_{-h/2}^{h/2} [Q]z^2 dz = \frac{1}{3} \sum_{i=1}^m [Q']^{(i)} \left[z^{(i)} \right]^3 - \left[z^{(i-1)} \right]^3 \Big] , [D^*] = \frac{12}{h^3} [D]$$

$[Q']^{(i)}$ = off-axis stiffness of the i-th ply group with angle $\theta^{(i)}$



$$\begin{Bmatrix} \sigma_1^f \\ \sigma_2^f \\ \sigma_6^f \end{Bmatrix} = \begin{bmatrix} D_{11}^* & D_{12}^* & D_{16}^* \\ D_{21}^* & D_{22}^* & D_{26}^* \\ D_{61}^* & D_{62}^* & D_{66}^* \end{bmatrix} \begin{Bmatrix} \varepsilon_1^f \\ \varepsilon_2^f \\ \varepsilon_6^f \end{Bmatrix}$$




$$\begin{Bmatrix} \varepsilon_1^f \\ \varepsilon_2^f \\ \varepsilon_6^f \end{Bmatrix} = \begin{bmatrix} d_{11}^* & d_{12}^* & d_{16}^* \\ d_{21}^* & d_{22}^* & d_{26}^* \\ d_{61}^* & d_{62}^* & d_{66}^* \end{bmatrix} \begin{Bmatrix} \sigma_1^f \\ \sigma_2^f \\ \sigma_6^f \end{Bmatrix}$$


Flexural stress-strain relations

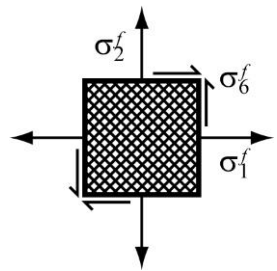
Normalised flexural stiffness

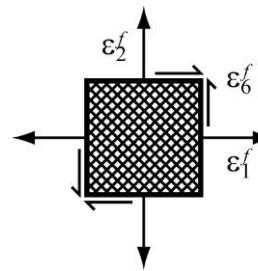
$$[D] = \int_{-h/2}^{h/2} [Q]z^2 dz = \frac{1}{3} \sum_{i=1}^m [Q']^{(i)} \left[z^{(i)} \right]^3 - \left[z^{(i-1)} \right]^3$$

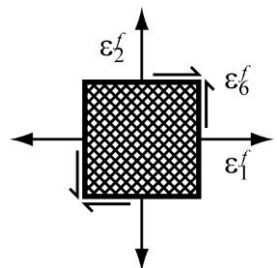
$$[D^*] = \frac{12}{h^3} [D]$$

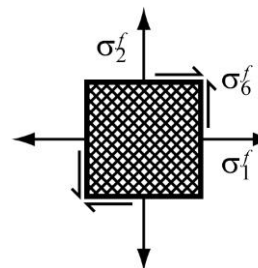
$[Q']^{(i)}$ = off-axis stiffness of the i-th ply group with angle $\theta^{(i)}$

Bend-twist coupling



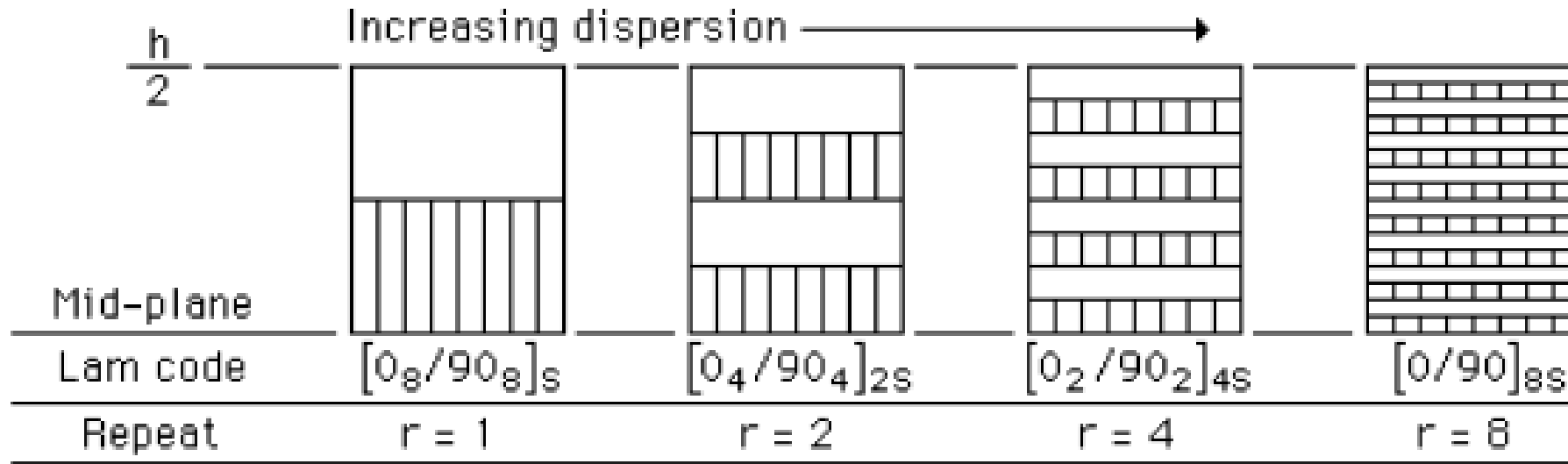
$$\begin{Bmatrix} \sigma_1^f \\ \sigma_2^f \\ \sigma_6^f \end{Bmatrix} = \begin{bmatrix} D_{11}^* & D_{12}^* & D_{16}^* \\ D_{21}^* & D_{22}^* & D_{26}^* \\ D_{61}^* & D_{62}^* & D_{66}^* \end{bmatrix} \begin{Bmatrix} \varepsilon_1^f \\ \varepsilon_2^f \\ \varepsilon_6^f \end{Bmatrix}$$




$$\begin{Bmatrix} \varepsilon_1^f \\ \varepsilon_2^f \\ \varepsilon_6^f \end{Bmatrix} = \begin{bmatrix} d_{11}^* & d_{12}^* & d_{16}^* \\ d_{21}^* & d_{22}^* & d_{26}^* \\ d_{61}^* & d_{62}^* & d_{66}^* \end{bmatrix} \begin{Bmatrix} \sigma_1^f \\ \sigma_2^f \\ \sigma_6^f \end{Bmatrix}$$


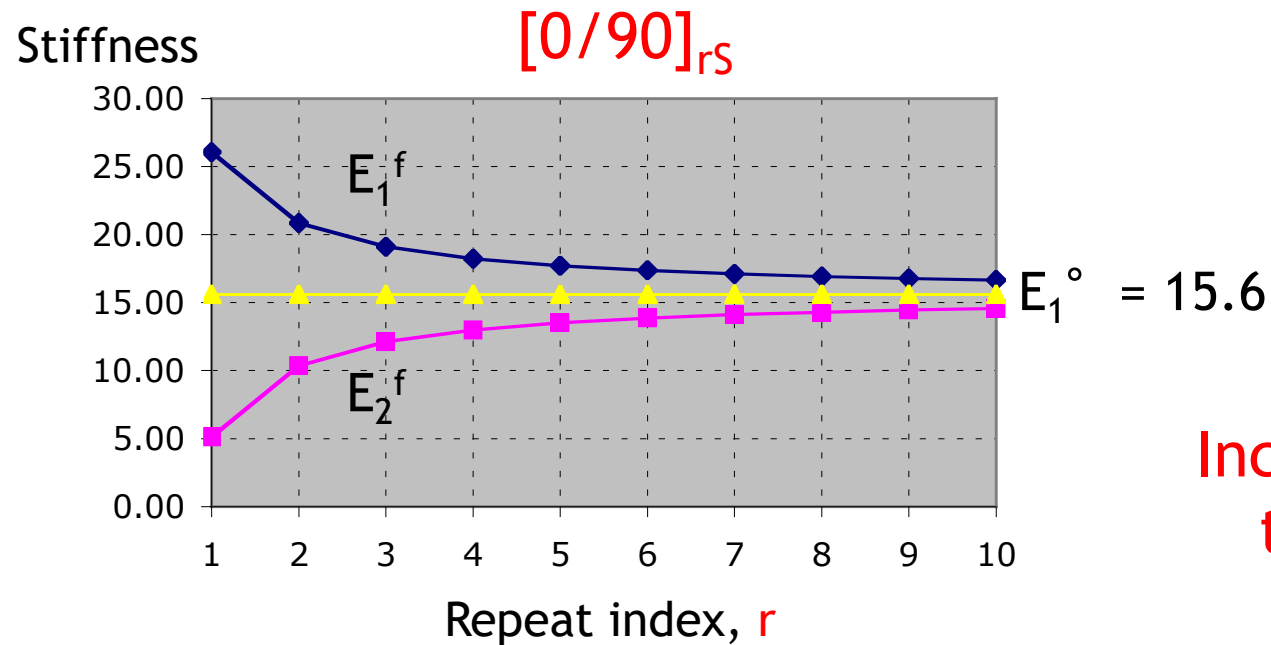
Off-axis (+/-θ) plies

Repeating sub-laminates



From: Tsai SW. *Composites Design Workshop*.
Stanford: Composites Design Group,
Department of Aeronautics and Astronautics,
Stanford University.

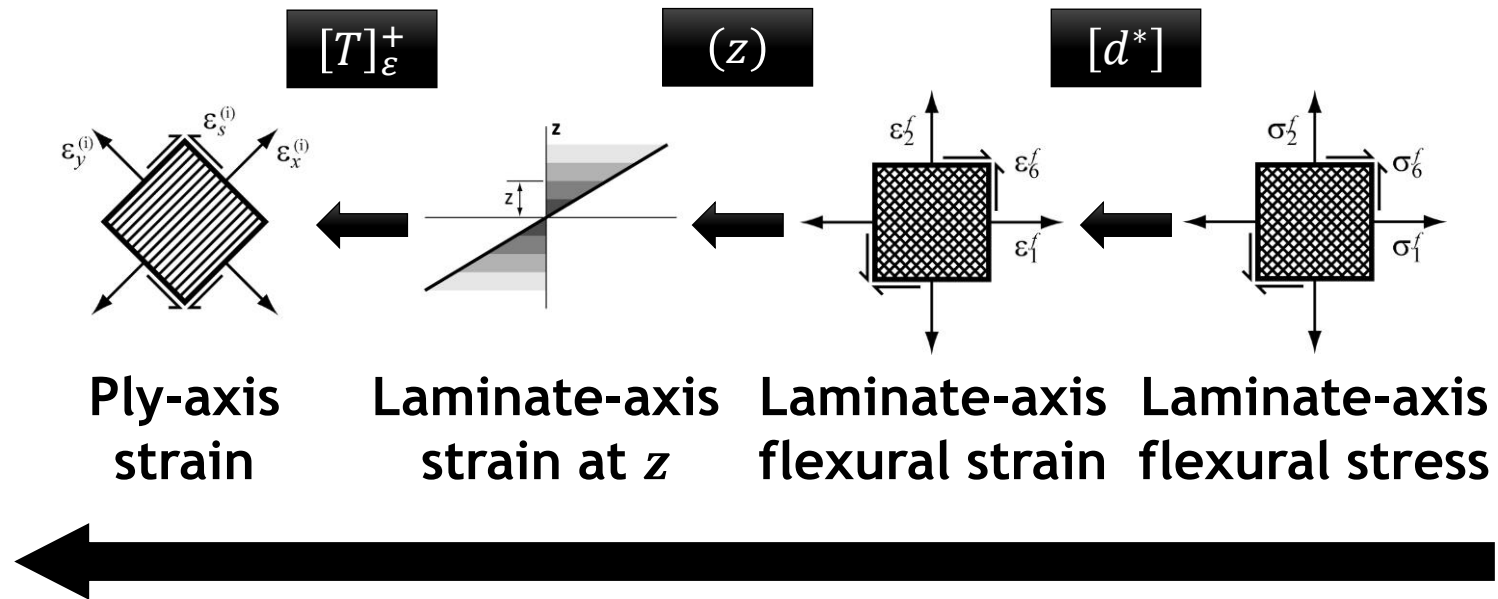
Repeating sub-laminates



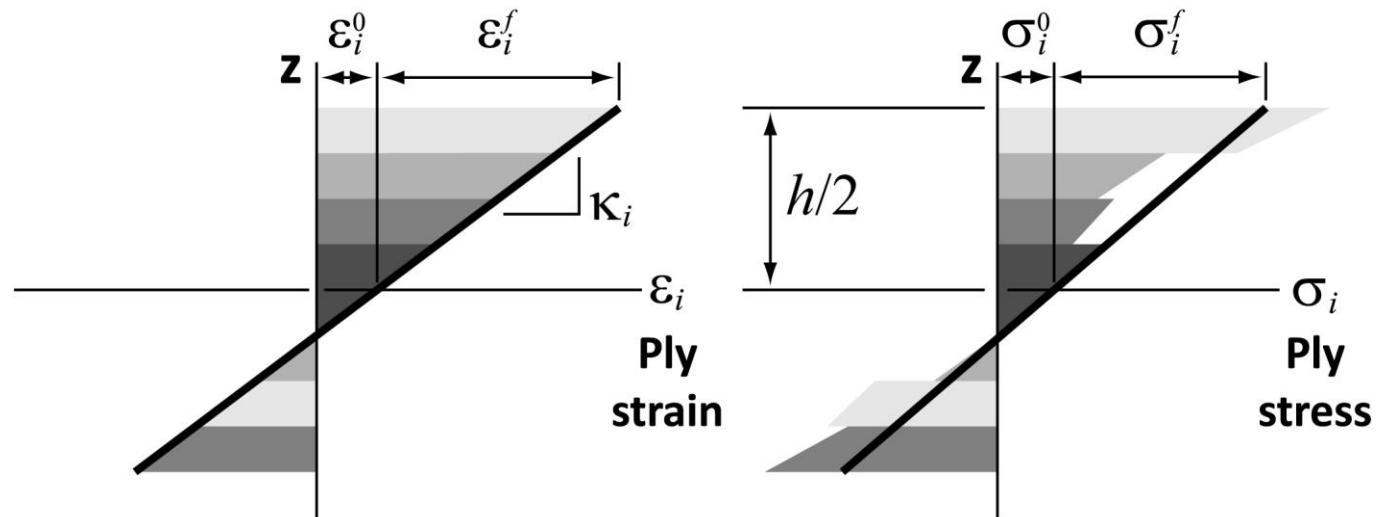
Increasing the repeat index leads to laminate homogenisation

From: Tsai SW. *Composites Design Workshop*.
Stanford: Composites Design Group,
Department of Aeronautics and Astronautics,
Stanford University.

Ply strain from laminate flexural stress



Unsymmetric laminates



$$\{\sigma^0\} = \frac{1}{h} \{N\}, \quad \{\sigma^f\} = \frac{6}{h^2} \{M\}, \quad \{\varepsilon^f\} = \frac{h}{2} \{\kappa\}$$

Unsymmetric laminates

$$\{N\} = \int_{-h/2}^{h/2} \{\sigma\} dz = \int_{-h/2}^{h/2} [Q] \{\underline{\varepsilon}\} dz = \int_{-h/2}^{h/2} [Q] [\{\underline{\varepsilon}^0\} + z\{\underline{\kappa}\}] dz$$

$$= \left[\int_{-h/2}^{h/2} [Q] dz \right] \{\underline{\varepsilon}^0\} + \left[\int_{-h/2}^{h/2} [Q] z dz \right] \{\underline{\kappa}\} = \underline{[A]} \{\underline{\varepsilon}^0\} + \underline{[B]} \{\underline{\kappa}\}$$

Bending-extension coupling

$$\{M\} = \int_{-h/2}^{h/2} \{\sigma\} z dz = \int_{-h/2}^{h/2} [Q] \{\underline{\varepsilon}\} z dz = \int_{-h/2}^{h/2} [Q] [\{\underline{\varepsilon}^0\} + z\{\underline{\kappa}\}] z dz$$

$$= \left[\int_{-h/2}^{h/2} [Q] z dz \right] \{\underline{\varepsilon}^0\} + \left[\int_{-h/2}^{h/2} [Q] z^2 dz \right] \{\underline{\kappa}\} = \underline{[B]} \{\underline{\varepsilon}^0\} + \underline{[D]} \{\underline{\kappa}\}$$

Bending-extension coupling

$$\{\sigma^0\} = \frac{1}{h} \{N\}, \quad \{\sigma^f\} = \frac{6}{h^2} \{M\}, \quad \{\varepsilon^f\} = \frac{h}{2} \{\kappa\}$$

$$[A^*] = \frac{1}{h} [A], \quad [B^*] = \frac{2}{h^2} [B], \quad [D^*] = \frac{12}{h^3} [D], \quad \text{in Pa}$$

Stress-strain relations

The general stress-strain relation for laminated plates can be written as:

$$\begin{Bmatrix} N \\ M \end{Bmatrix} = \begin{bmatrix} A & B \\ B & D \end{bmatrix} \begin{Bmatrix} \varepsilon_0 \\ K \end{Bmatrix}$$

with **A**, **B** and **D** the **extension (membrane)**, **bending/extension coupling** and **bending stiffness** matrices, ε_0 the **deformation** of the mid-plane, and **K** the **curvature**.

Stress-strain relations

Considering also non-mechanical loadings, for example temperature and moisture, then:

$$\begin{Bmatrix} N + N^T + N^H \\ M + M^T + M^H \end{Bmatrix} = \begin{bmatrix} A & B \\ B & D \end{bmatrix} \begin{Bmatrix} \varepsilon_0 \\ K \end{Bmatrix}$$

with T for **thermal** and H for **hygroscopic** effects.

Stress-strain relations

Bending-extension coupling

	ABSOLUTE	NORMALISED	RECOMMENDED
STIFFNESS	$\begin{Bmatrix} N_i \\ M_i \end{Bmatrix} = \begin{bmatrix} A_{ij} & B_{ij} \\ B_{ij} & D_{ij} \end{bmatrix} \begin{Bmatrix} \varepsilon_j^0 \\ \kappa_j \end{Bmatrix}$	$\begin{Bmatrix} \sigma_i^0 \\ \sigma_i^f \end{Bmatrix} = \begin{bmatrix} A_{ij}^* & B_{ij}^* \\ 3B_{ij}^* & D_{ij}^* \end{bmatrix} \begin{Bmatrix} \varepsilon_j^0 \\ \varepsilon_j^f \end{Bmatrix}$	
COMPLIANCE	$\begin{Bmatrix} \varepsilon_i^0 \\ \kappa_i \end{Bmatrix} = \begin{bmatrix} a_{ij} & b_{ij} \\ \tilde{b}_{ij} & d_{ij} \end{bmatrix} \begin{Bmatrix} N_j \\ M_j \end{Bmatrix}$	$\begin{Bmatrix} \varepsilon_i^0 \\ \varepsilon_i^f \end{Bmatrix} = \begin{bmatrix} a_{ij}^* & \frac{1}{3} b_{ij}^* \\ \tilde{b}_{ij}^* & d_{ij}^* \end{bmatrix} \begin{Bmatrix} \sigma_j^0 \\ \sigma_j^f \end{Bmatrix}$	

$$A_{ij}^*, B_{ij}^*, D_{ij}^* = \left[\frac{1}{h} A_{ij}, \frac{2}{h^2} B_{ij}, \frac{12}{h^3} D_{ij} \right]$$

Stress-strain relations

Bending-extension coupling

	ABSOLUTE	NORMALISED	
STIFFNESS	$\begin{Bmatrix} N_i \\ M_i \end{Bmatrix} = \begin{bmatrix} A_{ij} & B_{ij} \\ B_{ij} & D_{ij} \end{bmatrix} \begin{Bmatrix} \varepsilon_j^0 \\ \kappa_j \end{Bmatrix}$	$\begin{Bmatrix} \sigma_i^0 \\ \sigma_i^f \end{Bmatrix} = \begin{bmatrix} A_{ij}^* & B_{ij}^* \\ 3B_{ij}^* & D_{ij}^* \end{bmatrix} \begin{Bmatrix} \varepsilon_j^0 \\ \varepsilon_j^f \end{Bmatrix}$	RECOMMENDED
COMPLIANCE	$\begin{Bmatrix} \varepsilon_i^0 \\ \kappa_i \end{Bmatrix} = \begin{bmatrix} a_{ij} & b_{ij} \\ \tilde{b}_{ij} & d_{ij} \end{bmatrix} \begin{Bmatrix} N_j \\ M_j \end{Bmatrix}$	$\begin{Bmatrix} \varepsilon_i^0 \\ \varepsilon_i^f \end{Bmatrix} = \begin{bmatrix} a_{ij}^* & \frac{1}{3} b_{ij}^* \\ \tilde{b}_{ij}^* & d_{ij}^* \end{bmatrix} \begin{Bmatrix} \sigma_j^0 \\ \sigma_j^f \end{Bmatrix}$	

Rule to avoid bending-extension coupling:

- Laminate symmetry

Stress-strain relations

Bending-extension coupling

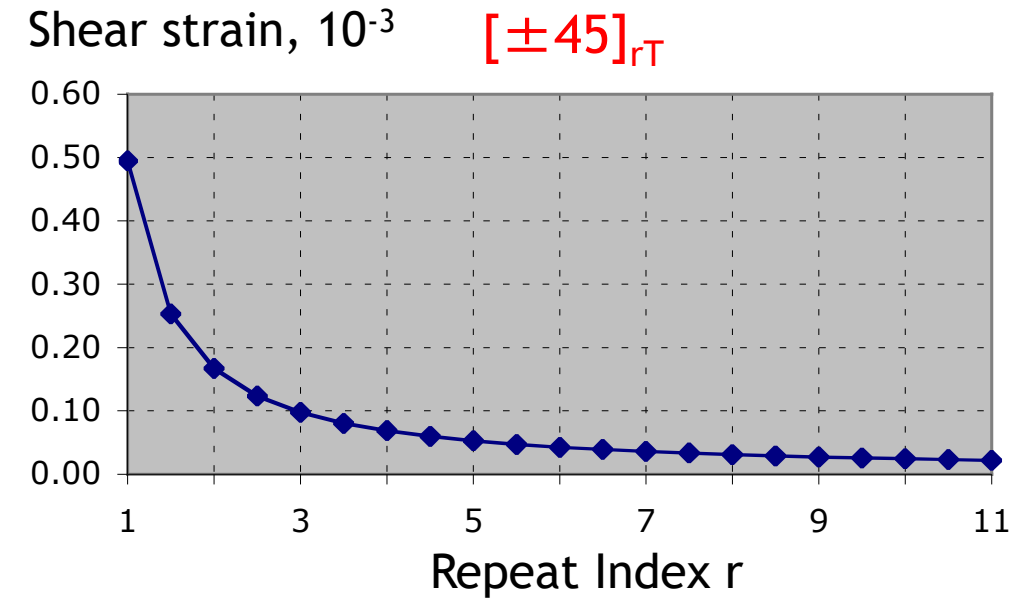
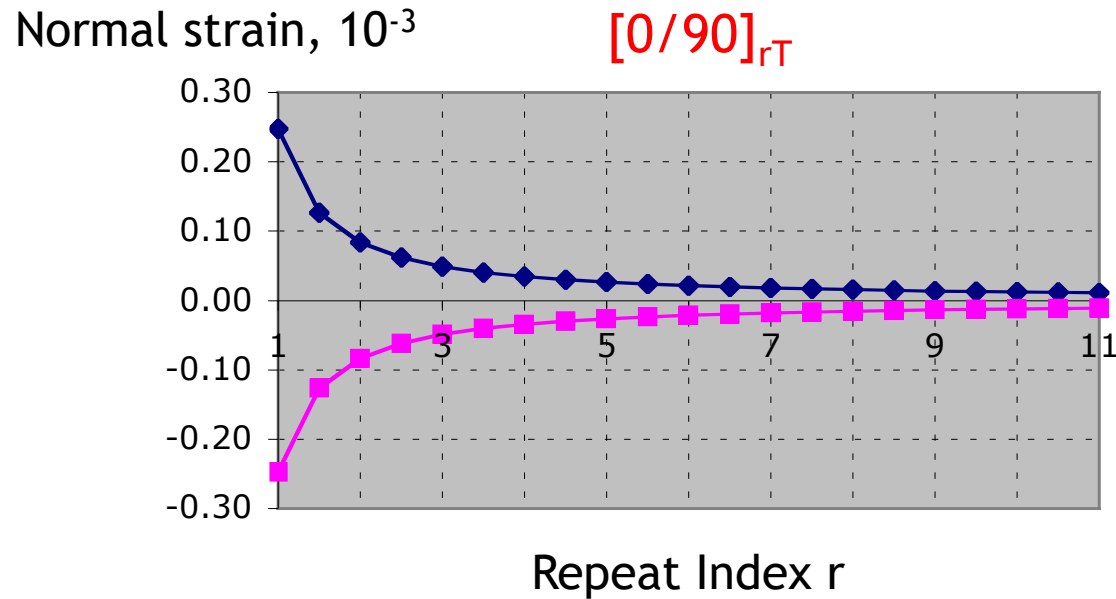
	ABSOLUTE	NORMALISED	
STIFFNESS	$\begin{Bmatrix} N_i \\ M_i \end{Bmatrix} = \begin{bmatrix} A_{ij} & B_{ij} \\ B_{ij} & D_{ij} \end{bmatrix} \begin{Bmatrix} \varepsilon_j^0 \\ \kappa_j \end{Bmatrix}$	$\begin{Bmatrix} \sigma_i^0 \\ \sigma_i^f \end{Bmatrix} = \begin{bmatrix} A_{ij}^* & B_{ij}^* \\ 3B_{ij}^* & D_{ij}^* \end{bmatrix} \begin{Bmatrix} \varepsilon_j^0 \\ \varepsilon_j^f \end{Bmatrix}$	RECOMMENDED
COMPLIANCE	$\begin{Bmatrix} \varepsilon_i^0 \\ \kappa_i \end{Bmatrix} = \begin{bmatrix} a_{ij} & b_{ij} \\ \tilde{b}_{ij} & d_{ij} \end{bmatrix} \begin{Bmatrix} N_j \\ M_j \end{Bmatrix}$	$\begin{Bmatrix} \varepsilon_i^0 \\ \varepsilon_i^f \end{Bmatrix} = \begin{bmatrix} a_{ij}^* & \frac{1}{3} b_{ij}^* \\ \tilde{b}_{ij}^* & d_{ij}^* \end{bmatrix} \begin{Bmatrix} \sigma_j^0 \\ \sigma_j^f \end{Bmatrix}$	

Homogeneous Plate: $[A^*] = [D^*]$, $[B^*] = 0$; $[\alpha^*] = [\delta^*]$, $[\beta^*] = 0$:

$$\{ \sigma^0 \pm \sigma^f \} = [A^*] \{ \varepsilon^0 \pm \varepsilon^f \} ; \{ \varepsilon^0 \pm \varepsilon^f \} = [\alpha^*] \{ \sigma^0 \pm \sigma^f \}$$

Warpage reduction by increasing r

Warping is drastically reduced by sub-laminate repetition (homogenisation)



Tsai SW. Composites Design Workshop. Stanford: Composites Design Group, Department of Aeronautics and Astronautics, Stanford University.

Questions?

Classical lamination theory

Part 2

SASCOM

Introductory course on composite materials 2021

Albertino Arteiro & Pedro P. Camanho

INEGI, University of Porto, Porto, Portugal

SASCOM

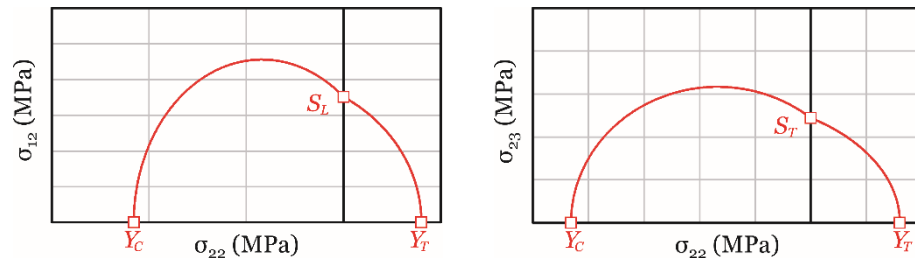
Introductory course on composite materials 2021

Designing with composite materials
Failure mechanisms and failure criteria

Introduction

- **Failure criteria** define the limit values in stress (or strain) space that separate “failed” states from “non-failed” states under any possible combination of stresses (or strains), extending test data on simple uniaxial or shear stress states to combined stress states.
- **Composite materials**
“Failure criteria are needed to extend the uniaxial and pure shear test data of unidirectional composite materials to combined stresses.”

Tsai et al. **Composite Materials Design and Testing.**
Stanford, 2015.



Johnson et al. *Engineering Plasticity*. New York, 1973.

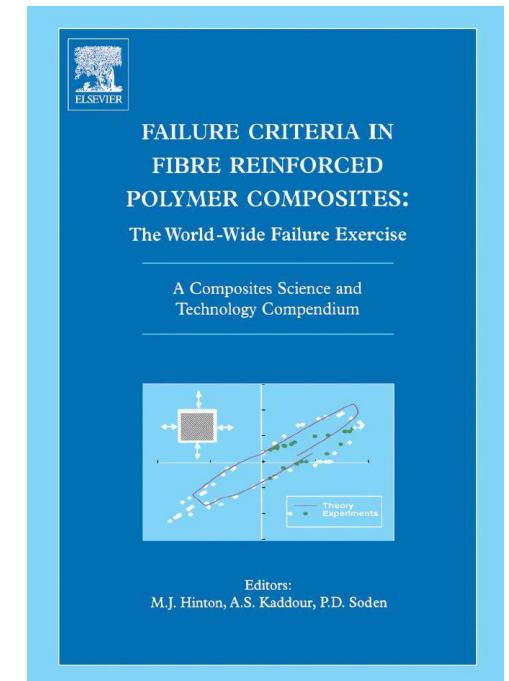
Chakrabarty. *Theory of Plasticity*. New York, 1987.

Gomes. *Mecânica dos Sólidos e Resistência dos Materiais*. Porto, 2004.

Camanho et al. In: Camanho et al. (eds.), *Numerical Modelling of Failure in Advanced Composite Materials*. Amsterdam, 2015. p. 111-150.

Introduction

Over more than one decade, in the 1990's and early 2000's, an international activity, known as the **World Wide Failure Exercise**, has been organised to improve the foundation on which failure criteria for composite materials are based.



Hinton *et al.* (eds.). *Failure Criteria in Fibre Reinforced Polymer Composites*. Amsterdam, 2004.

Micromechanics of failure: Failure mechanisms

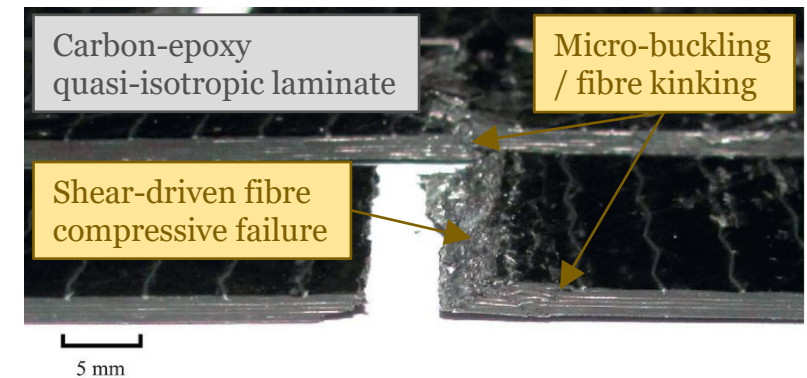
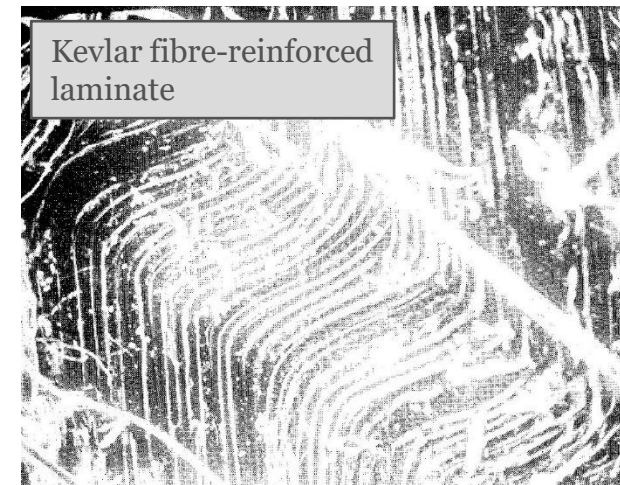
Longitudinal tension

- When loaded in the fibre direction, the phase with the lower ultimate strain, typically the fibre (e.g. polymer matrix composites), will fail first.

Micromechanics of failure: Failure mechanisms

Longitudinal compression

- Under longitudinal compression, failure is associated with **micro-buckling** or **kinking** of the fibres within the matrix, causing pronounced deformation in ductile fibres (e.g. aramid) or fracture planes in brittle fibres (e.g. carbon).
- In composites with high volume fractions and well-aligned fibres, **shear-driven compressive failure** may also occur.



Hahn *et al.* *Compression failure mechanisms of composite structures*. NASA report no. CR-3988, St. Louis, 1986.
Daniel *et al.* *Engineering Mechanics of Composite Materials*. New York, 1994.
Arteiro *et al.* *Compos Sci Technol* 2013;79:97-114.

Micromechanics of failure: Failure mechanisms

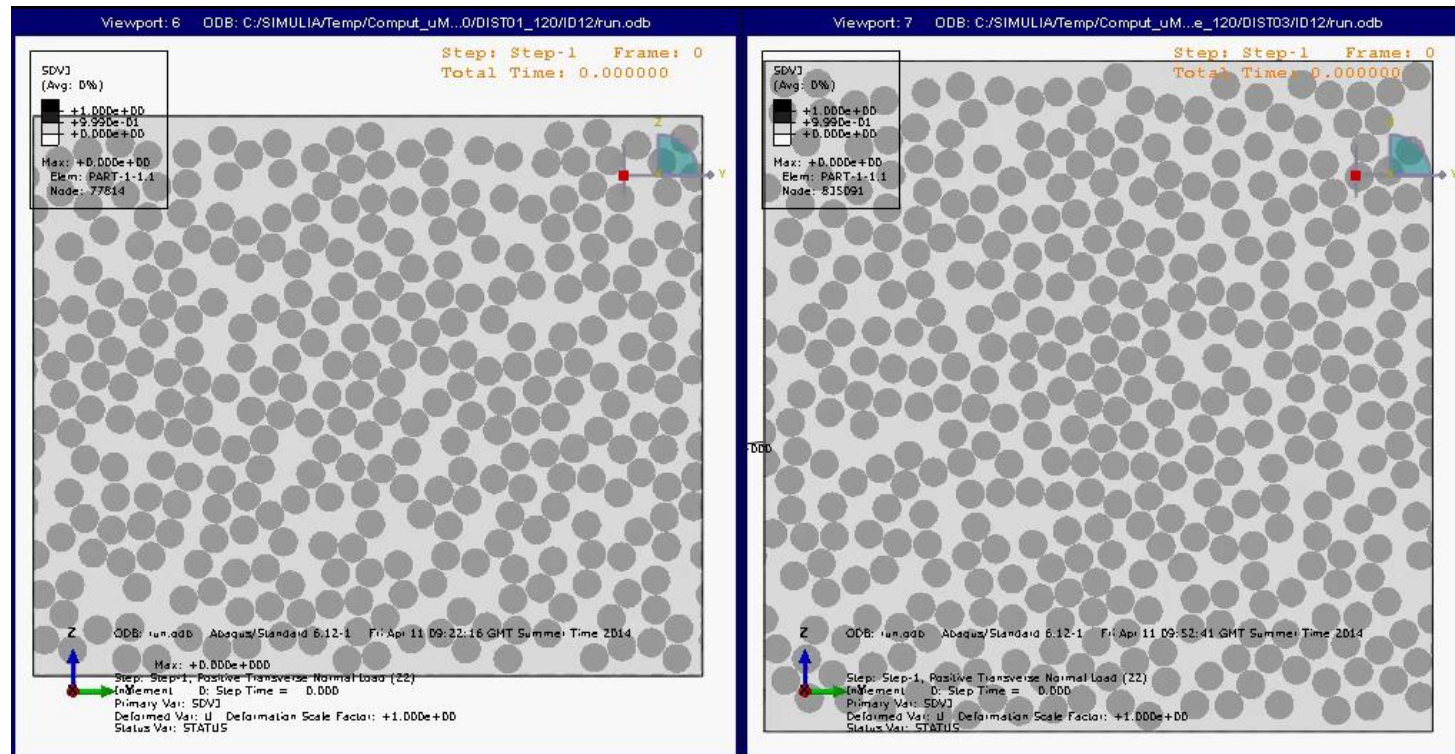
Transverse tension

- Transverse tension results in high stress and strain concentrations in the matrix and fibre-matrix interface.
- Failure takes the form of isolated interfacial microcracks increasing in number with loading and finally coalescing into a catastrophic transverse crack.

Micromechanics of failure: Failure mechanisms

Transverse tension

- (i) 0.100 mm
- (ii) 0.120 mm

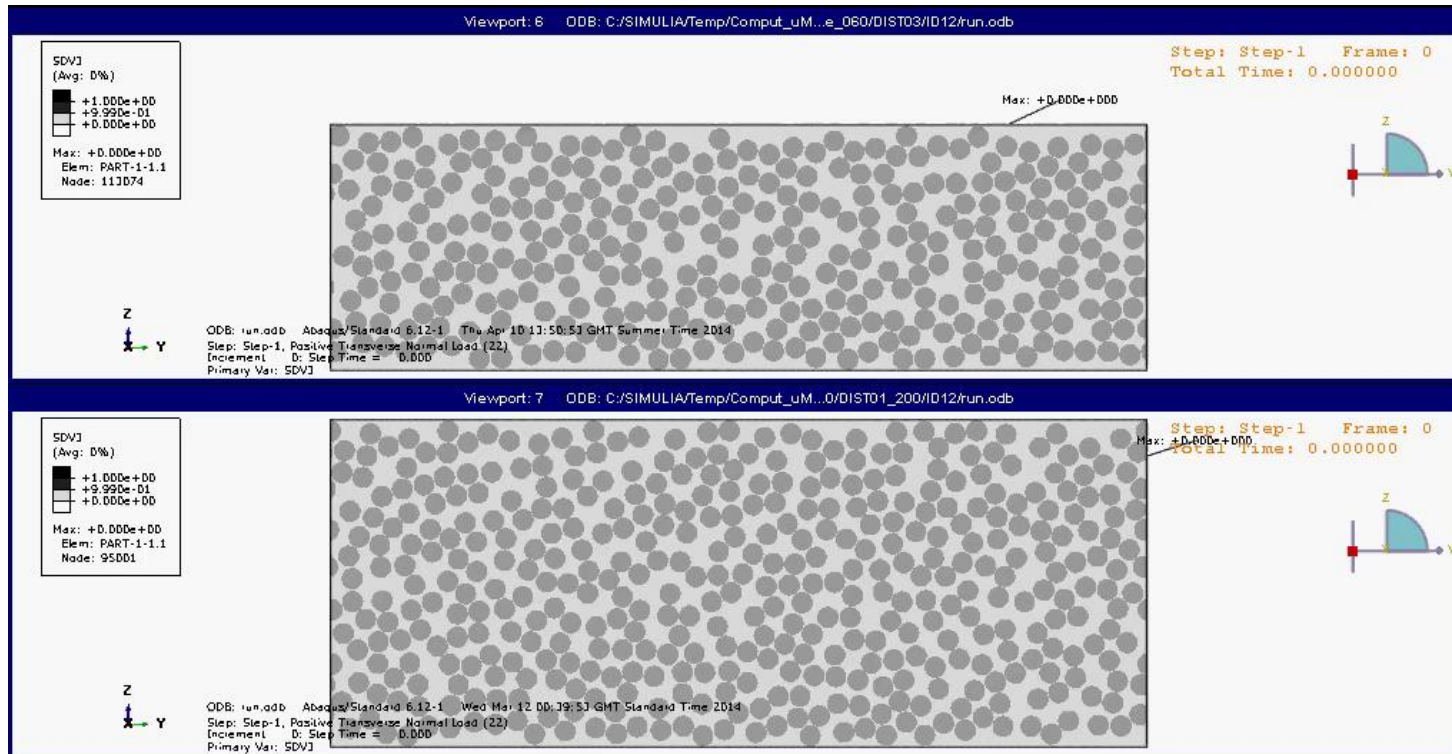


Arteiro et al. *Compos Struct* 2014;116:827-840.
Saito et al. *Adv Compos Mater* 2012;21:57-66.

Micromechanics of failure: Failure mechanisms

Transverse tension

- (i) 0.060 mm
- (ii) 0.080 mm

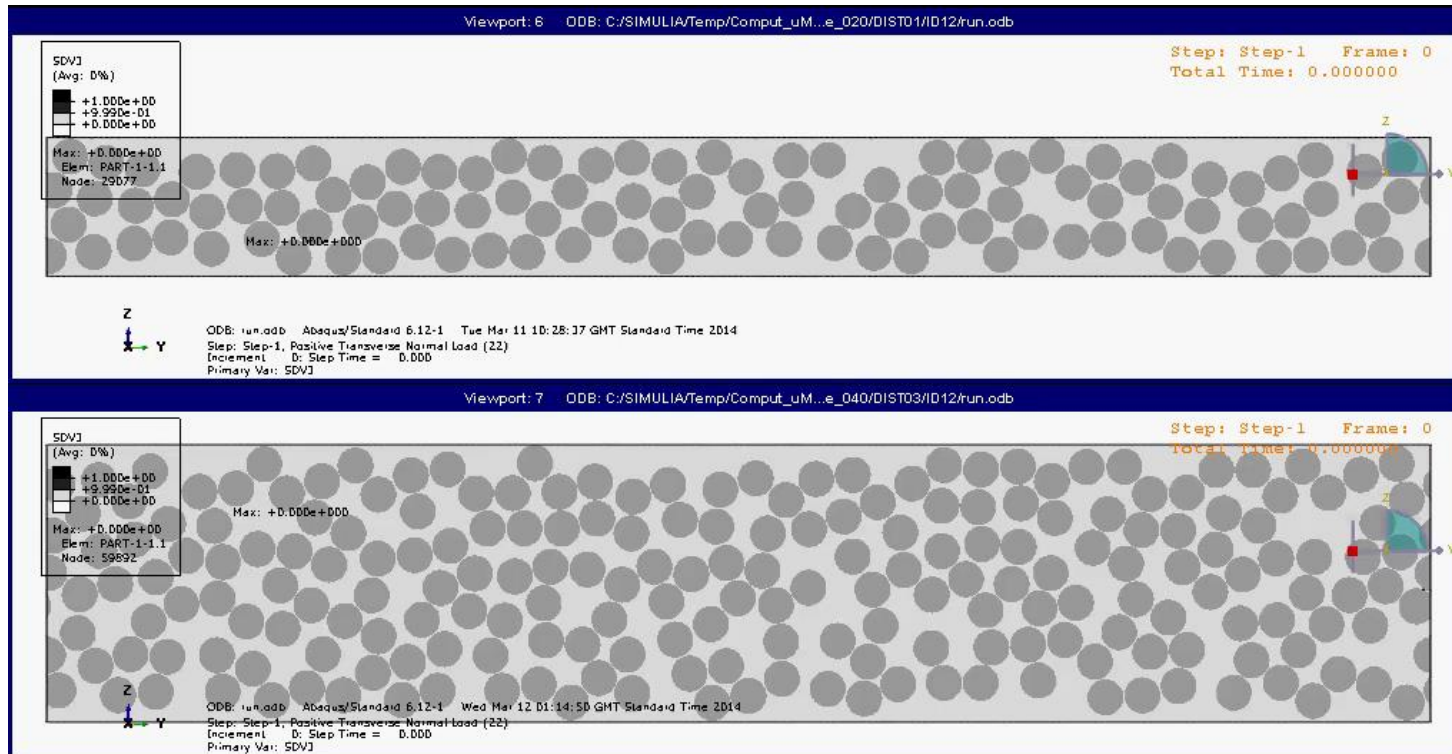


Arteiro *et al.* *Compos Struct* 2014;116:827-840.
Saito *et al.* *Adv Compos Mater* 2012;21:57-66.

Micromechanics of failure: Failure mechanisms

Transverse tension

- (i) 0.020 mm
- (ii) 0.040 mm

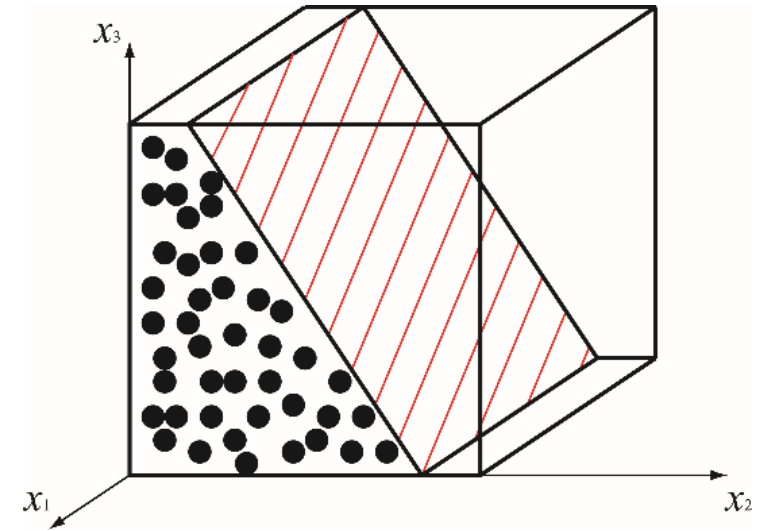


Arteiro *et al.* *Compos Struct* 2014;116:827-840.
Saito *et al.* *Adv Compos Mater* 2012;21:57-66.

Micromechanics of failure: Failure mechanisms

Transverse compression

- Under transverse compression, high interfacial shear stresses cause matrix shear failure and fibre-matrix debonding, leading to an overall shear failure mode characterised by a **wedge-shaped transverse fracture**.



Daniel et al. *Engineering Mechanics of Composite Materials*. New York, 1994.

González et al. *Compos Sci Technol* 2007;67:2795-2806.

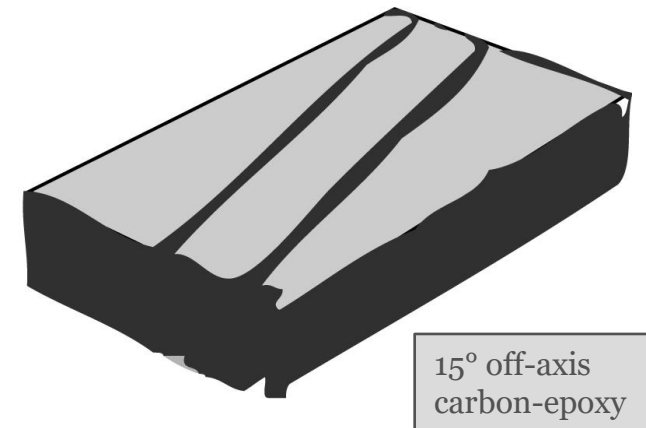
Arteiro et al. *Compos Part A-Appl S* 2015;79:127-137.

Micromechanics of failure: Failure mechanisms

In-plane shear

- Under in-plane shear, a high shear stress concentration develops at the fibre-matrix interface, causing **shear failure in the matrix** and/or fibre-matrix debonding.

In-plane shear failure mode



Daniel *et al.* *Engineering Mechanics of Composite Materials*. New York, 1994.
Koerber *et al.* *Mech Mater* 2010;42:1004-1019.

Maximum stress failure criterion

- Failure occurs when at least **one stress component** along the principal material axes **exceeds** the corresponding **strength** in that direction.
- **The maximum stress criterion is more appropriate for the brittle failure modes and does not consider any interaction under general stress states.**

$$\sigma_1 = \begin{cases} F_{1t} & \text{when } \sigma_1 > 0 \\ -F_{1c} & \text{when } \sigma_1 < 0 \end{cases}$$

$$\sigma_2 = \begin{cases} F_{2t} & \text{when } \sigma_2 > 0 \\ -F_{2c} & \text{when } \sigma_2 < 0 \end{cases}$$

$$|\tau_6| = F_6$$

Maximum strain failure criterion

- Failure occurs when at least **one strain component** along the principal material axes **exceeds** the corresponding **ultimate strain** in that direction.
- The maximum strain criterion allows for some **interaction** of stress components due to **Poisson's effect**.

$$\epsilon_1 = \begin{cases} \epsilon_{1t}^u & \text{when } \epsilon_1 > 0 \\ \epsilon_{1c}^u & \text{when } \epsilon_1 < 0 \end{cases}$$

$$\epsilon_2 = \begin{cases} \epsilon_{2t}^u & \text{when } \epsilon_2 > 0 \\ \epsilon_{2c}^u & \text{when } \epsilon_2 < 0 \end{cases}$$

$$|\gamma_6| = 2|\epsilon_{12}| = \gamma_6^u$$

- A non-interacting maximum allowable strain criterion is commonly used in phenomenological failure criteria to represent longitudinal tensile failure.

Daniel et al. *Engineering Mechanics of Composite Materials*. New York, 1994.
Dávila et al. *J Compos Mater* 2005;39(4):323-345.
Camanho et al. *Int J Solids Struct* 2015;55:92-107.

Tsai-Hill (deviatoric strain energy) failure criterion

- Hill modified the von Mises criterion for the case of **ductile metals with anisotropy** (e.g. laminated metal sheet).
- Later, Tsai adapted this criterion for unidirectional composite laminae with transverse isotropy.

$$\frac{\sigma_1^2}{F_1^2} + \frac{\sigma_2^2}{F_2^2} + \frac{\tau_6^2}{F_6^2} - \frac{\sigma_1 \sigma_2}{F_1^2} = 1$$

$$F_1 = \begin{cases} F_{1t} & \text{when } \sigma_1 > 0 \\ F_{1c} & \text{when } \sigma_1 < 0 \end{cases}$$

$$F_2 = \begin{cases} F_{2t} & \text{when } \sigma_2 > 0 \\ F_{2c} & \text{when } \sigma_2 < 0 \end{cases}$$

Daniel *et al.* *Engineering Mechanics of Composite Materials*. New York, 1994.

Tsai. *Theory of Composites Design*. Stanford, 2008.

Tsai *et al.* *Composite Materials Design and Testing*. Stanford, 2015.

Tsai-Hill (deviatoric strain energy) failure criterion

- The Tsai-Hill failure criterion is expressed in terms of a **single criterion**, and it allows for considerable **interaction** among the stress components.
- However, no distinction is made between tensile and compressive strengths. The strength parameters must be specified according to the signs of the normal stresses σ_1 and σ_2 .

$$\frac{\sigma_1^2}{F_1^2} + \frac{\sigma_2^2}{F_2^2} + \frac{\tau_6^2}{F_6^2} - \frac{\sigma_1 \sigma_2}{F_1^2} = 1$$

$$F_1 = \begin{cases} F_{1t} & \text{when } \sigma_1 > 0 \\ F_{1c} & \text{when } \sigma_1 < 0 \end{cases}$$

$$F_2 = \begin{cases} F_{2t} & \text{when } \sigma_2 > 0 \\ F_{2c} & \text{when } \sigma_2 < 0 \end{cases}$$

Tsai-Wu (interactive tensor polynomial) failure criterion

- The Tsai-Wu failure criterion is a modified **tensor polynomial criterion** for orthotropic or transversely isotropic laminae.
- It allows for the distinction between **tensile** and **compressive strengths** and it accounts for the **interaction** between the normal stresses.

Plane stress state

$$F_{xx}\sigma_x^2 + 2F_{xy}\sigma_x\sigma_y + F_{yy}\sigma_y^2 + F_{ss}\sigma_s^2 + F_x\sigma_x + F_y\sigma_y = 1$$

$$\frac{\sigma_x^2}{XX'} + \frac{2F_{xy}^* \sigma_x \sigma_y}{\sqrt{XX'YY'}} + \frac{\sigma_y^2}{YY'} + \frac{\sigma_s^2}{S^2} + \left[\frac{1}{X} - \frac{1}{X'} \right] \sigma_x + \left[\frac{1}{Y} - \frac{1}{Y'} \right] \sigma_y = 1$$

Daniel et al. *Engineering Mechanics of Composite Materials*. New York, 1994.

Tsai. *Theory of Composites Design*. Stanford, 2008.

Tsai et al. *Composite Materials Design and Testing*. Stanford, 2015.

Tsai-Wu (interactive tensor polynomial) failure criterion

- The **admissible range** of the normalised interaction term that ensures a **closed envelope** and **acceptable inclinations** of the tangents to the failure envelopes at the **four anchor points** is generally **between -1 and 0**.
- When the normalised interaction term is **-1/2**, the **von Mises failure criterion** can be **recovered** if anisotropy is reduced to **isotropy** and the **tensile and compressive strengths are equal**.

Plane stress state

$$F_{xx}\sigma_x^2 + 2F_{xy}\sigma_x\sigma_y + F_{yy}\sigma_y^2 + F_{ss}\sigma_s^2 + F_x\sigma_x + F_y\sigma_y = 1$$

$$\frac{\sigma_x^2}{XX'} + \frac{2F_{xy}^* \sigma_x \sigma_y}{\sqrt{XX'YY'}} + \frac{\sigma_y^2}{YY'} + \frac{\sigma_s^2}{S^2} + \left[\frac{1}{X} - \frac{1}{X'} \right] \sigma_x + \left[\frac{1}{Y} - \frac{1}{Y'} \right] \sigma_y = 1$$

Daniel et al. *Engineering Mechanics of Composite Materials*. New York, 1994.

Tsai. *Theory of Composites Design*. Stanford, 2008.

Tsai et al. *Composite Materials Design and Testing*. Stanford, 2015.

Tsai-Wu (interactive tensor polynomial) failure criterion

Other advantages:

- The Tsai-Wu failure criterion is a **closed-form, single-valued function**, operationally simple and readily amenable to computational procedures.
- It satisfies the invariant requirements of coordinate transformation, following normal transformation laws, and the strength tensors display similar symmetry properties as the stiffnesses and compliances.

However, **it is not possible to identify failure modes.**

Daniel *et al.* *Engineering Mechanics of Composite Materials*. New York, 1994.

Tsai. *Theory of Composites Design*. Stanford, 2008.

Tsai *et al.* *Composite Materials Design and Testing*. Stanford, 2015.

Hashin failure criteria

- Hashin proposed a set of interactive failure criteria for unidirectional composites that could model distinct failure modes for both two- and three-dimensional cases.

Tensile fibre failure—for $\sigma_{11} \geq 0$

$$\left(\frac{\sigma_{11}}{X_T}\right)^2 + \frac{\sigma_{12}^2 + \sigma_{13}^2}{S_{12}^2} = \begin{cases} > 1 \text{ failure} \\ \leq 1 \text{ no failure} \end{cases}$$

Compressive fibre failure—for $\sigma_{11} < 0$

$$\left(\frac{\sigma_{11}}{X_C}\right)^2 = \begin{cases} > 1 \text{ failure} \\ \leq 1 \text{ no failure} \end{cases}$$

Tensile matrix failure—for $\sigma_{22} + \sigma_{33} > 0$

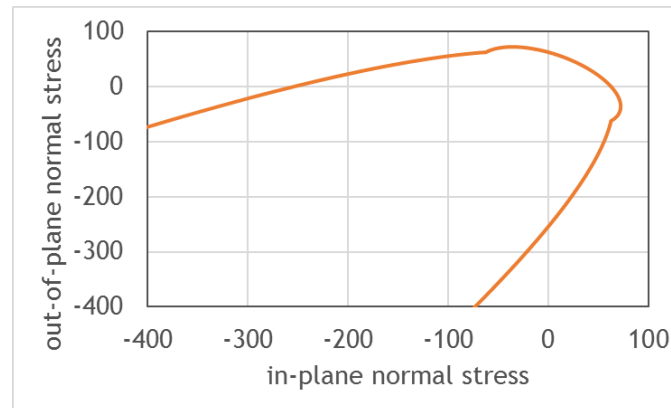
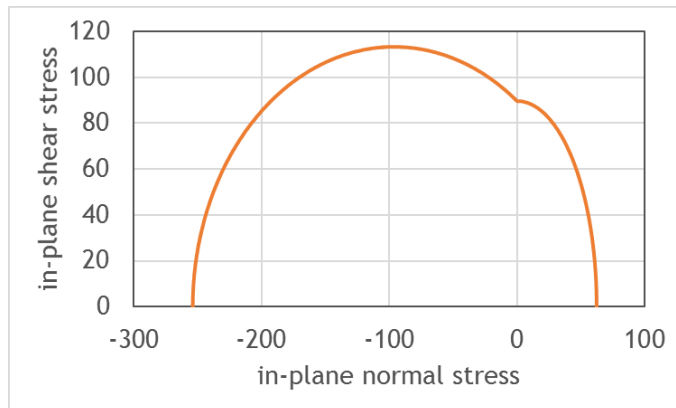
$$\left(\frac{\sigma_{22} + \sigma_{33}}{Y_T}\right)^2 + \frac{\sigma_{23}^2 - \sigma_{22}\sigma_{33}}{S_{23}^2}$$

$$+ \frac{\sigma_{12}^2 + \sigma_{13}^2}{S_{12}^2} = \begin{cases} > 1 \text{ failure} \\ \leq 1 \text{ no failure} \end{cases}$$

Compressive matrix failure—for $\sigma_{22} + \sigma_{33} < 0$

$$\left[\left(\frac{Y_C}{2S_{23}}\right)^2 - 1\right] \left(\frac{\sigma_{22} + \sigma_{33}}{Y_C}\right) + \frac{(\sigma_{22} + \sigma_{33})^2}{4S_{23}^2}$$

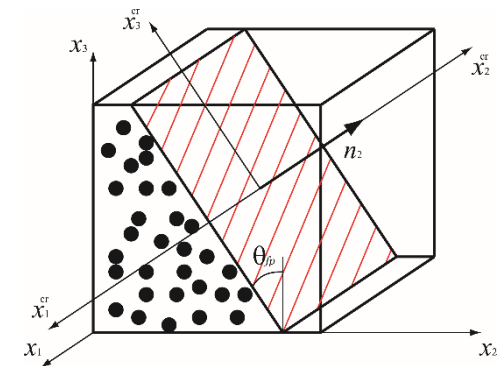
$$+ \frac{(\sigma_{23}^2 - \sigma_{22}\sigma_{33})}{S_{23}^2} + \frac{\sigma_{12}^2 + \sigma_{13}^2}{S_{12}^2} = \begin{cases} > 1 \text{ failure} \\ \leq 1 \text{ no failure} \end{cases}$$



Farooq et al. Acta Astronaut 2014;102:169-177.

Puck failure criteria

- Puck failure criterion for matrix transverse cracking is based on a **modified Mohr/Coulomb theory** for **brittle** transversely-isotropic materials.
- The **tractions** acting on the **fracture plane**, which needs to be determined, are used to assess failure under two fundamental regimes: transverse tension or transverse compression.



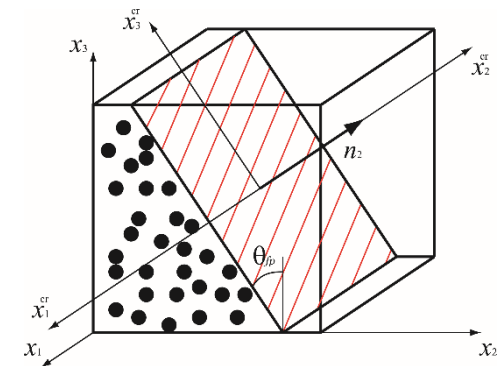
Puck *et al.* In: Hinton *et al.* (eds.), *Failure Criteria in Fibre Reinforced Polymer Composites*. Amsterdam, 2004. p. 264-297.

Camanho *et al.* *Int J Solids Struct* 2015;55:92-107.

Camanho *et al.* In: Camanho *et al.* (eds.), *Numerical Modelling of Failure in Advanced Composite Materials*. Amsterdam, 2015. p. 111-150.

Puck failure criteria

- The **orientation of the fracture plane** is determined when the plane of maximum stress effort is found. In general, a maximisation problem needs to be solved.
- In practice this is done varying the orientation of the fracture plane, calculating the failure index for every angle, and recording the orientation giving the maximum value of the failure index.



Puck *et al.* In: Hinton *et al.* (eds.), *Failure Criteria in Fibre Reinforced Polymer Composites*. Amsterdam, 2004. p. 264-297.

Camanho *et al.* *Int J Solids Struct* 2015;55:92-107.

Camanho *et al.* In: Camanho *et al.* (eds.), *Numerical Modelling of Failure in Advanced Composite Materials*. Amsterdam, 2015. p. 111-150.

Puck failure criteria

Fibre failure (FF)

Tensile

$$\frac{1}{\varepsilon_{ff}} \left(\varepsilon_1 + \frac{\nu_{f12}}{E_{fl}} m_{\sigma f} \sigma_2 \right) = 1$$

Compression (kinking)

$$\frac{1}{\varepsilon_{1c}} \left| \left(\varepsilon_1 + \frac{\nu_{f12}}{E_{fl}} m_{\sigma f} \sigma_2 \right) \right| = 1 - (10\gamma_{21})^2$$

Inter-fibre fracture (IFF)

Mode A, $\theta_{fp} = 0^\circ$

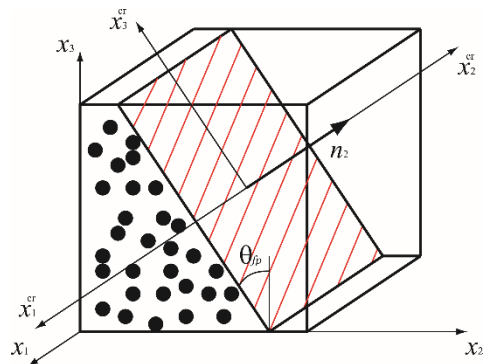
$$\sqrt{\left(\frac{\tau_{21}}{S_{21}} \right)^2 + \left(1 - p_{1\parallel}^{(+)} \frac{\gamma_T}{S_{21}} \right)^2 \left(\frac{\sigma_2}{Y_T} \right)^2} + p_{1\parallel}^{(+)} \frac{\sigma_2}{S_{21}} = 1 - \left| \frac{\sigma_1}{\sigma_{1D}} \right|$$

Mode B, $\theta_{fp} = 0^\circ$

$$\frac{1}{S_{21}} \left(\sqrt{\tau_{21}^2 + (p_{1\parallel}^{(-)} \sigma_2)^2} + p_{1\parallel}^{(-)} \sigma_2 \right) = 1 - \left| \frac{\sigma_1}{\sigma_{1D}} \right|$$

Mode C, $\cos \theta_{fp} = \sqrt{\frac{f_w R_{\perp\perp}^A}{(-\sigma_2)}}$

$$\left[\left(\frac{\tau_{21}}{2(1 + p_{1\parallel}^{(-)} S_{21})} \right)^2 + \left(\frac{\sigma_2}{Y_C} \right)^2 \right] \frac{Y_C}{(-\sigma_2)} = 1 - \left| \frac{\sigma_1}{\sigma_{1D}} \right|$$



Puck et al. In: Hinton et al. (eds.), *Failure Criteria in Fibre Reinforced Polymer Composites*. Amsterdam, 2004. p. 264-297.
Puck et al. In: Hinton et al. (eds.), *Failure Criteria in Fibre Reinforced Polymer Composites*. Amsterdam, 2004. p. 832-876.

Puck failure criteria

FF tension

$$\frac{1}{\epsilon_{1T}} \left(\epsilon_1 + \frac{\nu_{f12}}{E_{fl}} m_{\sigma f} \sigma_2 \right) = 1$$

Stress magnification factor of the transverse stress for the fibre (1.3 for glass and 1.1 for carbon)

FF compression

$$\frac{1}{\epsilon_{1C}} \left| \left(\epsilon_1 + \frac{\nu_{f12}}{\epsilon_{fl}} m_{\sigma f} \sigma_2 \right) \right| + (10\gamma_{21})^2 = 1$$

Empirical shear correction term

IFF mode A

$$\sqrt{\left(\frac{\tau_{21}}{S_{21}} \right)^2 + \left(1 - p_{\perp\parallel}^{(+)} \frac{\gamma_T}{S_{21}} \right)^2 \left(\frac{\sigma_2}{Y_T} \right)^2} + p_{\perp\parallel}^{(+)} \frac{\sigma_2}{S_{21}} = 1 - \left| \frac{\sigma_1}{\sigma_{1D}} \right|$$

Slopes of the failure envelope (fitted to the experimentally deduced slope)

Stress value for linear degradation

IFF mode B

$$\frac{1}{S_{21}} \left(\sqrt{\tau_{21}^2 + p_{\perp\parallel}^{(-)} \sigma_2^2} + p_{\perp\parallel}^{(-)} \sigma_2 \right) = 1 - \left| \frac{\sigma_1}{\sigma_{1D}} \right|$$

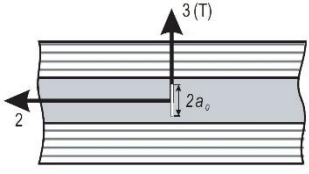
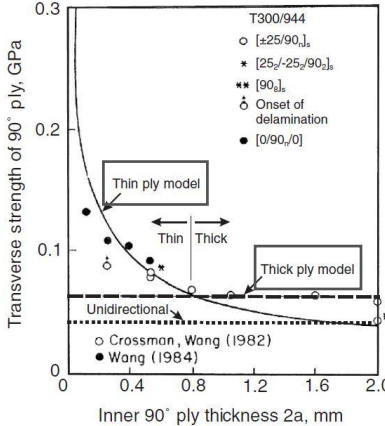
IFF mode C

$$\left[\left(\frac{\tau_{21}}{2(1 + p_{\perp\parallel}^{(-)} S_{21})} \right)^2 + \left(\frac{\sigma_2}{Y_C} \right)^2 \right] \frac{Y_C}{(-\sigma_2)} = 1 - \left| \frac{\sigma_1}{\sigma_{1D}} \right|$$

Puck et al. In: Hinton et al. (eds.), *Failure Criteria in Fibre Reinforced Polymer Composites*. Amsterdam, 2004. p. 264-297.
Puck et al. In: Hinton et al. (eds.), *Failure Criteria in Fibre Reinforced Polymer Composites*. Amsterdam, 2004. p. 832-876.

LaRC failure criteria

- Set of failure criteria for plane stress assumptions based on Hashin and Puck failure criteria.

Matrix tension, $\sigma_{22} \geq 0$	Matrix compression, $\sigma_{22} < 0$	
$FI_M = (1 - g) \left(\frac{\sigma_{22}}{Y_{is}^T} \right) + g \left(\frac{\sigma_{22}}{Y_{is}^T} \right)^2 + \left(\frac{\tau_{12}}{S_{is}^L} \right)^2$	$\sigma_{11} < -Y^C$ $FI_M = \left(\frac{\tau_{eff}^{mT}}{S^T} \right)^2 + \left(\frac{\tau_{eff}^{mL}}{S_{is}^L} \right)^2$	$\sigma_{11} \geq -Y^C$ $FI_M = \left(\frac{\tau_{eff}^T}{S^T} \right)^2 + \left(\frac{\tau_{eff}^L}{S_{is}^L} \right)^2$
In situ effect		
$Y_{is}^T = \sqrt{\frac{8G_{Ic}(L)}{\pi t \Lambda_{22}^0}}$ $S_{is}^L = \sqrt{\frac{8G_{IIc}(L)}{\pi t \Lambda_{44}^0}}$ $g = \frac{G_{Ic}(L)}{G_{IIc}(L)}$ <p style="text-align: center;">Thin</p>	$Y_{is}^T = 1.12\sqrt{2} Y^T$ $S_{is}^L = \sqrt{2} S^L$ $g = 1.12^2 \frac{\Lambda_{22}^0}{\Lambda_{44}^0} \left(\frac{Y^T}{S^L} \right)^2$ <p style="text-align: center;">Thick</p>	 $\Lambda_{22}^0 = 2 \left(\frac{1}{E_2} - \nu_{21}^2 \right)$ $\Lambda_{44}^0 = \frac{1}{G_{12}}$
		

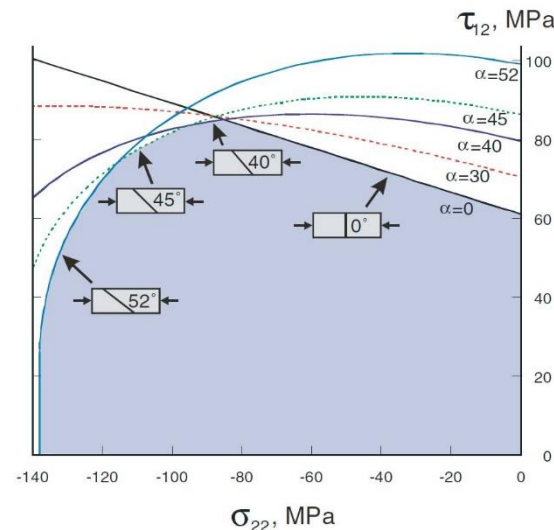
Dávila et al. J Compos Mater 2005;39(4):323-345.

LaRC failure criteria

- Set of failure criteria for plane stress assumptions based on Hashin and Puck failure criteria.

Matrix tension, $\sigma_{22} \geq 0$	Matrix compression, $\sigma_{22} < 0$	
$FI_M = (1 - g) \left(\frac{\sigma_{22}}{Y_{is}^T} \right) + g \left(\frac{\sigma_{22}}{Y_{is}^T} \right)^2 + \left(\frac{\tau_{12}}{S_{is}^L} \right)^2$	Biaxial compression	
	$\sigma_{11} < -Y^C$ $FI_M = \left(\frac{\tau_{eff}^{mT}}{S^T} \right)^2 + \left(\frac{\tau_{eff}^{mL}}{S_{is}^L} \right)^2$	$\sigma_{11} \geq -Y^C$ $FI_M = \left(\frac{\tau_{eff}^T}{S^T} \right)^2 + \left(\frac{\tau_{eff}^L}{S_{is}^L} \right)^2$

Fracture angle determined iteratively



$$\begin{cases} \tau_{eff}^T = \langle -\sigma_{22} \cos \alpha (\sin \alpha - \eta^T \cos \alpha) \rangle \\ \tau_{eff}^L = \langle \cos \alpha (|\tau_{12}| + \eta^L \sigma_{22} \cos \alpha) \rangle \end{cases}$$

$$\eta^T = \frac{-1}{\tan 2\alpha_0}$$

$$\eta^L \approx -\frac{S_{is}^L \cos 2\alpha_0}{Y^C \cos^2 \alpha_0} \quad \text{or from test data}$$

$$\alpha_0 = 53^\circ \quad \text{or from test data}$$

$$S^T = Y^C \cos \alpha_0 \left(\sin \alpha_0 + \frac{\cos \alpha_0}{\tan 2\alpha_0} \right)$$

Dávila et al. J Compos Mater 2005;39(4):323-345.

LaRC failure criteria

- Set of failure criteria for plane stress assumptions based on Hashin and Puck failure criteria.

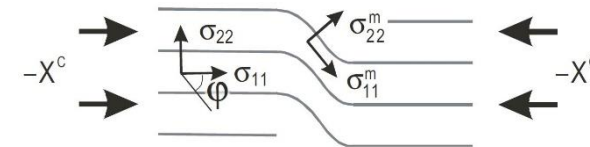
Fibre tension, $\sigma_{11} \geq 0$	Fibre compression, $\sigma_{11} < 0$	
$FI_F = \frac{\varepsilon_{11}}{\varepsilon_1^T}$ <p>Non-interacting maximum allowable strain criterion</p>	$\sigma_{22}^m < 0$ $FI_F = \left\langle \frac{ \tau_{12}^m + \eta^L \sigma_{22}^m}{S_{is}^L} \right\rangle$	$\sigma_{22}^m \geq 0$ $FI_F = (1 - g) \left(\frac{\sigma_{22}^m}{Y_{is}^T} \right) + g \left(\frac{\sigma_{22}^m}{Y_{is}^T} \right)^2 + \left(\frac{\tau_{12}^m}{S_{is}^L} \right)^2$

LaRC failure criteria

- Set of failure criteria for plane stress assumptions based on Hashin and Puck failure criteria.

Fibre tension, $\sigma_{11} \geq 0$	Fibre compression, $\sigma_{11} < 0$	
$FI_F = \frac{\varepsilon_{11}}{\varepsilon_1^T}$	$\sigma_{22}^m < 0$ $FI_F = \left\langle \frac{ \tau_{12}^m + \eta^L \sigma_{22}^m}{S_{is}^L} \right\rangle$	$\sigma_{22}^m \geq 0$ $FI_F = (1 - g) \left(\frac{\sigma_{22}^m}{Y_{is}^T} \right) + g \left(\frac{\sigma_{22}^m}{Y_{is}^T} \right)^2 + \left(\frac{\tau_{12}^m}{S_{is}^L} \right)^2$

Fibre compressive failure is modelled as the collapse of the fibres as a result of shear kinking and damage of the supporting matrix.



LaRC failure criteria

- Set of failure criteria for plane stress assumptions based on Hashin and Puck failure criteria.

Fibre tension, $\sigma_{11} \geq 0$	Fibre compression, $\sigma_{11} < 0$	
$FI_F = \frac{\varepsilon_{11}}{\varepsilon_1^T}$	$\sigma_{22}^m < 0$ $FI_F = \left\langle \frac{ \tau_{12}^m + \eta^L \sigma_{22}^m}{S_{is}^L} \right\rangle$	$\sigma_{22}^m \geq 0$ $FI_F = (1 - g) \left(\frac{\sigma_{22}^m}{Y_{is}^T} \right) + g \left(\frac{\sigma_{22}^m}{Y_{is}^T} \right)^2 + \left(\frac{\tau_{12}^m}{S_{is}^L} \right)^2$

Fibre compressive failure is modelled as the collapse of the fibres as a result of shear kinking and damage of the supporting matrix.

Ply stresses in the misalignment frame

$$\sigma_{11}^m = \cos^2 \varphi \sigma_{11} + \sin^2 \varphi \sigma_{22} + 2 \sin \varphi \cos \varphi \tau_{12}$$

$$\sigma_{22}^m = \sin^2 \varphi \sigma_{11} + \cos^2 \varphi \sigma_{22} - 2 \sin \varphi \cos \varphi \tau_{12}$$

$$\tau_{12}^m = -\sin \varphi \cos \varphi \sigma_{11} + \sin \varphi \cos \varphi \sigma_{22} + (\cos^2 \varphi - \sin^2 \varphi) \tau_{12}$$

Misalignment angle

$$\varphi = \frac{|\tau_{12}| + (G_{12} - X^C)\varphi^C}{G_{12} + \sigma_{11} - \sigma_{22}}$$

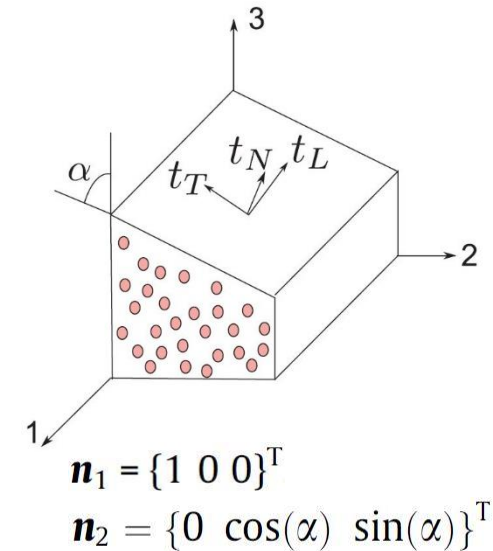
Total misalignment angle for pure longitudinal compression

$$\varphi^C = \tan^{-1} \left(\frac{1 - \sqrt{1 - 4(S_{is}^L/X^C + \eta^L)(S_{is}^L/X^C)}}{2(S_{is}^L/X^C + \eta^L)} \right)$$

Dávila et al. J Compos Mater 2005;39(4):323-345.

3D failure criteria (LaRC 3D)

- Improved 3D failure criteria, based on Puck failure criteria, were proposed to address more **general stress states** in a **consistent way**, providing not only the **predictions for the onset of ply damage**, but also additional information regarding the **type of failure** and the **orientation of the fracture plane**.



Components of the traction tensor

$$t_N = \mathbf{t} \cdot \mathbf{n}_2, \quad t_L = \mathbf{t} \cdot \mathbf{n}_1, \quad t_T = \mathbf{t} \cdot (\mathbf{n}_1 \times \mathbf{n}_2)$$

Catalanotti et al. *J Compos Mater* 2013;95:63-79.

Camanho et al. *Int J Solids Struct* 2015;55:92-107.

Camanho et al. In: Camanho et al. (eds.), *Numerical Modelling of Failure in Advanced Composite Materials*. Amsterdam, 2015. p. 111-150.

3D failure criteria (LaRC 3D)

Failure criterion for transverse compression

$$\phi_{MC} = \left(\frac{t_L}{S_L^{is} - \eta_L t_N} \right)^2 + \left(\frac{t_T}{S_T^{is} - \eta_T t_N} \right)^2$$

In situ strengths

$$Y_C^{is} = -\frac{S_L^{is} (2 \cos^2(\alpha_0) - 1)}{\eta_L \cos^2(\alpha_0)}$$

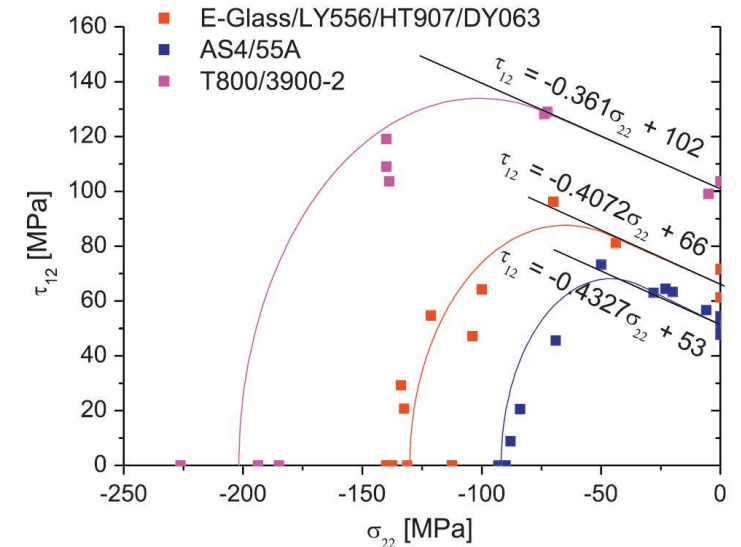
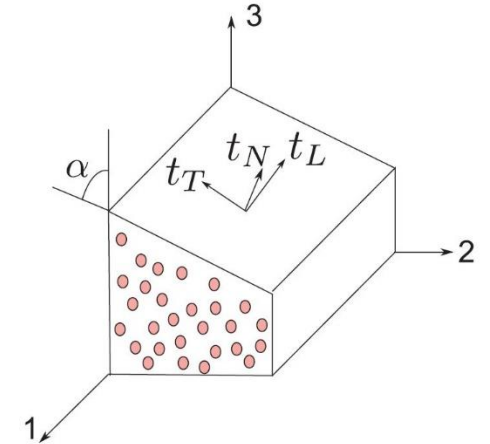
$$S_T^{is} = \frac{1}{2} \frac{(2 \sin^2(\alpha_0) - 1) S_L^{is}}{\sqrt{1 - \sin^2(\alpha_0)} \sin(\alpha_0) \eta_L}$$

Off-axis compression

$$\eta_L = -\left. \frac{\partial t_L}{\partial t_N} \right|_{t_N=0}$$

$$\eta_T = -\left. \frac{\partial t_T}{\partial t_N} \right|_{t_N=0}$$

$$\eta_L / \eta_T = S_L^{is} / S_T^{is}$$



Catalanotti et al. J Compos Mater 2013;95:63-79.

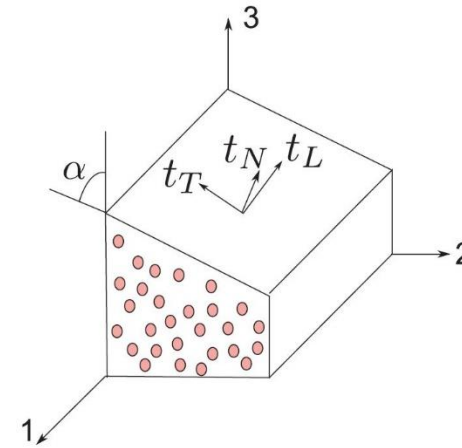
3D failure criteria (LaRC 3D)

Failure criterion for transverse tension

$$\phi_{MT} = \left(\frac{t_N}{S_T^{is}}\right)^2 + \left(\frac{t_L}{S_L^{is}}\right)^2 + \left(\frac{t_T}{S_T^{is}}\right)^2 + \lambda \left(\frac{t_N}{S_T^{is}}\right) \left(\frac{t_L}{S_L^{is}}\right)^2 + \kappa \left(\frac{t_N}{S_T^{is}}\right)$$

$$\kappa = \frac{S_T^{is2} - Y_T^{is2}}{S_T^{is} Y_T^{is}}$$

$$\lambda = 2 \eta_L S_T^{is} / S_L^{is} - \kappa$$



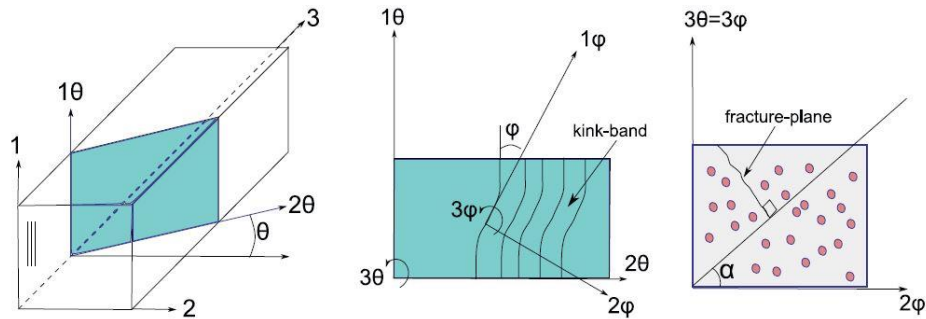
Failure criterion for longitudinal tension

$$\phi_{LT} = \varepsilon_{11} / \varepsilon_1^T$$

Maximum strain criterion

3D failure criteria (LaRC 3D)

Failure criterion for longitudinal compression



$$\sigma^{(\varphi)} = \mathbf{R}^{(\varphi)} \cdot \sigma^{(\theta)} \cdot \mathbf{R}^{(\varphi)T}$$

$$\sigma^{(\theta)} = \mathbf{R}^{(\theta)} \cdot \sigma \cdot \mathbf{R}^{(\theta)T}$$

$$\mathbf{R}^{(\varphi)} = \begin{bmatrix} \cos(\varphi) & \sin(\varphi) & 0 \\ -\sin(\varphi) & \cos(\varphi) & 0 \\ 0 & 0 & 1 \end{bmatrix}$$

$$\mathbf{R}^{(\theta)} = \begin{bmatrix} 1 & 0 & 0 \\ 0 & \cos(\theta) & \sin(\theta) \\ 0 & -\sin(\theta) & \cos(\theta) \end{bmatrix}$$

$$\theta = \arctan(\tau_{13}/\tau_{12})$$

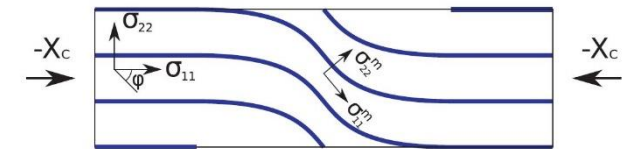
or

$$\theta = \frac{1}{2} \arctan\left(\frac{2\tau_{23}}{\sigma_{22} - \sigma_{33}}\right)$$

$$\varphi = \text{sgn}\{\tau_{12}\}(\varphi_0 + \gamma_m)$$

$$\gamma_m = \frac{\varphi_0 G_{12} + |\tau_{12}^{(\theta)}|}{G_{12} + \sigma_{11}^{(\theta)} - \sigma_{22}^{(\theta)}} - \varphi_0$$

$$\varphi_0 = \varphi_C - \gamma_{mC}$$



$$\gamma_{mC} = \frac{\sin(2\varphi_C)X_C}{2G_{12}} \approx \frac{\varphi_C X_C}{G_{12}}$$

$$\varphi_C = \arctan\left(\frac{1 - \sqrt{1 - 4\left(\frac{S_L^{is}}{X_C} + \eta_L\right)\frac{S_L^{is}}{X_C}}}{2\left(\frac{S_L^{is}}{X_C} + \eta_L\right)}\right)$$

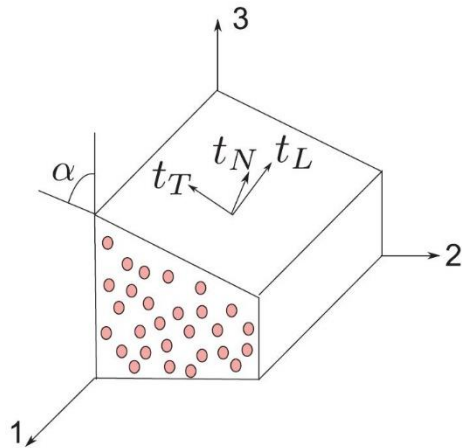
3D failure criteria (LaRC 3D)

Failure criterion for longitudinal compression

$$t_N^{(\varphi)} = \cos^2(\alpha)\sigma_{22}^{(\varphi)} + 2 \cos(\alpha) \sin(\alpha)\tau_{23}^{(\varphi)} + \sin^2(\alpha)\sigma_{33}^{(\varphi)}$$

$$t_T^{(\varphi)} = -\sin(\alpha) \cos(\alpha) (\sigma_{22}^{(\varphi)} - \sigma_{33}^{(\varphi)}) + (\cos^2(\alpha) - \sin^2(\alpha))\tau_{23}^{(\varphi)}$$

$$t_L^{(\varphi)} = \cos(\alpha)\tau_{12}^{(\varphi)} + \sin(\alpha)\tau_{13}^{(\varphi)}$$



If $t_N^{(\varphi)} < 0$ the failure index becomes:

$$\phi_{KMC} = \left(\frac{t_L^{(\varphi)}}{S_L^{is} - \eta_L t_N^{(\varphi)}} \right)^2 + \left(\frac{t_T^{(\varphi)}}{S_T^{is} - \eta_T t_N^{(\varphi)}} \right)^2$$

while if $t_N^{(\varphi)} \geq 0$ the failure index reads:

$$\phi_{KMT} = \left(\frac{t_N^{(\varphi)}}{S_T^{is}} \right)^2 + \left(\frac{t_L^{(\varphi)}}{S_L^{is}} \right)^2 + \left(\frac{t_T^{(\varphi)}}{S_T^{is}} \right)^2 + \lambda \left(\frac{t_N^{(\varphi)}}{S_T^{is}} \right) \left(\frac{t_L^{(\varphi)}}{S_L^{is}} \right)^2 + \kappa \left(\frac{t_N^{(\varphi)}}{S_T^{is}} \right)$$

3D invariant-based failure criteria

- New **3D failure criteria** with an **invariant quadratic formulation** based on structural tensors that accounts for the preferred directions of the anisotropic material.
- With this formulation, anisotropy is derived using **structural tensors** and not symmetry conditions based on a reference coordinate system.
- The structural tensors represent the material symmetries of the respective anisotropy class as an intrinsic material property, which enables an elegant **coordinate system-free description** of anisotropy using isotropic tensor functions.

3D invariant-based failure criteria

Preferred direction

$$\mathbf{a} = [1 \ 0 \ 0]^T$$

Structural tensor of transverse isotropy

$$\mathbf{A} = \mathbf{a} \otimes \mathbf{a}$$

Functional basis for transverse isotropy

$$\text{tr} \boldsymbol{\sigma}, \text{tr} \boldsymbol{\sigma}^2, \text{tr} \boldsymbol{\sigma}^3, \text{tr}(\mathbf{A}\boldsymbol{\sigma}) \text{ and } \text{tr}(\mathbf{A}\boldsymbol{\sigma}^2)$$

Transversely isotropic invariants

$$I_1 = \frac{1}{2} \text{tr}(\boldsymbol{\sigma}^p)^2 - \mathbf{a}(\boldsymbol{\sigma}^p)^2 \mathbf{a}$$

$$I_2 = \mathbf{a}(\boldsymbol{\sigma}^p)^2 \mathbf{a}$$

$$I_3 = \text{tr} \boldsymbol{\sigma} - \mathbf{a}\boldsymbol{\sigma}\mathbf{a}$$

$$\boldsymbol{\sigma}^r = \frac{1}{2}(\text{tr} \boldsymbol{\sigma} - \mathbf{a}\boldsymbol{\sigma}\mathbf{a})\mathbf{1} - \frac{1}{2}(\text{tr} \boldsymbol{\sigma} - 3\mathbf{a}\boldsymbol{\sigma}\mathbf{a})\mathbf{A}$$

$$\boldsymbol{\sigma}^p = \boldsymbol{\sigma} - \boldsymbol{\sigma}^r$$

3D invariant-based failure criteria

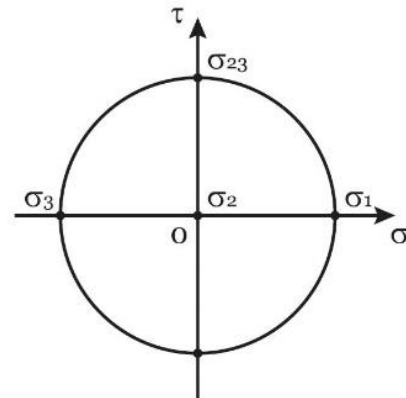
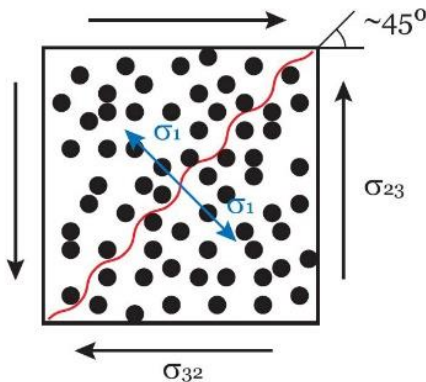
Matrix failure

$Y_T, Y_{BT}, Y_C, Y_{BC}, S_L, S_T (= Y_T)$

$$I_1 = \frac{1}{4} \sigma_{22}^2 - \frac{1}{2} \sigma_{22} \sigma_{33} + \frac{1}{4} \sigma_{33}^2 + \sigma_{23}^2$$

$$I_2 = \sigma_{12}^2 + \sigma_{13}^2$$

$$I_3 = \sigma_{22} + \sigma_{33}$$



Matrix tension ($I_3 > 0$)

$$f_M = \alpha_1 I_1 + \alpha_2 I_2 + \alpha_3^t I_3 + \alpha_{32}^t I_3^2$$

$$\alpha_1 = \frac{1}{S_T^2}$$

$$\alpha_2 = \frac{1}{S_L^2}$$

$$\alpha_{32}^t = \frac{1 - \frac{Y_T}{2Y_{BT}} - \alpha_1 \frac{Y_T^2}{4}}{Y_T^2 - 2Y_{BT}Y_T}$$

$$\alpha_3^t = \frac{1}{2Y_{BT}} - 2\alpha_{32}^t Y_{BT}$$

Matrix compression ($I_3 \leq 0$)

$$f_M = \alpha_1 I_1 + \alpha_2 I_2 + \alpha_3^c I_3 + \alpha_{32}^c I_3^2$$

$$\alpha_1 = \frac{1}{S_T^2}$$

$$\alpha_2 = \frac{1}{S_L^2}$$

$$\alpha_{32}^c = \frac{1 - \frac{Y_C}{2Y_{BC}} - \alpha_1 \frac{Y_C^2}{4}}{Y_C^2 - 2Y_{BC}Y_C}$$

$$\alpha_3^c = \frac{1}{2Y_{BC}} - 2\alpha_{32}^c Y_{BC}$$

3D invariant-based failure criteria

Fibre failure

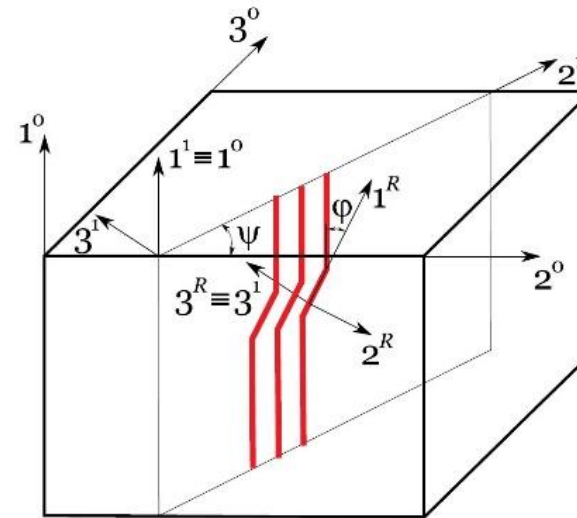
G_{12}, ε_1^T (or X_T), $X_C, Y_T, Y_{BT}, Y_C, Y_{BC}, S_L, S_T (= Y_T), \beta$

Fibre tension ($\sigma_{11} \geq 0$)

$$f_F = \frac{\varepsilon_{11}}{\varepsilon_1^T} \quad \text{Maximum strain criterion}$$

Fibre compression ($\sigma_{11} < 0$)

If $\sigma_{12} = 0$ and $\sigma_{13} = 0$	Otherwise
$\psi = \frac{1}{2} \arctan \left(\frac{2\sigma_{23}}{\sigma_{22} - \sigma_{33}} \right)$	$\psi = \arctan \frac{\sigma_{13}}{\sigma_{12}}$



$$\alpha_1 = \frac{1}{S_T^2}$$

$$\alpha_2 = \frac{1}{S_L^2}$$

$$\alpha_{32}^t = \frac{1 - \frac{Y_T}{2Y_{BT}} - \alpha_1 \frac{Y_T^2}{4}}{Y_T^2 - 2Y_{BT}Y_T}$$

$$\alpha_{32}^c = \frac{1 - \frac{Y_C}{2Y_{BC}} - \alpha_1 \frac{Y_C^2}{4}}{Y_C^2 - 2Y_{BC}Y_C}$$

$$\alpha_3^t = \frac{1}{2Y_{BT}} - 2\alpha_{32}^t Y_{BT}$$

$$\alpha_3^c = \frac{1}{2Y_{BC}} - 2\alpha_{32}^c Y_{BC}$$

Camanho et al. *Int J Solids Struct* 2015;55:92-107.

Camanho et al. In: Camanho et al. (eds.), *Numerical Modelling of Failure in Advanced Composite Materials*. Amsterdam, 2015. p. 111-150.

3D invariant-based failure criteria

Fibre failure

Fibre compression ($\sigma_{11} < 0$)

$$\varphi = \text{sgn} \left\{ \sigma_{12}^{(R)}(\varphi_0, \psi) \right\} \left\{ \varphi_0 + \left| \frac{\sigma_{12}^{(R)}(\varphi_0, \psi)}{G_{12}} + \beta \left[\sigma_{12}^{(R)}(\varphi_0, \psi) \right]^3 \right| \right\}$$

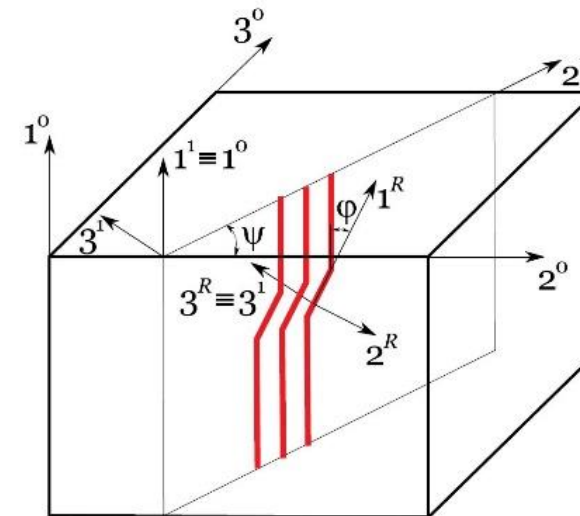
$$\varphi_0 = \varphi_C \left(1 + \frac{|X_C|}{G_{12}} \right)^{-1}$$

$$\varphi_C = \frac{1}{2} \arccos \left\{ \left[4 \sqrt{\alpha_1 - 4\alpha_2 + \alpha_2^2 X_C^2 + (\alpha_3^c)^2 + 2\alpha_2 \alpha_3^c X_C + 4\alpha_{32}^c} + (\alpha_1 + 4\alpha_{32}^c) X_C + 4\alpha_3^c \right] \cdot [(\alpha_1 - 4\alpha_2 + 4\alpha_{32}^c) X_C]^{-1} \right\}$$

$$\sigma_{12}^{(R)}(\varphi_0, \psi) = \frac{1}{2} \left[-\sigma_{11} + \sigma_{22} \cos^2 \psi + \sigma_{33} \sin^2 \psi + \sigma_{23} \sin 2\psi \right] \sin 2\varphi_0 + (\sigma_{12} \cos \psi + \sigma_{13} \sin \psi) \cos 2\varphi_0$$

Preferred direction

$$\mathbf{a} = \begin{bmatrix} \cos \varphi \\ \cos \psi \sin \varphi \\ \sin \psi \sin \varphi \end{bmatrix}$$



Camanho et al. *Int J Solids Struct* 2015;55:92-107.

Camanho et al. In: Camanho et al. (eds.), *Numerical Modelling of Failure in Advanced Composite Materials*. Amsterdam, 2015. p. 111-150.

3D invariant-based failure criteria

Fibre failure

Fibre compression ($\sigma_{11} < 0$)

$$\mathbf{A} = \mathbf{a} \otimes \mathbf{a}$$

$$\boldsymbol{\sigma}^r = \frac{1}{2}(\text{tr } \boldsymbol{\sigma} - \mathbf{a}\boldsymbol{\sigma}\mathbf{a})\mathbf{1} - \frac{1}{2}(\text{tr } \boldsymbol{\sigma} - 3\mathbf{a}\boldsymbol{\sigma}\mathbf{a})\mathbf{A}$$

$$\boldsymbol{\sigma}^p = \boldsymbol{\sigma} - \boldsymbol{\sigma}^r$$

$$I_1 = \frac{1}{2} \text{tr}(\boldsymbol{\sigma}^p)^2 - \mathbf{a}(\boldsymbol{\sigma}^p)^2\mathbf{a}$$

$$I_2 = \mathbf{a}(\boldsymbol{\sigma}^p)^2\mathbf{a}$$

$$I_3 = \text{tr } \boldsymbol{\sigma} - \mathbf{a}\boldsymbol{\sigma}\mathbf{a}$$

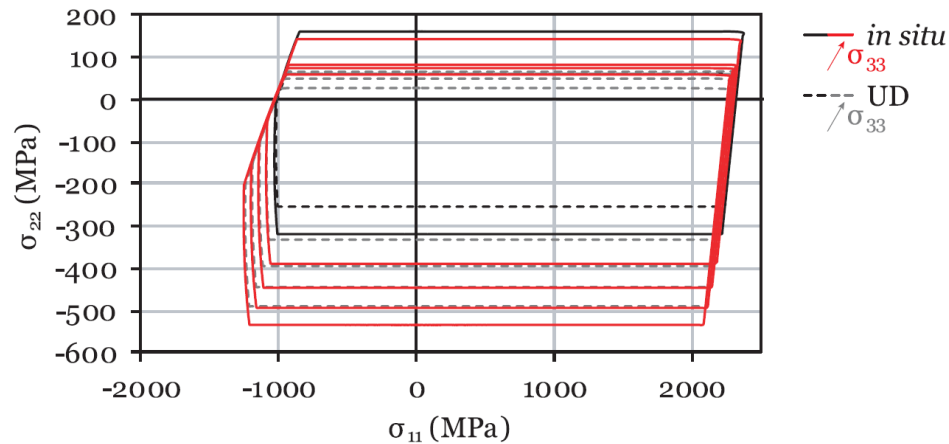
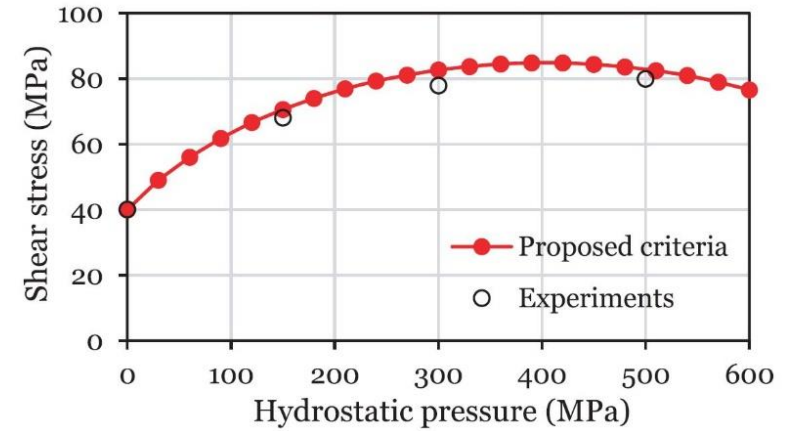
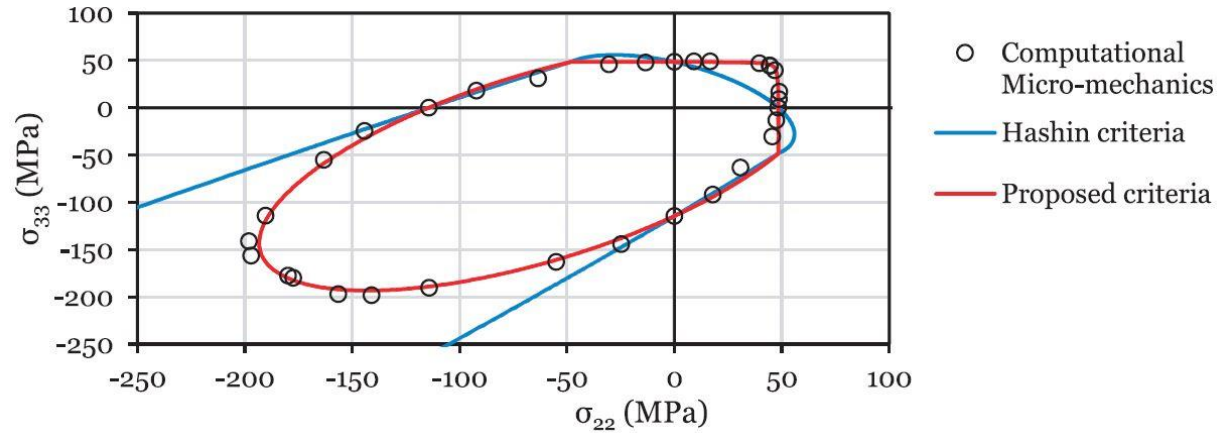
Matrix tension ($I_3 > 0$)

Matrix compression ($I_3 \leq 0$)

$$f_K = \alpha_1 I_1 + \alpha_2 I_2 + \alpha_3^t I_3 + \alpha_{32}^t I_3^2$$

$$f_K = \alpha_1 I_1 + \alpha_2 I_2 + \alpha_3^c I_3 + \alpha_{32}^c I_3^2$$

3D invariant-based failure criteria



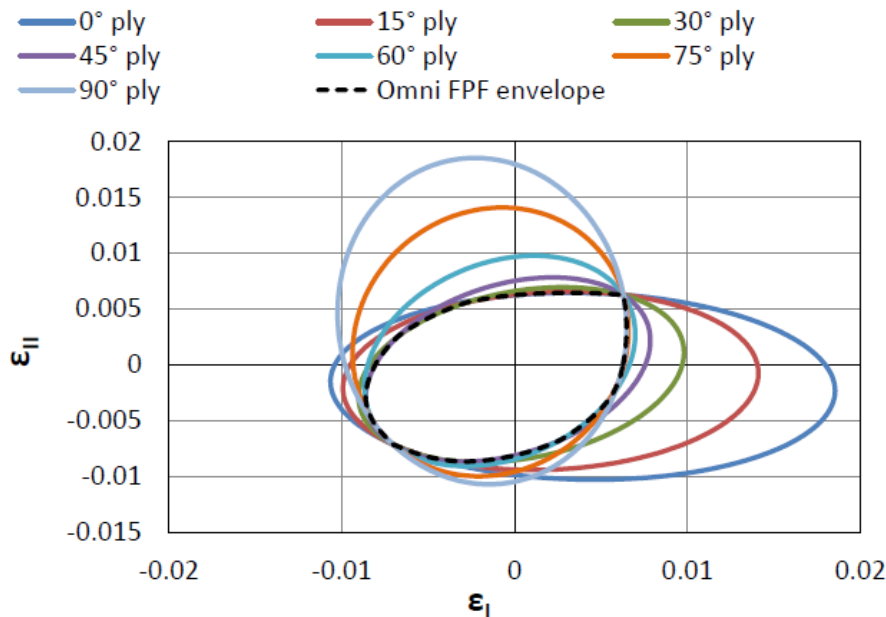
Camanho et al. *Int J Solids Struct* 2015;55:92-107.

Camanho et al. In: Camanho et al. (eds.), *Numerical Modelling of Failure in Advanced Composite Materials*. Amsterdam, 2015. p. 111-150.

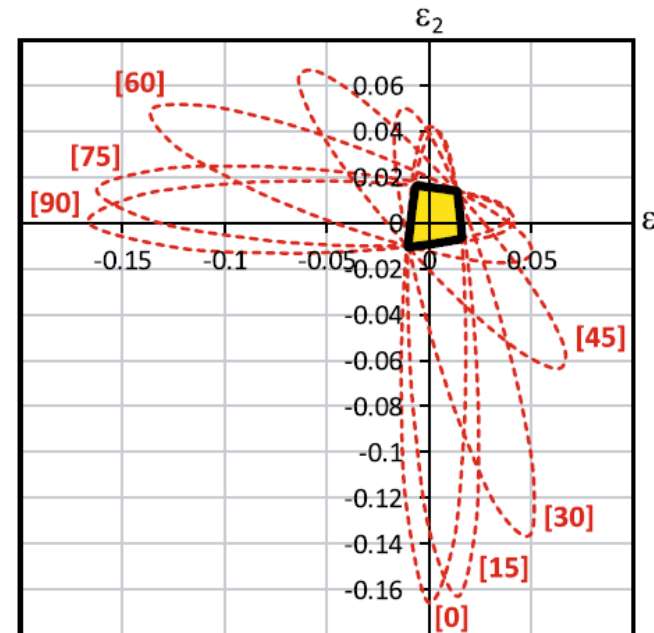
Laminate failure criteria - omni failure envelopes

- The **omni strain failure envelope** is defined as a material property independent of laminate layup configuration.

FPF envelope - intact stiffness



LPF envelope - degraded stiffness

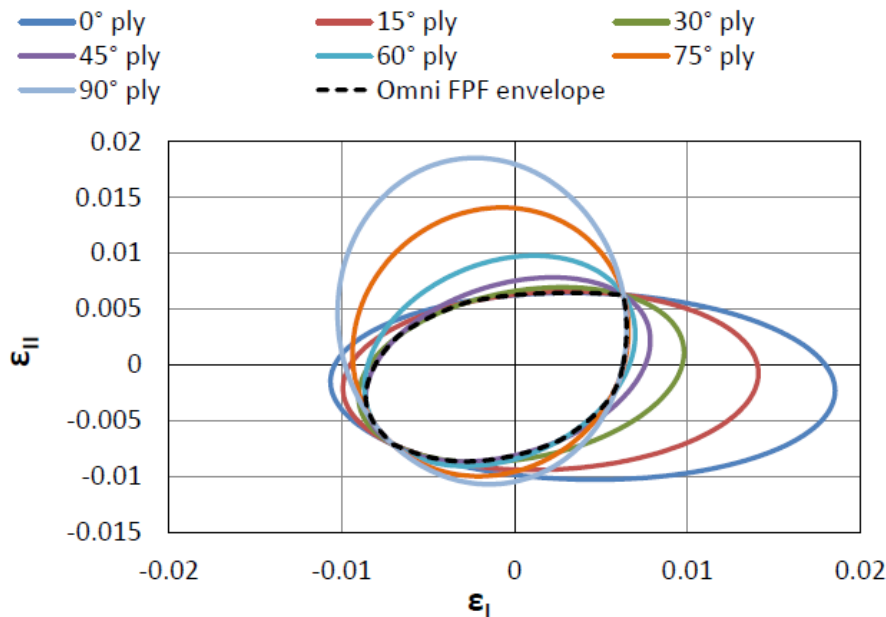


Tsai et al. *Compos Sci Technol* 2014;100:237-243.
Arteiro et al. *Arch Comput Meth Eng* 2019;26:1445-1487.
Corrado et al. *Submitted for publication*, 2021.

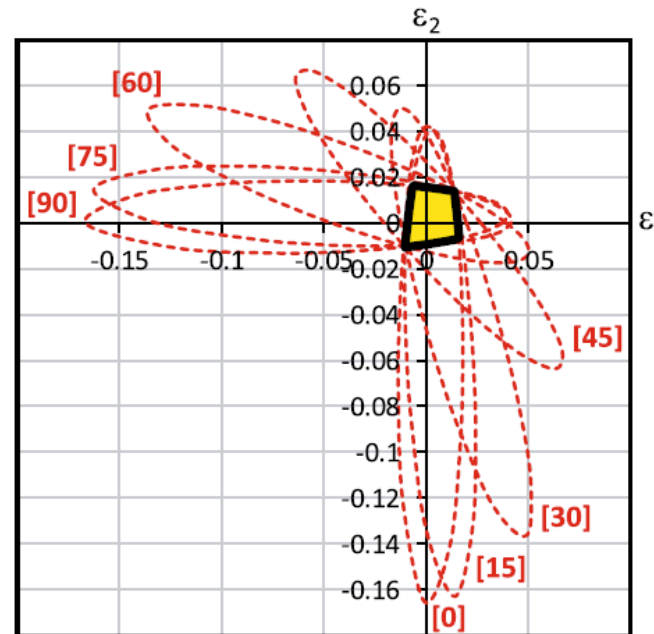
Laminate failure criteria - omni failure envelopes

- A representation in the **strain space** is selected because in this case failure envelopes are invariant, i.e. their shapes remain the same independently of the presence of other plies.

FPF envelope - intact stiffness



LPF envelope - degraded stiffness

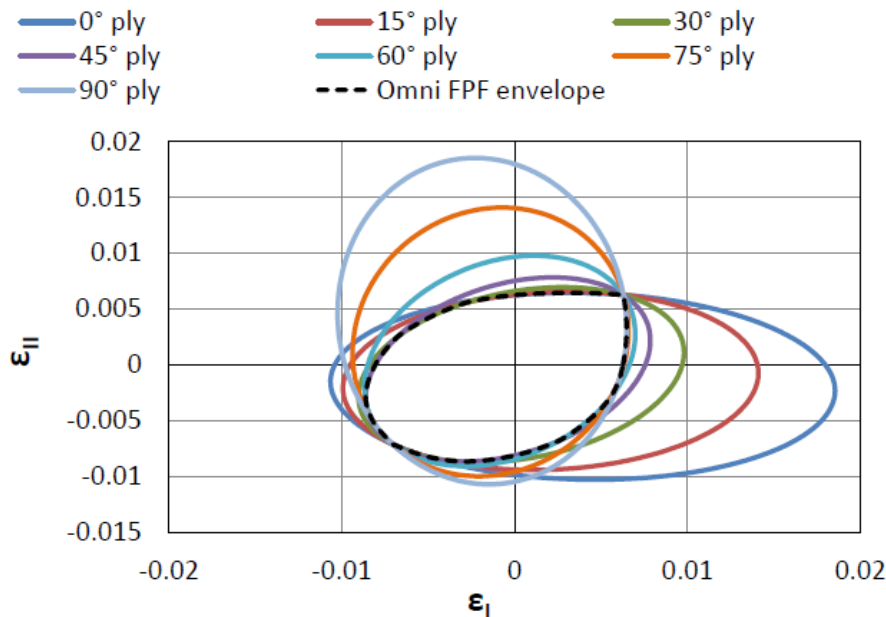


Tsai et al. *Compos Sci Technol* 2014;100:237-243.
Arteiro et al. *Arch Comput Meth Eng* 2019;26:1445-1487.
Corrado et al. *Submitted for publication*, 2021.

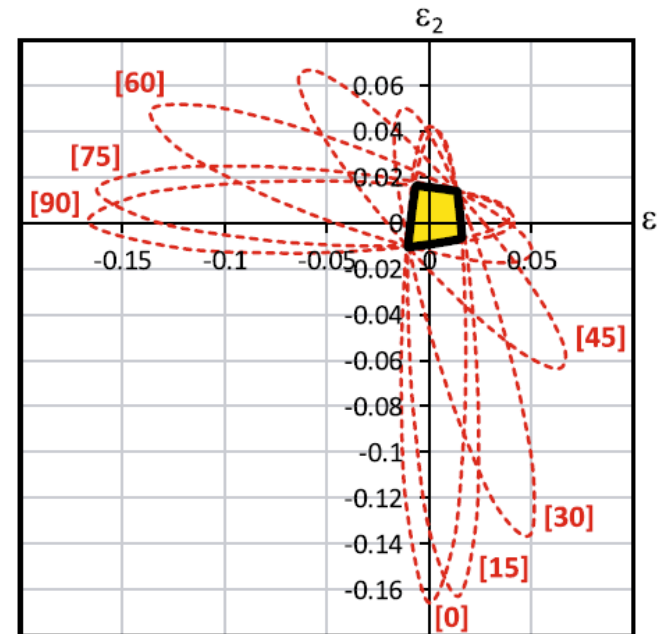
Laminate failure criteria - omni failure envelopes

- The **inner envelope** can be determined by finding the **controlling ply** that would fail first.

FPF envelope - intact stiffness



LPF envelope - degraded stiffness

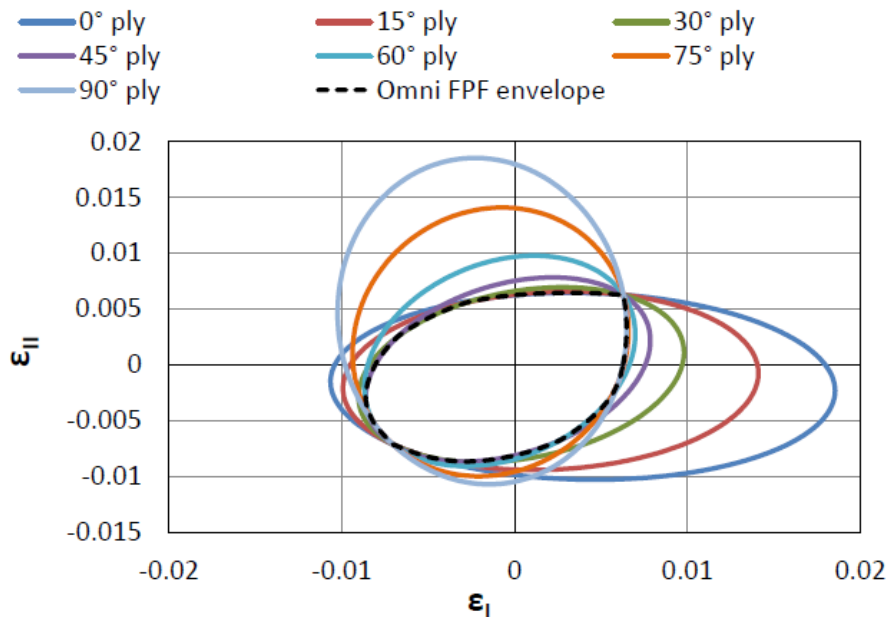


Tsai et al. *Compos Sci Technol* 2014;100:237-243.
Arteiro et al. *Arch Comput Meth Eng* 2019;26:1445-1487.
Corrado et al. *Submitted for publication*, 2021.

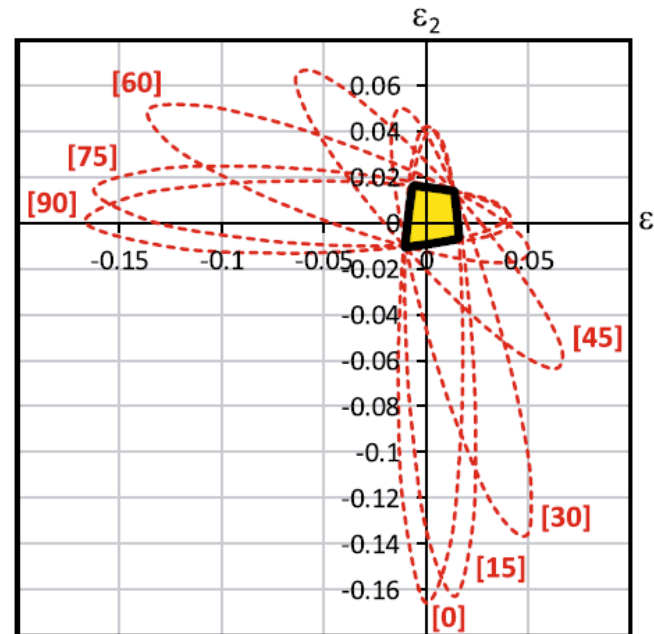
Laminate failure criteria - omni failure envelopes

- The inner envelope thus becomes an invariant that defines the **FPF** (first-ply failure) and **LPF** (last-ply failure) envelopes for all ply orientations of a given material.

FPF envelope - intact stiffness



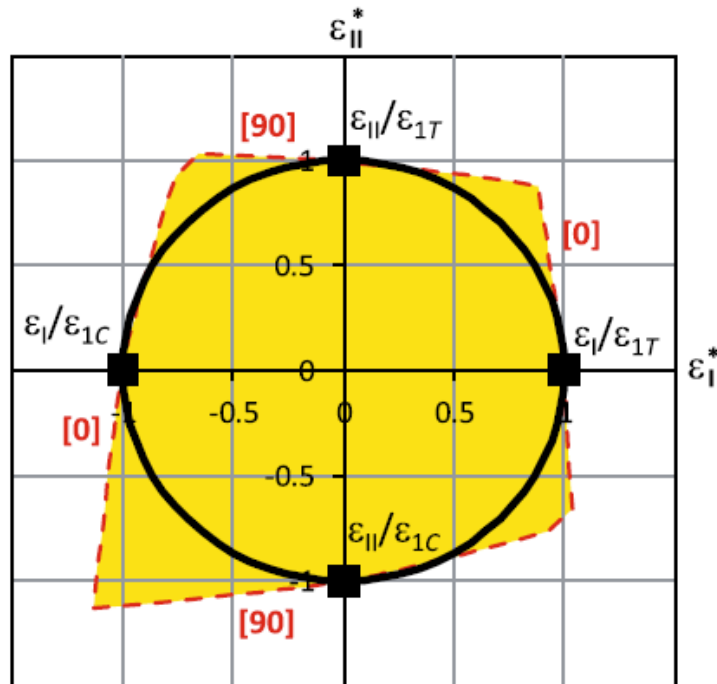
LPF envelope - degraded stiffness



Tsai et al. *Compos Sci Technol* 2014;100:237-243.
Arteiro et al. *Arch Comput Meth Eng* 2019;26:1445-1487.
Corrado et al. *Submitted for publication*, 2021.

Laminate failure criteria - omni failure envelopes

- To make laminate failure analysis simpler, the LPF omni strain envelope can be approximated by a **unit circle** in the normalised principal strain space.



$$\text{Failure index: } k = \sqrt{k_1^2 + k_2^2}$$

$$\begin{cases} k_1 = \varepsilon_I/e_x & \text{and} & k_2 = \varepsilon_{II}/e_x & \text{if } \{\varepsilon_I, \varepsilon_{II}\} \geq 0 \\ k_1 = \varepsilon_I/e_x' & \text{and} & k_2 = \varepsilon_{II}/e_x' & \text{if } \{\varepsilon_I, \varepsilon_{II}\} < 0 \end{cases}$$

$$e_x = X_T/E_x \quad e_x' = X_C/E_x$$

Only two strength properties are required: X_T and X_C

Questions?

Designing with composite materials
Failure mechanisms and failure criteria

SASCOM

Introductory course on composite materials 2021

Designing with composite materials
Effects of stress concentrations

References

Marques AT. Composite Systems: Design and Manufacture for Durability, University of Porto, September 2019.

Design with composite systems

To take advantage of the potential of composites and make them competitive:



Be creative - Conceptual design
- Integral solutions

Composites
(identify advantages and limitations)



Anisotropic materials



Structural engineer “creates” the material and integrates components



Specific design philosophy



Selection of **constituents** (fibres, matrices, hybrids, etc.), reinforcement **architectures** (fabric uni-, bi- or multiaxial, braided, etc.), **manufacturing** process, **curing/consolidation**, **post-curing**, etc.

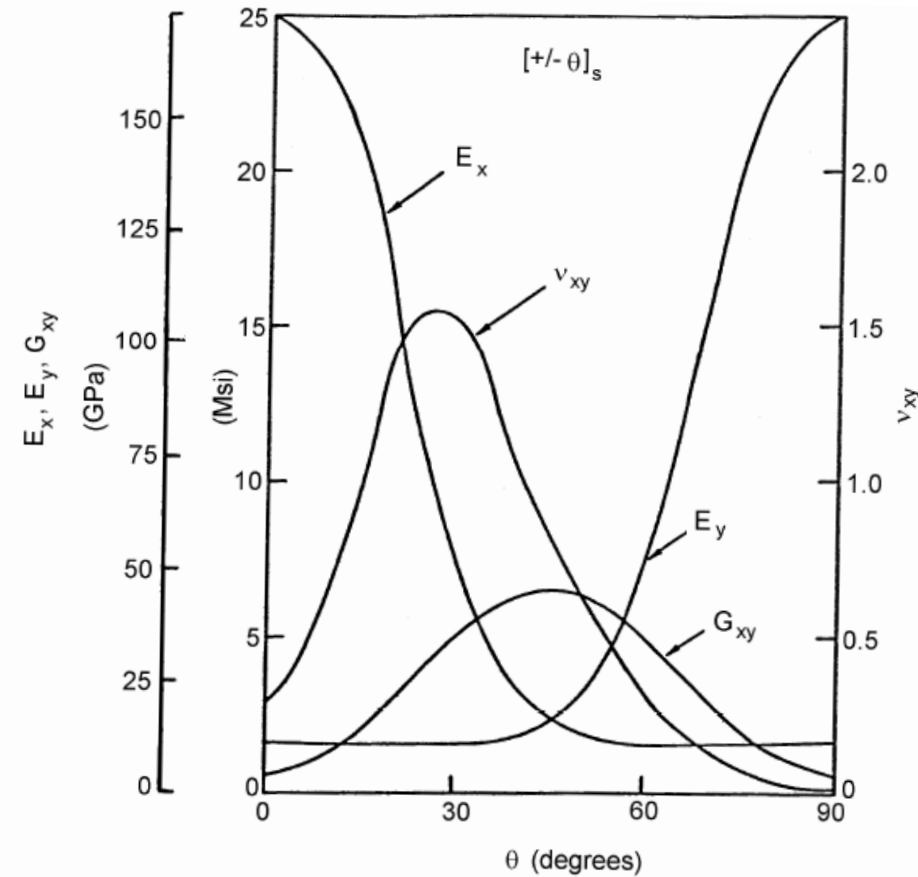
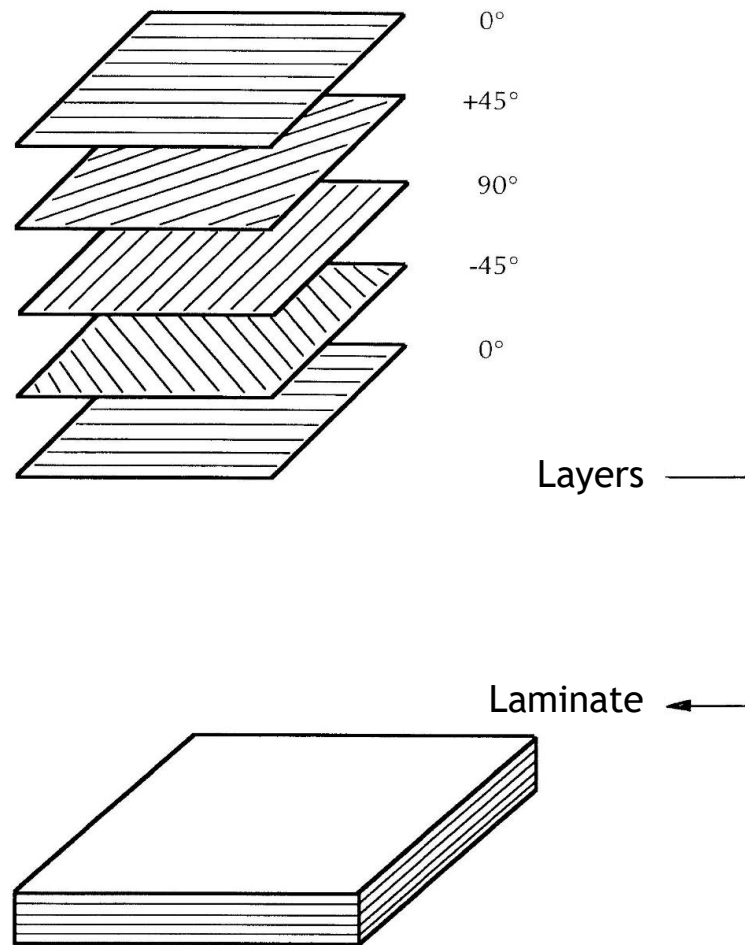
Structural Engineer

- Integrates the conceptual design with manufacturing strategies.
- Develops test programs to validate choices (materials and/or components in the short and long term, combining environmental effects with mechanical stress), identifying failure modes and damage mechanisms.
- Develops detailed design tools (stress analysis, structural integrity, predictive models, joints).
- Sets quality control strategies.
- Defines methodologies for inspection, non-destructive testing (NDT), repairing and life cycle analysis.

Composite systems

- It is possible to optimise the mechanical and physical properties.
- Composites (with brittle matrices) can be considered almost elastic until failure.
- Excellent fatigue behaviour.
- Polymer matrices are viscoelastic, creep and stress relaxation must be considered, if applicable.
- Can be moulded to complex shapes.
- It is possible to reduce the number of components.
- Connections (joints) should be considered from the beginning.

Laminated structures



CMH-17-3G COMPOSITE MATERIALS HANDBOOK VOLUME 3. POLYMER MATRIX COMPOSITES MATERIALS USAGE, DESIGN, AND ANALYSIS. 2012.

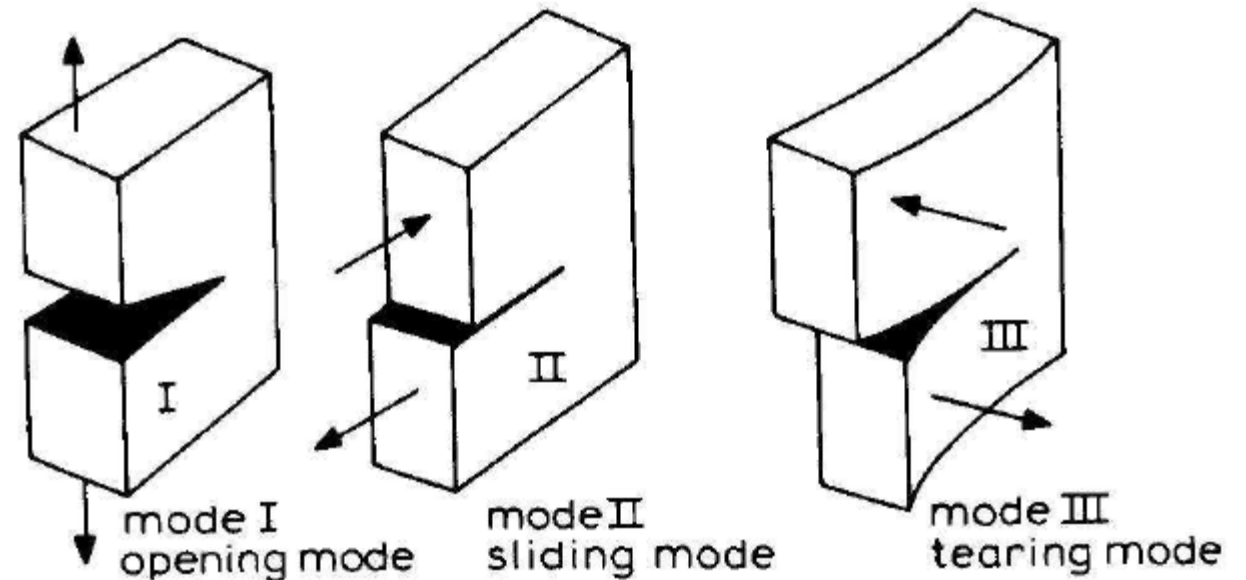
Interlaminar fracture mechanics

- Composite materials are especially vulnerable to **interfacial cracks**, commonly referred to as **delaminations**.
- The study of fracture of polymeric composite materials is largely based on the **Linear Elastic Fracture Mechanics** and the **Strain Energy Release Rate** approach.

Interlaminar fracture mechanics

Often referred to as **Griffith Crack Theory**, this approach represents an energy balance between a decrease in **potential energy** of the body **U** and an increase in **surface energy** associated with the creation of a **crack surface A**.

$$G = \frac{\partial W}{\partial A} - \frac{\partial U}{\partial A}$$



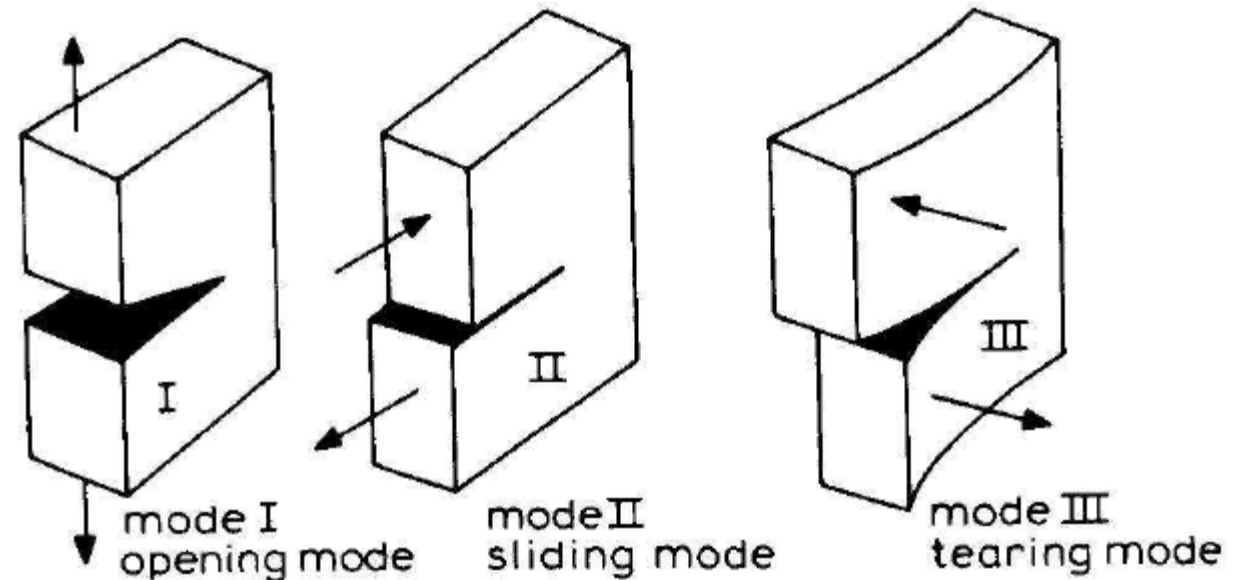
CMH-17-3G COMPOSITE MATERIALS HANDBOOK VOLUME
3. POLYMER MATRIX COMPOSITES MATERIALS USAGE,
DESIGN, AND ANALYSIS. 2012.

Interlaminar fracture mechanics

Often referred to as **Griffith Crack Theory**, this approach represents an energy balance between a decrease in **potential energy** of the body **U** and an increase in **surface energy** associated with the creation of a **crack surface A**.

$$G_I = \frac{\lim}{2\Delta A \rightarrow 0} \int_A \sigma_z u_z dA$$

$$G_{II} = \frac{\lim}{2\Delta A \rightarrow 0} \int_A \sigma_{yz} u_y dA$$



CMH-17-3G COMPOSITE MATERIALS HANDBOOK VOLUME
3. POLYMER MATRIX COMPOSITES MATERIALS USAGE,
DESIGN, AND ANALYSIS. 2012.

Interlaminar fracture mechanics

- In the prediction of delamination initiation and/or growth behaviour in advanced composite structures, the **interlaminar fracture mechanics approach** has several advantages over stress-based methods.
- An elastic analysis of a delamination will reveal **stress singularities** at the “crack tip” of these macroscopic, ply level, discontinuities.
- A fracture mechanics-based analysis and characterization of this problem has been adopted to **avoid the uncertainties** associated with **analysing singular stress fields**.

Interlaminar fracture mechanics

Practical implementation of interlaminar fracture mechanics involves calculation of strain energy release rates, which can also be obtained using the **finite element method (FEM)** in combination with different **computational fracture mechanics** approaches:

- J-Integral;
- Crack Tip Element;
- Virtual crack closure technique (VCCT);
- Cohesive elements; etc.

Interlaminar fracture mechanics

Crack Tip Element

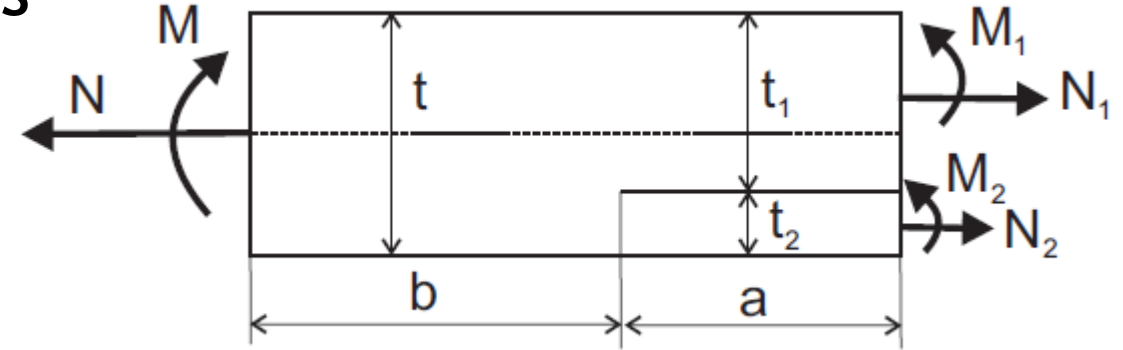
$$G = \frac{1}{2} (c_{11}N_c^2 + c_{22}M_c^2 + 2\sqrt{c_{11}c_{22}}N_cM_c \sin \Gamma)$$

$$\sin \Gamma = \frac{c_{12}}{\sqrt{c_{11}c_{22}}}$$

$$c_{11} = A'_1 + A'_2 + B'_1t_1 - B'_2t_2 + \frac{D'_1t_1^2}{4} + \frac{D'_2t_2^2}{4}$$

$$c_{22} = D'_1 + D'_2$$

$$c_{12} = \frac{D'_2t_2}{2} - \frac{D'_1t_1}{2} - B'_1 - B'_2$$



2D Crack Tip Element

$$\begin{bmatrix} A'_i & B'_i \\ B'_i & D'_i \end{bmatrix} = \begin{bmatrix} A_i & B_i \\ B_i & D_i \end{bmatrix}^{-1}$$

$$\begin{bmatrix} N_i \\ M_i \end{bmatrix} = \begin{bmatrix} A_i & B_i \\ B_i & D_i \end{bmatrix} \begin{bmatrix} \epsilon_i^0 \\ \kappa_i \end{bmatrix}$$

classical laminated plate theory

Interlaminar fracture mechanics

Crack Tip Element

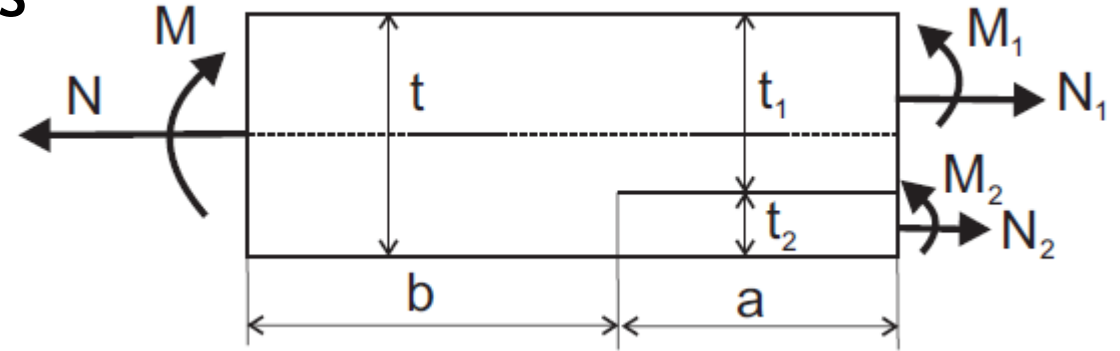
$$G = \frac{1}{2} (c_{11}N_c^2 + c_{22}M_c^2 + 2\sqrt{c_{11}c_{22}}N_cM_c \sin \Gamma)$$

$$N_c = -N_1 + a_{11}N + a_{12}M$$

concentrated crack tip force

$$M_c = M_1 - N_1 \frac{t_1}{2} + \left(a_{11} \frac{t_1}{2} - a_{21} \right) N + \left(a_{12} \frac{t_1}{2} - a_{22} \right) M$$

concentrated crack tip moment



2D Crack Tip Element

$$a_{11} = A_1 A'_u + \left(B_1 - \frac{A_1 t_2}{2} \right) B'_u$$

$$a_{12} = A_1 B'_u + \left(B_1 - \frac{A_1 t_2}{2} \right) D'_u$$

$$a_{21} = B_1 A'_u + \left(D_1 - \frac{B_1 t_2}{2} \right) B'_u$$

$$a_{22} = B_1 B'_u + \left(D_1 - \frac{B_1 t_2}{2} \right) D'_u$$

(*u* refers to the uncracked region)

Interlaminar fracture mechanics

Crack Tip Element

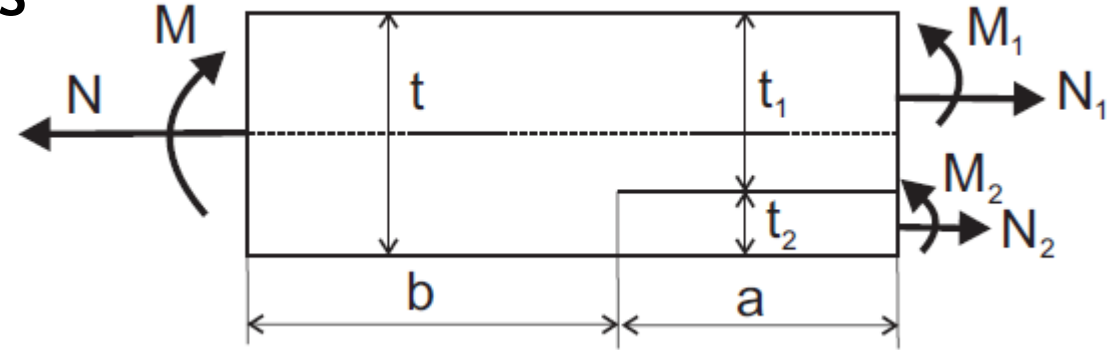
Mode partitioning

$$\mathcal{G}_I = \frac{1}{2} [-N_c \sqrt{c_{11}} \sin(\Omega) + M_c \sqrt{c_{22}} \cos(\Omega + \Gamma)]^2$$

$$\mathcal{G}_{II} = \frac{1}{2} [N_c \sqrt{c_{11}} \cos(\Omega) + M_c \sqrt{c_{22}} \sin(\Omega + \Gamma)]^2$$

$$\Omega = \left\{ \begin{array}{ll} -24 & \eta < -0.468 \\ 60.409\eta - 41.738\eta^3 & \text{if } -0.468 < \eta < 0.468 \\ 24 & \eta > 0.468 \end{array} \right\} \quad (\Omega \text{ calculated in degrees})$$

$$\eta = \log_{10} \left(\frac{t_2}{t_1} \right)$$



2D Crack Tip Element

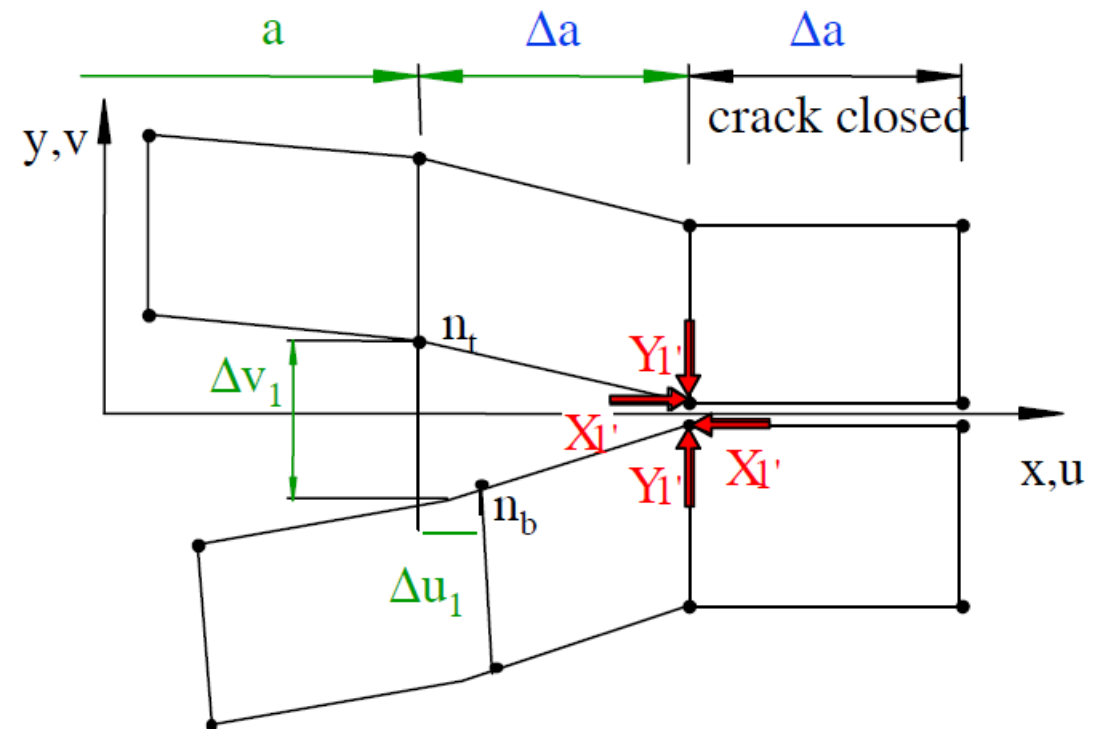
Interlaminar fracture mechanics

Virtual crack closure technique (VCCT)

- Two-dimensional linear continuum element

$$G_I = \frac{1}{2b\Delta a} Y_1' \Delta v_1$$

$$G_{II} = \frac{1}{2b\Delta a} X_1' \Delta u_1$$



CMH-17-3G COMPOSITE MATERIALS HANDBOOK VOLUME
3. POLYMER MATRIX COMPOSITES MATERIALS USAGE,
DESIGN, AND ANALYSIS. 2012.

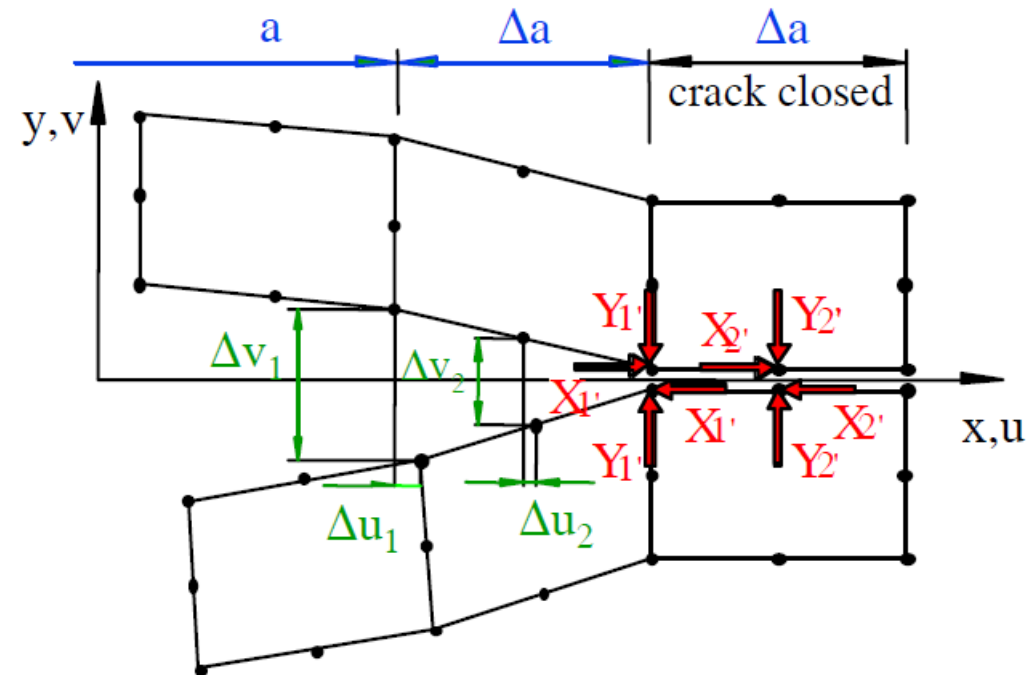
Interlaminar fracture mechanics

Virtual crack closure technique (VCCT)

- Two-dimensional quadratic continuum element

$$G_I = \frac{1}{2b\Delta a} (Y'_1 \Delta v_1 + Y'_2 \Delta v_2)$$

$$G_{II} = \frac{1}{2b\Delta a} (X'_1 \Delta u_1 + X'_2 \Delta u_2)$$



CMH-17-3G COMPOSITE MATERIALS HANDBOOK VOLUME
3. POLYMER MATRIX COMPOSITES MATERIALS USAGE,
DESIGN, AND ANALYSIS. 2012.

Interlaminar fracture mechanics

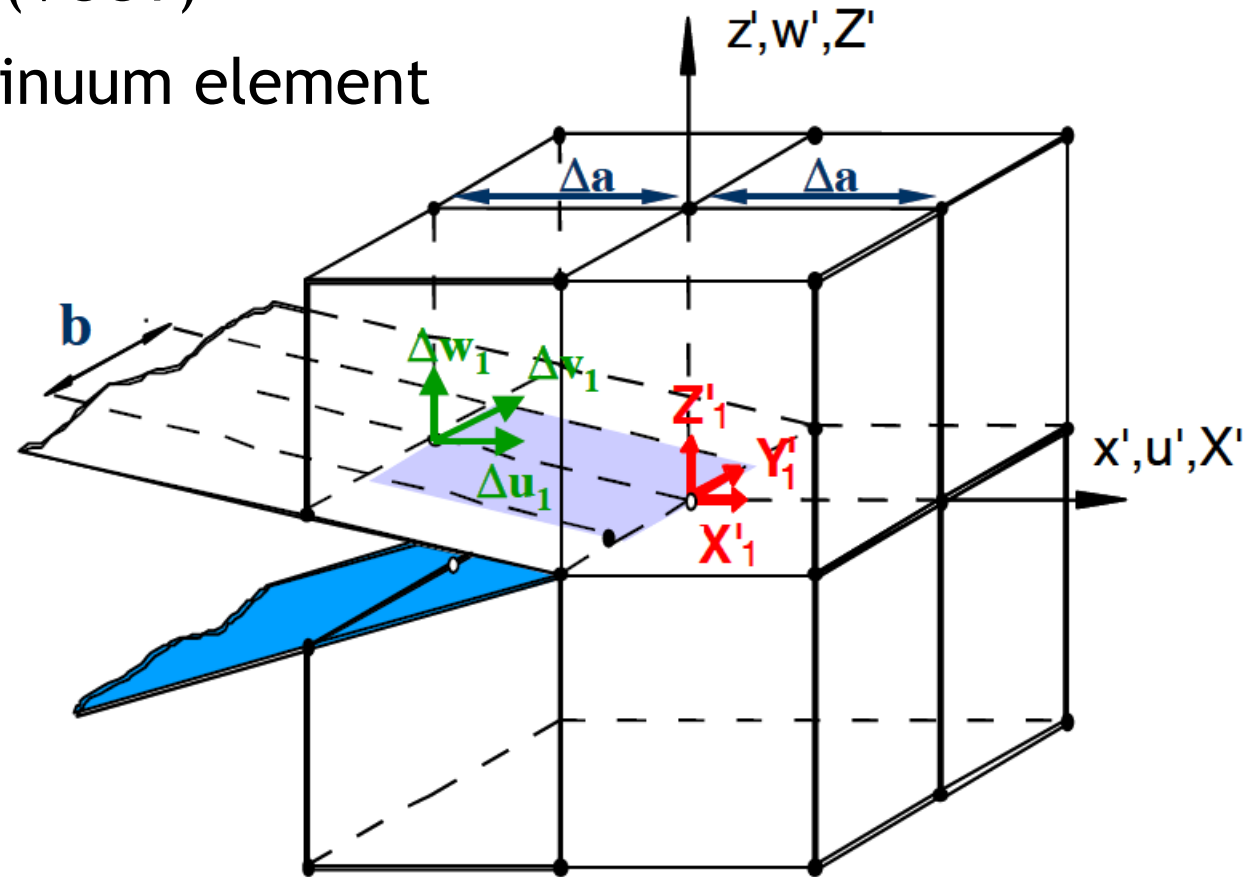
Virtual crack closure technique (VCCT)

- Three-dimensional linear continuum element

$$G_I = \frac{1}{2b\Delta a} Z'_1 \Delta w_1$$

$$G_{II} = \frac{1}{2b\Delta a} X'_1 \Delta u_1$$

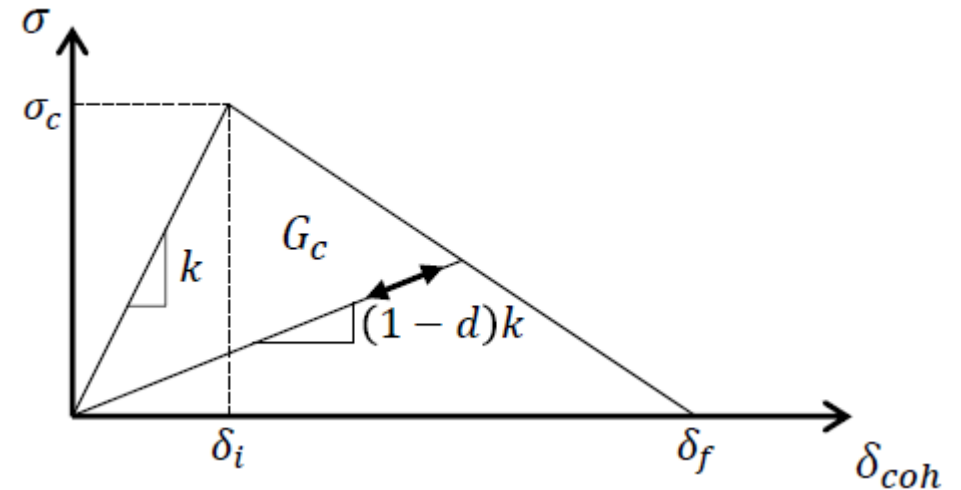
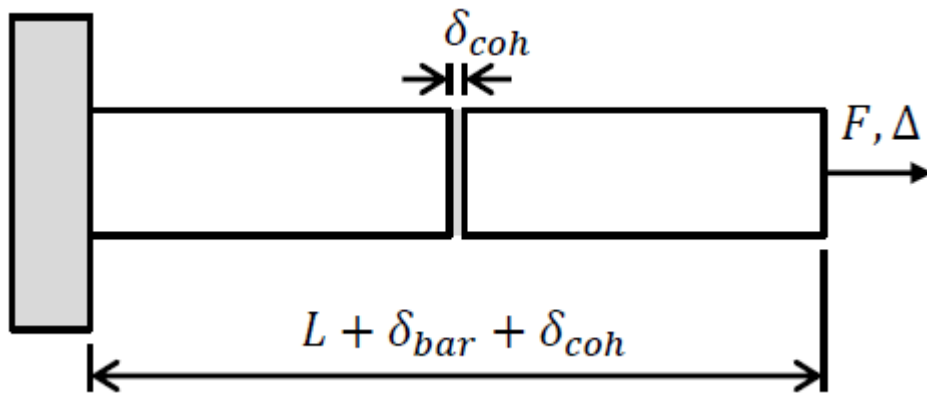
$$G_{III} = \frac{1}{2b\Delta a} Y'_1 \Delta v_1$$



CMH-17-3G COMPOSITE MATERIALS HANDBOOK VOLUME
3. POLYMER MATRIX COMPOSITES MATERIALS USAGE,
DESIGN, AND ANALYSIS. 2012.

Interlaminar fracture mechanics

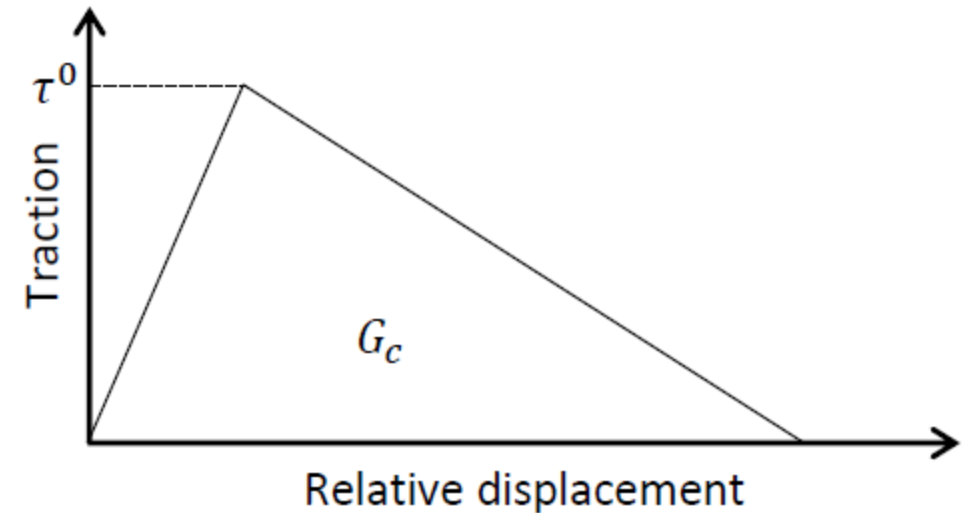
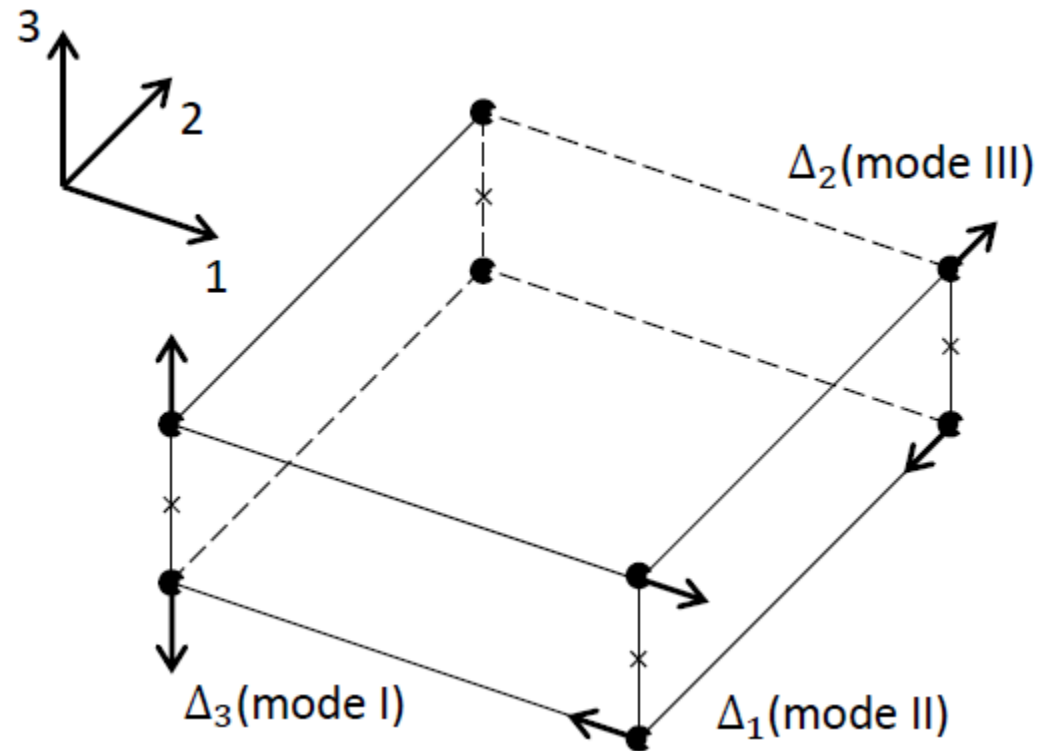
Cohesive zone models



A. Arteiro. Technology development and structural mechanics of composites built of spread tow thin-ply technology. Master's thesis, University of Porto, Porto, 2012.

Interlaminar fracture mechanics

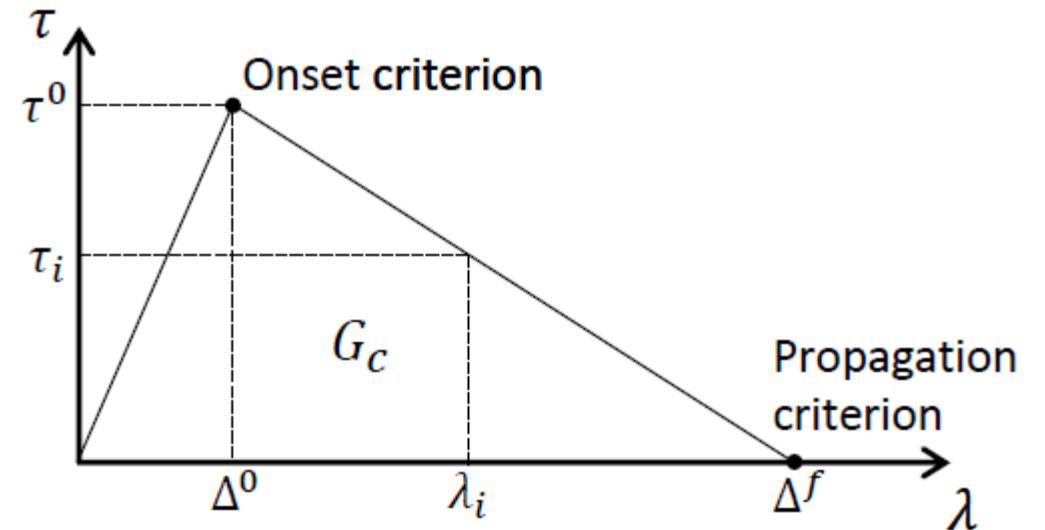
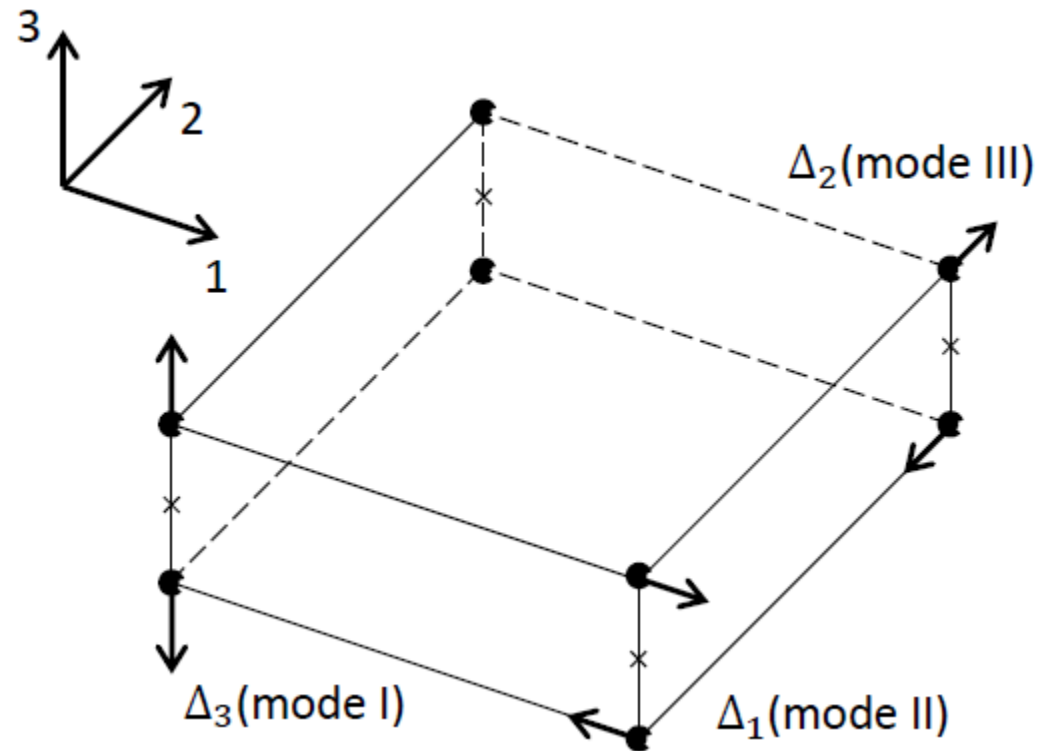
Cohesive elements



A. Arteiro. Technology development and structural mechanics of composites built of spread tow thin-ply technology. Master's thesis, University of Porto, Porto, 2012.

Interlaminar fracture mechanics

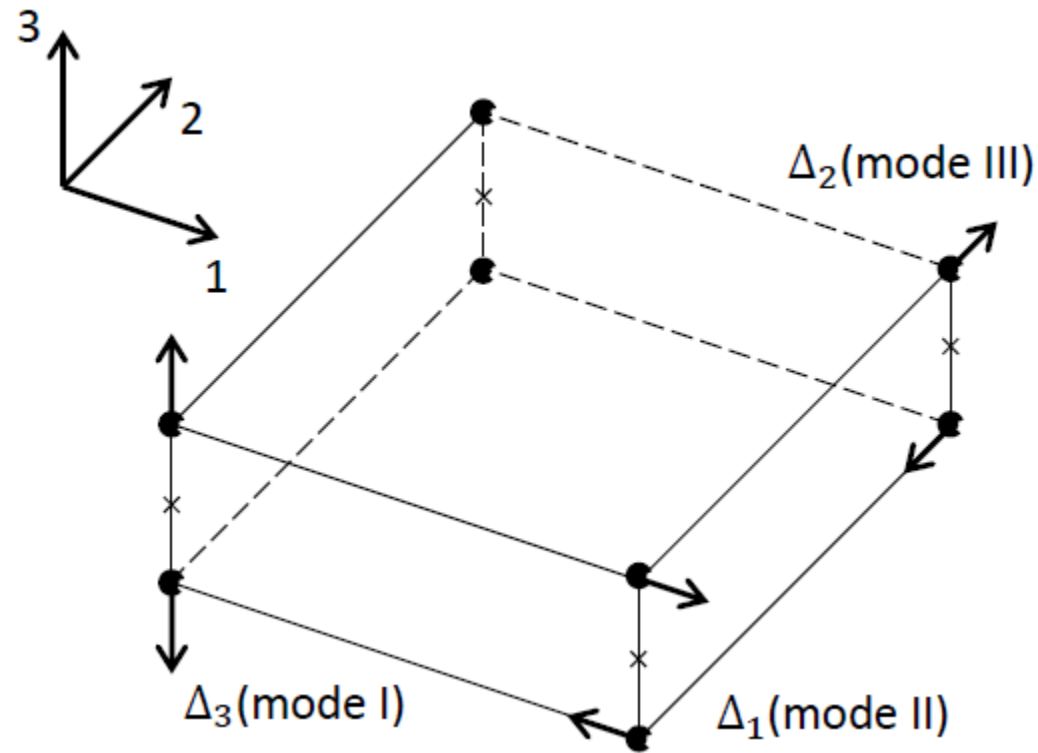
Cohesive elements



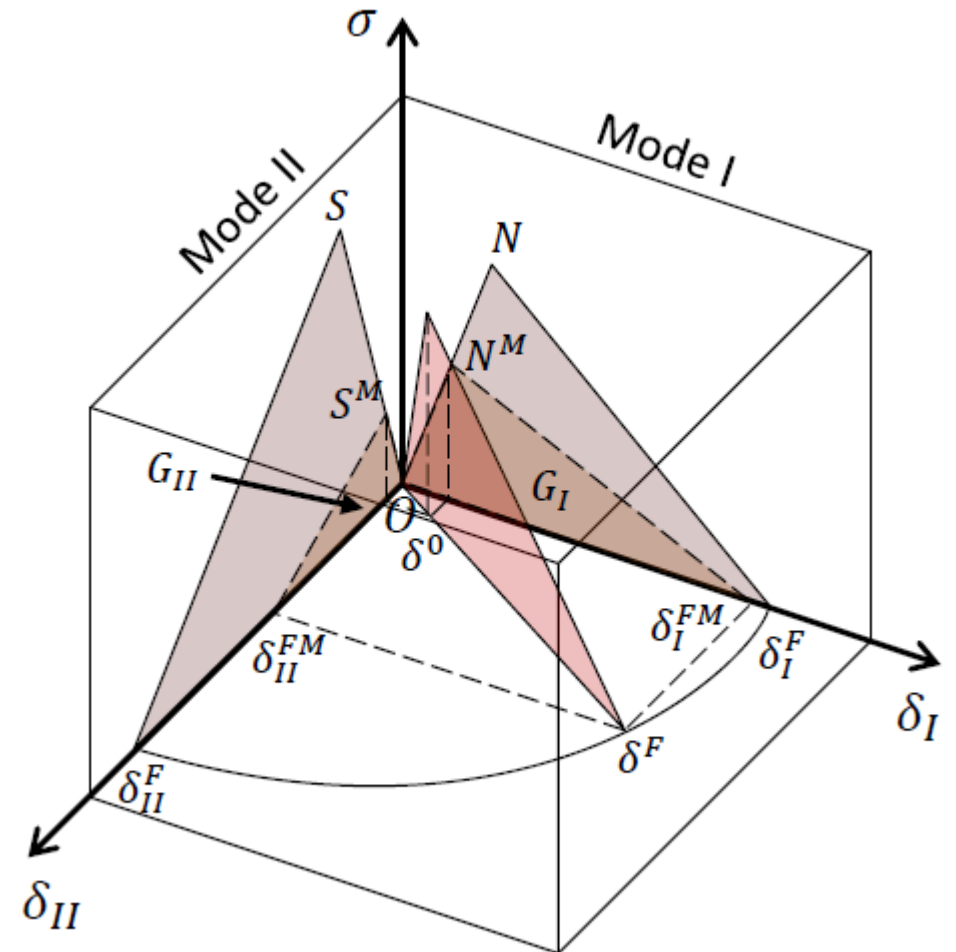
A. Arteiro. Technology development and structural mechanics of composites built of spread tow thin-ply technology. Master's thesis, University of Porto, Porto, 2012.

Interlaminar fracture mechanics

Cohesive elements



A. Arteiro. Technology development and structural mechanics of composites built of spread tow thin-ply technology. Master's thesis, University of Porto, Porto, 2012.

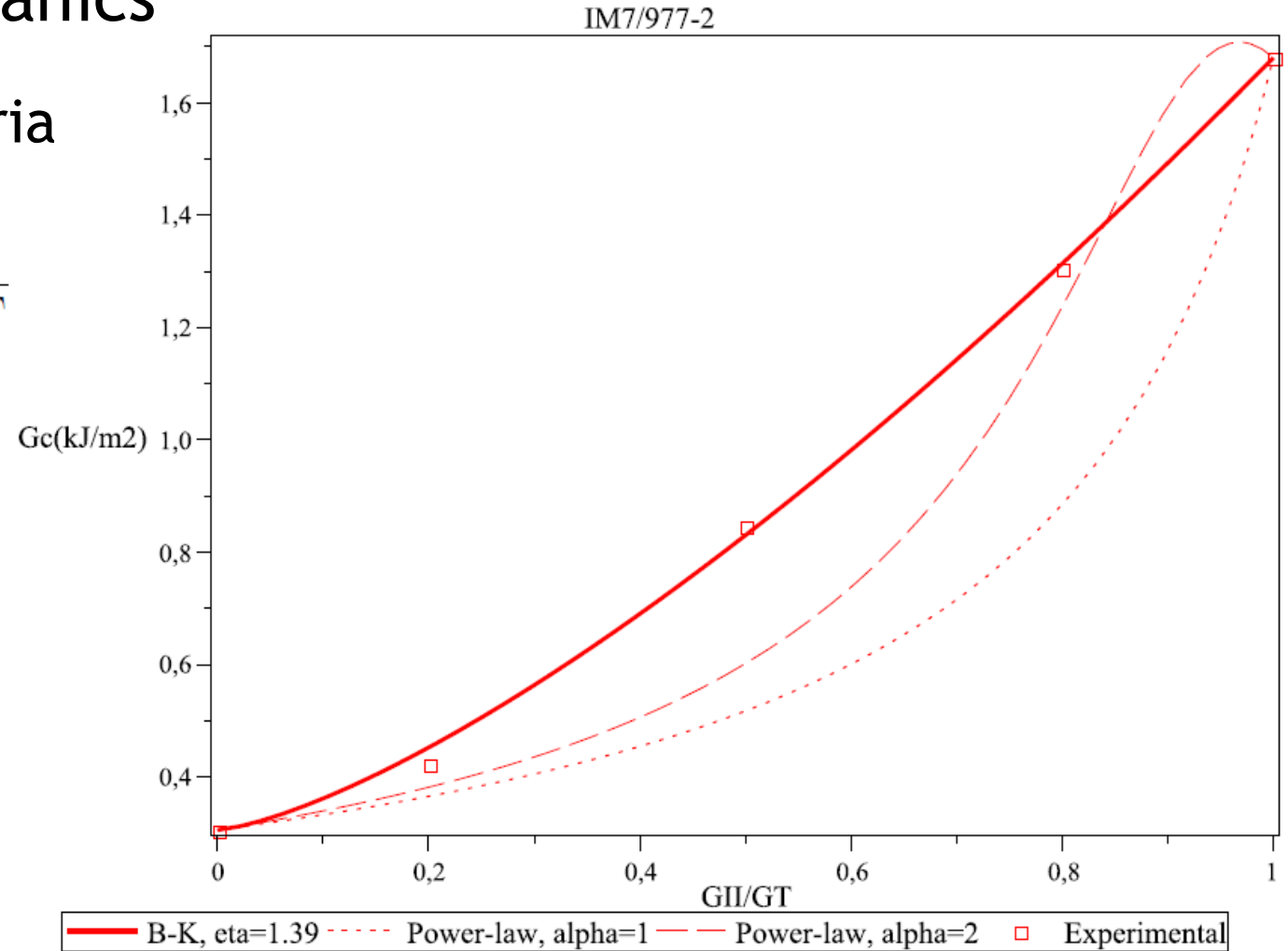


Interlaminar fracture mechanics

Delamination propagation criteria

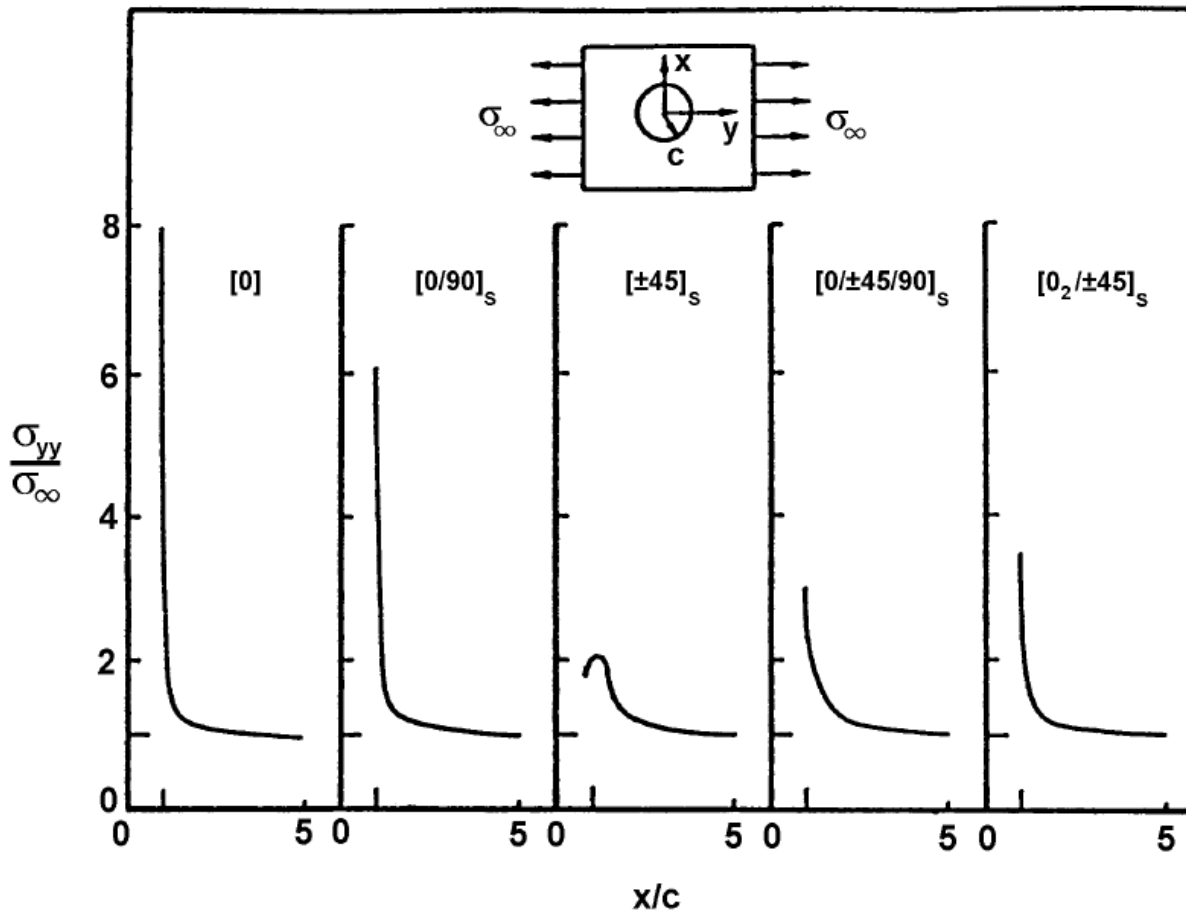
$$\mathcal{F}_{BK} := \frac{G_I + G_{II}}{G_{Ic} + (G_{IIc} - G_{Ic}) \left(\frac{G_{II}}{G_I + G_{II}} \right)^\eta} \geq \frac{1}{SF}$$

$$\left(\frac{G_I}{G_{Ic}} \right)^\alpha + \left(\frac{G_{II}}{G_{IIc}} \right)^\alpha \geq \frac{1}{SF}$$



P.P. Camanho, A. Turon, C.S. Lopes, D. Trias. DELAT Technical Note 2: Best Practice Analysis Methods. June 2010.

Stress concentrations



$$\sigma'_M = \sigma' \times \left\{ 1 + \sqrt{2 \left(\sqrt{\frac{E_x}{E_y} - \nu_{xy}} \right) + \frac{E_x}{G_{xy}}} \right\}$$

Maximum stress in the laminate, where:

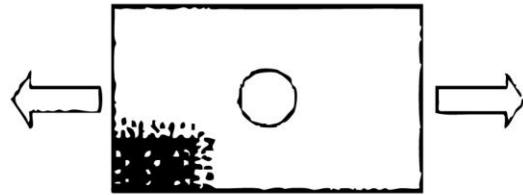
E_x and E_y are the moduli of elasticity in the 0° and 90° directions;

G_{xy} is the shear modulus;

ν_{xy} is the Poisson's ratio.

CMH-17-3G COMPOSITE MATERIALS HANDBOOK VOLUME 3. POLYMER MATRIX COMPOSITES MATERIALS USAGE, DESIGN, AND ANALYSIS. 2012. Daniel Gay, Suong V. Hoa, Stephen W. Tsai. Composite materials - design and application. CRC Press LLC, 2000.

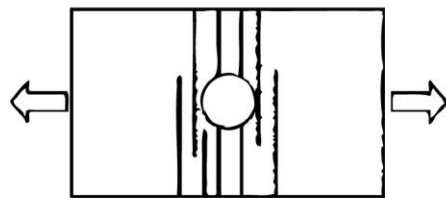
Stress concentrations



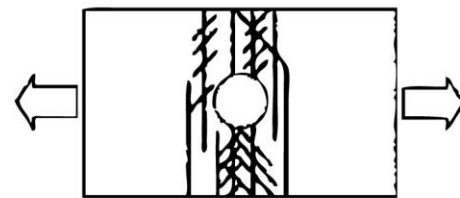
$$\sigma'_M = \sigma' \times \left\{ 1 + \sqrt{2 \left(\sqrt{\frac{E_x}{E_y} - \nu_{xy}} \right) + \frac{E_x}{G_{xy}}} \right\}$$

Maximum stress in the laminate, where:

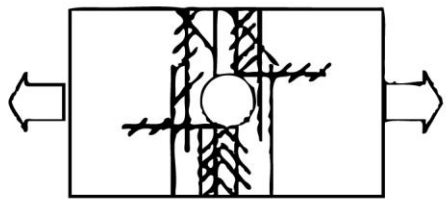
E_x and E_y are the moduli of elasticity in the 0° and 90° directions;
 G_{xy} is the shear modulus;
 ν_{xy} is the Poisson's ratio.



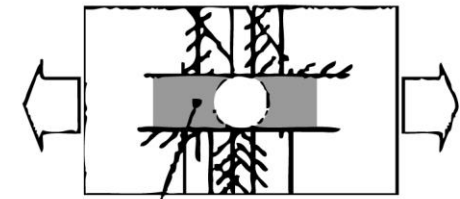
90° ply fracture
(matrix)



+/-45° ply fracture
(matrix)



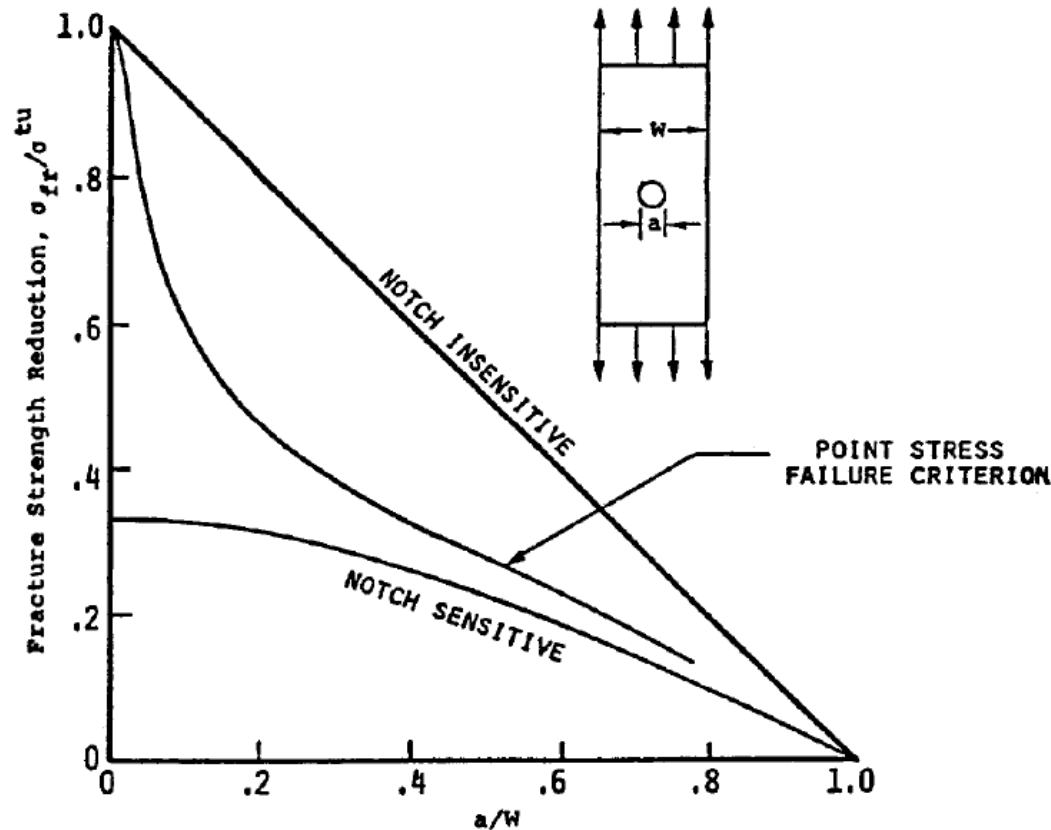
0° ply split cracking
(matrix)



Delamination
Deformation around the hole

Daniel Gay, Suong V. Hoa, Stephen W. Tsai. Composite materials - design and application. CRC Press LLC, 2000.

Stress concentrations



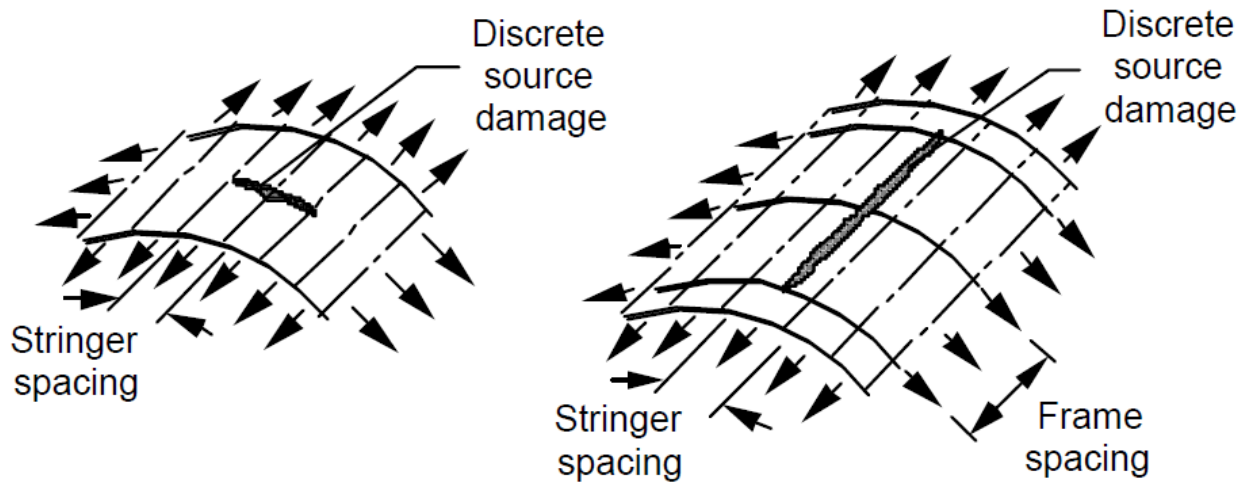
$$\sigma'_M = \sigma' \times \left\{ 1 + \sqrt{2 \left(\sqrt{\frac{E_x}{E_y} - \nu_{xy}} \right) + \frac{E_x}{G_{xy}}} \right\}$$

Maximum stress in the laminate,
where:

E_x and E_y are the moduli of elasticity
in the 0° and 90° directions;
 G_{xy} is the shear modulus;
 ν_{xy} is the Poisson's ratio.

CMH-17-3G COMPOSITE MATERIALS HANDBOOK VOLUME 3. POLYMER
MATRIX COMPOSITES MATERIALS USAGE, DESIGN, AND ANALYSIS. 2012.
Daniel Gay, Suong V. Hoa, Stephen W. Tsai. Composite materials -
design and application. CRC Press LLC, 2000.

Residual strength



Linear elastic fracture mechanics (LEFM)

$$\bar{\sigma}^\infty = \frac{\mathcal{K}_{Ic}}{\chi Y \sqrt{\pi a}}$$

Laminate fracture toughness \mathcal{K}_{Ic}

Orthotropy rescaling¹ χ

FWC factor² Y

Length of the inherent flaw a

Inherent flaw model (IFM)³

$$\bar{\sigma}^\infty = X_T^L \sqrt{\frac{a_0}{a + a_0}} \sqrt{\frac{1 - \left[\frac{2(a + a_0)}{W} \right]^2}{1 - \left(\frac{2a_0}{W} \right)^2}}$$

Laminate tensile strength X_T^L

a_0

$a + a_0$

$\frac{2(a + a_0)}{W}$

$\frac{2a_0}{W}$

¹ Suo et al. *Int J Solids Struct* 1991;28(2):235-248.

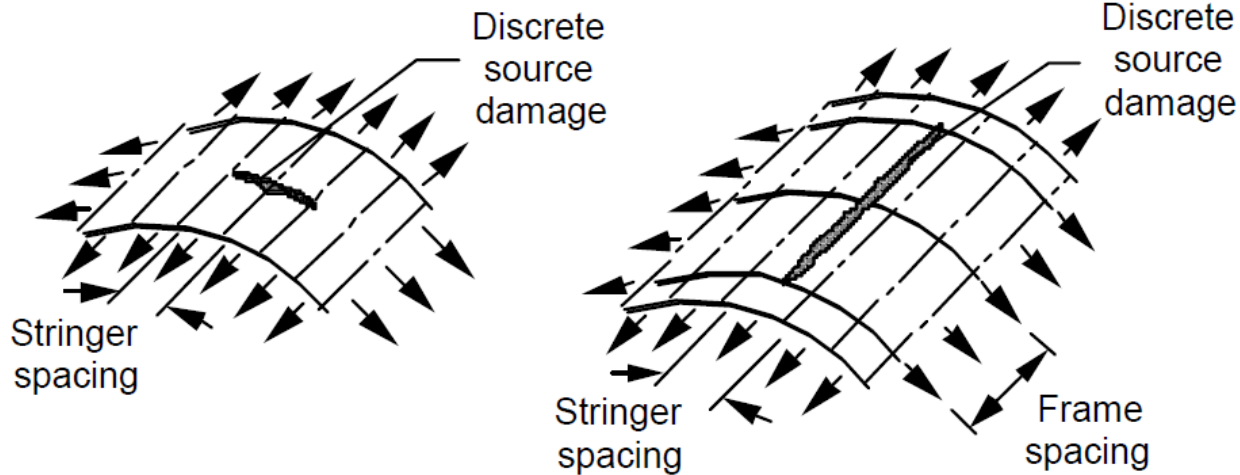
² Chen et al. *Int J Fracture* 1992;55:R3-R8.

³ Waddoups et al. *J Compos Mater* 1971;5:446-454.

⁴ Whitney and Nuismer. *J Compos Mater* 1974;8:253-265.

⁵ Camanho et al. *Compos Part A-Appl S* 2012;43:1219-1225.

Residual strength



Point stress (PS) model⁴ $\sigma_{yy}(x, 0)|_{x=a+r_{ot}} = X_T^L$

Characteristic distance

Average stress (AS) model⁴ $\frac{1}{r_{ot}} \int_a^{a+r_{ot}} \sigma_{yy}(x, 0) dx = X_T^L$

Finite Fracture Mechanics (FFMs) model⁵ $\left\{ \begin{array}{l} \frac{1}{\bar{l}} \int_a^{a+\bar{l}} \sigma_{yy}(x, 0) dx = X_T^L \\ \frac{1}{\bar{l}} \int_a^{a+\bar{l}} \mathcal{K}_I^2(a) da = \mathcal{K}_{Ic}^2 \end{array} \right.$

Crack extension at failure

¹ Suo et al. *Int J Solids Struct* 1991;28(2):235-248.

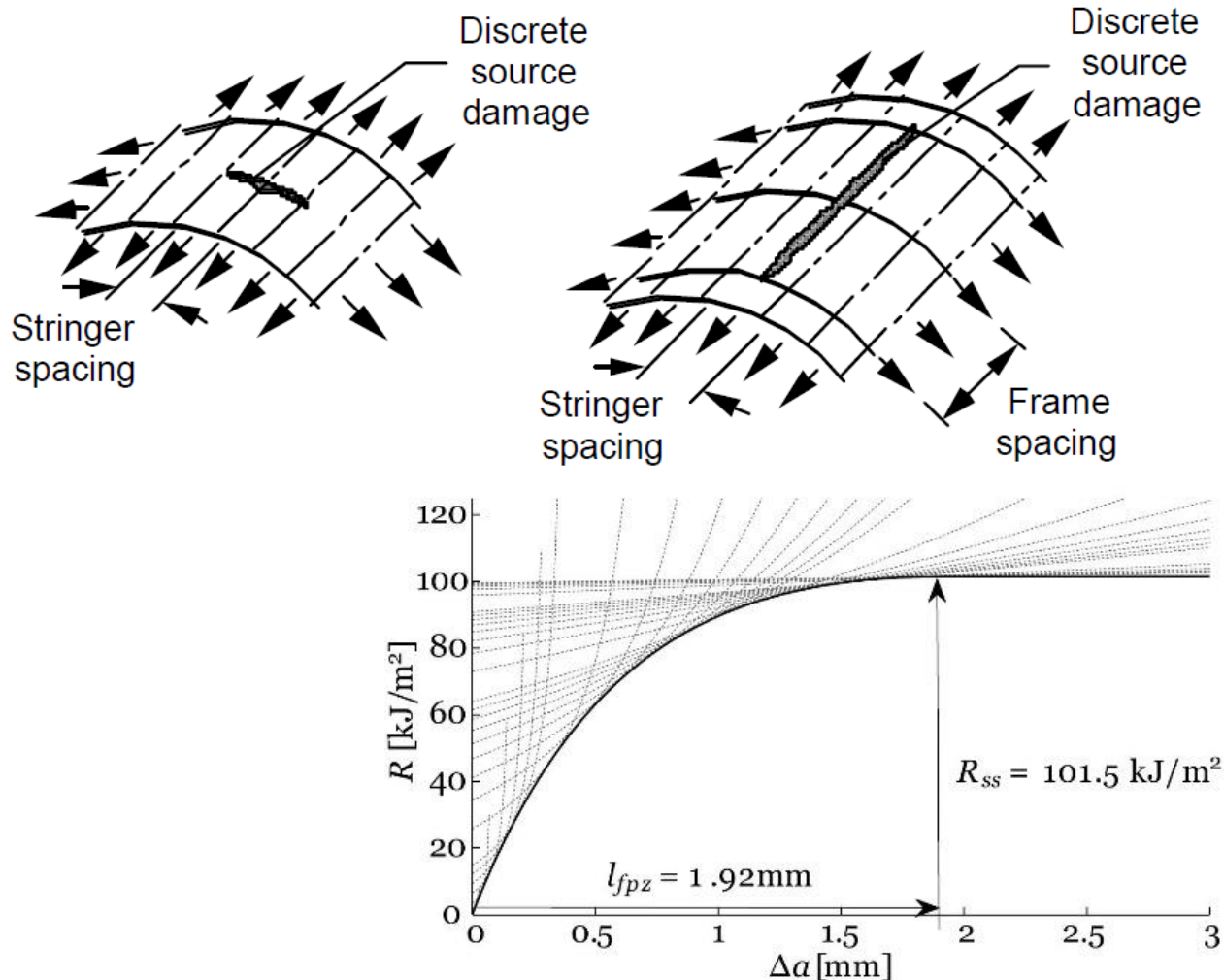
² Chen et al. *Int J Fracture* 1992;55:R3-R8.

³ Waddoups et al. *J Compos Mater* 1971;5:446-454.

⁴ Whitney and Nuismer. *J Compos Mater* 1974;8:253-265.

⁵ Camanho et al. *Compos Part A-Appl S* 2012;43:1219-1225.

Residual strength



Point stress (PS) model⁴ $\sigma_{yy}(x, 0)|_{x=a+r_{ot}} = X_T^L$

Characteristic distance

Average stress (AS) model⁴ $\frac{1}{r_{ot}} \int_a^{a+r_{ot}} \sigma_{yy}(x, 0) dx = X_T^L$

Finite Fracture Mechanics (FFMs) model⁵ $\begin{cases} \frac{1}{l} \int_a^{a+l} \sigma_{yy}(x, 0) dx = X_T^L \\ \int_a^{a+l} \mathcal{G}_I(a) da = \int_0^l \mathcal{R}(\Delta a) d\Delta a \end{cases}$

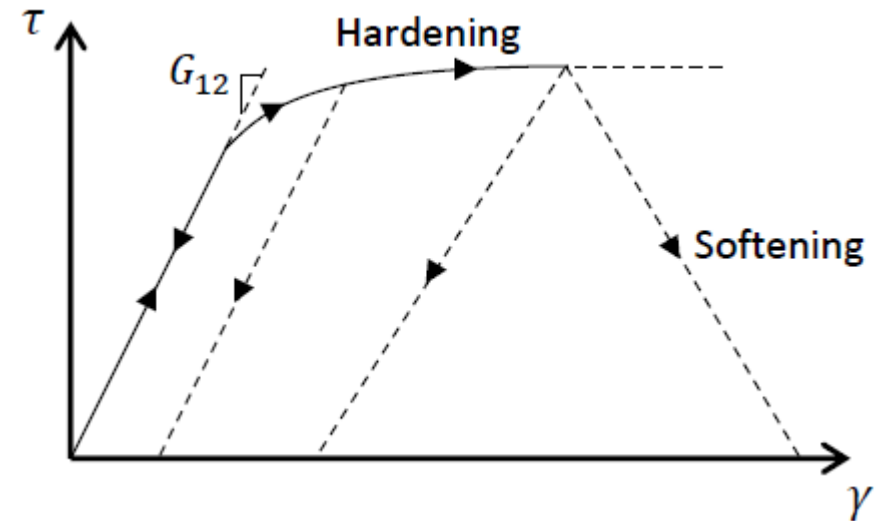
R-curve of the laminate

$$\mathcal{R}(\Delta a) = \begin{cases} \mathcal{R}_{SS} [1 - (1 - \zeta \Delta a)^\eta] & , \Delta a \leq l_{fpz} \\ \mathcal{R}_{SS} & , \Delta a > l_{fpz} \end{cases}$$

⁵ Arteiro et al. *Compos Part A-Appl S* 2014;63:110-122.

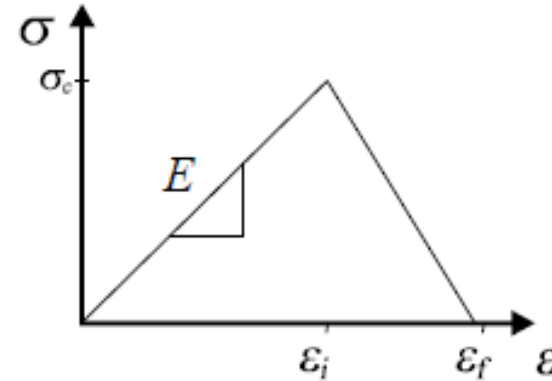
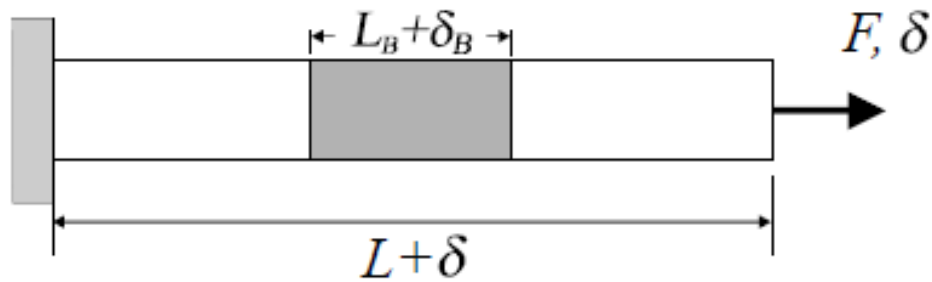
Progressive damage mechanics

- All materials exhibit **irreversible nonlinearities**, such as **plasticity**, **damage**, and **fracture**, which can be identified by comparing the *unloading paths* to the *loading paths*.
- **Hardening** is a macroscopic irreversible material response that smears the stress concentrations and eliminates any stress singularities.
- **Softening** corresponds to the development and coalescence of voids and microcracks, conducting to damage localized along a fracture surface and elastic unload adjacent to the fracture surface.



A. Arteiro. Technology development and structural mechanics of composites built of spread tow thin-ply technology. Master's thesis, University of Porto, Porto, 2012.

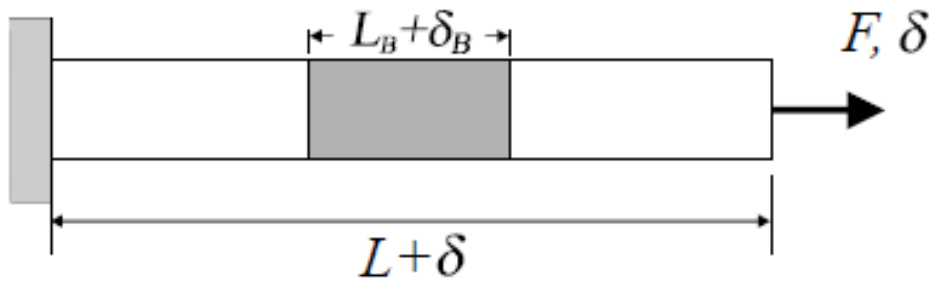
Progressive damage mechanics



$$\sigma(\epsilon) = \begin{cases} E\epsilon, & \epsilon \leq \epsilon_i \\ (1-d)E\epsilon, & \epsilon_i < \epsilon < \epsilon_f, \quad d = \frac{\epsilon_f(\epsilon - \epsilon_i)}{\epsilon(\epsilon_f - \epsilon_i)} \\ 0, & \epsilon > \epsilon_f \end{cases}$$

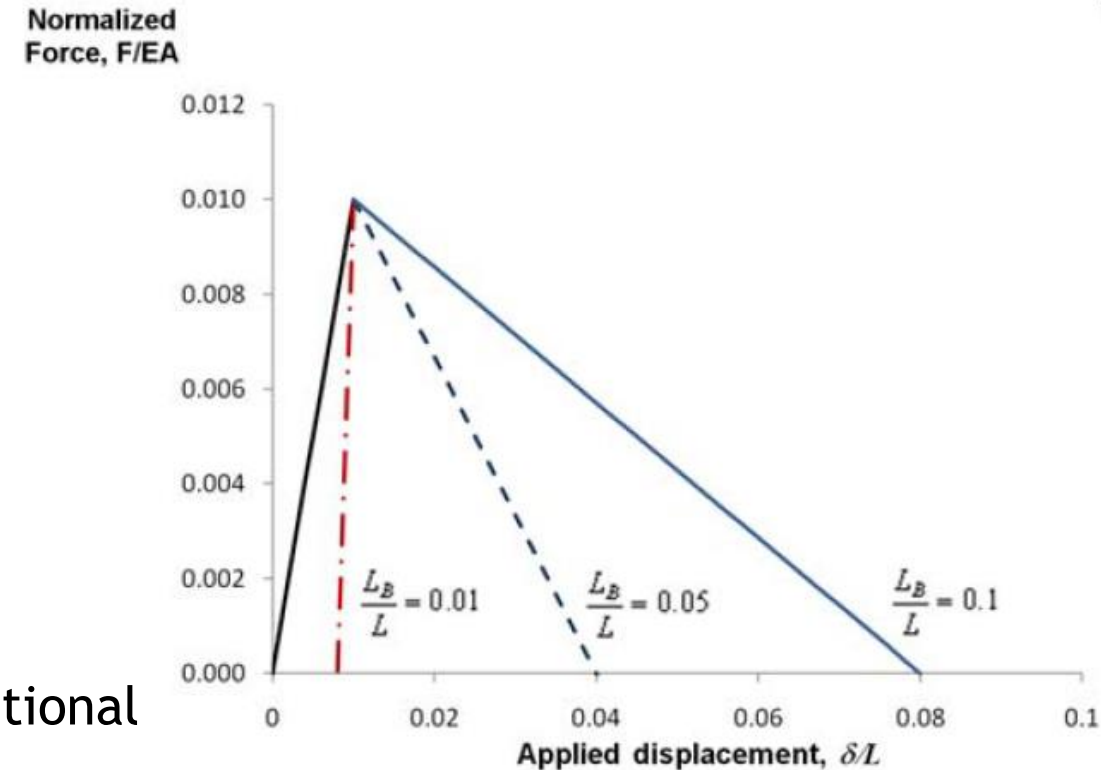
Carlos G. Dávila, Cheryl A. Rose, Endel Iarve. Modeling fracture and complex crack networks in laminated composites. In: Vladislav Mantič, editor, Mathematical Methods and Models in Composites. World Scientific Publishing, 2014.

Progressive damage mechanics



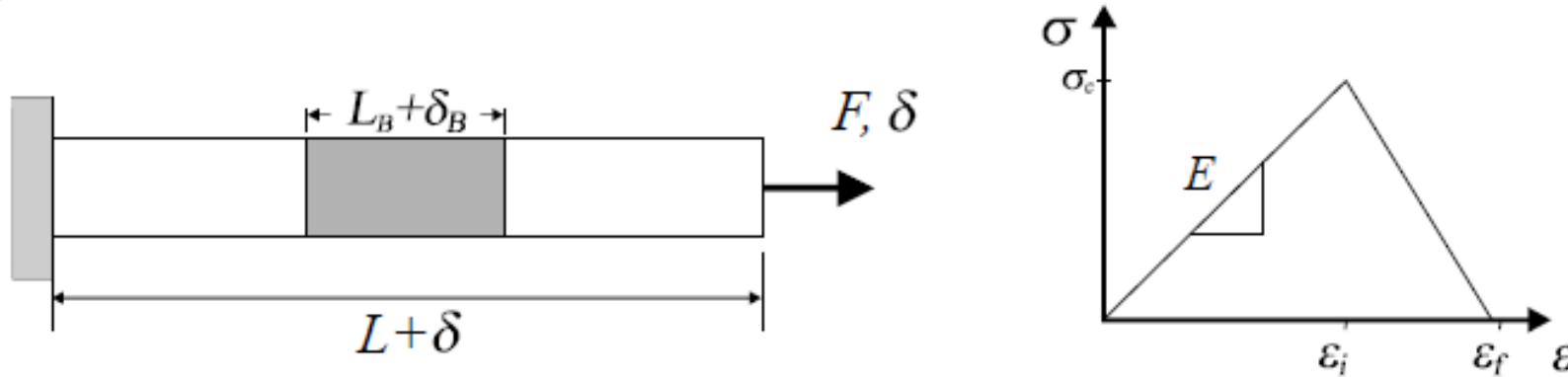
In finite element analyses, the length L_B is associated with the element length.

When the element size tends to zero, the computational model predicts failure without any energy being dissipated, a physically unacceptable result.



Carlos G. Dávila, Cheryl A. Rose, Endel Larve. Modeling fracture and complex crack networks in laminated composites. In: Vladislav Mantič, editor, Mathematical Methods and Models in Composites. World Scientific Publishing, 2014.

Progressive damage mechanics

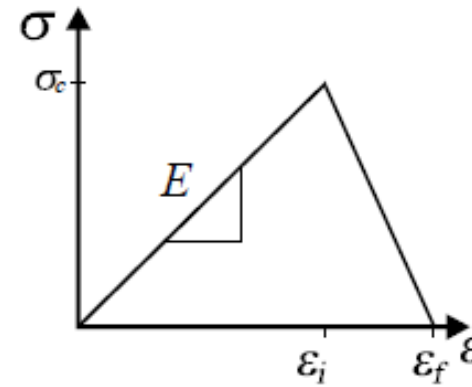
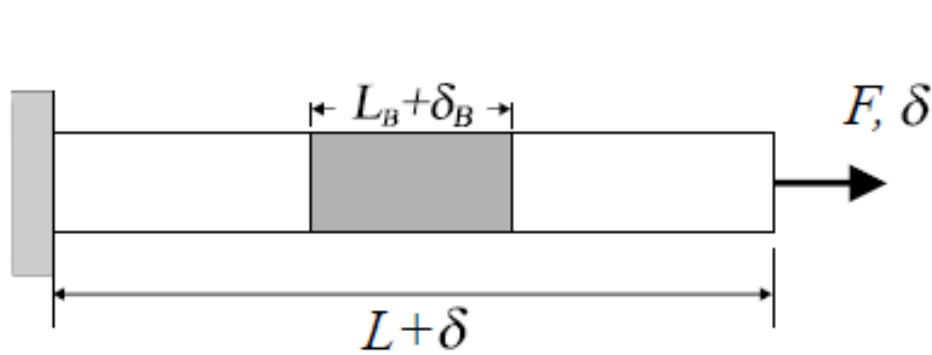


$$\int_V \int_0^{\epsilon_f} \sigma d\epsilon dV = G_c A \Rightarrow AL_e \frac{E \epsilon_i \epsilon_f}{2} = G_c A \Rightarrow \epsilon_f = \frac{2G_c}{L_e E \epsilon_i}$$

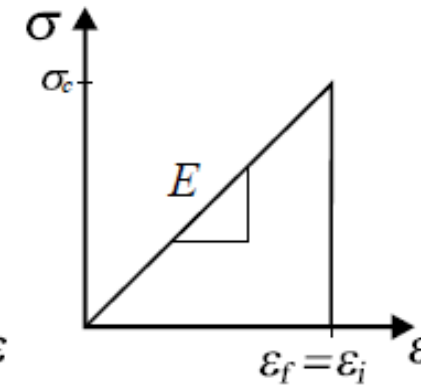
The **objectivity** of the numerical solution can be simply achieved by adjusting the post-peak material response using a **characteristic element length** L_e .

Carlos G. Dávila, Cheryl A. Rose, Endel Larve. Modeling fracture and complex crack networks in laminated composites. In: Vladislav Mantič, editor, Mathematical Methods and Models in Composites. World Scientific Publishing, 2014.

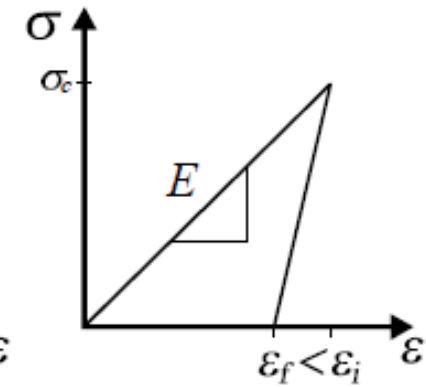
Progressive damage mechanics



Softening



Limit



Snap-back

$$AL_e^{Max} \frac{\sigma_c^2}{2E} = G_c A \Rightarrow L_e^{Max} = \frac{2EG_c}{\sigma_c^2}$$

Carlos G. Dávila, Cheryl A. Rose, Endel larve. Modeling fracture and complex crack networks in laminated composites. In: Vladislav Mantič, editor, Mathematical Methods and Models in Composites. World Scientific Publishing, 2014.

Progressive damage mechanics

The thermodynamics of irreversible processes can be used to formulate the constitutive equations using phenomenological criteria as damage activation functions.

Definition of the complementary free energy density in the laminated composite material

$$\begin{aligned}
 G = & \frac{\sigma_{11}^2}{2(1-d_1)E_1} + \frac{\sigma_{22}^2}{2(1-d_2)E_2} - \frac{\nu_{12}}{E_1} \sigma_{11} \sigma_{22} \\
 & + \frac{\sigma_{12}^2}{2(1-d_6)G_{12}} + (\alpha_{11}\sigma_{11} + \alpha_{22}\sigma_{22})\Delta T \\
 & + (\beta_{11}\sigma_{11} + \beta_{22}\sigma_{22})\Delta M
 \end{aligned}$$

$$\varepsilon = \frac{\partial G}{\partial \sigma} = \mathbf{H} : \sigma + \alpha \Delta T + \beta \Delta M$$

$$\mathbf{H} = \frac{\partial^2 G}{\partial \sigma^2} = \begin{bmatrix} \frac{1}{(1-d_1)E_1} & -\frac{\nu_{21}}{E_2} & 0 \\ -\frac{\nu_{12}}{E_1} & \frac{1}{(1-d_2)E_2} & 0 \\ 0 & 0 & \frac{1}{(1-d_6)G_{12}} \end{bmatrix}$$

P. Maimí, P.P. Camanho, J.A. Mayugo, C.G. Dávila. A continuum damage model for composite laminates: Part I - Constitutive model. *Mechanics of Materials* 39 (2007) 897-908.

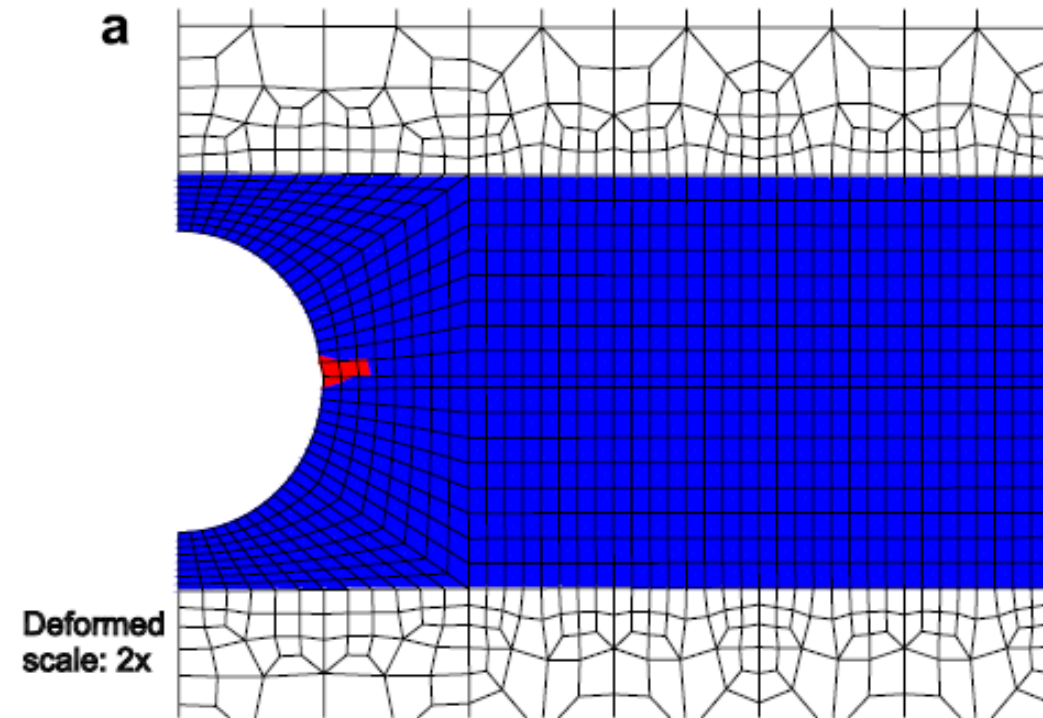
Progressive damage mechanics

The thermodynamics of irreversible processes can be used to formulate the constitutive equations using phenomenological criteria as damage activation functions.

Definition of the complementary free energy density in the laminated composite material

$$G = \frac{\sigma_{11}^2}{2(1 - d_1)E_1} + \frac{\sigma_{22}^2}{2(1 - d_2)E_2} - \frac{\nu_{12}}{E_1} \sigma_{11} \sigma_{22} + \frac{\sigma_{12}^2}{2(1 - d_6)G_{12}} + (\alpha_{11} \sigma_{11} + \alpha_{22} \sigma_{22}) \Delta T + (\beta_{11} \sigma_{11} + \beta_{22} \sigma_{22}) \Delta M$$

P.P. Camanho, P. Maimí, C.G. Dávila. Prediction of size effects in notched laminates using continuum damage mechanics. *Composites Science and Technology* 67 (2007) 2715-2727.



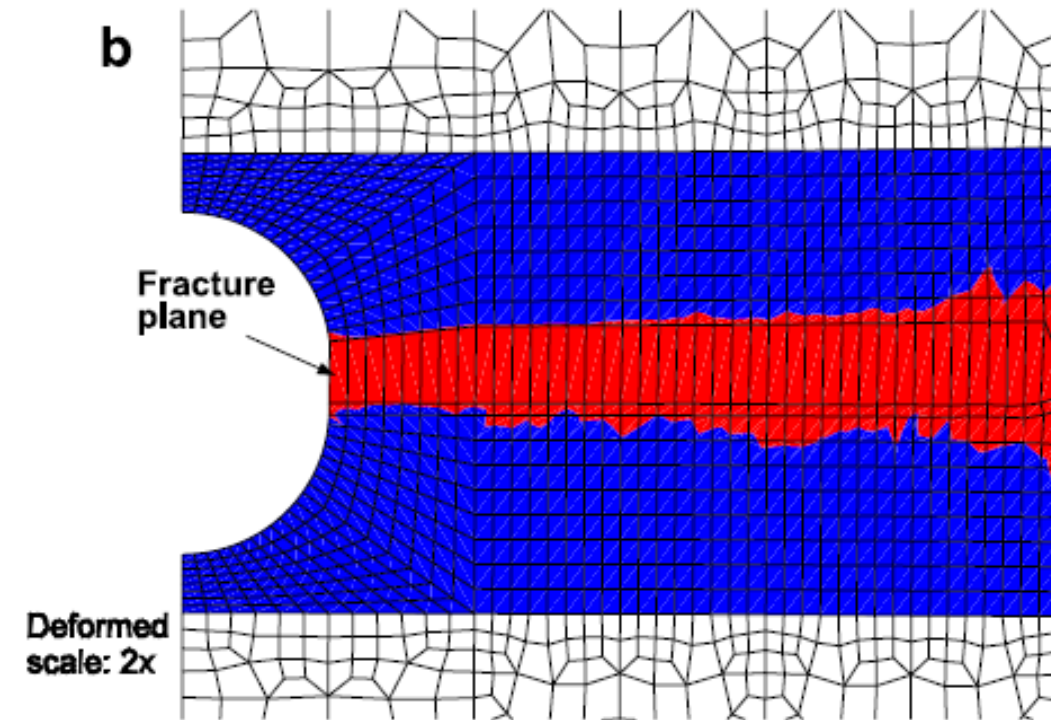
Progressive damage mechanics

The thermodynamics of irreversible processes can be used to formulate the constitutive equations using phenomenological criteria as damage activation functions.

Definition of the complementary free energy density in the laminated composite material

$$G = \frac{\sigma_{11}^2}{2(1-d_1)E_1} + \frac{\sigma_{22}^2}{2(1-d_2)E_2} - \frac{\nu_{12}}{E_1} \sigma_{11} \sigma_{22} + \frac{\sigma_{12}^2}{2(1-d_6)G_{12}} + (\alpha_{11} \sigma_{11} + \alpha_{22} \sigma_{22}) \Delta T + (\beta_{11} \sigma_{11} + \beta_{22} \sigma_{22}) \Delta M$$

P.P. Camanho, P. Maimí, C.G. Dávila. Prediction of size effects in notched laminates using continuum damage mechanics. *Composites Science and Technology* 67 (2007) 2715-2727.

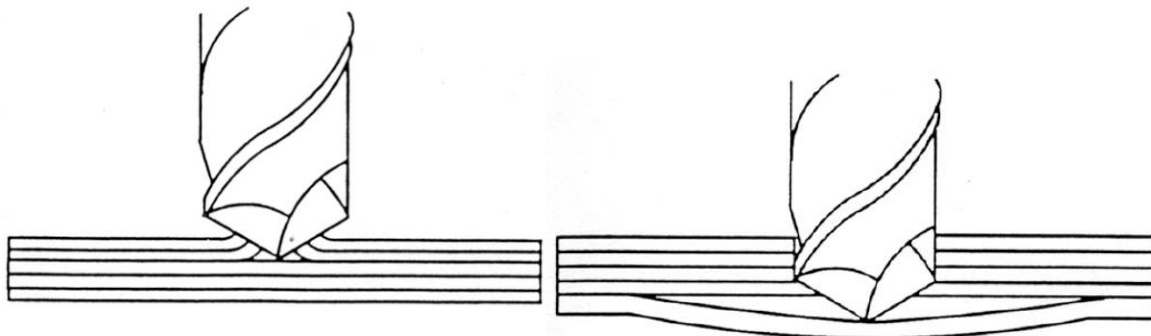


Composite joints

Mechanically fastened joints	Bonded joints
<ul style="list-style-type: none"> ✓ Drilling - probability of inducing damage ✓ Different coefficients of thermal expansion between composite and joining elements can cause deterioration of the joint (particularly in harsh, cyclic environments) 	<ul style="list-style-type: none"> ✓ More vulnerable to environment ✓ Lower assembly/unmounting flexibility ✓ Lower stress concentration ✓ Well designed provide a better alternative

Peel-up delamination at hole entry

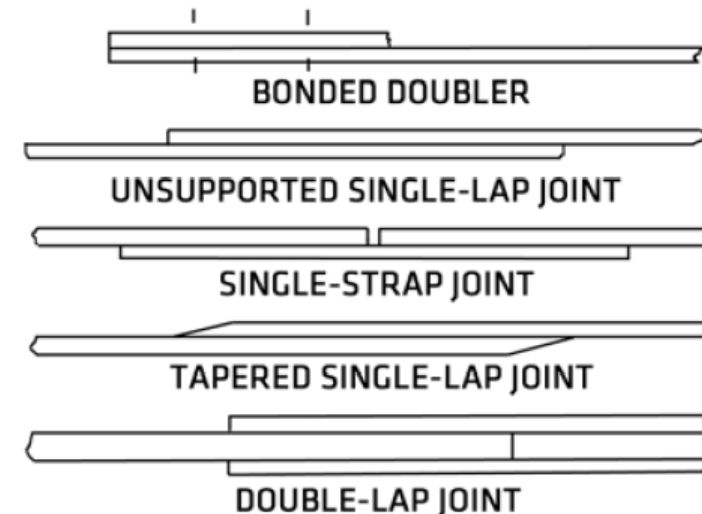
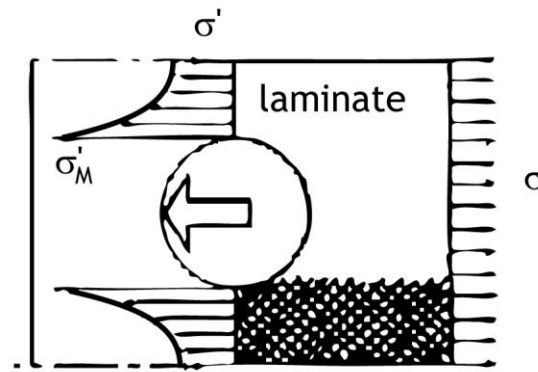
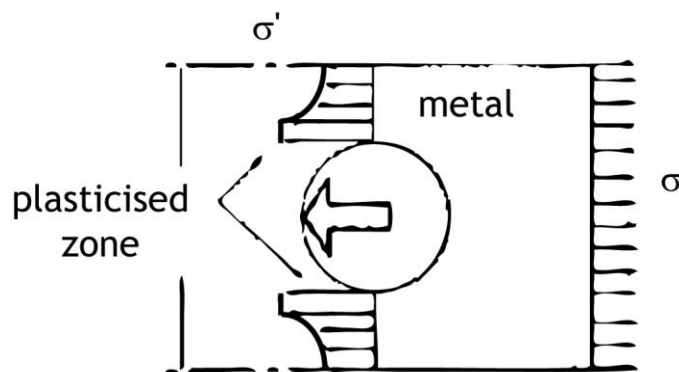
Push-out delamination at hole exit



Composite joints

CMH-17-3G COMPOSITE MATERIALS HANDBOOK VOLUME 3. POLYMER MATRIX COMPOSITES MATERIALS USAGE, DESIGN, AND ANALYSIS. 2012.

Mechanically fastened joints	Bonded joints
<ul style="list-style-type: none"> ✓ Drilling - probability of inducing damage ✓ Different coefficients of thermal expansion between composite and joining elements can cause deterioration of the joint (particularly in harsh, cyclic environments) 	<ul style="list-style-type: none"> ✓ More vulnerable to environment ✓ Lower assembly/unmounting flexibility ✓ Lower stress concentration ✓ Well designed provide a better alternative

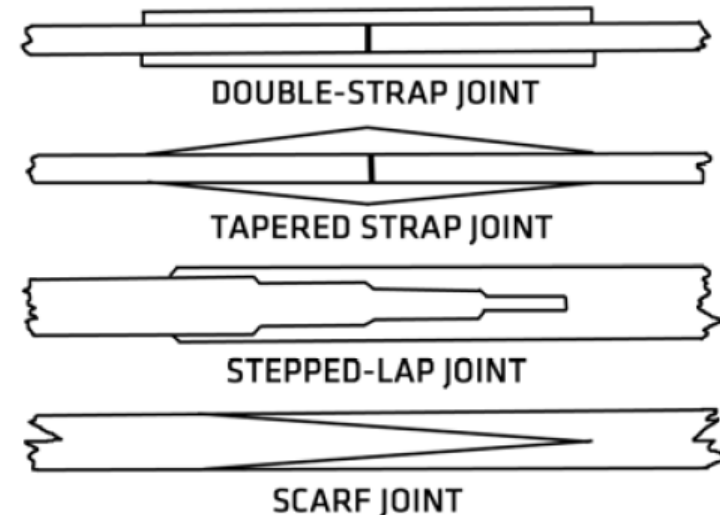
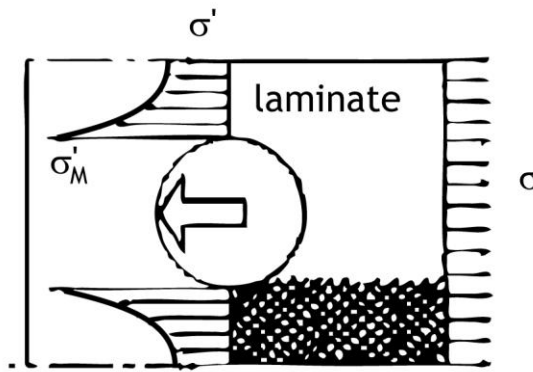
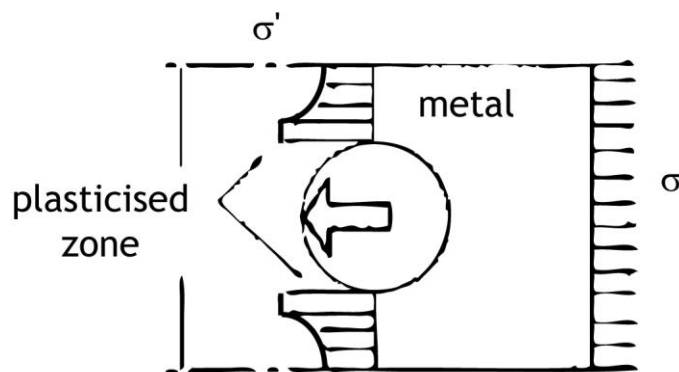


Daniel Gay, Suong V. Hoa, Stephen W. Tsai. Composite materials - design and application. CRC Press LLC, 2000.

Composite joints

CMH-17-3G COMPOSITE MATERIALS HANDBOOK VOLUME 3. POLYMER MATRIX COMPOSITES MATERIALS USAGE, DESIGN, AND ANALYSIS. 2012.

Mechanically fastened joints	Bonded joints
<ul style="list-style-type: none"> ✓ Drilling - probability of inducing damage ✓ Different coefficients of thermal expansion between composite and joining elements can cause deterioration of the joint (particularly in harsh, cyclic environments) 	<ul style="list-style-type: none"> ✓ More vulnerable to environment ✓ Lower assembly/unmounting flexibility ✓ Lower stress concentration ✓ Well designed provide a better alternative

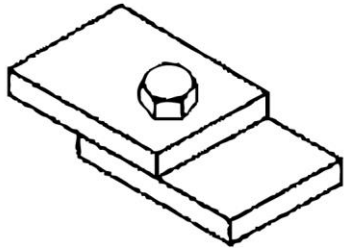


Daniel Gay, Suong V. Hoa, Stephen W. Tsai. Composite materials - design and application. CRC Press LLC, 2000.

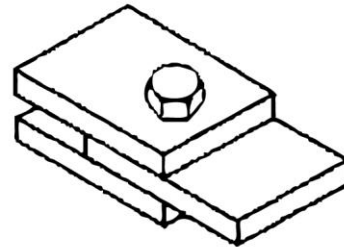
Composite joints

Mechanically fastened joints

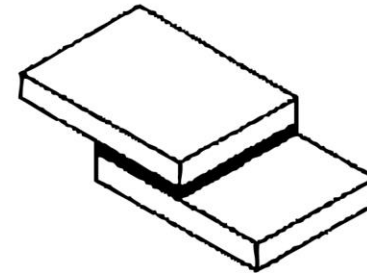
Bonded joints



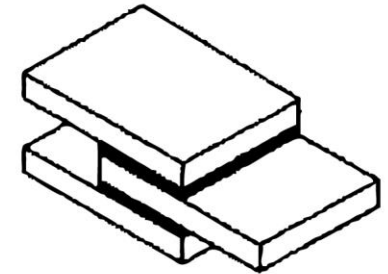
single-lap joint



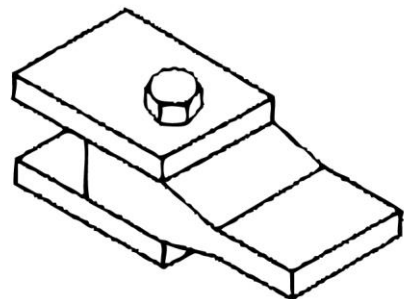
double-lap joint



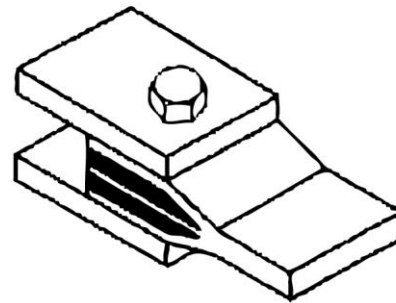
single-lap joint



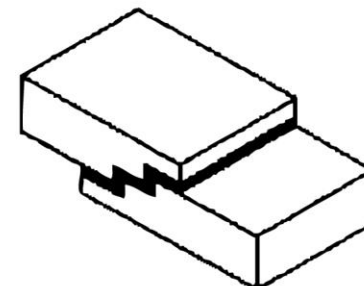
double-lap joint



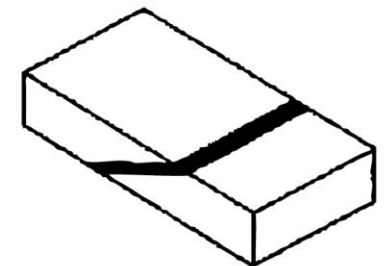
reinforced-edge joint



shimmed joint



stepped-lap joint



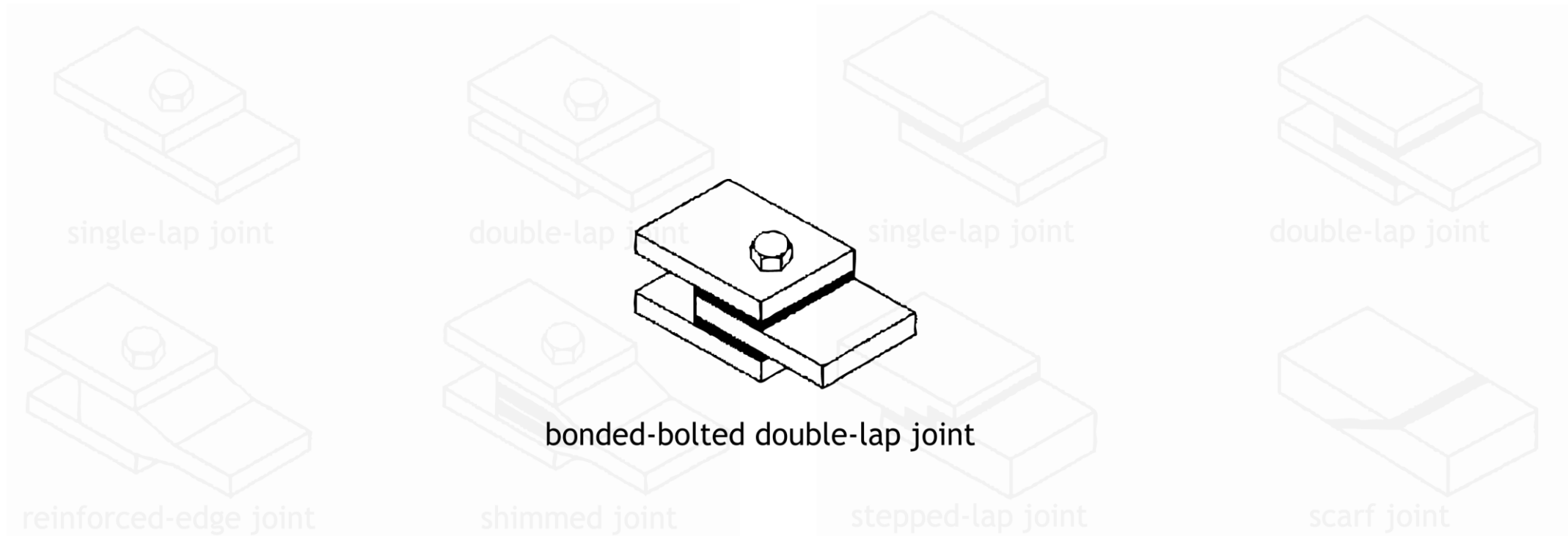
scarf joint

Jones, Robert M. Mechanics of composite materials – 2nd ed.
Taylor & Francis Group, LLC, 1999.

Composite joints

Mechanically fastened joints

Bonded joints

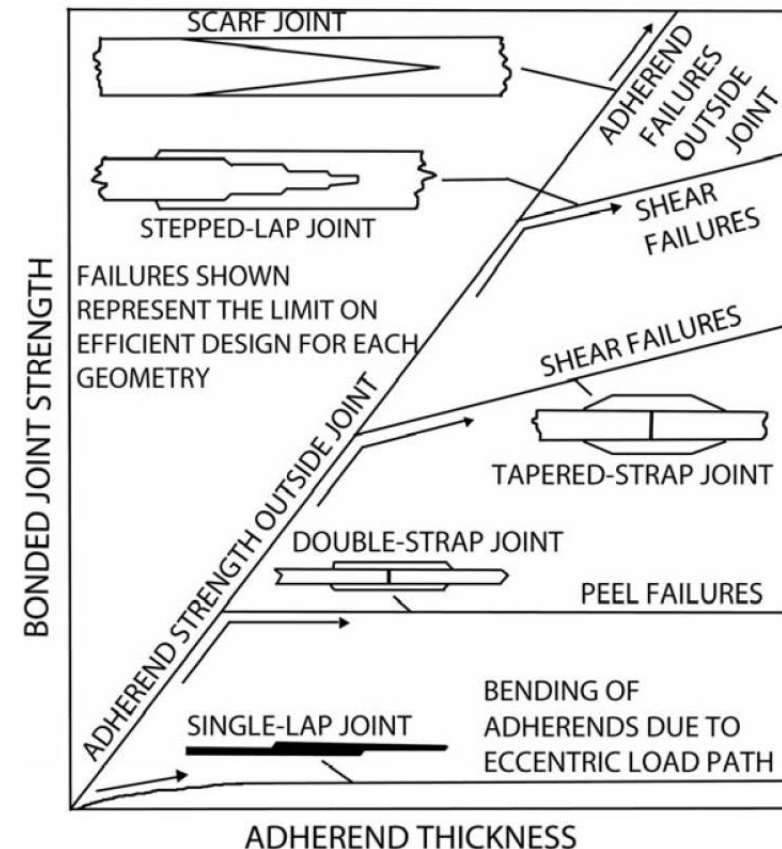
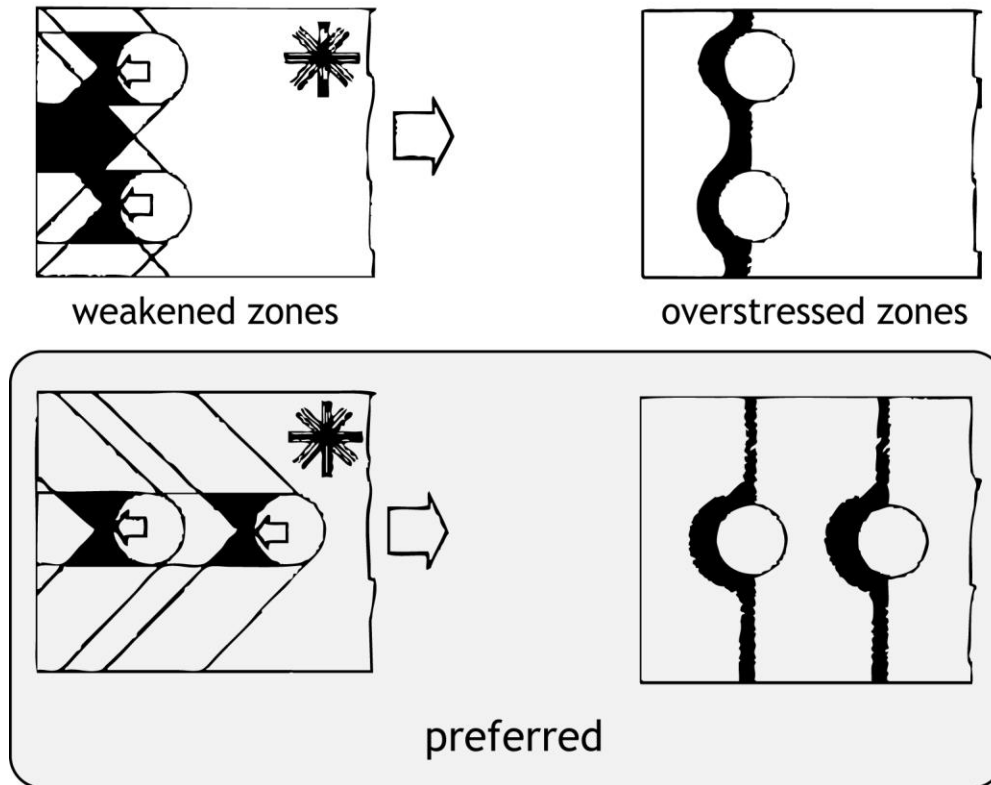


Jones, Robert M. Mechanics of composite materials – 2nd ed.
Taylor & Francis Group, LLC, 1999.

Composite joints

CMH-17-3G COMPOSITE MATERIALS HANDBOOK VOLUME 3. POLYMER MATRIX COMPOSITES MATERIALS USAGE, DESIGN, AND ANALYSIS. 2012.

Mechanically fastened joints	Bonded joints
-------------------------------------	----------------------

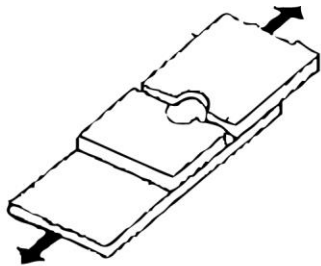


Daniel Gay, Suong V. Hoa, Stephen W. Tsai. Composite materials - design and application. CRC Press LLC, 2000.

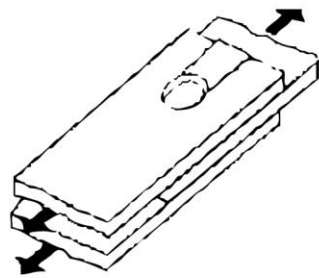
Composite joints

CMH-17-3G COMPOSITE MATERIALS HANDBOOK VOLUME 3. POLYMER MATRIX COMPOSITES MATERIALS USAGE, DESIGN, AND ANALYSIS. 2012.

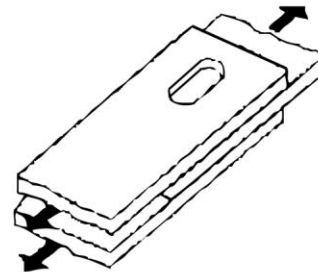
Mechanically fastened joints	Bonded joints
------------------------------	---------------



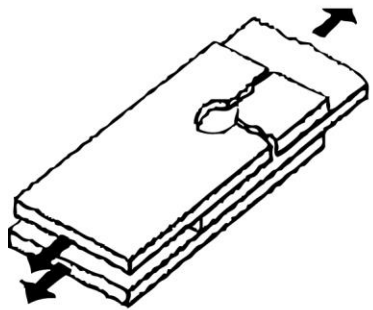
tensile fracture
(insufficient number of 0° plies)



shear fracture
(insufficient number of +/-45° plies)



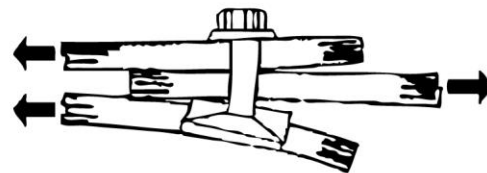
bearing failure
(insufficient thickness)



tensile na normal fracture

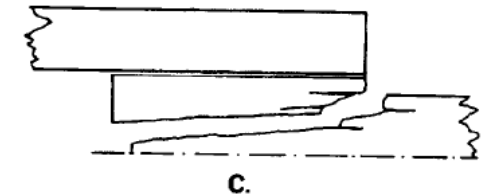
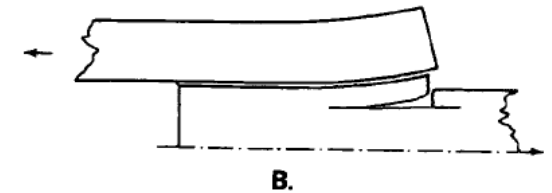
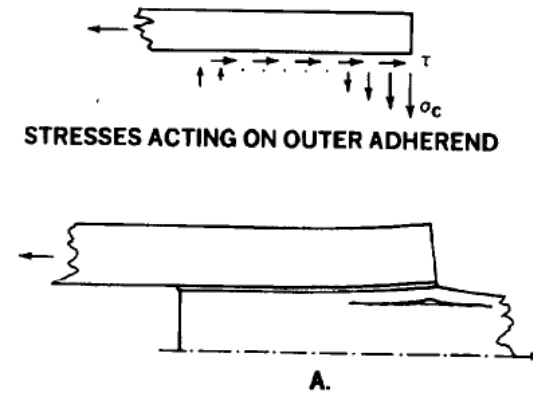


bolt fracture

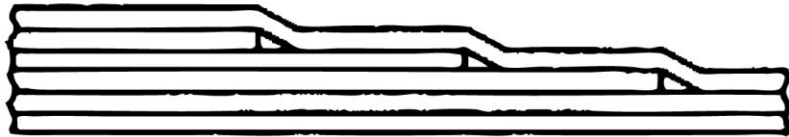


bolt lifting

Daniel Gay, Suong V. Hoa, Stephen W. Tsai. Composite materials - design and application. CRC Press LLC, 2000.

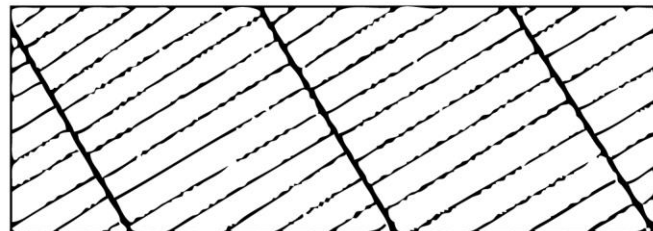
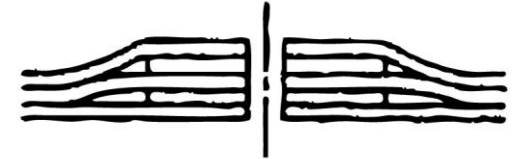


Thickness variations

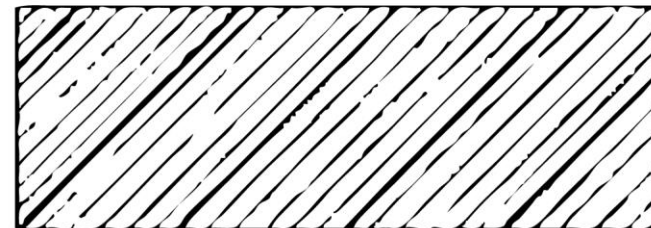


Ply drops

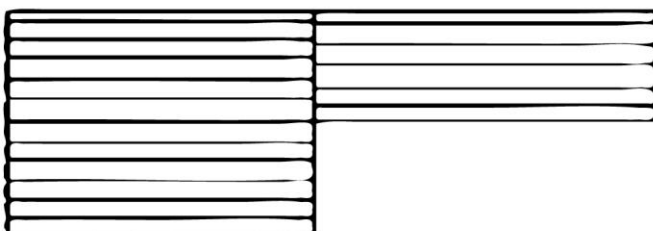
Increase bearing capacity



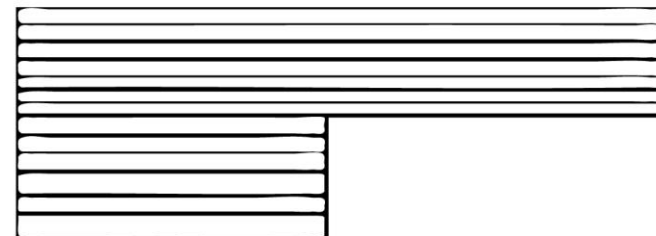
Bad



Good



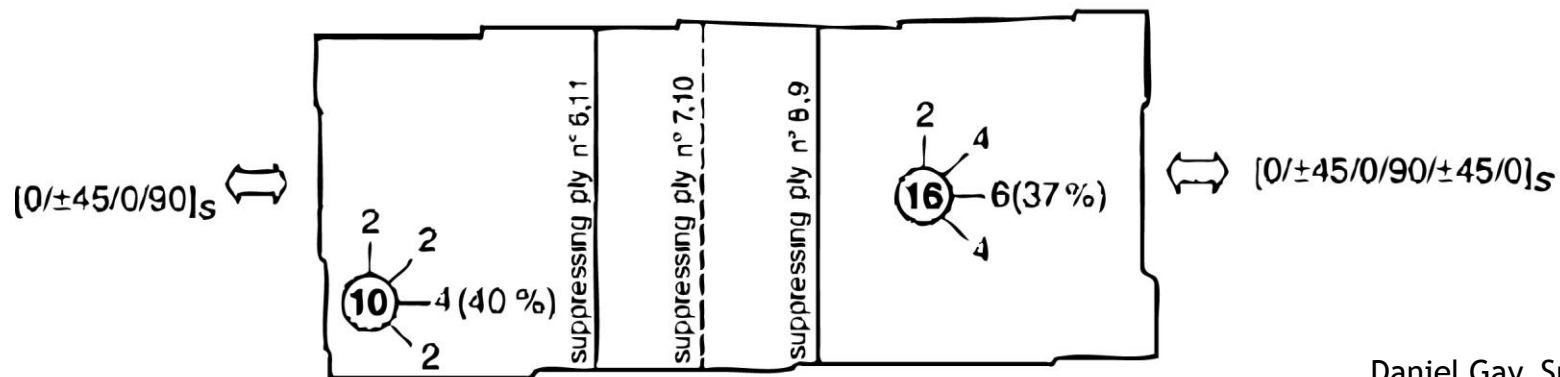
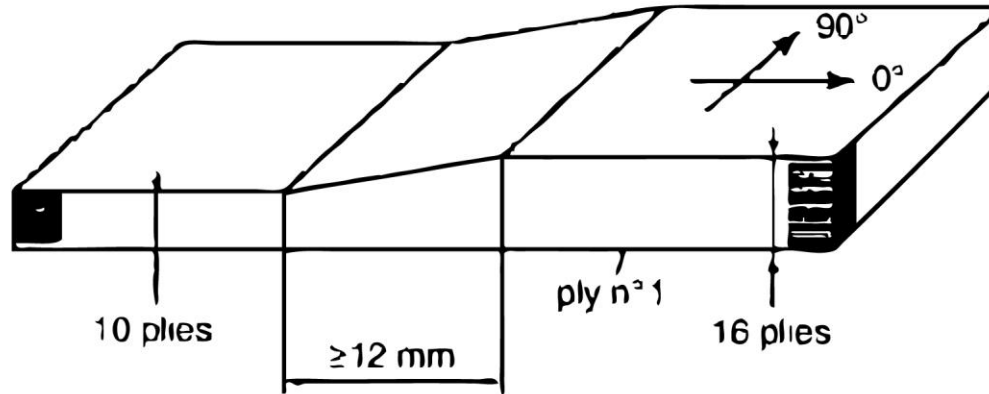
Bad



Good

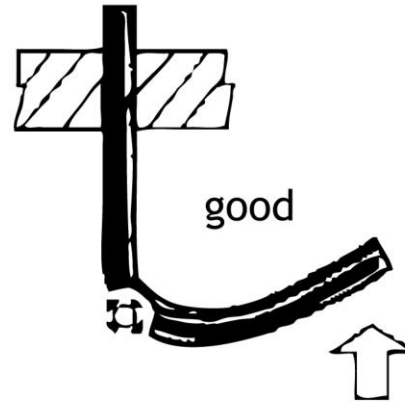
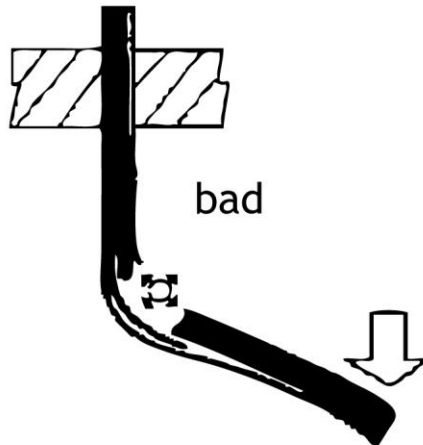
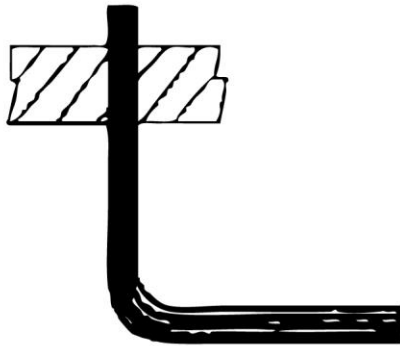
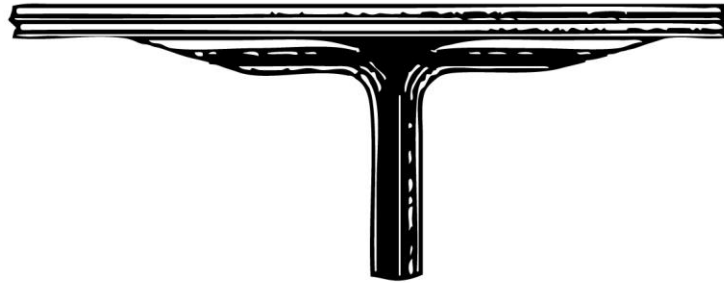
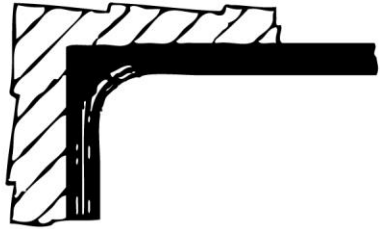
Jones, Robert M. Mechanics of composite materials – 2nd ed. Taylor & Francis Group, LLC, 1999.
Daniel Gay, Suong V. Hoa, Stephen W. Tsai. Composite materials - design and application. CRC Press LLC, 2000.

Thickness variations



Daniel Gay, Suong V. Hoa, Stephen W. Tsai. Composite materials - design and application. CRC Press LLC, 2000.

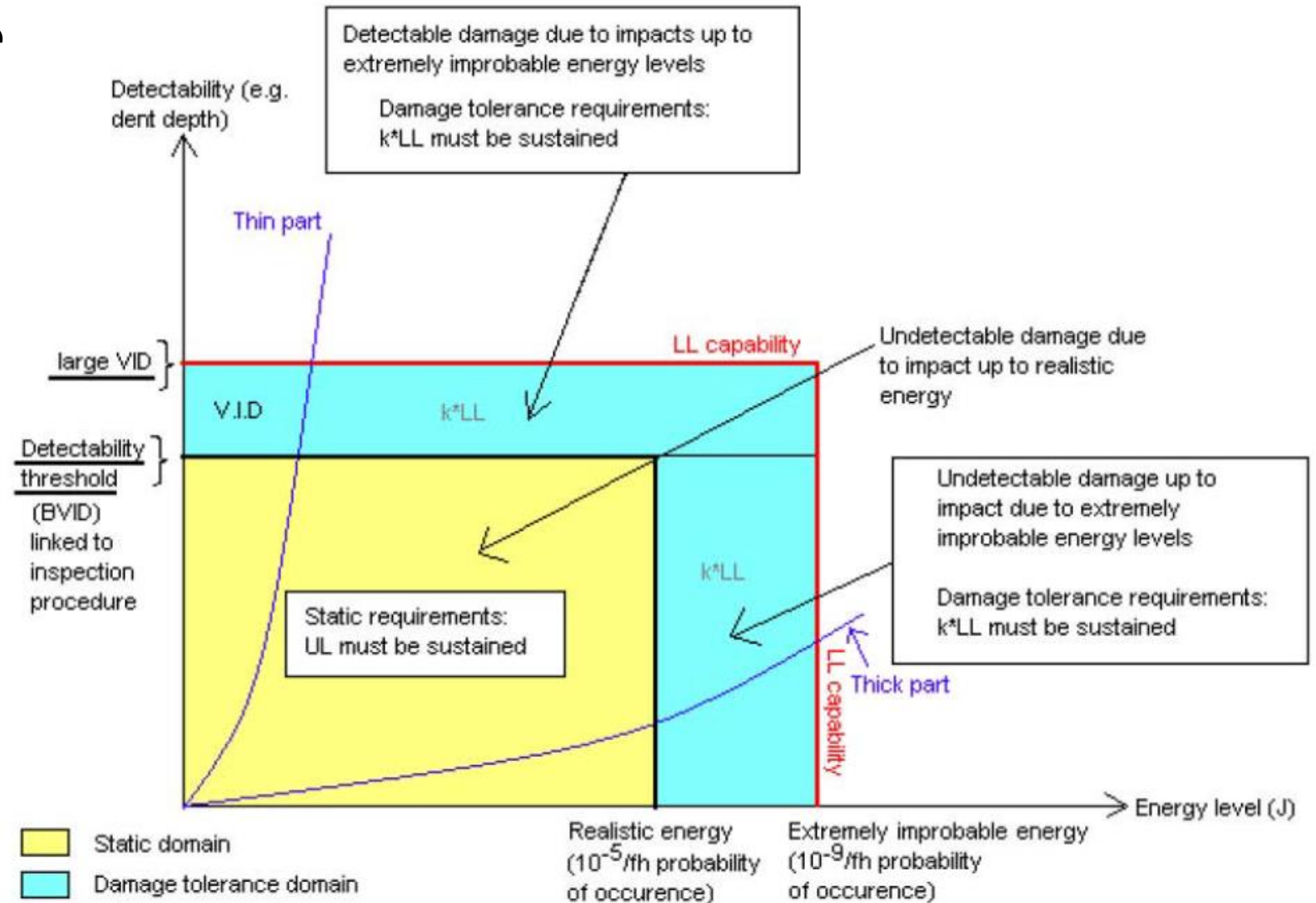
Corners



tendency to
ply delamination

Daniel Gay, Suong V. Hoa, Stephen W. Tsai. Composite materials
- design and application. CRC Press LLC, 2000.

Damage tolerance



CMH-17-3G COMPOSITE MATERIALS
HANDBOOK VOLUME 3. POLYMER MATRIX
COMPOSITES MATERIALS USAGE, DESIGN,
AND ANALYSIS. 2012.

Recommended safety factors

a) For general composites

Static:	Short term	2
	Long term	4

Long-term intermittent situation:

	Cyclic	5
	Shock	10

b) Advanced Composites

1.3 to 1.8

Questions?

Designing with composite materials
Effects of stress concentrations
